N° D'ORDRE : 41375

MINES DOUAI **UNIVERSITE LILLE 1**

THESE

présentée en vue
d'obtenir le grade de

DOCTEUR
en

Spécialité : Génie Civil

par

Zengfeng ZHAO

DOCTORAT DELIVRE CONJOINTEMENT
PAR L'ECOLE DES MINES DE DOUAI ET L'UNIVERSITE LILLE 1

Titre de la thèse :
Valorisation des sables de béton recyclé pour la fabrication de mortiers
(Re-use of fine recycled concrete aggregates for the manufacture of mortars)

Soutenue le 14 Février 2014 devant le jury d'examen :

Rapporteur	*Eric GARCIA-DIAZ, Professeur, Mines Alès*
Rapporteur	*Ahmed LOUKILI, Professeur, Centrale Nantes*
Membre	*Anne-Lise BEAUCOUR, Maître de Conférences, Université de Cergy-Pontoise*
Membre	*André LECOMTE, Professeur, IUT Nancy Brabois*
Membre	*Jean-Eric Poirier, Directeur Scientifique, Groupe COLAS*
Membre	*Thierry SEDRAN, Ingénieur IFSTTAR*
Directeur de thèse	*Sébastien REMOND, Professeur, Mines Douai*
Co-directeur de thèse	*Denis DAMIDOT, Professeur, Mines Douai*

Laboratoire d'accueil : Département Génie Civil et Environnemental de l'Ecole des Mines Douai

Thèse codirigée par le Professeur Weiya XU, Université de HOHAI

Ecole Doctorale SPI 072 (Lille I)

Acknowledgements

My deepest gratitude goes first to Professors Sébastien REMOND and Denis DAMIDOT, my supervisors, for their constant encouragements and guidance during all my thesis. They helped me to find the right way of doing research and to solve the problems with endless passions, which will be big fortune in all my life. Without their selfless helps, this thesis could not reach its present form.

Secondly, I would like to express my sincere gratitude to my Chinese supervisor Professor Weiya XU at Hohai University, who encouraged me to study in a foreign country and go further in the research road.

Heartfelt thanks are due to Professor Eric GARCIA-DIAZ from Mines Alès and Professor Ahmed LOUKILI from Centrale Nantes for their willingness to evaluate my work despite of their tight schedule, for their useful suggestions and comments.

Thanks are due to Professor André LECOMTE from IUT Nancy Brabois for accepting to be the president of the jury of my thesis. My thanks also go to Doctor Anne-Lise BEAUCOUR from Université de Cergy-Pontoise, Doctor Jean-Eric Poirier from COLAS, and Doctor Thierry SEDRAN from IFSTTAR for their interests in this thesis and for examining my work.

I would also like to thank all the researchers and technicians in the Civil engineering and environmental department for their help in the research and experiments. Their names are as follows: David BULTEEL, Ghislain LOUIS, Vincent THIERY, Christine LORS, Guillaume POTIER, Dominique DUBOIS, Johanna CABOCHE, Damien BETRANCOURT, Christophe CAPPELAERE, Michael D'HELFT, Carole DELCHAMBRE, Jacqueline WOITRAIN, Rachid ZENTAR, Georges AOUAD, Frédéric BECQUART, Nor Edine ABRIAK, Claire ALARY, Mahfoud BENZERZOUR, Patrick PIZETTE.

I would also like to thank all my colleagues and friends for their help in my daily life. They are Dongxing WANG, Kai WU, Adolphe KIMBONGUILA, samira BRAKNI, Hassane AZRAR, Thomas VALEYRE, Alexandra BOURDOT, Raouf ACHOUR, Coralie DEPARIS, Moussa DIA, Jean DUCASSE LAPEYRUSSE, Abdelhafid KASMI, Issameddine KHEZAMI, Erwan SIMON, Feiyi DU, Baochao LI, Dulin CHEN, Yi HOU, Zaobao LIU, Jia WANG, Fanfei ZENG, Sijia ZHANG.

I would like to thank Chinese Scholarship Council (CSC) for the funding support of my thesis, and MINES DOUAI for the accommodation.

Finally, I would like to thank my beloved family for their loving considerations and great confidence in the past twenty-nine years, especially my parents Zaiyong ZHAO, Jiaoying JIN my sister Qianqian ZHAO, and my girl friend Yanyun LU who stayed with me for the last years spent in France and will continue to live with me for all the rest life.

Abstract

Very large quantities of construction and demolition wastes and especially concrete wastes are produced yearly. At the same time, high amounts of natural aggregates are needed for construction industry. Up to now, only a small fraction of these concrete wastes is re-used as recycled concrete aggregates (RCA) for the manufacture of concrete. RCA are composed of an intimate mix between aggregates and hardened cement paste (HCP). Hardened cement paste is much more porous than the natural aggregates and the properties and proportions of HCP largely influence the properties of RCA. As a consequence, the fine fraction of RCA (FRCA), essentially composed of mortar and cement paste, possesses a large water demand which makes it harder to recycle into concrete.

The objective of this research was to better understand the role played by HCP on the properties of RCA in relation with the improvement of the characterization methods of these materials and their reuse in the manufacture of mortar or concrete. Firstly, an experimental method based on salicylic acid attack of RCA allowed us to determine a soluble fraction in salicylic acid (SFSA) that is related to the HCP content. FRCA properties were then studied as a function of SFSA, particle sizes and properties/composition of the original concrete. From the obtained relationship between water absorption and SFSA, the water absorption coefficient of the smaller fraction (0/0.63mm) was estimated as it is not accurately measured with the standard methods. Secondly, different industrial RCA were characterized which allowed us to expand the preceding conclusions to “real RCA”, meanwhile, the influence of carbonation on the properties of FRCA was also carried out.

Finally, the influence of the saturation state of FRCA on the properties of fresh and hardened mortars and on their microstructure was explored. The recycled mortars with dried FRCA had better compressive strength than that made with saturated FRCA, which was confirmed by the study of ITZ properties. The mechanical properties of mortars with different RCA content and replacement fraction were determined. The finer fraction of RCA had a worse influence on the mechanical properties of RAC than the coarser fraction.

Key words: fine recycled concrete aggregates, water absorption, hardened cement paste content, carbonation, recycled mortar, interfacial transition zone

Résumé

De très grandes quantités de déchets de construction et de démolition sont produites chaque année, en même temps, de grandes quantités de granulats naturels sont nécessaires pour la construction. Jusqu'à présent, seule une petite fraction de ces déchets est réutilisée comme granulats pour la fabrication du béton. Les Granulats Recyclés (GR) sont principalement composés d'un mélange intime de granulats naturels et de pâte de ciment durcie (PCD). La pâte de ciment durcie possède généralement une porosité nettement plus élevée que celle des granulats naturels, la teneur et les propriétés physico-chimiques de la pâte de ciment présente dans les GR a ainsi une forte influence sur leurs propriétés. Les sables recyclés qui contiennent essentiellement du mortier et de la pâte, possèdent généralement un coefficient d'absorption d'eau très élevé, ce qui freine considérablement leur valorisation dans le béton. L'objectif principal de cette étude était de mieux comprendre le rôle joué par la PCD sur les propriétés des GR afin d'améliorer les méthodes de caractérisation de ces matériaux et de les réutiliser dans la fabrication de mortiers ou de bétons.

Tout d'abord, une méthode expérimentale basée sur l'attaque de la pâte de ciment par l'acide salicylique a été développée et a permis de déterminer la fraction soluble dans l'acide salicylique (FSAS) des GR. Les propriétés des GR ont ensuite été étudiées en fonction de la FSAS, de la taille des particules et de la composition du béton d'origine. De la relation obtenue entre l'absorption d'eau et la FSAS, le coefficient d'absorption d'eau de la fraction fine (0/0.63mm) peut être estimé. Différents GR industriels ont ensuite été caractérisés afin d'étendre les conclusions précédentes à des GR produits dans des conditions plus réalistes. Par ailleurs, l'influence de la carbonatation sur les propriétés des GR a également été étudiée.

Enfin, l'influence de l'état de saturation des GR sur les propriétés des mortiers frais et durci et sur leur microstructure a été explorée. Les mortiers recyclés avec GR sec ont présenté une meilleure résistance à la compression que ceux avec GR saturés. Ces résultats ont été confirmés par l'étude des propriétés de l'ITZ. Les propriétés mécaniques de mortiers fabriqués avec des teneurs variables en GR ou avec des fractions de substitution différentes ont été étudiées. Les résultats obtenus ont montré que la fraction fine des GR avait une influence plus néfaste sur les propriétés des bétons recyclés que la fraction grossière.

Mots clés: fines des granulats recyclés, absorption d'eau, teneur en pâte de ciment, carbonatation, mortier recyclé, zone de transition

Content

Notations

Abstract

RCA: Recycled concrete aggregates

FRCA: Fine recycled concrete aggregates

HCP: Hardened cement paste

GR: Granualts recyclés

PCD: Pâte de ciment durcie

ITZ: Interfacial transition zone

Chapter 1

RAC: Recycled aggregate concrete

C&DW: Construction and demolition wastes

CRCA: Coarse recycled concrete aggregates

SSD: Saturated surface dry

TSMA: Two-stage mixing approach

Chapter 2

OPC: Ordinary Portland Cement

W/C: Water to cement ratio

OCx: Original concrete x

Fraction D1/D2 mm: The minimal and maximal particle sizes of the granular class are D1 and D2 respectively.

RCA-OCx-28/90: Recycled concrete aggregates manufactured from the original concrete x which has been cured during 28/90 days in water.

CP-0.6-90: Cement paste which is made with W/C=0.6 and cured 90 days in water.

CPC: Cement paste content

XRD: X-ray diffraction

TGA: Thermogravimetric analysis

$ML_{105-600}$: Mass loss between 105 and 600°C.

SSA: Specific surface area

BET: Brunauer-Emmett-Teller analysis for the measuring of specific surface area

BJH: Barrett-Joyner-Halenda analysis for the determining of pore area and volume on desorption isotherms from BET.

SFSA: Soluble fraction in salicylic acid

HPC: Hydrated paste content

RCA-OCx-90-carbo D1/D2mm: Recycled concrete aggregates manufactured from the original concrete x which has been cured 90days in water, these recycled concrete aggregates are carbonated in the laboratory under accelerated conditions, and the minimal and maximal particle sizes of the granular class are D1 and D2 respectively.

MIP: Mercury intrusion porosimetry for the measuring of porosity

EN: notation for water absorption coefficient determined from NF EN 1097-6

IFSTTAR: notation for water absorption coefficient determined from IFSTTAR method number 78

Chapter 3

RCA-Colas1: Industrial RCA produced by Colas company in the site Valormat of Amien

RCA-Colas2: Industrial RCA produced by Colas company in the plant of Louvres

RCA-PNR: Industrial RCA produed for the French nationl projet Recybéton

Chapter 4

CM: Calcareous mortar with the natural calcareous sand

RM: Recycled motar with recycled sand

RM-W/C-S/D: Recycled mortar manufactured with saturated sand (S) and dried sand (D), and water to cement ratio= W/C

RM-W/C-Proportion for example RM-0.5-10: Recycled mortar manufactured with water to cement ratio 0.5 and 10% of natural sand is replaced by the same volume of recycled sand.

RM-W/C-Fraction for example RM-0.5-0/0.63: Recycled mortar manufactured with water to cement ratio 0.5 and fraction of natural sand 0/0.63mm is replaced by the same volume of recycled sand 0/0.63mm.

SEM and EDX: Scanning Electron Microscopy and Energy-dispersive X-ray analysis

CPS/D: Cement paste manufactured with saturated/dried grain

List of tables

List of figures

General introduction

Very large quantities of natural aggregates are used yearly for the construction of roads, buildings or civil engineering infrastructures. In the same time, the demolition of concrete structures produces high amounts of wastes that could be recycled as concrete aggregates in order to decrease the amounts of natural aggregates that are used.

Up to now, only a small fraction of these materials is re-used for the manufacture of concrete and a better understanding of the properties of recycled concrete aggregates (RCA) and of mortars or concretes made with RCA would allow to reduce the amounts of wastes that have to be disposed in landfills and as a consequence would preserve natural resources.

Recycled concrete aggregates are composed of an intimate mix between aggregates and hardened cement paste (HCP). Hardened cement paste is much more porous than the natural aggregates generally used for the manufacture of concrete and the properties and proportions of HCP largely influence the properties of RCA. The coarse fraction of RCA, essentially composed of gravel (surrounded by mortar) generally possesses satisfying properties for the re-use as concrete aggregates. On the contrary, the fine fraction of RCA (FRCA), essentially composed of mortar and hardened cement paste, possesses a large water demand which makes it harder to recycle into concrete. A better understanding of the role played by HCP on the properties of FRCA is essential for improving the use of FRCA in concrete. This necessitates a better characterization of HCP content in FRCA.

The objectives of this research are twofold. Firstly, we aim at studying the properties of fine recycled concrete aggregates (FRCA) as a function of hardened cement paste content, particle sizes and properties/composition of the original concrete. Secondly, the influence of the

saturation state of FRCA on the properties of fresh and hardened mortars and on their microstructure is explored.

The first chapter of this manuscript presents a literature review on the properties of RCA and of concretes manufactured with RCA. From this literature review the main scientific issues and research objectives are defined. In the second chapter, properties of laboratory made RCA are studied. An experimental method allowing measuring the HCP content of RCA is presented and FRCA are then characterized for different parent concretes. In the third chapter, different industrial RCA are characterized in order to extend the preceding conclusions to "real RCA". Chapter four presents the study carried out on mortars containing RCA that were defined in Chapter three. The influence of saturation state of RCA on the variation of slump with time is first studied. Then, the mechanical properties of mortars are determined for different RCA contents in the mortars and different saturation states of the aggregates. The influence of saturation state on the microstructure of mortars, especially on the interfacial transition zone is studied. Finally, the general conclusions and some perspectives of this work are exposed.

All this research work has been carried out at the civil and environmental engineering department (Mines Douai) under the supervision of Profs. Damidot and Rémond. It has been done in collaboration with Prof. Xu (Hohai University, China) with the financial support of the China Scholarship Council (CSC) and Mines Douai.

Chapter 1 Literature review

1.1 Introduction

This chapter presents a review of previous research works on the use of recycled concrete aggregate (RCA) to make recycled aggregate concrete (RAC). The literature review will focus first on the global issue of construction and demolition wastes (C&DW), then on the properties of RCA, and finally on the properties of RAC.

1.2 Construction and demolition wastes

Due to the growth of population and rapid development of construction industry, large amounts of construction and demolition wastes (C&DW) are generated annually and these quantities are expected to increase in the future. When structures are demolished, the wastes are either dumped in landfill sites or recycled in new applications. Therefore, it is very important to recycle C&DW in order to protect the environment and save natural aggregates[1-2].

1.2.1 Recycling situation

European Union

The generation of C&DW in the European Union reached 850 million tonnes in 2008, which represents 31% of total waste generation in the EU [3]. Since the total population of EU is 500 millions, the annual production of C&DW per habitant in EU is about 1.7 ton. Figure 1-1 shows that most countries of EU have a recycling percentage over 60%. Denmark,

Netherlands, Germany recycle nearly 90%, while United Kingdom and France only recycle 60%.

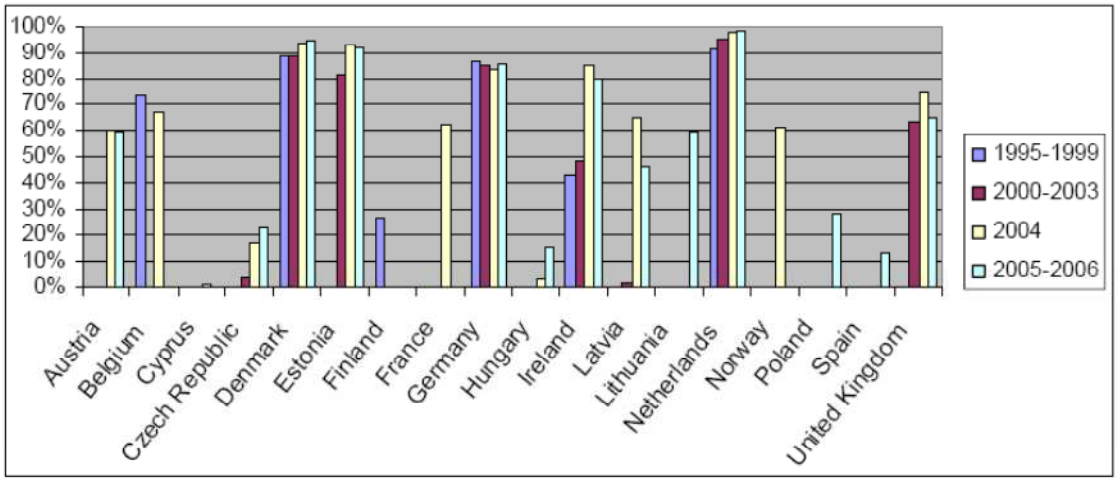

Figure 1-1 Recycling of C&DW in percentage of generated amount in the EU[3]

In 2005, the production of recycled materials for aggregates use accounted for 6% of the total production of aggregates used in civil works and building activity in Europe. The use of recycled materials from C&DW is encouraged especially in areas where there is a lack of natural resources [4]. Figure 1-2 shows that France uses a very little percentage of recycled aggregates from C&DW in comparison to Germany, UK, and Netherlands. The consumption of aggregates in France is about 379 million tons, while the production of recycled aggregates is about 15 million tons in 2009 [5]. France therefore has a very large potential for reusing recycled aggregates.

China

In China, the generation of C&DW comes from two different sources, one is the normal demolition of constructions, and the other is the abnormal demolition like earthquakes and other natural disasters. For example, Wenchuan Earthquake which happened in 2008 in

Sichuan Province (China) killed 90000 persons and caused approximately 380 million tons of C&DW [6].

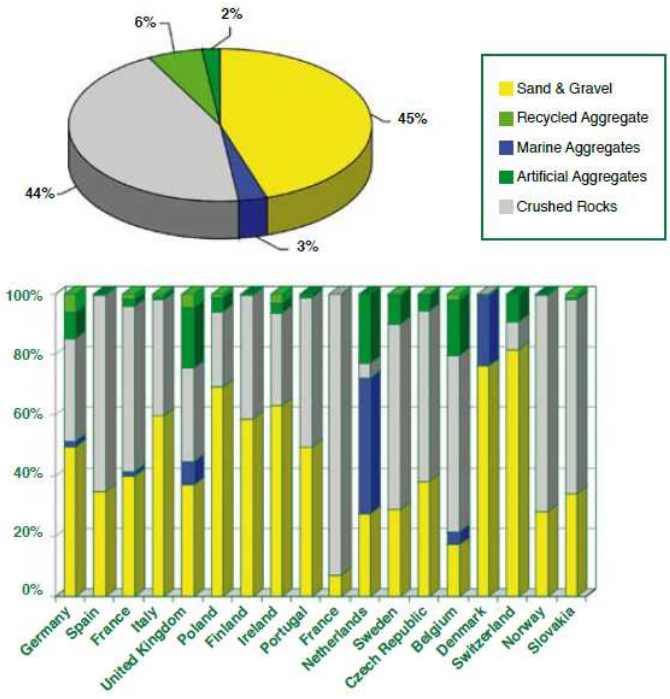

Figure 1-2 Aggregates (including Recycled Aggregates) production in EU 2005 [4]

According to Shi and Xu [7], the quantity of C&DW reached 239 million tons in 2010 in China. Due to rapidly developing construction, about 820 million tons of cement and 8 billion tons of aggregates are consumed yearly to satisfy this large demand [8]. Therefore, natural aggregates could be used out in the future. The reuse and recycling in China is less developed than in EU, and most of the C&DW is dumped in landfills [9]. But fortunately government and society are paying more attention to reuse and recycling of C&DW. In 2003, the "Law of the People's Republic of China on Promotion of Cleaner Production" has been established in order to develop circular economy, and promote companies to make good use of resources and wastes.

From the statistics of EPD (Environmental Protection Department) of Hongkong, 20 million tons of C&DW are generated every year which represents 38% of the solid wastes in Hongkong [10-12].

1.2.2 Recycling process

The production of RCA from the crushing of C&DW uses a similar industrial process than that used for the production of natural aggregates. Various types of crushers, screens, transfer equipment and devices for the removal of foreign matter as magnetic tools to separate metals are employed. C&DW are crushed to produce granular materials of small particle size. Figure 1-3 shows the process of producing RCA [13]. One of the limiting factors in reuse and recycling of the C&DW is their complex composition which may include concrete, bitumen, mortar, gypsum, glass, soil, metals and others [14-16]. The main constituent of C&DW is waste concrete as shown in Figure 1-4. Indeed, the amount of concrete in C&DW varies from 32% to 75% [17-20].

Crushing is the most important step in converting C&DW into usable products. In some operations, one step crushing (a primary crusher) is used. Sometimes two or three steps, with several crushers are used to produce high quality aggregates [21-22]. Crushers such as jaw crushers, impact crushers, and cone crushers are used to crush C&DW. According to Ogawa and Nawa [23], jaw crushers can provide good grain-size distributions of recycled aggregates for concrete production. Tam et al. [24] showed that good quality RCA could be manufactured and used in applications if waste concrete was first crushed with a primary jaw crusher, then followed by passing the material through a magnetic separator and the hammer crusher. Cone crusher is suitable as a secondary crusher with small feed size. Impact crushers can provide good grain-size for applications in road construction [13].

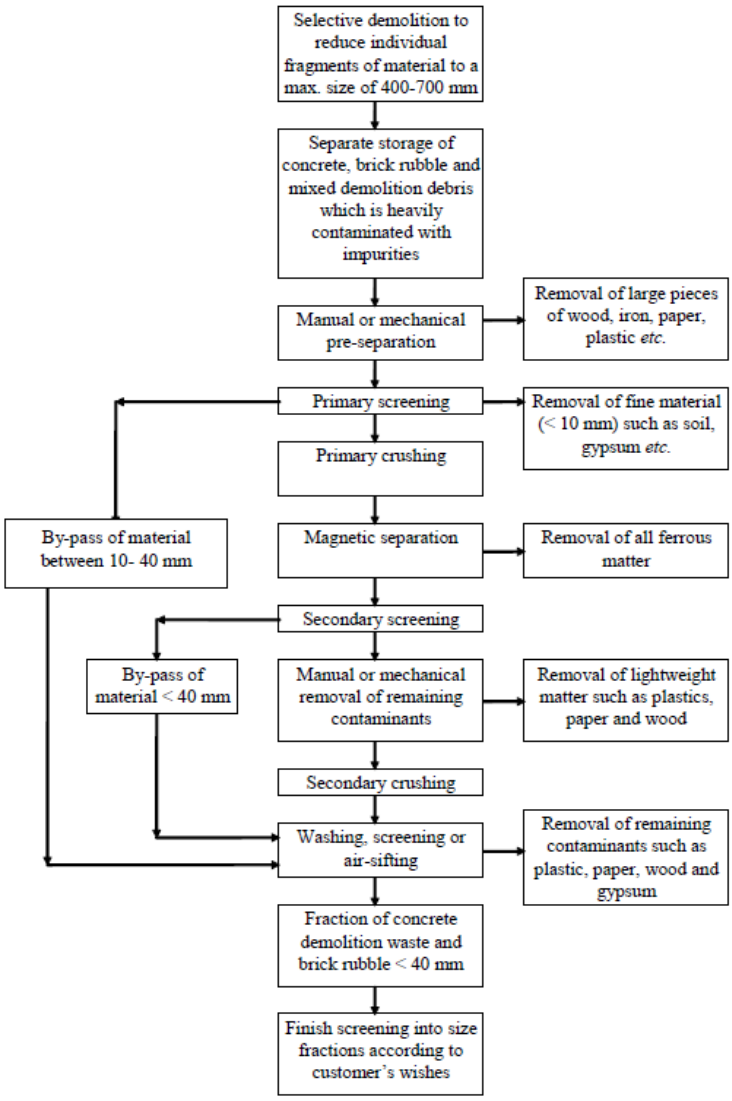

Figure 1-3 Processing of C&DW [13]

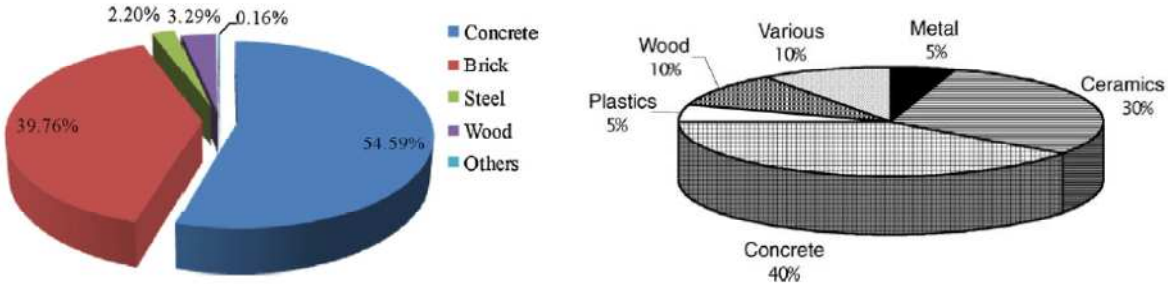

Figure 1-4 Compositions of C&DW from Xiao [18] (left) and Nik.D. [25] (right)

1.2.3 Application and problem

As the quantities of C&DW are becoming larger and larger, recycling C&DW becomes more important for the society and for the environment. Up to now, most of recycled C&DW has been used as a base and sub-base material or as a capping layer in road construction, while only a small proportion is re-used as RCA in the manufacture of new concrete [26-28]. The use of RCA as road base and sub-base material is comparable to the natural sub-materials in practical construction for road engineering [29-31]. However, when used in concrete RCA might not have the same quality and performances as natural aggregates, but the cost of dumping C&DW can be saved. Moreover, it can decrease the use of natural aggregates, and protect the environment and natural resources [32]. However, lack of appropriate technology and proper standards are serious barriers in promoting widespread use of recycled aggregate from recycled C&DW in concrete [33].

1.3 Properties of RCA

Generally, two typical grades of recycled concrete aggregates can be classified by size gradation: Coarse Recycled Concrete Aggregates (CRCA), which are larger than 5mm, and Fine Recycled Concrete Aggregates (FRCA) whose sizes are smaller than 5mm. RCA are mainly composed of an intimate mix between natural aggregates and cement paste (Figure 1-5). Adherent cement paste generally presents a much larger porosity than natural aggregates, the content and the physicochemical properties of adherent cement paste therefore have a large influence on the properties of RCA, such as density, porosity, and water absorption.

Figure 1-5 Composition of recycled concrete aggregates (RCA)

1.3.1 Adherent mortar and cement paste content

When concrete is crushed, some cement paste remains attached around the original aggregates. Adherent cement paste is much more porous than natural aggregates generally used for the manufacture of concrete. Therefore, quality and quantity of adherent cement paste are at the origin of the poorer properties of RCA that are comparatively to natural aggregates: lower density, higher water absorption, higher Los Angeles abrasion and higher sulphate content. The determination of adherent cement paste content is however difficult to carry out experimentally, and several experimental methods have been developed in order to measure adherent mortar content, which is easier to quantify. Therefore, in the following we study both adherent cement paste and adherent mortar in RCA.

Methods for the determination of adherent cement paste and mortar content

Thermal treatment [34] : this method is based on several cycles of soaking in water and heating of the aggregates (500°C), which allows detaching progressively adherent mortar from coarse aggregates surface because of micro cracks occurring at the interface between aggregates and mortar. After several steps, some mortar remains attached and a rubber hammer is used to scratch the surface. The sample is screened to obtain the coarse aggregate for which all the mortar has been removed. Mortar content is calculated by the mass loss between the original recycled aggregates and the obtained coarsed aggregates. This method is only suitable for measuring the adherent mortar content in CRCA.

Treatment with a solution of hydrochloric acid: this method is based on the dissolution of cement paste in a solution of hydrochloric acid [35]. The adherent cement paste is determined from the weight loss due to dissolution in a dilute solution of hydrochloric acid. Unfortunately, the treatment with hydrochloric acid cannot be used with limestone aggregates, which are also dissolved by this acid.

Sodium sulphate solution treatment [36]: this method is based on a few daily cycles of freezing and thawing in a sodium sulphate solution. Representative samples of RCA are obtained, then dried for 24h at 105°C. The samples are immersed for 24h in a 26% (by weight) sodium sulphate solution. After five daily cycles of freezing and thawing, the samples are washed with tap water, then they are placed in an oven for 24h at 105°C. Mortar content is calculated by the mass loss between the original recycled aggregates and the obtained aggregates after treatment. This method is only suitable for measuring adherent mortar content in CRCA.

Image analysis [36]: image analysis is used to quantify the amount of residual mortar on flat polished concrete section with CRCA particle in a white cement paste. Image analysis is not

suitable for the quantification of adherent cement paste content of FRCA. Indeed, the distinction between fine aggregates and cement paste is more difficult to carry out. Moreover, this method is long to perform as a statistical approach is needed.

Linear traverse method [37]: a representative sample of RCA is mixed with a red-colored cement and cast into cubes. After hardening, the cubes are cut into slices and polished. The volume percentage of old mortar content is determined on a representative number of samples by means of a linear traverse method, similar in principle to the method which is described in ASTM C457-71, "Standard Recommended Practice for Microscopical Determination of Air-Void Content and Parameters of the Air-Void System in Hardened Concrete".

Influence factors on the determination of adherent cement paste and mortar content

Adherent mortar content results are very different when using different test methods. De Juan et al. [34] pointed out that adherent mortar content are (25-70%) for treatment with hydrochloric acid solution, (25-65%) for the production of a new concrete followed by image analysis, and (40-55%) for thermal treatment. Abbas et al. [36] reported that the adherent mortar content of two industrial CRCA (RCA1 was obtained from a demolition concrete in which the original aggregate was limestone, RCA2 was made with river-bed gravel) were 39-43%, and 21%-26% respectively by using image analysis. They found similar results by sodium solution method, adherent mortar contents were 39-44%, and 20-30% respectively.

Lots of authors pointed out that the size of granular class of RCA had an important influence on adherent mortar content. They showed that the adherent mortar content was lower for larger size CRCA [21, 34-38] (Table 1-1). But, Yagishita et al. [39] reported that mortar content increased as the grain sizes increased, which is contradictory to other studies.

Table 1-1 Summary of adherent mortar or cement paste content from literature

Author, Year (Reference no.)	Test methods	Fractions of RCA (mm)	Adherent mortar or cement paste content (%)
Etxeberria et al. [21]	Not metioned	CRCA 4/10, 10/25	40% for fraction 4/10; 20% for fraction 10/25
De Juan et al. [34]	Thermal method	15 samples of CRCA 4/8, 8/16	33-55% for fraction 4/8; 23-44% for fraction 8/16
Nagataki et al. [35]	hydrochloric acid solution method	CRCA 5/20	52.3-55% for level 1; 30.2-32.4% for level 3
Yagishita et al. [39]	hydrochloric acid solution method	CRCA 5/10, 10/20	40.2% for low-grade fraction 10/20, 35.2 for low-grade fraction 5/10; 26% for medium -grade fraction 10/20, 16.7 for low-grade fraction 5/10
Abbas et al. [36]	Image analysis mehtod and sodium sulphate solution method	Two CRCA 4.75/9.5, 9.5/12.7,12.7/19	RCA2 results. Image analysis:30%,21%,21% for 4.75/9.5, 9.5/12.7, 12.7/19 respectively; Sodium sulphate solution method: 26%,22%,21% for 4.75/9.5, 9.5/12.7, 12.7/19 respectively
Hansen and Narud [37]	Linear traverse method	CRCA 4/8, 8/16, 16/32	58-64% for fraction 4/8; 38-39% for fraction 8/16; 25-35% for fraction 16/32
Topçu et al. [38]	Linear traverse method	CRCA 4/8, 16/32	60% for fraction 4/8; 30% for fraction 16/32

Some authors reported that the mortar content is influenced by the crushing method. Increasing crushing times allows to reduce the mortar content of RCA [35, 39]. Nagataki et al. [35] determined the adherent mortar content of CRCA by hydrochloric acid dissolution method. As can be seen in Table 1-2, using only jaw and impact crushers (level 1), the adherent mortar content of the CRCA (fraction 5/20mm) made from high, medium, and low quality concrete were 52.3%, 55.0% ,52.3% respectively. Using several grinding equipments after first crushing (level 3), the adherent mortar content were reduced to 30.2%, 32.4%, 32.3%. In this study, the w/c ratio of original concrete had little influence on the adherent mortar content in RCA. Several crushing can therefore decrease the adherent mortar content of CRCA, meanwhile it increases the quantity of FRCA.

Table 1-2 Properties of recycled coarse aggregates [35]

Quality of source concrete	Process level	Adhered mortar content (%)	Density SSD (g/cm^3)	Water absorption (%)	Soundness loss (%)	100 KN crushing value (%)
High (W/C=0.35)	1	52.3	2.42	4.88	29.7	3.83
	3	30.2	2.51	3.14	8.10	1.53
Medium(W/C=0.45)	1	55.0	2.41	5.58	48.3	5.19
	3	32.4	2.50	3.19	18.4	1.73
Low (W/C=0.63)	1	52.3	2.37	6.27	49.1	6.30
	3	32.3	2.48	3.76	22.5	2.28

Globally, the quantity of adherent mortar increases with the decrease in size of RCA, as can be seen in Figure 1-6. In the literature, lots of studies present results on the quantification of adherent mortar content in CRCA. However, there is a larger dispersion of data.

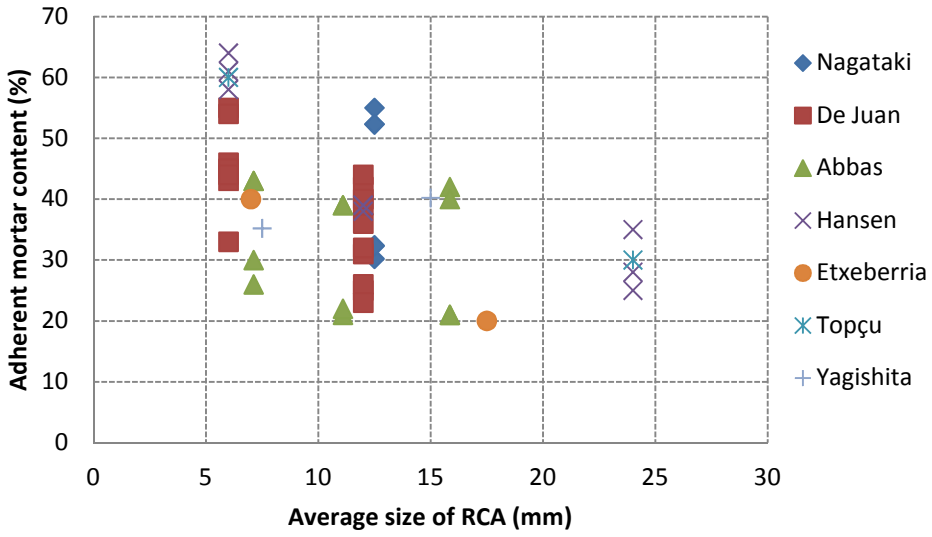

Figure 1-6 Adehrent mortar content as a function of average size of RCA

1.3.2 Water absorption and density

Water absorption and density are very important engineering properties of RCA when used in concrete. Generally, RCA have a higher water absorption and a lower density than natural aggregates which are caused by porous adherent cement paste attached on the surface of aggregates.

The determination of water absorption is therefore of great importance for the characterization of RCA. Up to now, there is no particular standard for the measurement of water absorption coefficient of RCA. Therefore, standards used for natural aggregates such as EN 1097-6 [40], ASTM C127 (for coarse aggregate) [41], ASTM C128 (for fine aggregate)[42] are also used for the characterization of RCA. The principle of these methods is similar, the water absorption coefficients of sand and gravel are determined based on the water content at saturated surface dry (SSD) state. The SSD state of sand dried progressively under warm air is identified using a slump test. The SSD state of gravel is identified by drying aggregates with dry cloths until no water is visible at the surafce of particles.

Tam et al. [43] indicated that the soaking of recycled aggregates in water may detach some attached cement paste and the drying at 105°C to obtain the oven-dried mass may remove some water contained in the hydrates of the attached cement paste. In order to avoid these problems, they proposed a new method named real-time assessment of water absorption (RAWA) for RCA. In RAWA, the oven-dried mass is obtained by placing them in an oven at 75±5°C. Then the aggregates are placed into a pyknometer fully filled with distilled water. The water absorbed is noted at different time intervals. One natural aggregate and three recycled aggregates from different recycling plants and demolition sites (from 5 to 40mm) were tested by the proposed method. They showed that the standard duration of 24h of saturation was not suitable for recycled aggregate, but water absorption rate was larger in the first 5h which produced up to 80% of the total water absorption. The results of the standard 24h measurement were 5.72% and 8.28% compared with the values of 5.92% and 8.72% for two recycled aggregates (96h and 120h measurement), respectively. The difference is quite small.

Djerbi Tegguer [44] studied the kinetics of water absorption of natural and recycled aggregates by a new method (LCPC) based on hydrostatic weighing, consisting in measuring

the mass variations of a sample immersed in water. The aggregates sample was first dried in the oven at a temperature of 110±5°C until a difference in mass less than 0.1%, then they were immersed in water to obtain the mass of absorbed water with time. Two types of natural aggregates with fractions 4-12.5mm and 12.5-20mm (limestone aggregates and limestone-siliceous aggregates), together with RCA crushed from unknown waste concrete (fractions 5-12mm and 12-20mm), were tested by the proposed method. They found that the water absorption standard values were slightly higher than hydrostatic weighing approach, and the water absorption coefficient of RCA for 24h of soaking produced about 60% and 70% of the total water absorption for fraction 12.5-20mm and fraction 5-12.5mm respectively.

Mechling et al. [45] presented a simple method by recording the evaporation rate of the sample in a moderate temperature regulated drying oven (40±5°C). The change in the rate of evaporation that appeared between the external and internal water in the aggregate permitted to determine the critical water content, corresponding to the desired absorption. They studied the water absorption of different sands by this evaporometry method, especially the fine fraction of porous materials (mineral admixtures), and found the values of water absorption were between1.2-3.7% for natural sand (calcareous sand and siliceous sand), 4.2-7.4% for additional fillers, and 14.6-31.1% for the fine recycled materials.

Density of RCA is related to the adherent cement paste content. De Juan et al. [34] studied the relationship between mortar content and density, and found that the density of RCA decreased as the amount of attached mortar increased. They found that the water absorption varied from 5.1 to 11.5% for fraction 4-8mm, and from 4.2 to 8.8% for fraction 8-16mm. They also pointed out that the water absorption increased as the amount of attached mortar increased.

Poon et al. [46] studied the effect of microstructure of ITZ on compressive strength of concrete prepared with RCA. They found that the typical crushed granite aggregates had a

density of approximately 2600-2650 kg/m^3 and a water absorption capacity of approximately 1%, while RCA density varied from 2200 to 2400 kg/m^3 and water absorption capacity varied from 5 to 15%, which was due to the difference in properties of the initial mortar. The water absorption of RCA crushed from normal-strength concrete was 8.82%, while that of RCA crushed from high-performance concrete was 6.77%, and the water absorption of natural crushed granite was only 1.25%.

José [47] compared properties of RCA with natural aggregate (Table 1-3). The total porosity showed large differences between RCA and natural aggregate, which reached 2.82% for natural aggregate and 14.86% for the 5/10mm gravel fraction of RCA. Water absorption of the 5/10mm gravel fraction of RCA was 6.81% while for natural aggregate it was only 1.13%.

Table 1-3 Properties of recycled aggregate and NA [47]

Property	RCA			Natural aggregate		
	10/20mm	5/10mm	0/5mm	12/20mm	5/12mm	0/5mm
Dry specific gravity(kg/m^3)	2280	2260	2170	2570	2640	2570
Specific gravity (surface dry) (kg/m^3)	2410	2420	2350	2590	2670	2600
Water absorption (100%)	5.83	6.81	8.16	0.88	1.13	1.49
Total porosity (%)	13.42	14.86	-	2.70	2.82	-

Martin-Morales et al. [48] studied the characteristics of recycled aggregates which were produced in a recycling plant. Four different fractions were studied: the sample 001 was the unselected fraction which was crushed simply before the vibrating screen process (fraction 0/50mm); the samples 002, 003 and 004 were the 10/50, 6/10 and 0/6 mm recycled aggregates produced in plant respectively. Water absorption values of RCA varied from one fraction to another (Table 1-4). They observed that higher water absorption values were related to the larger particle size of samples. Given by the authors, a possible reason for this could be the higher absorption rate of cement mortar attached to aggregate particles in the case of the fraction with larger particles, and thus, with a higher water absorption capacity. As particle size decreased, the amount of cement particles adhering to them was lower, and consequently,

the water absorption capacity also decreased. These conclusions are contradictory with others studies [34, 46, 49]. Indeed several studies show that as the size of RCA decreases, their density decreases and water absorption increases.

Table 1-4 Properties of recycled aggregates [48]

Properties	Fraction			
	Sample001 (0/50mm)	Sample002 (10/50mm)	Sample003 (6/10mm)	Sample 004 (0/6mm)
Dry density(kg/m^3)	2230	2140	2150	2500
Water absorption (%)	10.64	10.74	8.43	3.74

1.3.3 Other factors affecting the properties of RCA

The properties of RCA depend on lots of factors as follows:

Contaminants

One of the problems in the use of recycled aggregates for the manufacture of new concrete is the presence of contaminants in the RCA [50]. Khalaf and De Venny [51] studied the recycling of demolished masonry rubble as coarse aggregate in new concrete. They showed that bitumen, mortar, gypsum, organic matter, chlorides and sulfates, glass could be found in the recycled aggregates, decreasing their properties. Lamond et al. [52] summarized strength loss based on inclusion of contaminants in RCA. They showed that volume percentage of impurities (7% for lime plaster, 5% for soil, 4% for wood, 3% for gypsum, 2% for asphalt) can result in 15% or greater reduction of compressive strength as compared to reference concrete. Debieb et al. [53] showed the effect of contaminated crushed concrete aggregate on the mechanical properties and durability properties of RAC. They found significant difference in these properties when using contaminated RCA and uncontaminated RCA. Concrete containing contaminated RCA were more sensitive to chlorides than sulphates. Therefore, precautions and specific measurement need to be taken, especially with aggregates from hazardous origin such as concrete under marine environment.

Properties of original concrete

Hansen and Narud [37] studied the compressive strength of recycled concrete made from CRCA crushed from original concretes with three different w/c ratios (0.4,0.7,1.2). Three grades of CRCA (noted as Recycle H, Recycle M and Recycle L) were prepared by the crushing of original high-strength, medium-strength, and low-strength concrete in jaw crushing which was set at an opening of 25mm with the jaws in a closed position. They found that the properties of RCA was influenced by the w/c ratios and paste volume of the original concrete (Table 1-5). The compressive strength of RAC can be as good as or better than the original concrete when the w/c ratio of the original concrete is the same or lower than that of new concrete.

Table 1-5 Properties of natural gravel and recycled coarse aggregates[37], B.S. crushing value is determined according to british standard BS 812:110 [54]

Type of aggregate	Size fraction (mm)	Specific gravity (g/cm^3)	Water absorption (%)	Los Angeles abrasion (%)	B.S. crushing value (%)	Volume of attached mortar (%)
Natural gravel	4-8	2.50	3.7	25.9	21.8	0
	8-16	2.62	1.8	22.7	18.5	0
	16-32	2.61	0.8	18.8	14.5	0
Recycled (H)	4-8	2.34	8.5	30.1	25.6	58
	8-16	2.45	5.0	26.7	23.6	38
	16-32	2.49	3.8	22.4	20.4	35
Recycled (M)	4-8	2.35	8.7	32.6	27.3	64
	8-16	2.44	5.4	29.2	25.6	39
	16-32	2.48	4.0	25.4	23.2	28
Recycled (L)	4-8	2.32	8.7	41.4	28.2	61
	8-16	2.42	5.7	37.0	29.6	39
	16-32	2.49	3.7	31.5	27.4	25

Poon et al. [46] studied the influence of recycled aggregates on the microstructure of RAC. They used two types of RCA, one was from normal-strength concrete, and the other was from high-performance concrete that had been prepared with silica fume as a partial cement substitute. The physical properties of natural and recycled aggregates are presented in Table 1-6. The recycled aggregates were more porous, less dense and weaker than the crushed

granite, and the water absorption of RCA was much higher than that of crushed granite. The water absorption capacity of the RCA derived from normal-strength concrete (NC) was larger than that of high-performance concrete (HPC). But the compressive strength and constituents of NC and HPC are not presented in details. The mercury intrusion porosities of the coarse aggregates (natural aggregate, recycled NC and recycled HPC) were 1.60%, 16.81%, and 7.86%, respectively. The higher porosities of recycled aggregates can be attributed to the adherent cement paste. The pores in the NC aggregate were mainly distributed between 0.01 and 1μm whereas the majority of pores in the HPC aggregate were lower than 0.1μm. For the authors, the finer pore size distribution of the recycled HPC was due to the use of pozzolanic admixtures, but the lower w/c ratio certainly also plays very important role which is not mentioned here.

Table 1-6 Physical properties of natural and recycled coarse aggregates[46], ten percent fines crushing value is determined according to BS 812:110 [54]

Type of coarse aggregate	Ten percent fines crushing value(kN)	Apparent density (g/cm^3)	Water absorption(%)	
			10mm	20mm
Crushed granite	159.7	2.620	1.25	1.24
Recycled NC	101.9	2.409	8.82	7.89
Recycled HPC	123.8	2.390	6.77	6.53

Padmini et al. [55] studied the influence of parent concrete on the properties of RCA. The properties of granite and recycled concrete aggregate are shown in Table 1-7. Three maximum sizes of crushed granite aggregates and three w/c ratios (0.58, 0.43 and 0.34) were manufactured as parent concrete. They found that the water absorption of RCA increased with an increase in strength of parent concrete (the volume of paste certainly also plays very important role which is not mentioned in this study), while it decreased with an increase in maximum size of aggregate. The specific gravity of RCA reduced marginally with an increase in strength of parent concrete, and the quantity of adherent mortar was relatively lower for the RCA produced from lower strength parent concrete. They also showed that for a given

compressive strength, the split tensile strength, flexural strength and modulus of elasticity were lower for RAC than parent concrete.

Table 1-7 Properties of fresh granite and recycled concrete aggregate [55], NA means the crushed natural granite aggregates

Property	NA of maximum size (mm)			RCA of maximum size								
	10	20	40	10mm			20mm			40mm		
Maximum size of NA in parent concrete (mm)	-	-	-	10	10	10	20	20	20	40	40	40
Compressive strength of parent concrete (MPa)	-	-	-	35	49	56	37	50	58	31	45	52
Specific gravity g/cm^3	2.8	2.8	2.8	2.46	2.4	2.38	2.52	2.51	2.48	2.56	2.53	2.52
Water absorption (%)	0.3	0.3	0.3	4.60	4.8	5.0	3.65	4.1	4.86	2.2	2.5	2.8
Abrasion value (%)	29	26	26	48	46	46	38	35	33	30	29	29

Tam et al. [56] studied the relationship between properties of demolished concrete, recycled aggregates and RAC using regression analysis. Ten samples from ten demolition sites were used to investigate their characteristics and properties. They showed that there were correlations between characteristics of demolished concretes samples, RCA and RAC. The properties of RCA (particle size distribution, density, porosity and water absorption) were correlated with the properties of demolished concrete (density, absorption, porosity, carbonation depth).

Limbrchiya et al. [57] studied the chemical and mineralogical characteristics of CRCA and their influence on concrete performances. They concluded that for CRCA samples obtained by crushing C&D debris from different sites, there was no significant variation in quality, indicating no significant effect if adequate quality control criteria during RCA production was adopted.

We can conclude that some authors point out that the properties of RCA depend on that of the original concrete, whereas some authors conclude that there is no or little effect of the original concrete.

Crushing method

Yagishita et al. [39] studied the behaviour of reinforced concrete beams containing CRCA. They showed that the coefficient of water absorption of the high-grade recycled coarse aggregate (after three time crushing) used for the experiments was 1.03 times larger than that of natural coarse aggregate on the average, while the coefficient of the low-grade recycled coarse aggregate (one time crushing) was 3.44 times larger. Therefore, the quality of CRCA was improved by number of successive crushing.

Tomas et al. [58-59] studied the influence parameters of impact crushers (crushing time, impact velocity and energy). With good control of parameters of impact crushers, good quality of RCA can be obtained.

Molin et al. [60] studied some relevant factors influencing the quality of reused crushed concrete. They tested two main crushing techniques (jaw crusher and rotation crusher) with respectively 45 and 100mm opening. They concluded that jaw crusher was somewhat better than rotation crusher and the big opening was slightly better than the small one. The jaw crusher imposed more micro-cracks than percussion from the rotation crusher, and so it removes more mortar from the aggregates. However, it has to be noted that removing more mortar from CRCA improves their quality but leads in the same time to the production of larger quantity of FRCA.

Weathering (carbonation)

Weathering influence includes two parts, one part is the weathering influence on the properties of original concrete, and the other part is the weathering influence (storage conditions, temperature, and relative humidity) on properties of RCA after crushing the demolished concrete. For the first part, the environment exposure conditions (temperature, relative humidity) are the major factors influencing the carbonation of original concretes.

Carbonation is a procedure where carbon dioxide (CO_2) in the atmosphere penetrates and diffuses through the pore water and reacts with calcium hydroxide ($Ca(OH)_2$), producing calcium carbonate ($CaCO_3$) and water (Equation 1-1).

$$Ca(OH)_2 + H_2CO_3 \rightarrow CaCO_3 + H_2O \qquad \text{Equation 1-1}$$

In addition, hydrated calcium silicate (C-S-H) can also react with CO_2 [61-63]. The depth of carbonation can be determined by spraying phenolphthalein indicator, which is a colorless indicator, that turns purple when the pH is above 9 [64]. The carbonation depth increases with the concentration of CO_2, age, w/c ratio, and porosity of concrete. Any factors which increase the concrete permeability can also increase the carbonation rate. For example, the carbonation depth with w/c=0.4 was 50% lower than that of 0.6 [65]. A typical carbonation depth with w/c=0.5 was between 5 and 10 mm after normal exposure for 10 years [56].

Roy et al. [66] studied the accelerated carbonation and weathering of concrete in the laboratory. Five different grades of concrete with w/c ratios of 0.8, 0.7, 0.65, 0.6, and 0.55 were selected to study the effect of humidity levels on the depth of carbonation. They found as the humidity level increased from 52 to 75% there was a significant increase in the carbonation depth. There was a decrease in carbonation depth as the relative humidity increased from 75 to 84% and the carbonation depth increased once again as the relative humidity was finally increased to 92%. Fernandez Bertos et al. [62] pointed out that the carbonation rate is faster at a relative humidity of 50-70% and decreases at higher and lower relative humilities, which was explained by the fact that diffusion of CO_2 and reaction kinetics are two conflicting processes.

Thiery et al. [67] investigated the chemical kinetics of carbonation on ordinary Portland cement paste and concretes. The carbonation depth was determined by TGA and by gammadensitometry after the accelerated carbonation tests. Gammadensitometry is a non-

destructive method able to measure the total penetrated CO_2 and to monitor the carbonation process during the accelerated tests [68]. The results indicated that CO_2 is chemically bounded as $CaCO_3$, which precipitates in various forms, namely: stable (Calcite, decomposes from 780 to 990ºC), metastable (vaterite and aragonite, decomposes from 680 to 780ºC), and amorphous (decomposes from 550 to 680ºC). The unstable form (amorphous) of $CaCO_3$ was preferentially associated with C-S-H carbonation. It seems that the higher the level of carbonation leads to more C-S-H carbonation leading to greater quantity of unstable $CaCO_3$. Some authors [69-70] also pointed out the different crystallized forms of $CaCO_3$ (calcite, aragonite and vaterite) formed during the carbonation.

Ngala and Page [71] investigated the effect of carbonation on pore structure and diffusional properties of hydrated cement pastes. The pore size distribution, total porosity and coarse capillary porosity of non-carbonated and fully carbonated specimens of OPC, OPC/30% fly ash and OPC/65% slag pastes were determined. The results showed that the total porosity for all the studied pastes reduced after the carbonation (it is due to the deposition of $CaCO_3$ formed, which volume exceeds that of original hydrates, and thus causing a reduction of porosity). Also the authors observed a redistribution of pore sizes, the proportion of large pores (diameter > 30nm) increased slightly for OPC pastes (it is due to the formation of additional silica gel by the decomposition of C-S-H gel), but much more significantly for the fly ash and slag pastes.

Johannesson and Utgenannt [72] investigated the microstructure changes (specific surface area and pore size distribution) of an OPC cement mortar. Specific surface area determined by the BET equation (simplest one layer expression) for well-carbonated and noncarbonated cement paste was 29.4 and 31.8 m^2/g, respectively. The well-carbonated cement mortar had a larger volume of pores in the pore size range of 2-7nm than the noncarbonated mortar.

Arandigoyen et al. [73] studied the variations of microstructure with carbonation of paste of lime blended with cement. The porosity, pore size distribution, and specific surface area were investigated with both carbonated and non-carbonated pastes. The results showed that carbonation decreased around 10% the porosity, but not with the same intensity in all pore size ranges. The specific surface area decreased in lime pastes as a consequence of the decrease of the small porosity (<0.03µm), but increased when there was cement in the paste, which would due to the deterioration of C-S-H (opening of gel pores) and appearance of microcracking. Lawrence et al. [74] studied the effect of carbonation on the pore structure of non-hydraulic lime mortars. They showed that there was an increase in pore volume in the 0-0.1µm pore diameter range across all mortar types which were due to the transformation of portlandite to calcite. There was also a monotonic increase in the volume of pores with diameter below 0.3µm.

Improving methods

It is very important to improve the properties of RCA in order to make good application of RCA in new concrete. Because of the large varieties of contaminants in the RCA, separation techniques are proposed and discussed by some authors. Hendriks and Xing [75] showed that the possible separation techniques were size separation (classification of materials by size), density separation (separation of particles by different densities), and magnetic separation (removal of ferrous metals). Ulsen et al. [22] studied the separation techniques of recycling sand from C&DW. They processed by tertiary impact crushing, together with sieving and density and magnetic separations. Density separation was realised by heavy liquid media elutriation and magnetic separation on the Frantz barrier field separator. They found that both density and magnetic separation were effective for the reduction of residual cement paste content.

Ogawa and Nawa [23] studied the quality of recycled fine aggregate by selective removal of brittle defects. Fourteen FRCA were manufactured by three types of processes including a jaw crushing, ball mill, and granulator. They showed that jaw crusher slightly changed the defects in FRCA, ball mill made the grains more round and surface more regular, and the granulator made more round but retained the original irregular shape.

Tsujino et al. [76] studied the application of low-quality recycled coarse aggregate to concrete by surface modification treatment. They used two types of surface agent, oil-type and silane-type to improve the properties of RCA. The results showed that the silane-type surface agent reduced greatly the strength of concrete. The water absorption of low quality RCA was 1% after treatment for a silane-type agent comparing to no treatment 5.5%, 3.5% after treatment for oil-type agent.

Grabiec et al. [77] studied the modification of RCA by calcium carbonate biodeposition with bacteria. They showed that this method can reduce the water absorption of RCA, and the effect was visible in case of finer RCA from the inferior-quality old concrete. The water absorption with biodeposition was 4.1-4.7 % comparing to 5.2-5.5 % without biodeposition.

Tam et al. [78] investigated the practices of RCA in constructions and studied three pre-soaking treatment approach in order to reduce the mortar attached to RCA. Three acidic solvents named hydrochloric acid (HCl), sulfuric acid (H_2SO_4) and phosphoric acid (H_3PO_4) with a concentration of 0.1mol/l were used in the study. After the authors, a concentration 0.1 mol/l of the acidic solution can provide a suitable acidic environment for the aggregate to remove the old cement mortar and will not lower the quality of aggregate. The results showed that the treatment applied can effectively improve the aggregate quality: water absorption rates after the pre-treatments have been significantly reduced (reduction between 7.3% and 12.2% in comparison to the untreated RCA). However, it has to be noted that the RCA used in this study had water absorption relatively low in comparison to classical RCA. Perhaps with

lower quality RCA the results could be better? The pre-treatments could effectively remove old cement mortar from RCA, which helps improving the weak bound between RCA and new cement mortar. Although the chloride and sulphate contents increased after the pre-treatments, they were still within the limits of 0.05% and 1%.

Ahn et al. [79] studied the recovery of aggregates from concrete by heating and grinding method. They heated the waste concrete at 400-500°C and ground by ball mill, and obtained good quality RCA with specific gravity above 2.5 g/cm^3, and water absorption below 3.0%.

Nakagawa et al. [80] developed a new recycling process of fine aggregate from waste concrete particle using high-pressure carbon dioxide solution. The recycling process is composed of three types of treatment: high-pressure CO_2 aqueous solution, grinding with a ball mill, and classification. They found that single ball mill crushing can reduce water absorption to 5.3% after 60mins treatment. Combined treatment with ball mill 30mins and 6h treatment with CO_2 can reduce water absorption from 15% to 3.2%.

1.4 Standards for RCA

In order to make good use of RCA in concrete, standards for recycled concrete and classification of RCA have to be followed. Several requirement considering RCA can be found such as pr EN 933-11(European Union) [81], BS8500-2(England) [82], JIS(Japan), DG/TJ08-2018-2007 (China).

RILEM specifications

RILEM [83] classified the CRCA into three types which are shown in Table 1-8. These recommendations suggest maximum allowable values for impurities in RCA. Here type I aggregates means that aggregates originate from masonry rubble, type II signifies that aggregates originate from concrete rubble; type III aggregates means a blend of recycled

aggregate and natural aggregates. The composition of type III aggregates shall meet the following additional requirements: the minimum content of natural aggregates is at least 80% (m/m), the maximum content of type I aggregate is 10% (m/m). CRCA can be used in plain and reinforced concrete under the provision mentioned in Table 1-9 .

Table 1-8 Classification of recycled coarse aggregates for concrete (RCAC) [83]

Mandatory requirements	RCAC type I	RCAC type II	RCAC type III	Test method
Min. dry particle density (kg/m^3)	1500	2000	2400	ISO 6783& 7033
Max. water absorption (% m/m)	20	10	3	ISO 6783& 7033
Max. content of material with SSD <2200 kg/m^3 (% m/m)	-	10	10	ASTM C123
Max. content of material with SSD <1800 kg/m^3 (% m/m)[a]	10	1	1	ASTM C123
Max. content of material with SSD <1000 kg/m^3 (% m/m)	1	0.5	0.5	ASTM C123
Max. content of foreign material (metal, glass, soft material, bitumen) <1000 kg/m^3 (% m/m)	5	1	1	Visual
Max. content of metal (% m/m)	1	1	1	Visual
Max. content of organic material (% m/m)	1	0.5	0.5	NEN 5933
Max. content of filler (< 0.063mm) (% m/m)	3	2	2	prEN 933-1
Max. content of sand (< 4mm) (% m/m)[b]	5	5	5	prEN 933-1
Max. content of sulfate (% m/m)[c]	1	1	1	BS 812, part 118

[a] Water saturated surface dry condition (SSD).
[b] If the maximal allowable content of sand is exceeded, this part of the aggregates shall be considered together with the total sand fraction.
[c] Water soluble sulfate content calculated as SO_3.

Table 1-9 Provisions for the use of recycled concrete [83]

Recycled aggregates	RCAC type I	RCAC type II	RCAC type III
Max. allowable strength class	C16/20[a]	C50/60	No limit
Additional testing required when used in exposure class 1[b]	None	None	None
Additional testing required when used in exposure class 2a,4a	ASR expansion test [c] Use in class 4a not allowed	ASR expansion test	ASR expansion test
Additional testing required when used in exposure class 2b,4b	Use in classes 2b,4b not allowed	ASR expansion test Bulk freeze-thaw test	ASR expansion test Bulk freeze-thaw test
Additional testing required when used in exposure class 3	Use in class 3 not allowed	ASR expansion test Bulk freeze-thaw test Deicing salt test	ASR expansion test Bulk freeze-thaw test Deicing salt test

a However, the strength class may be increased to C30/37 subject to the condition that the saturated surface dry (SSD) density of the recycled aggregates exceeds 2000 kg/m^3.
b Conforming with ENV 206.
c Expansion test to evaluate alkali silica reactivity.

For concrete with recycled aggregates used in exposure classes 2, 3 and 4 (Table 1-9), attention should be paid to the durability aspects of reinforced concrete. The use of recycled fine aggregates is limited in this standard due to the larger amounts of contaminants, higher water absorption, larger adherent cement paste content.

JIS (Japanese Industrial Standard)

Japan has a history of more than a quarter century of research on the reuse of recycled aggregates in new concrete, and three classes of recycled aggregates are defined in Japan. JIS A5021 [84] was established for high-quality recycled aggregate H for concrete in 2005. JIS A5022 [85] and JIS A5023 [86] are dedicated to recycled concrete using recycled class M and class L, respectively (Table 1-10). The JIS Technical Report, TR A 0006 "Recycled concrete using recycled aggregate" classified recycled concrete into three classes as "Normal", "Chloride controlled", "Flexible use" [87]. "Normal" recycled concrete should be used for filling concrete and leveling concrete which are no-structural members where high strength and high durability are not required. "Chloride controlled" recycled concrete is used similarly as "Normal" concrete but for members with steel reinforcement. "Flexible use" recycled concrete is used for a wider range of members, sometimes for structural use, under the guidance of an engineer who has expert knowledge of recycled concrete (Table 1-11).

Table 1-10 Specified values of recycled aggregate in JIS [84-86]

Recycled aggregates properties	Class-H		Class-M		Class-L	
	Coarse	Fine	Coarse	Fine	Coarse	Fine
Oven-dry density (g/cm^3)	Not less than 2.5	Not less than 2.5	Not less than 2.3	Not less than 2.3	-	-
Water absorption (%)	Not more than 3.0	Not more than 3.5	Not more than 5.0	Not more than 7.0	Not more than 7.0	Not more than 13.0

Table 1-11 Specifications for recycled concrete[87]

Class	Nominal strength (MPa)	Gmax (mm)	Slump (cm)	Chloride content (kg/m^3)
"Normal"	12	20 or 25	Less than 15	-
"Chloride controlled"	12	20 or 25	Less than 15	Less than 0.6
"Flexible use"	Less than 18	As required	As required	As required

Chinese standard (DG/TJ08-2018-2007)

The first standard for recycled aggregate concrete in China (Technical code on the application of recycled concrete [88]) was issued in 2007 in Shanghai. In this code, only coarse RCA (minimum size of RCA over 5mm) is allowed to use in recycled concrete (Recycled concrete used as block, pavement, and element which strength class is less than RC40, including RC40). In terms of density, water absorption and masonry content, two classes of RCA are defined in Table 1-12.

Table 1-12 Classification of recycled coarse aggregates for concrete in DG/TJ08-2018-2007 [88]

Items	Type I	Type II
Apparent density (kg/m^3)	≥2400	≥2200
Water absorption (%)	≤7	≤10
Masonry content (%)	≤5	≤10
Flakiness index (%)	≤15	
Crushing value (%)	≤30	
Soundness (mass loss %)	≤18	
Impurity content (%)	≤1	

1.5 Properties of recycled aggregate concrete

As discussed in section 1.3, CRCA essentially composed of natural gravel generally possess satisfying properties for the re-use as concrete aggregates. Lots of studies have been dedicated to the properties of concretes containing CRCA or FRCA.

1.5.1 Fresh properties of recycled aggregate concrete

Sagoe-Crentsil et al. [89] studied fresh and hardened properties of RAC made with commercially produced CRCA and natural fine sand. The properties of RCA and basalt aggregates are shown in Table 1-13. The concrete mixture proportions and slump of RAC are shown in Table 1-14. The RAC contained 100% CRCA and fine natural sand while the normal concrete mixture contained only natural coarse and fine aggregates. The RCA were presaturated for 10 min in the mixture. The slump of RAC was 75mm while the slump of normal concrete was 90mm.

Table 1-13 Properties of recycled concrete aggregate and basalt aggregate [89]

Property	Recycled concrete aggregate	Basalt
Aggregate crushing value,% (AS1141.21)	23.1	15.7
Bulk density, kg/m^3 (AS1141.6)	2394	2890
Water absorption,% (AS1141.6)	5.6	1.0

Table 1-14 Mix designation and mixture details of concrete specimens[89]

Mix designation	Cement (kg/m^3)	Water-cement ratio	Coarse aggregate	Wet density (kg/m^3)	Entrapped air content (%)	Slump (mm)
C0912A	242	0.76	basalt	2466	2.4	90
C0912B	240	0.73	recycled	2335	2.4	75

J.M. Khatib [90] investigated the properties of concrete containing FRCA and natural coarse aggregates. Five different mixes were employed to examine the influence of incorporating FRCA as shown in Table 1-15. The free w/c ratio for all mixes was 0.5. The slump values of RC varied from 170 to 190 mm. There was a systematic increase in slump as the content of FRCA in the mix increased, the slump of fresh concrete was 170mm, 175mm, 185 mm, and 190 mm respectively as the substitution of FRCA was 25%, 50%, 75% and 100% (by weight). However, the method to prepare FRCA (using FRCA with SSD state or dried state) is not mentioned precisely in the article.

Table 1-15 Details of concrete mixes (kg/m^3)[90]

Mix	Cement	Water	Sand(Class M)	FRCA	Coarse Aggregate	Slump(mm)
Control	325	162	649	0	1298	145
RC25	322	161	483	161	1288	170
RC50	320	159	320	320	1277	175
RC75	317	158	158	475	1267	185
RC100	315	157	0	629	1257	190

Tam et al. [91-94] proposed a new approach in concrete mixing, 'two-stage mixing approach (TSMA)' which is shown in the Figure 1-7, in order to improve the compressive strength of recycled concrete. During the first stage of mixing, TSMA uses half of the required water for mixing leading to form a thin layer of cement slurry which fills up some pores and cracks in the RCA. At the second stage of mixing, the remaining water is added to complete the mixing process. Under the examination of SEM, both the new ITZ and old ITZ of RAC are improved after the TSMA comparing to normal mixing approach. Improvement of strength was recorded up to 21% for 20% of RCA used after 28days of curing. They also suggested that using pozzolanic materials (silica fume, fly ash) into concrete combined with TSMA could improve the properties of RAC.

Roesler et al. [27] studied the effects of RCA on the concrete's fresh and strength properties for airfield rigid pavement application using TSMA. Various concrete mixtures with different percentages of RCA and mineral admixtures as partial replacement of Portland cement were tested. The RCA were kept in moisture conditions of approximately 80% of their absorption capacity. The mix water was adjusted according to the water absorption of RCA. The results showed that TSMA can be an effective method for improving properties of RAC. The slump value for the RAC gave similar results comparing to control concrete (concrete with natural aggregates). Thus, TSMA with higher initial absorbed moisture reduced the negative workability effects associated with RCA. The RCA mixtures with silica fume or fibers reduced workability as expected.

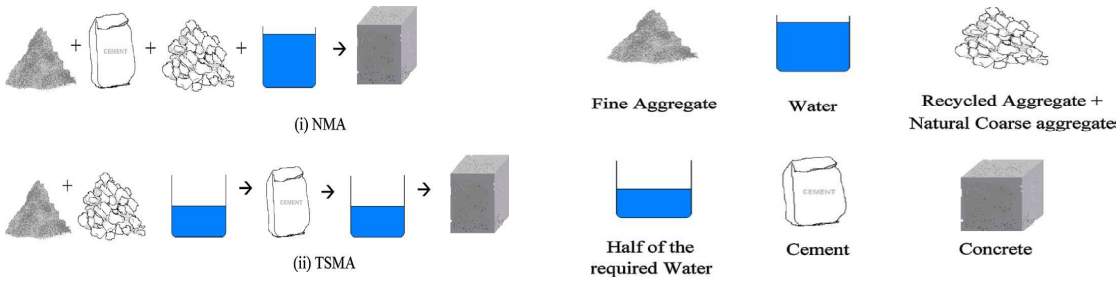

Figure 1-7 Mixing procedures of (i) normal mixing approach and (ii) two-stage mixing approach[91]

Kou et al. [95] studied the properties of concretes that were prepared with FRCA and crushed natural coarse aggregate. They used two methods to design the concrete mixes, one with a fixed water/cement ratio and the other with a fixed slump range. Saturated surface dried conditions of aggregates were used to design the concrete mixes, but unfortunately they didn't mention how SSD condition was determined. Water compensation was made during concrete batching. But they didn't mention the state of moisture of FRCA used in the mixing procedure. The slump of fresh concrete Mixes I was 75mm, 98mm, 120 mm, and 135 mm as the substitution of FRCA was 25%, 50%, 75%, and 100% respectively at the fixed water/cement ratio. The slump value of the concrete Mixes II maintained at approximately the same value (between 60-80mm) by reducing the added free water. The free water decreased as the substitution of FRCA increased. The results illustrated how the water absorption properties of FRCA affected the free water required in the concrete mixes which influenced directly the slump value of fresh concrete. But they didn't mention the method used to evaluate the water absorption of FRCA.

Poon et al. [96] studied the influence of moisture states of natural and recycled aggregates on the properties of fresh and hardened concretes. The moisture states of aggregates were controlled at air-dried (AD), oven-dried (OD) and saturated surface-dried (SSD) states. The fine aggregates used were natural river sand with a fineness modulus of 2.11. The natural

coarse aggregates used were crushed granite with nominal sizes of 10 and 20mm. The CRCA were crushed and obtained from a single source at the old Kai Tak airport in Hong kong. The physical and mechanical properties of the natural and CRCA are shown in Table 1-16.

Table 1-16 Properties of the natural and recycled coarse aggregates[96]

Type	Nominal size (mm)	Density (kg/m^3)	Water absorption (%)	Strength (10% fine value) KN	Porosity (%)
Crushed granite	10	2620	1.25	159	1.60
	20	2620	1.24		
Recycled aggregate	10	2330	7.56	117	10.45
	20	2370	6.28		

All the mixes had a free water content of 205 kg/m^3, a free water-to-cement ratio (w/c) of 0.57 and a fine aggregate to total aggregate ratio of 0.375. The amount of water was adjusted according to the actual moisture contents of the aggregates. When the AD and the OD aggregates were used, an additional amount of water was needed to saturate the aggregates. The actual mass of water and materials used in 12 mixes are shown in Table 1-17.

The test results showed that initial slump values of the concrete mixtures were dependent on the initial free water contents, and the slump loss values of the mixtures were related to the moisture states of the aggregates. The changes of slump with time are shown in Figure 1-8. For the mixes prepared with all the coarse aggregate being replaced by the recycled aggregate, the initial slump values of OD4 mix was about 145mm, while that of AD4 mix was 125mm. In contrast, the mix with SSD coarse aggregate still maintained at initial slump of 100mm. The concrete with OD coarse aggregate showed a higher initial slump which was due to the higher initial free water content in the mix. The slump value of these mixes decreased to zero at 135min for mix OD1 and at 165 min for mix AD1 and SD1 after initial mixing. Overall, it was clear that if the recycled aggregates were used in the SSD state, there was only a small change in the initial slump of the concrete. Due to the absorption of water by the dry aggregate, which reduced quickly the amount of free water in the mixture, the mixes prepared

with 20-100% recycled aggregates in the SSD state showed a slower process of slump loss and the slump did not reach zero during the test period of 165 min. In comparison, the OD mixes showed a faster loss of slump than the SSD mixes.

Table 1-17 Actual mass of water and materials used in different mixes[96]

Mix	Combination of coarse aggregate	Moisture state of coarse aggregate	Proportions (kg/m^3)						
			Water	Cement	Sand	Crushed granite		Recycled aggregate	
						10mm	20mm	10mm	20mm
AD1	100% crushed granite	AD	214	353	667	362	724		
OD1		OD	221	353	667	360	720		
SSD1		SSD	209	353	666	364	729		
AD2	80% crushed granite + 20% recycled concrete	AD	217	353	660	287	574	70	139
OD2		OD	230	353	661	284	569	67	135
SSD2		SSD	206	353	661	288	576	72	144
AD3	50% crushed granite + 50% recycled concrete	AD	229	353	647	176	351	170	343
OD3		OD	247	353	647	175	349	164	332
SSD3		SSD	207	353	649	177	354	177	354
AD4	100% recycled concrete	AD	241	353	625			330	663
OD4		OD	271	353	625			317	642
SSD4		SSD	209	353	625			342	684

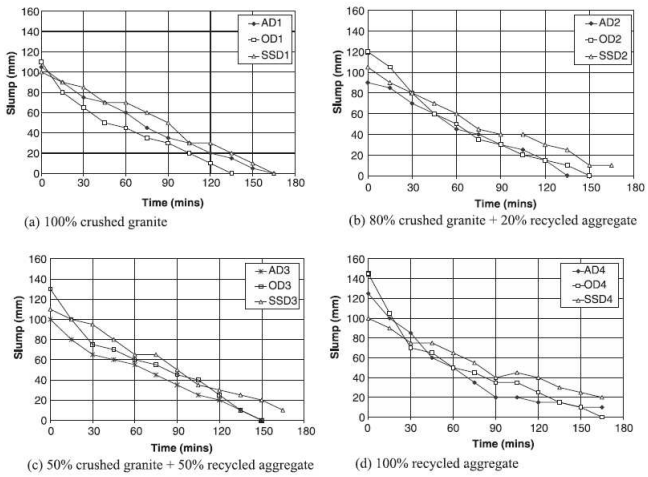

Figure 1-8 Changes of slump of concrete mixes with different types of coarse aggregates and at different moisture states[96]

Poon et al. [97] studied the properties of fresh concrete prepared with recycled aggregates. They prepared the concrete mixtures with a design compressive strength of 35 MPa, the mix proportions of concretes are shown in Table 1-18. The fine aggregates used were natural river sand with a fineness modulus of 2.11. The recycled aggregate was used at the air-dried

condition with initial moisture content of the aggregate at mixing much lower than its absorption capacity. The changes in slump of concrete mixes without fly ash and with 25% fly ash are shown in Figure 1-9 and Figure 1-10, respectively. The initial slump increased with an increase in the percentage of recycled aggregate.

Table 1-18 Mix proportion of concrete[97]

Notation	Recycled aggregate (%)	Constitution (kg/m^3)					
		water	cement	sand	Fly ash	granite	Recycled aggregate
R0	0	225	410	642	-	1048	0
R20	20	225	410	642	-	840	204
R50	50	225	410	642	-	524	506
R80	80	225	410	642	-	210	814
R100	100	225	410	642	-	0	1017
R0F25	0	225	307.5	628	102.5	1048	0
R20F25	20	225	307.5	628	102.5	840	204
R50F25	50	225	307.5	628	102.5	524	506
R80 F25	80	225	307.5	628	102.5	210	814
R100 F25	100	225	307.5	628	102.5	0	1017

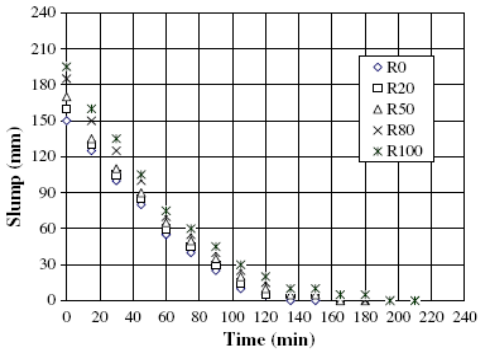

Figure 1-9 Changes of slump of concrete mixes without fly ash [97]

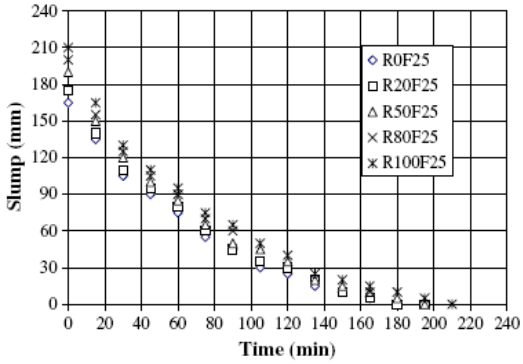

Figure 1-10 Changes of slump of concrete mixes with 25% fly ash [97]

The mix prepared with 100% recycled aggregate showed the greatest slump of 195mm and it took about 3h to decrease to the zero slump, while the mix without recycled aggregate took about 130 min. For the mixes with 25% fly ash, all the mixes showed higher initial slumps when compared to the corresponding without fly ash. The highest initial slump of 210 mm was recorded for the mix with 100% recycled aggregate and 25% Fly ash. The rate of slump

loss with time was also lower for the mixes with fly ash. As a result, the slump of these mixes took longer to reach zero than the mixes without fly ash.

Globally, we can conclude that the moisture state of the recycled aggregates affects the workability properties of concrete made with RCA. The slump loss of the concrete is influenced by the moisture state. Attention should be paid to the preparation of recycled aggregates before mixing.

1.5.2 Mechanical properties of recycled aggregate concrete

J.M.Khatib [90] found that compressive strength reduction occurred when natural sand was replaced by FRCA. The compressive strength for all mixes at 1, 7, 28, and 90 days are shown in Figure 1-11. After 90 days curing, the reduction could reach 27% at the replacement level of 100%, while it was only 15% for the replacement of 25% at the fixed water/cement ratio of 0.5.

Evangelista [98] studied the influence of FRCA which was produced in laboratory in the production of structural concrete. They used FRCA to partially or globally replace natural sand in the RAC. For replacement ratios up to 30%, the compressive strength was only decreased by 3.7%, the modulus of elasticity was decreased by 3.7%. For the replacement ratio up to 100%, the compressive strength was only decreased by 7.6%, the modulus of elasticity was decreased by 18.5%. Globally they concluded that the use of FRCA does not jeopardize the mechanical properties of concrete, however it was contradictory to [90, 95].

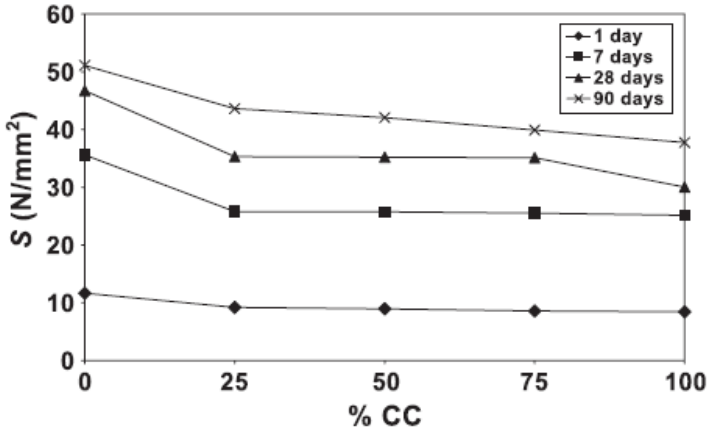

Figure 1-11 Effect of FRCA content on compressive strength(S)[90]

Kou et al. [95] studied the properties of concretes that were prepared with FRCA as fine aggregates. They used two methods to design the concrete mixes, one was the fixed water/cement ratio of 0.53 and the other one was the fixed slump range of 60-80mm. The concrete mixes were designed on the saturated surface dried condition. But they didn't mention the state of moisture of FRCA used in the mixing procedure. Water compensation was made during concrete batching. They pointed out that at a fixed W/C and at fixed slump, the compressive strength of concrete with replacement of 100% decreased 25%, 26% respectively compared to control concrete (Figure 1-12 and Figure 1-13). After the authors, the poorer mechanical strength of concrete mixes of fixed water/cement ratio might be due to the high initial free water content used in the mixes rendered bleeding and poorer interfacial bonding between the aggregates and the cement pastes.

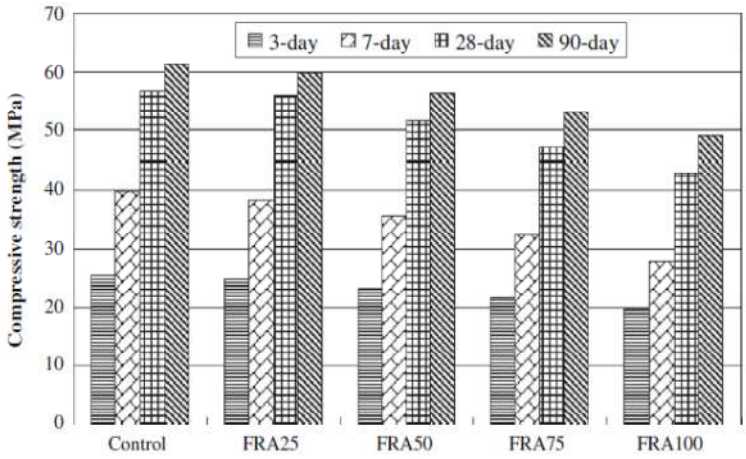

Figure 1-12 Compressive strength of concrete mixes in Series I(fixed w/c)[95]

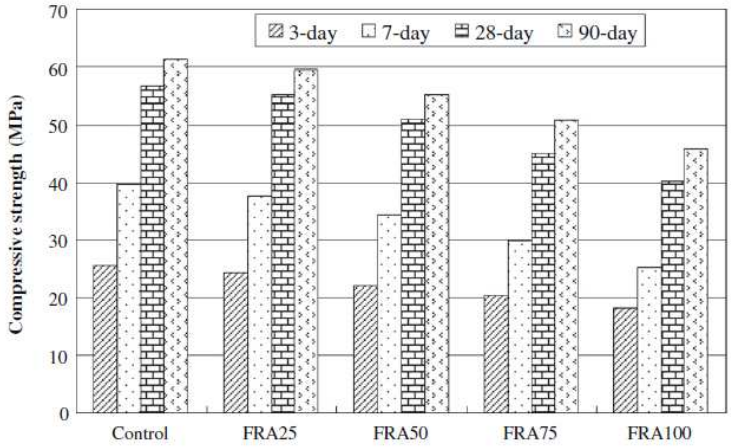

Figure 1-13 Compressive strength of concrete mixes in Series II(fixed slump)[95]

Poon et al. [99] used recycled aggregates to produce concrete bricks and paving blocks obtained from C&DW. Series of laboratory trial tests were carried out to determine the properties of the bricks and blocks prepared with and without recycled aggregates. The test results showed that the replacement of coarse and fine natural aggregates by recycled aggregates at the levels of 25% and 50% had little effect on the compressive strength of the brick and block specimens, but at the levels of 100% it was decreased by 27% and 13% compared to the control brick and block respectively. Paving blocks with a 28-day

compressive strength of not less than 49 MPa can be produced without the incorporation of fly ash, and paving blocks for footway uses with a lower compressive strength of 30 MPa and masonry bricks can be produced with the incorporation of fly ash.

Xiao et al. [100] studied the compressive strength and the stress-strain curve of RAC under uniaxial loading with different replacement percentages of CRCA (0%, 30%, 50%, 70%, 100%). The fine aggregate used was river sand. The used CRCA were pre-soaked before mixing. The mix proportions and properties of concrete are shown in Table 1-19.

Table 1-19 Mix proportions and properties of concrete(kg/m^3)[100]

No.	RCA replacement percentage	W/C	C	S	NCA	RCA	Mixing water	Slump (mm)	Compressive strength (MPa)
NC	0	0.43	430	555	1295	-	185	42	35.9
RC-30	30	0.43	430	534	872	374	185	33	34.1
RC-50	50	0.43	430	522	609	609	185	41	29.6
RC-70	70	0.43	430	510	357	832	185	40	30.3
RC-100	100	0.43	430	492	-	1149	185	44	26.7

They concluded that the failure mode of RAC was a shear mode and the failure process of RAC was relatively short. The inclination angle between the failure plane and the vertical load plumb was about 63-79º, while the inclination angle of the normal concrete was about 58-64º. The RCA replacement percentage had a considerable influence on the stress-strain curves of RAC which is shown in Figure 1-14. The stress-strain curves of RAC indicate a decrease in the peak stress and an increase in the peak strain. The compressive strengths generally decreased with increasing RCA contents. The elastic modulus of RAC was lower than that of the normal concrete. It decreased as the RCA content increased. For a RCA replacement percentage equals to 100%, the elastic modulus was reduced by 45%. The peak strain of RAC was higher than that of normal concrete. It increased with the increase in RCA

contents. For a RCA replacement percentage equals to 100%, the peak strain was increased by 20%.

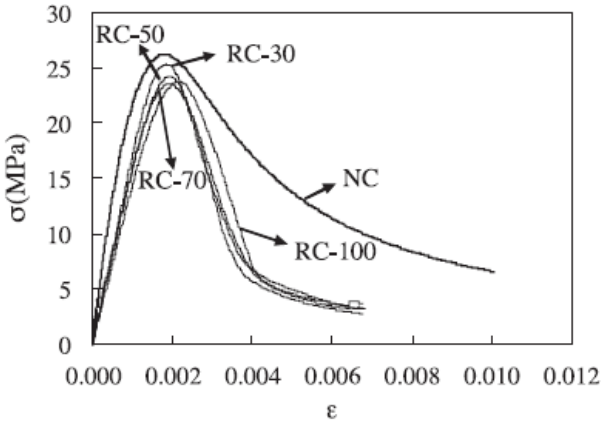

Figure 1-14 Typical stress-strain curves of RAC[100]

Etxeberria et al. [21] studied the shear behavior and strength of beams made with RAC. Twelve beam specimens with the same compressive strength, four concrete mixtures using different percentages of CRCA (0%, 25%, 50% and 100%) and three different transverse reinforcement arrangements were cast and tested up to failure. They concluded that a substitution of less than 25% of coarse aggregate was suitable for structural use by considering all measures related to dosage, compressive strength and durability.

Xiao et al. [101] studied the mechanical properties of RAC by collecting 1200 test results of experimental works published in the literature. The relationships between the compressive strength and the density, the splitting tensile strength, the flexural strength, the elastic modulus of RAC are shown in Figure 1-15 to Figure 1-18 respectively. A linear relationship between compressive strength and the density was found. They concluded that the equations used for the description of mechanical properties of normal concrete cannot be directly applied to the recycled aggregate concrete. Therefore they presented improved equations for the description of RAC after the statistical analysis of the collected experimental results. The

difference between proposed relations and equations suggested by ACI are shown in Table 1-20.

Table 1-20 Difference between proposed relations and equations suggested by ACI [101]

Xiao [101]	ACI Code
$f_{sp}=0.24f_{cu}^{0.65}$	$f_{sp}=0.49f_{cu}^{0.50}$
$f_f = 0.75\sqrt{f_{cu}}$	$f_f = 0.54\sqrt{f_{cu}}$
$E_c = 7770f_{cu}^{0.33}$	$E_c = 4127f_{cu}^{0.33}$

Globally, compressive strength of RAC decreases as the content of RCA increases both for FRCA and CRCA replacement (Table 1-21). Generally, authors showed that the reasonable use of CRCA doesn't decrease the compressive strength a lot and can satisfy the project needs. A few authors mentioned that the use of FRCA does not jeopardize the mechanical properties of concrete until the replacement of RCA up to 30%. But for other authors the use of FRCA is not good for the properties of RAC due to their high water absorption and mortar content.

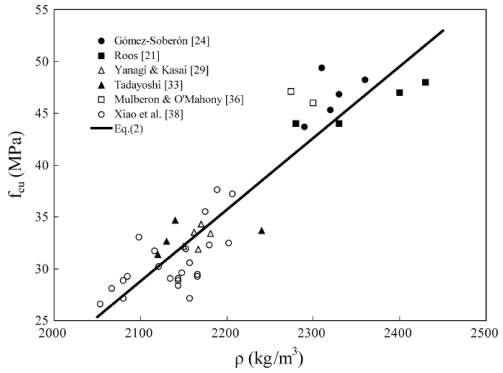

Figure 1-15 Relationship between the compressive strength and the density of RAC[101]

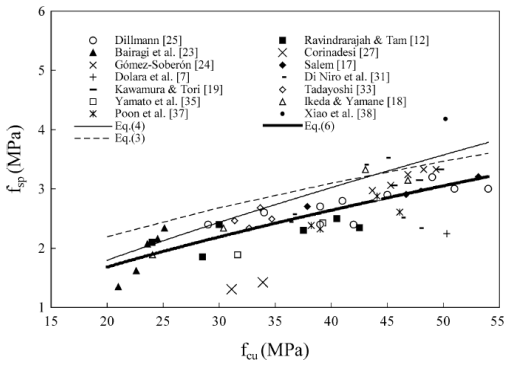

Figure 1-16 Relationship between the splitting tensile strength and the compressive strength of RAC[101]

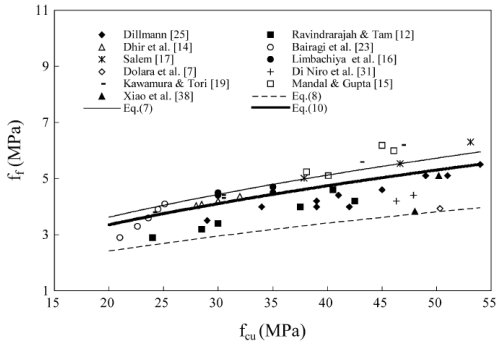

Figure 1-17 Relationship between the flexural strength and the compressive strength of RAC[101]

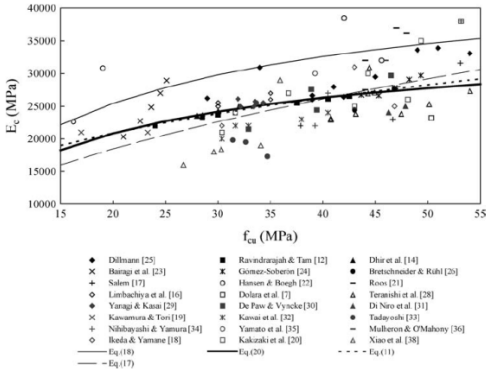

Figure 1-18 Relationship between the elastic modulus and the compressive strength of RAC[101]

Table 1-21 Summary of properties of RAC from literature

Author, Year (Reference no.)	Composition information	Compressive strength MPa (28days) Relative strength	Modulus of elasticity GPa (28days)
J.M Khatib 2005 [90]	w/c constant, FRCA replace with 0%,25%,50%,75%,100%	46.7,35.3,35.2,35.1,30 (1.00,0.76,0.75,0.75,0.64)	48.1,44.7,42.5,42.3,39.1(1.00,0.93,0.88,0.81)
L.Evangelista et al. 2007 [98]	cement constant,FRCA replace with0%,10%,20%,30%,50%,100%,Superplasticizer	59.3,59.0,57.3,57.1,58.8,54.8 (1.00,0.99,0.97,0.96,0.96,0.99,0.92)	35.5,34.2,28.9 (1.00,0.96,0.81) for 0%,30%,100%
Kou Shi-Cong et al. 2009 [95]	I:w/c constant,FRCA replace with 0%,25%,50%,75%,100%; II:slump constant,FRCA replace with 0%,25%,50%,75%,100%	I:57,56,52,47.5,42.5 (1.00,1.00,0.93,0.85,0.76); II:57,55,52.5,45,40.5 (1.00,0.96,0.92,0.79,0.71)	-
P.Pereira et al 2012 [102]	FRCA replace with 0%,10%,30%,50%,100%, Superplasticizer	53.3,53.7,51,47.8,45.1 (1.00,1.01,0.96,0.90,0.85)	-
C.S Poon et al 2002 [99]	cement constant,both FRCA and CRCA replace with 0%,25%,50%,75%,100%, Fly ash	46.6,44.7,46.5,45.4,40.1 (1.00,0.96,1.00,0.97,0.86)	-
Jianzhuang Xiao et al 2005 [100]	w/c constant, CRCA replace with 0%,30%,50%,70%,100%	35.9,34.1,29.6,30.3,26.7 (1.00,0.95,0.82,0.84,0.74)	-
M.Etxeberria et al 2007 [21]	compressive strength constant, CRCA replace with 0%,25%,50%,100%	29,28,29,28	32.56,31.3,28.59,27.74 (1.00,0.96,0.88,0.85)
Torben C. Hansen et al 1985 [103]	CRCA repalce with 100%	-	15-30% reduction
C.S Poon et al 2007 [12]	w/c constant, CRCA replace with 0%,30%,50%,70%,100%	48.6,45.3,42.5,39.2,37.1 (1.00,0.93,0.87,0.81,0.76)	-
C.S Poon et al 2004 [96]	cement constant, CRCA replace with 0%,25%,50%,75%,100%	SSD: 46,43.0,38.1,39.1 (1.00,0.93,0.83,0.85)	-
José M.V. Gomez-Soberon 2002 [47]	w/c constant, CRCA replace with 0%,15%,30%,60%,100%	39,38.1,37,35.8,34.5 (1.00,0.98,0.95,0.92,0.88)	29.7,29.1,27.8,26.6,26.7 (1.00,0.98,0.94,0.90,0.90)
Valeria Corinaldesi	w/c constant, CRCA repalce with 0%,30%	51.2,38.1 (1.00,0.74)	35.6,27.2 (1.00,0.76)

2010 [104]	(w/c=0.5)		
Amnon Katz 2003 [105]	w/c constant, both FRCA and CRCA replace with 0%,100%	30% reduction for OPC, 24% reduction for White PC	25% reduction
A.K. Padmini et al 2009 [55]	CRCA repalce with 100%	20-35% reduction for 10mm maximum size;14-35% reduction for 20mm maximum size;10-25% for 40mm maximum size	-
Ilker Bekir Topçu et al 2004 [106]	CRCA replace with 0%,30%,50%,,70%,100%	23.5% reduction for C20 concrete;33% reduction for C16 concrete	-
Sami W.Tabsh et al 2009 [107]	CRCA replace with 0%,30%,50%,70%,100%	30% reduction for C30 concrete;10% reductioni for C50 concrete	-
Benito Mas et al 2012 [108]	CRCA replace with 0%,25%,50%,75% and no Superplasticizer for C15;CRCA replace with 0%,20%,40% and Superplasticizer for C25 and C65	18-21% reduction for C15; 13% reduction for C25; 26-39% reduction for C65	-
M.Casuccio et al 2008 [109]	CRCA replace with 0%,100% and no Superplasticizer for C18; CRCA replace with 0%,100% and Superplasticizer for C37 and C48	1-15% reduction	13%-18% reudction

1.5.3 Mechanical properties of mortars made with FRCA

Like the recycled concrete, recycled mortar manufactured with FRCA generally present a lower strength and a lesser durability than similar mortar composed of natural sand. Generally, compressive strength of mortar decreases as the content of FRCA increases [110-112]. A few authors mentioned that the use of FRCA does not jeopardize the mechanical properties of mortar up to a replacement of 30%. But for other authors the use of FRCA is not good for the properties of mortar due to the high water absorption and adherent cement paste content.

Dapena et al. [113] studied the effect of recycled sand content on the characteristics of mortars and concretes. Using recycled sand contents of 0, 5, 10, 15, 20, and 50%, the strength drop of recycled mortars increased from 0 to 50%. The strength reduction was 14% and 31% comparing to the control mortar with siliceous sand when the recycled sand content was 10% and 20% respectively. With calcareous sand and an addition of superplasticizer, the

compressive strength of recycled mortar with 20% and 50% recycled sand were 51.8, 51.1MPa respectively (control mortar with 0% recycled sand was 61MPa). Replacing recycled sand up to 10% had no appreciable effect on the compressive strength of recycled mortar.

Braga et al. [114] found that it was feasible to use up to 15% of fine recycled concrete aggregate in mortar composition. I.Vegas et al. [115] presented that the critical characteristics of FRCA used in the manufacture of masonry mortar were their water absorption and sulfur compounds content. After these authors, cement-based masonry mortar may contain up to 25% FRCA with no detriment to their performance in terms of mechanical strength, workability or shrinkage. Miranda et al. [112] found that replacement ratios of up to 40% by volume didn't significantly affect the properties of low strength mortar, with the exception of density and workability.

Lee [116] studied the influence of recycled fine aggregates on the resistance of mortars to magnesium sulfate attack. Mortar specimens were prepared with FRCA at different replacement levels (0%, 25%, 50%, 75% and 100% of natural sand by mass). The results showed that the compressive strengths of mortars were 48.5, 42.8, 41.1, 37.6, 35.2MPa respectively. This study showed that the recommendable replacement level of recycled fines was up to around 50% by the used materials.

Corinaldesi et al. [117] studied mortars containing 100% FRCA. They showed that adding polypropylene fibers and stainless steel fibers in the mortars can reduce the shrinkage of mortars and improve the flexural strength, which allows to obtain good performances, in particular when coupled with bricks.

Corinaldesi and Moriconi [118-119] evaluated the mechanical and rheological behavior of mortars with three different 100% FRCA (from precast concrete, recycled bricks, from recycling plant). Mortars with FRCA developed low mechanical strength with respect to the

reference mortar (28MPa for reference mortar, 21, 16 and 17MPa for the three recycled mortars), particularly with the recycled bricks.

1.5.4 ITZ properties

Concrete can be considered as a three phase composite: aggregate, Interfacial Transition Zone (ITZ), and matrix [120-123]. The formation of ITZ around aggregates can be explained by several factors such as wall effect, bleeding during the vibration of concrete before setting, unidirectional growth of hydrates [124-126]. When the cement grains encounter the wall of an aggregate, a gradient of water and cement grains surrounds the aggregate due to the packing constraints imposed by the surface [127-128]. A region of higher porosity near the aggregate surface is therefore created.

RILEM TC 159-ETC [129] pointed out that ITZ should not be viewed as a well defined material but rather as a system which properties depend on the overall composition as well as on the method of fabrication of the cement composite. The microstructure of the ITZ can be quantified experimentally and by modeling in terms of gradients of microstructure [130-132]. The ITZ microstructure would depend to a large extent on the particle size distribution of the binder and its ability to efficiently pack at the aggregate surface. Bentz [133] stated that the microstructure of ITZ between cement paste and aggregate depended strongly on the nature of the aggregate, specially its porosity and water absorption.

In recycled aggregate concrete, three kinds of ITZ can be distinguished: the old ITZ between natural aggregate and old adherent cement paste (in the RCA), the new ITZ between the old adherent cement paste and new cement paste, and the new ITZ between new cement paste and natural aggregate (in the RCA), which are shown in Figure 1-19. Different experimental methods are used to characterize the properties of ITZ, including the optical microscopy,

scanning electron microscopy (SEM), energy dispersive X-ray analysis (EDX), mercury intrusion porosimetry (MIP), atomic force microscope (AFM), and nanoindentation. The typical width of the ITZ between the aggregate and matrix is 50μm. However, different researchers obtained different thickness of the ITZ from their tests.

1-Original aggregate 2-Adhered cement paste 3-New cement paste
Old ITZ between original aggregate and adhered cement paste
New ITZ between original aggregate and new cement paste
New ITZ between old adhered cement paste and new cement paste

Figure 1-19 Schematic representation of ITZs

Poon et al. [46] studied the microstructure of ITZ in RAC by SEM. SEM observations revealed that the normal concrete (NC) aggregate-cement interfacial zone consisted mainly of loose and porous hydrates whereas the high performance concrete (HPC) aggregate-cement interfacial zone consisted mainly of dense hydrates. The interfacial transition zone microstructure in concrete with RCA appeared to be an important factor in governing strength development of the RAC. It was expected that the mechanical properties of RAC can be improved by modifying the surface properties and the pore structure of the RCA.

Tam et al. [91] studied the microstructure of the ITZ between RCA and cement paste to assess the benefits gained from the two-stage mixing approach (TSMA). They pointed out that the quality of ITZ depends on the surface characteristics of the aggregate particles, the degree of

bleeding, chemical bonding and the specimen preparation technique. They found that ITZ of the RAC is improved by the TSMA, which fills up the cracks and pores within RCA. The compressive strengths and other mechanical properties of RAC are enhanced from the laboratory experiments.

Xiao et al. [134-136] investigated the properties of ITZ (old and new ITZ) in the RAC by AFM, SEM, and nanoindentation. The RCA used for casting RAC specimens were presoaked before mixing. The water amount used to presoak the RCA was according to the water absorption capacity. From the SEM results, obvious voids and higher concentration of calcium hydroxide can be found in both old ITZ and new ITZ in RAC. The thickness of the old ITZ and new ITZs measured by nanoindentation are respectively in the range 40-50 μm and in the range 55-65 μm. The average indentation modulus of old ITZ is 70-80% of that of old paste matrix, while the average indentation modulus of new ITZ is 80-90% of that of new paste matrix. For the old ITZ, they showed that the indentation modulus of old ITZ around limestone is higher than that of old ITZ around gravel, and the thickness of old ITZ around limestone is thinner than that around gravel. But they didn't mention the type of gravel used in this study. The mix proportion and hydration degree have no obvious effects on the nanomechanical properties of the old ITZ in RAC. Adding fly ash can increase the average indentation modulus of the new ITZ, and decrease the thickness of new ITZ. With the increase of hydration degree, the new ITZ thickness appears to be reduced and the microstructure of the new ITZ tends to become denser.

Lee et al. [137] studied the ITZ properties of recycled aggregate in RAC by micro-hardness tests. However, the saturation state of RCA used was not mentioned. In the compressive and tensile tests, RAC in general failed by cracks through the RCA, and partly through the ITZ between the RCA and mortar. Bigger ITZ cracks were observed in RAC. They pointed out

that the micro-hardness value in the old ITZ was the lowest, the micro-hardness value in the new ITZ was higher than in the old ITZ. The old ITZ was weak compared to the new ITZ because of cracks and voids created by impacts during production process of RCA.

1.6 Summary

The RCA can be obtained through the demolition of concrete from different sources. Adherent cement paste is much more porous than natural aggregates generally used for the manufacture of concrete. Therefore, quality and quantity of adherent cement paste is at the origin of the lower properties of RCA comparatively to natural aggregates. It is important to control the quality of RCA by reducing the hardened cement paste content and the water absorption.

A lot of researchers studied adherent mortar content in the CRCA, while there is a little about the adherent cement paste content in FRCA. Concerning the links between particle sizes and mortar content, most of the studies mentioned lower quantities of adherent mortar in CRCA with larger particle sizes. But relationships between the adherent cement paste and particle sizes are not studied, and therefore it should be studied more precisely. Most of the studies mentioned that the high water absorption is connected with the high mortar content.

A few studies mention the relationship between water absorption and original concrete properties. Some authors showed that the RCA properties are affected by the composition of the original concrete. The RCA crushed from normal-strength concrete (NC) has higher mortar content and water absorption than the RCA crushed from high-performance concrete (HPC). But some authors showed that the RCA properties are not connected with the original concrete, there is no significant variation in quality for different crushed concretes. The links between RCA sizes, original concrete, crushing methods, weathering of the RCA before use,

adherent cement paste content and water absorption should be studied in more details and more systematically.

Many authors studied the properties of RAC connected with the proportions of coarse and/or fine recycled concrete aggregates. As the replacement of RCA increases, the properties of RAC decrease. Generally, the properties of RAC both for the fresh properties and the hardened properties vary from the compositions of concrete. The moisture state of RCA also plays a very important role in the slump of concrete. Some authors concluded that the air-dried state, the oven-dried state, and the surface-dried state influence the slump value. So, more attention should be paid to the preparation of RCA, especially the saturation state of FRCA. It is necessary to accurately measure the water absorption of FRCA. Some authors mentioned that the slump of RAC is larger as the replacement of RCA increases.

Globally, compressive strength of RAC decreases as the content of RCA increases. A few authors mentioned that the use of FRCA does not jeopardize the mechanical properties of concrete up to a replacement of 30%. But for other authors the use of FRCA is not good whatever the percentage of replacement for the properties of RAC due to the high water absorption and mortar content. The replacement of natural aggregates by CRCA has less effect on the compressive strength than FRCA. Generally, most authors showed that the reasonable use of CRCA doesn't decrease significantly the compressive strength and thus can satisfy the project needs.

The quality of ITZ depends on the surface characteristics of the aggregate particles, the degree of bleeding, and chemical bonding. The saturation state of used RCA may also influence the properties of ITZ, some authors do not mention this used RCA situation, few studies about the saturation state on the properties of ITZ are carried out. Obvious voids and higher

concentration of calcium hydroxide are found in both old ITZ and new ITZ in RAC. The thicknesses of the old ITZ and new ITZs are about 50 µm. The average indentation modulus of old ITZ is similar or a little higher than new ITZ. Microstructure and nanomechanical properties of ITZ can influence the mechanical properties and durability of RAC.

The influence of dimensions of RCA on their properties has not been studied frequently. The properties of RCA crushed in the laboratory and those made in plants seem to be different. However few studies have been devoted to understand these differences for these two kinds of RCA. The relationships between particle sizes, adherent cement paste content and water absorption have also been less studied.

1.7 Research objective

The literature review has shown that the reuse of CRCA in optimized percentages allows the manufacture of concrete possessing satisfying properties at least for normal concrete. On the contrary FRCA, due to their high adherent paste content and resulting high water absorption, lead to a significant decrease in the fresh and hardened properties of concrete. Since the moisture state has a large influence on the properties of fresh and hardened concrete, it is of great importance to be able to quantify this state, and so to measure the water absorption coefficient. The characterization of RCA as a function of their size has not been carried out systematically in the literature, however it seems that a better knowledge of the relation between properties of RCA and size is needed if one wants to optimize the reuse of RCA as aggregates. Moreover, this relation has to be studied with regard to original concrete composition, which could both influence the properties of RCA as a function of their sizes.

The main objective of this research is twofold. Firstly, we aim at studying the properties of fine recycled concrete aggregates (laboratory produced FRCA and industrial FRCA) as a

function of hardened cement paste content, particle sizes and properties/composition of the original concrete. Secondly, we want to explore the influence of the saturation state of FRCA on the properties of fresh and hardened mortars and on their microstructure.

The previous objectives will be addressed by answering the following questions:

(1) Can we define accurate experimental methods allowing to measure the water absorption coefficient and the adherent cement paste content of the different fractions of FRCA?

(2) What is the link between properties of original concrete (W/C ratio, cement paste volume) and properties of RCA made with it?

(3) What is the link between size and properties of FRCA (cement paste content, density, water absorption, porosity...)?

(4) What is the influence of the conditions of conservation of the RCA (carbonation) on their properties?

(5) What is the influence of FRCA (replacement percentage and replacement fraction) on the properties of recycled mortars?

(6) What is the influence of the moisture state of FRCA on the properties of recycled mortars?

In order to answer the questions mentioned above, three steps were followed in our studies which are shown in Figure 1-20.

In the first step (chapter 2), three original concretes with various compositions (two W/C and two volumes of cement paste) are designed and manufactured. They are then crushed with a jaw crusher for the production of RCA, and sieved in different granular classes. These RCA are then used to define accurate experimental methods for the measurement of water absorption and adherent cement paste content. Then, the defined methods are used to

characterize systematically the laboratory produced RCA. The influence of carbonation on the properties of FRCA was also studied.

In the second step, three industrial FRCA sourced from different recycling plants are characterized with the experimental methods defined previously (Chapter 3).

In the third step, the influence of moisture state of FRCA (saturated or dried) on the rheological behaviour, on the compressive strength, and properties of ITZ of recycled mortars were studied (Chapter 4).

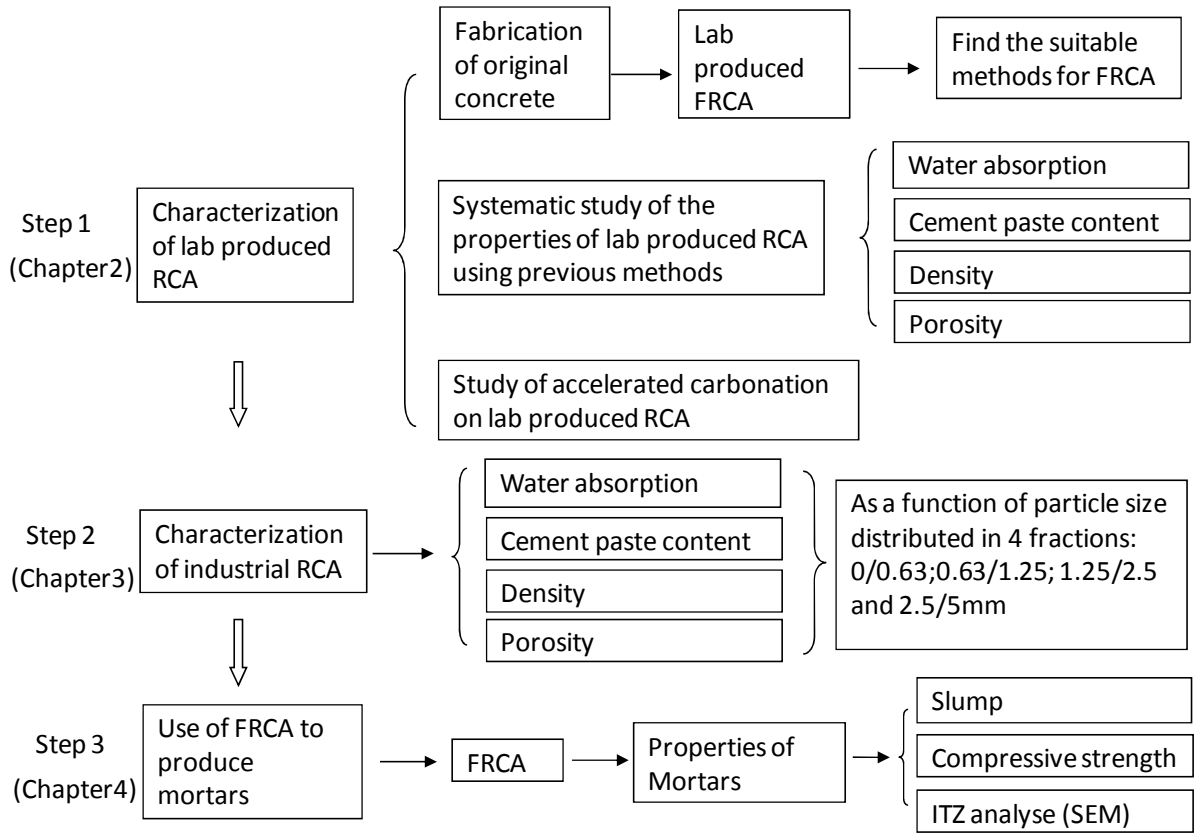

Figure 1-20 Research outline

Chapter 2 Characteristics of laboratory produced RCA

2.1 Introduction

In this chapter, experimental methods allowing to measure the cement paste content and the water absorption coefficient of FRCA are presented. A method based on the dissolution of the major part of the cement paste by salicylic acid has been developed for the measurement of cement paste content. These methods have been established by using RCA of well known composition, produced from the crushing of laboratory made concrete. Using these well defined laboratory made materials allows us to study the influence of properties of original concrete on the properties of FRCA. The relationships between adherent cement paste content and other properties of FRCA are presented. The influence of carbonation on the properties of laboratory produced FRCA are also presented.

2.2 Materials

Three original concretes with two different W/C ratios and volumes of paste were designed and manufactured for production of FRCA. Materials used in this study are as follows.

2.2.1 Cement

The cement used throughout this study was a white OPC (CEM I 52.5 “superblanc”) provided by Lafarge company whose mineralogical composition is shown in Table 2-1. Grey cement

CEM II 52.5 provided by Holcim company was also used only to test the salicylic acid disslution method.

Table 2-1 Mineralogical composition of cements determined by XRD-Rietveld

	C_3S	C_2S	C_3A	C_4AF	Anhydrite	Calcite	Periclase	Gypsum
CEM I 52.5 Superblanc (%)	73.90	21.87	1.46	-	0.52	1.53	0.72	-
Grey cement CEM II 52.5 (%)	52.74	8.07	8.92	8.95	0.74	18.06	0.46	2.06

2.2.2 Natural aggregates

Crushed calcareous coarse and fine aggregates sourced from Tournai (provided by Holcim France Benelux) were used for production of all original concretes. The water absorption coefficients of natural coarse and fine aggregates were respectively 0.8% and 1.05% according to standard EN 1097-6 [40]. Sieve analysis of natural coarse and fine aggregates was carried out by the standard EN 933-1 [138] as shown in Figure 2-1.

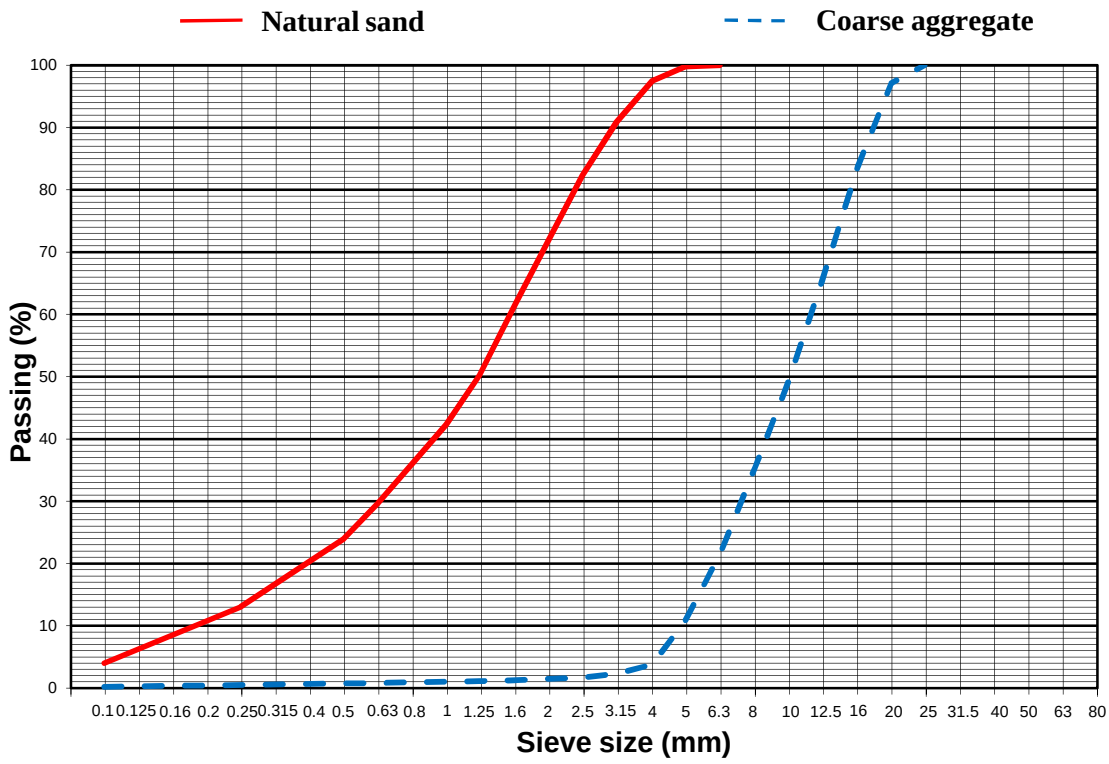

Figure 2-1 Particle size distributions of natural sand and coarse aggregate

2.2.3 Original concretes and production of RCA

Three original concretes with two different W/C ratios and volumes of paste were designed and manufactured for production of FRCA. Table 2-2 shows the details of original concrete compositions. OC1 and OC2 had the same W/C ratio and OC2 and OC3 had the same volume of cement paste.

Table 2-2 Original concrete compositions made in the laboratory (1 m^3)

Type of original concrete	OC1	OC2	OC3
Aggregate (kg)	1138.3	1040.7	1018.9
Sand (kg)	756.4	691.5	677.0
Cement (kg)	298.8	375.7	474.8
Efficient water(kg)	179.3	225.4	189.9
Absorbed water(kg)	17.2	15.7	15.4
Total water(kg)	196.5	241.1	205.3
Coarse Aggregate/Sand	1.505	1.505	1.505
W/C ratio	0.6	0.6	0.4
Volume of cement paste (dm^3)	278	350	347
Density of fresh concrete(kg/m^3)	2390	2349	2376
Slump (cm)	5.8	20.3	5.6
fc_{28} (MPa)	41.1	40.8	51.0
fc_{90}(MPa)	47.3	46.4	57.6

After 28 (RCA-28) and 90 (RCA-90) days curing in water, original concretes were crushed in the laboratory by using a jaw crusher with the same opening size (10mm). After crushing, RCA were dried in the oven at 105°C. The cumulated and partial particle size distributions of all the crushed RCA are given in Figure 2-2 and Figure 2-3. These figures show that, with the same jaw crusher opening, very similar particle size distributions (PSD) can be obtained for all the concretes produced in the laboratory, whatever their properties and compositions. Nevertheless, RCA-90 for the three concretes are coarser than RCA-28. All the crushed RCA were separated into CRCA and FRCA. In this study we focus on the properties of FRCA (0/5mm). FRCA were then separated by sieving in four different granular classes (0/0.63, 0.63/1.25, 1.25/2.5, 2.5/5mm) in order to study the influence of granular class on the

properties of FRCA. Each granular class is represented by its average particle size (0.315, 0.94, 1.875, 3.75mm), corresponding to the average value of the minimal and maximal particle sizes of the granular class. Each class was divided with a sample splitter and then tested for cement paste content, water absorption, density, porosity and mass loss between 105°C and 600°C ($ML_{105\text{-}600}$).

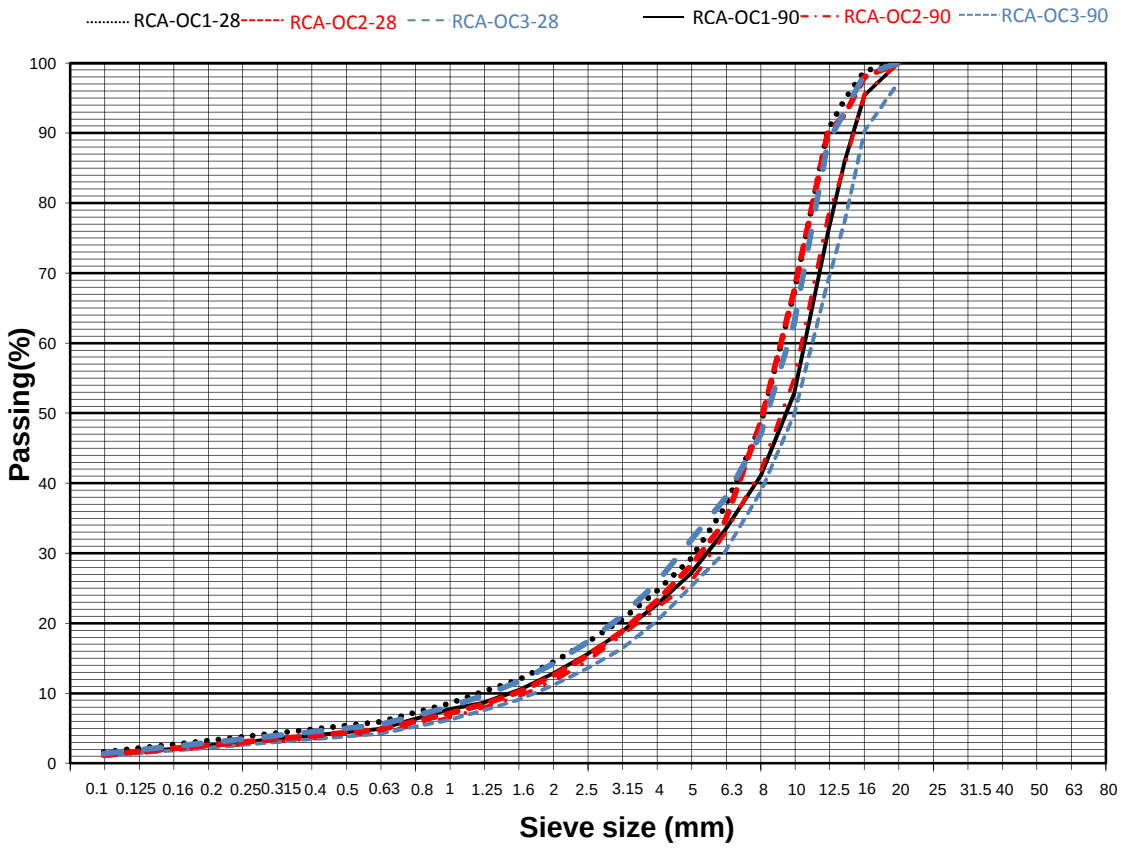

Figure 2-2 Cumulated particle size distributions of crushed RCA

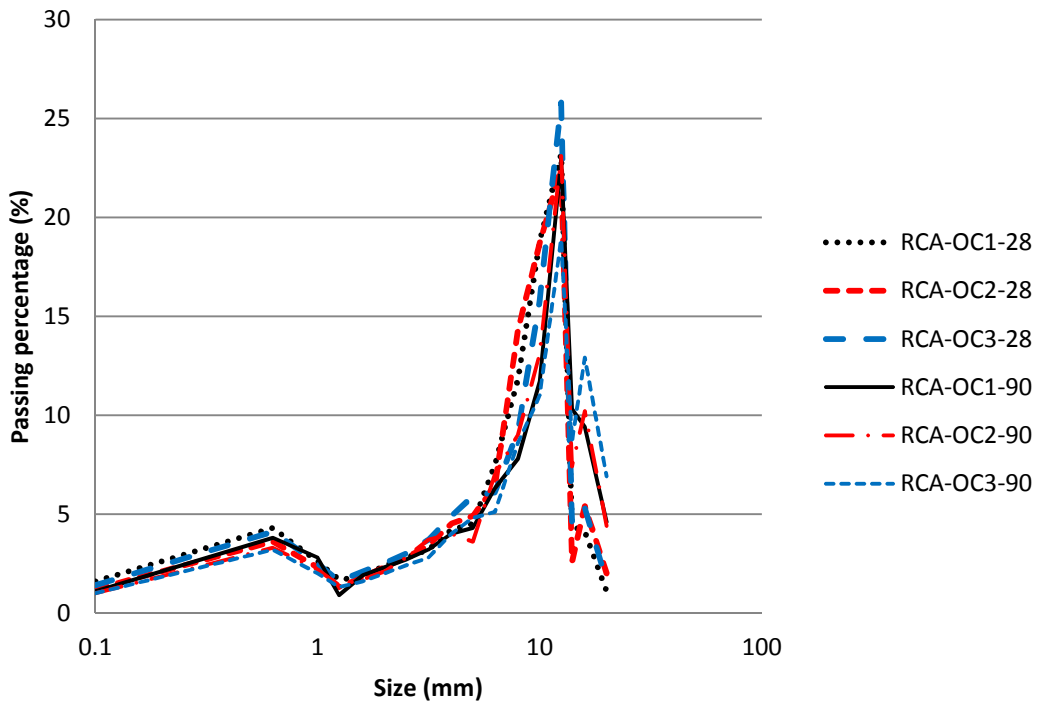

Figure 2-3 Partial particle size distributions of crushed RCA

2.2.4 Manufacture of cement pastes

Cement pastes with several W/C ratios (0.4, 0.5 and 0.6) were manufactured in a mortar mixer and poured into plastic bottles that were sealed after casting and rotated during 24h (until hardening) in order to prevent segregation. The cement used for all pastes was CEM I 52.5 Superblanc the same as used for the manufacture of original concrete. Grey cement paste with w/c ratio of 0.5 was manufactured only to test the salicylic acid disslution method. After 90days curing in the water, cement pastes (CP-90) were crushed by the same jaw crushers with the same opening size as for manufacture of RCA. Fraction 1.25/2.5mm of cement paste was obtained for the salicylic acid dissolution and carbonation test. CP-0.6-90 refers to the cement paste which is made with w/c=0.6 and curing 90 days in water.

2.3 Experimental methods

2.3.1 Water absorption

Water absorption of FRCA plays an important role in the manufacture of concrete. The water absorption coefficient of each granular class of the FRCA was measured with two different methods: the European standard method EN 1097-6 and the method n°78 of IFSTTAR [139]. Three samples of each granular class of FRCA were measured to obtain the average value.

The principle of these methods is similar: in both cases, samples are saturated 24 hours in water and then the water absorption coefficient is determined based on the water content at saturated surface dry (SSD) state. However, the drying method and the way to identify the SSD state are totally different. In the standard method (EN 1097-6), saturated aggregates are exposed to a gentle current of warm air to evaporate surface moisture and to reach the SSD state. The latter is identified using a slump test on the drying sample, which allows detecting the existence of cohesion forces due to surface moisture. A metal cone mould is filled with the drying sample and lifted gently to let the aggregate flow under the effect of gravity. The shape of the aggregate cone obtained after lifting allows the SSD state to be determined (Figure 2-4). In the IFSTTAR method, the aggregates are dried progressively with different sheets of colored absorbent paper until no trace of water can be seen on the paper (the surface of each sheet of coloured absorbent paper is wiped carefully with a brush to ensure that no fine particles remain attached on the paper). In that state (SSD state), no moisture remains at the surface of particles (third sheet of paper in Figure 2-5).

Figure 2-4 Shape of cone corresponding to the SSD state (EN 1097-6 method)

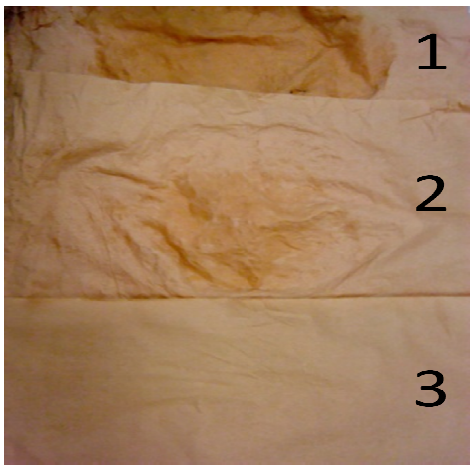

Figure 2-5 Trace of water after successive dryings with absorbent paper (IFSTTAR method)

2.3.2 Density

For each RCA and each granular class, representative samples were pre-dried in the oven at a temperature of 105°C, and then specific density was measured by using helium pycnometer (Micromeritics AccuPyc 1330, Figure 2-6).

Figure 2-6 Helium pycnometer

2.3.3 Cement paste content estimated by the soluble fraction in salicylic acid (SFSA)

A method based on the dissolution of cement paste by salicylic acid was developed in this work to estimate the cement paste content in FRCA as salicylic acid would not dissolve common aggregates such as quartz or limestone.

The experimental protocol used for salicylic acid dissolution is the following:

a) A representative sample (about 100g) is dried at 105°C, then grinded until passing 0.2mm sieve;

b) 0.5g of dried representative sample is then immersed in a solution of 14g of salicylic acid in 80ml of methanol, and stirred during 1h;

c) The solid fraction is filtered on glass filter (Pyrex N°4, pores: 10-16μm) and washed 4 times using methanol (2-3mm high on top of filter);

d) The solid residue is dried in the oven at 70°C for 30 min;

e) The cement paste content (CPC) is then estimated from the soluble fraction in salicylic acid (SFSA) as follows:

$$SFSA(\%) = \frac{M_1 - M_2}{M_1} \times 100 = \frac{\Delta M}{M_1} \times 100 \qquad \text{Equation 2-1}$$

where M_1 is the mass of dried material before dissolution and M_2 is the mass of dried filtrate.

The accuracy of the estimate of CPC by SFSA mostly depends on the amount of soluble versus insoluble phases contained in the cement paste of FRCA. In order to assess the impact of insoluble and soluble phases in salicylic acid and methanol, experiments where performed on pure cement paste with a grey cement Holcim (CEM II 52.5) and a white cement Lafarge Superblanc (CEM I 52.5). These cement pastes made with W/C ratio of 0.5 were studied after 28days of hydration (fraction 1.25/2.5mm) by the X-ray Diffraction (XRD) before and after

dissolution such as RCA-OC1-90 0.63/1.25mm. The samples were tested with XRD using a Bruker D8 Advance diffractometer, according to the diffraction powder method, with a Co $K\alpha_1$ radiation, sweep from 10° to 100° 2θ. The results were compared with the ICDD database. Table 2-3 shows the XRD results before and after dissolution of cements and cement pastes (corresponding XRD diffractograms are shown in Figure 2-7 to Figure 2-14).

Table 2-3 XRD results before and after dissolution in salicylic acid and methanol for cements and pastes

Sample	Insoluble phases
1. After dissolution of white cement	Calcite $Ca(CO_3)$****, Calcium sulfate $Ca(SO_4)$ **, Syngenite $K_2Ca(SO_4)_2.H_2O$*, Calcium Sulfate Hydrate $Ca(SO4)(H_2O)_{0.5}$*, Calcium Aluminum Oxide Ca_3Al2O_6***, Calcite, magnesian $Ca,Mg(CO_3)$**
2. After dissolution of grey cement	Calcite $Ca(CO_3)$****, Brownmillerite $Ca_2(Al,Fe^{+3})_2MgO_5$**, Anhydrite Ca(SO4)**, Gypsum $Ca(SO_4).2H_2O$*, Quartz SiO_2*, Calcium Sulfate Hydrate $Ca(SO_4)(H_2O)_{0.5}$*, Calcium Aluminum Oxide $Ca_3Al_2O_6$***
3. Before dissolution of white cement paste	Portlandite $Ca(OH)_2$****, Larnite Ca_2SiO_4**, Calcite $Ca(CO_3)$*, Hatrurite Ca_3SiO_5*, Calcium Silicate Hydrate $Ca_{1.5}SiO_{3.5}xH_2O$*
4. Before dissolution of grey cement paste	Portlandite $Ca(OH)_2$****, Calcite $Ca(CO_3)$***, Larnite Ca_2SiO_4**, Calcium Silicate Ca_2SiO_4* Calcium Aluminum Oxide Carbonate Hydroxide Hydrate (AFm hemi carbonate) $Ca_4Al_2O_6(CO_3)_{0.5}(OH).11.5H2O$**, Brownmillerite $Ca_2(Al,Fe^{+3})_2O_5$*
5.After dissolution of white cement paste	Calcite $Ca(CO_3)$****, Calcium Sulfate Hydrate $Ca(SO_4).0.5H_2O$***, Bassanite $Ca(SO_4).0.5H_2O$***
6.After dissolution of grey cement paste	Calcite $Ca(CO_3)$****, Quartz SiO_2* Calcium Aluminum Oxide $Ca_3Al_2O_6$*, Brownmillerite $Ca_2(Al,Fe^{+3})_2O_5$**, Calcium Sulfate Hydrate $Ca(SO_4).0.5H_2O$*, Calcium Aluminum Iron Oxide $Ca_3(Al,Fe)_2O_6$*
7. Before dissolution of RCA-OC1-90 0.63/1.25mm	Calcite $Ca(CO_3)$****, Quartz SiO_2**, Portlandite $Ca(OH)_2$**
8. After dissolution of RCA-OC1-90 0.63/1.25mm	Calcite $Ca(CO_3)$****, Quartz SiO_2**, Dolomite $CaMg(CO_3)_2$*

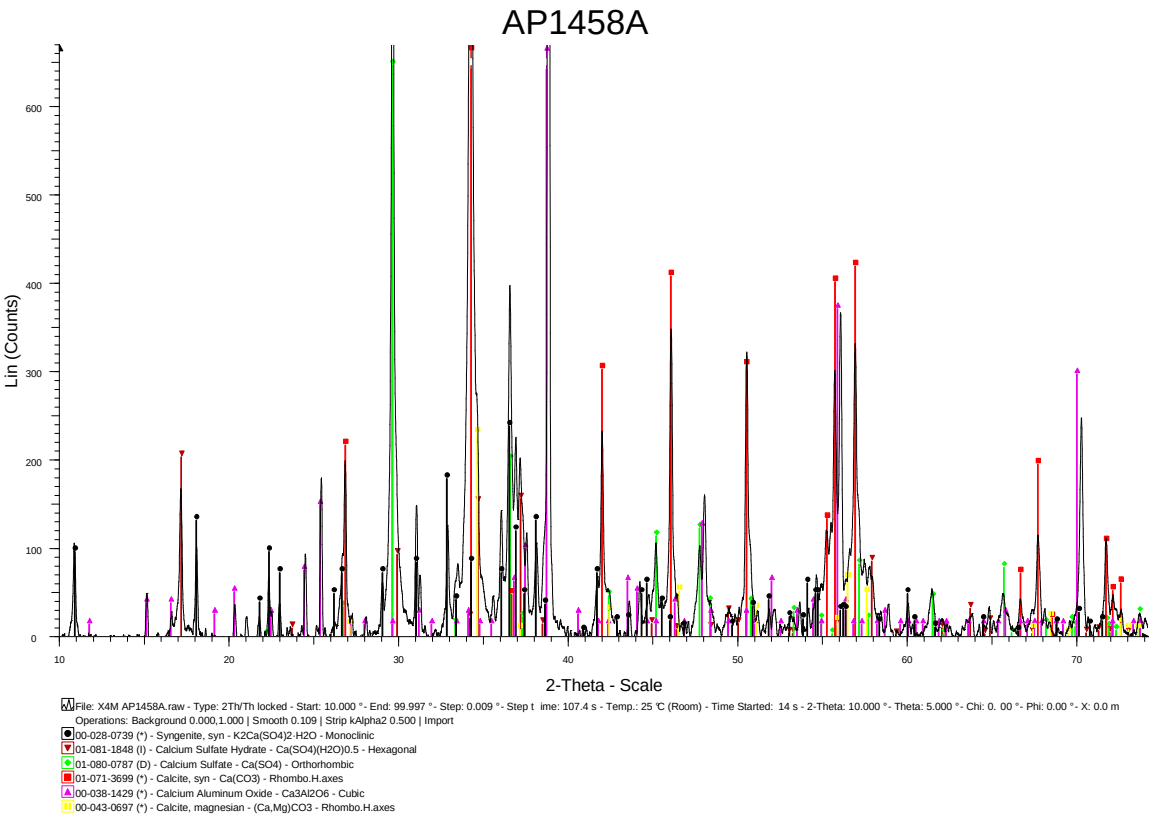

Figure 2-7After dissolution of white cement

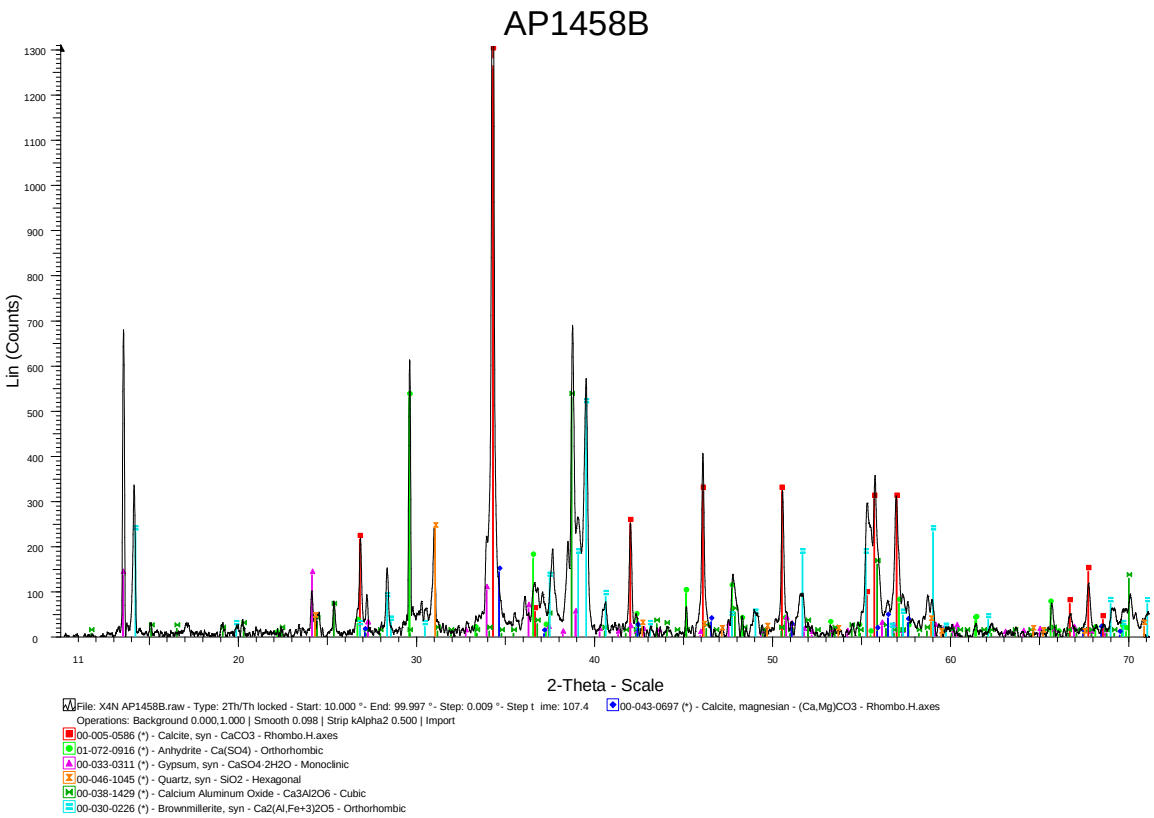

Figure 2-8 After dissoluion of grey cement

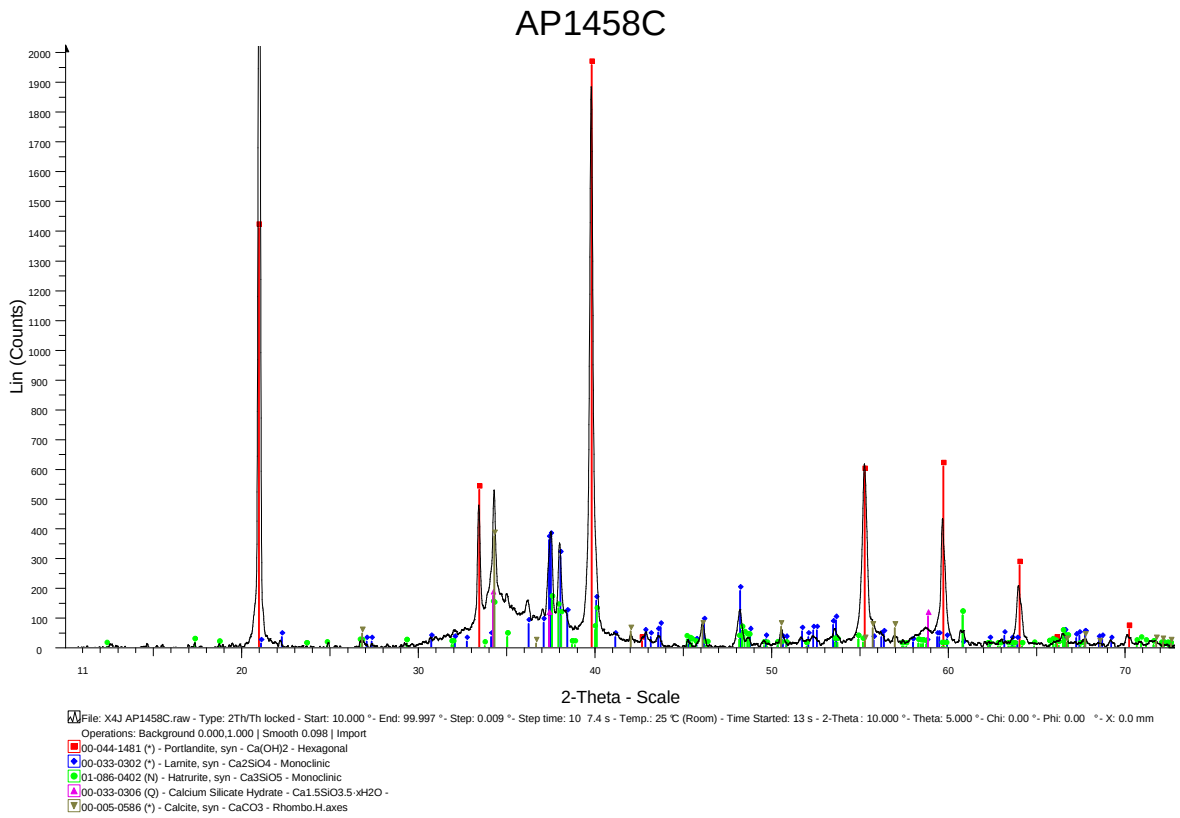

Figure 2-9 Before dissoluion of white cement paste

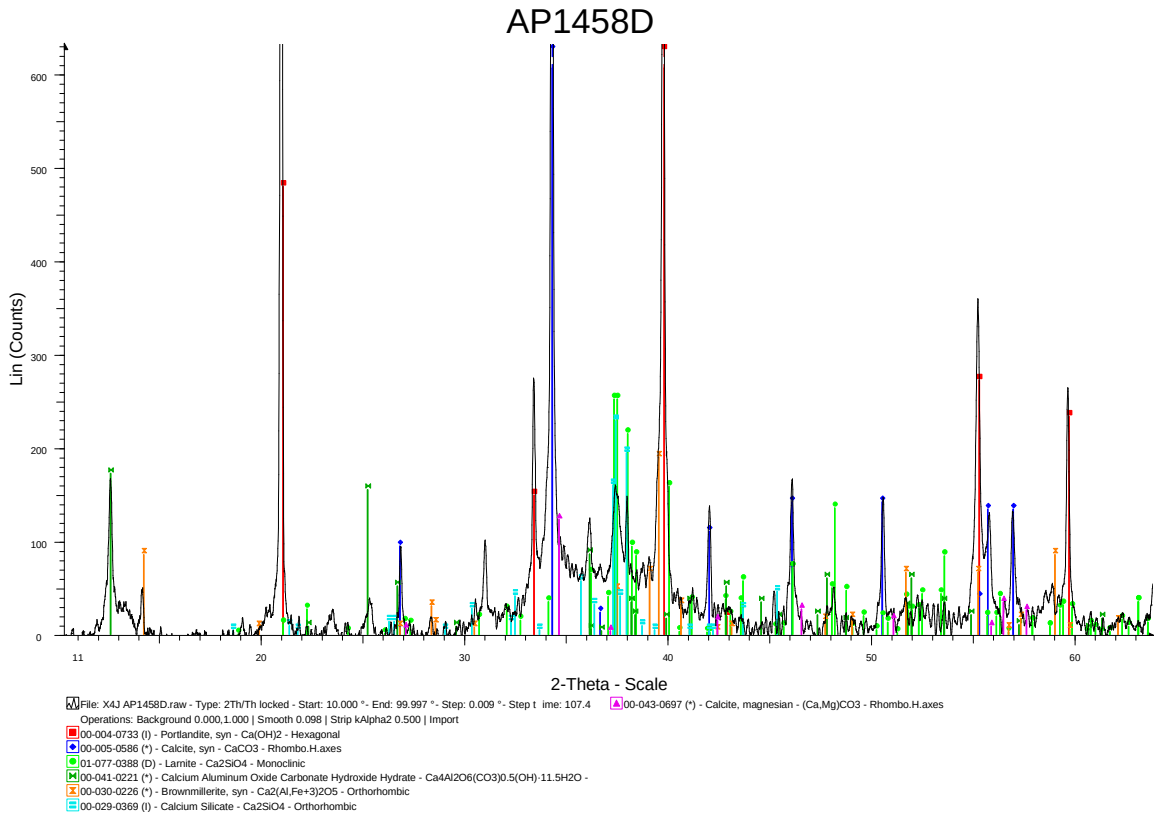

Figure 2-10 Before dissoluion of grey cement paste

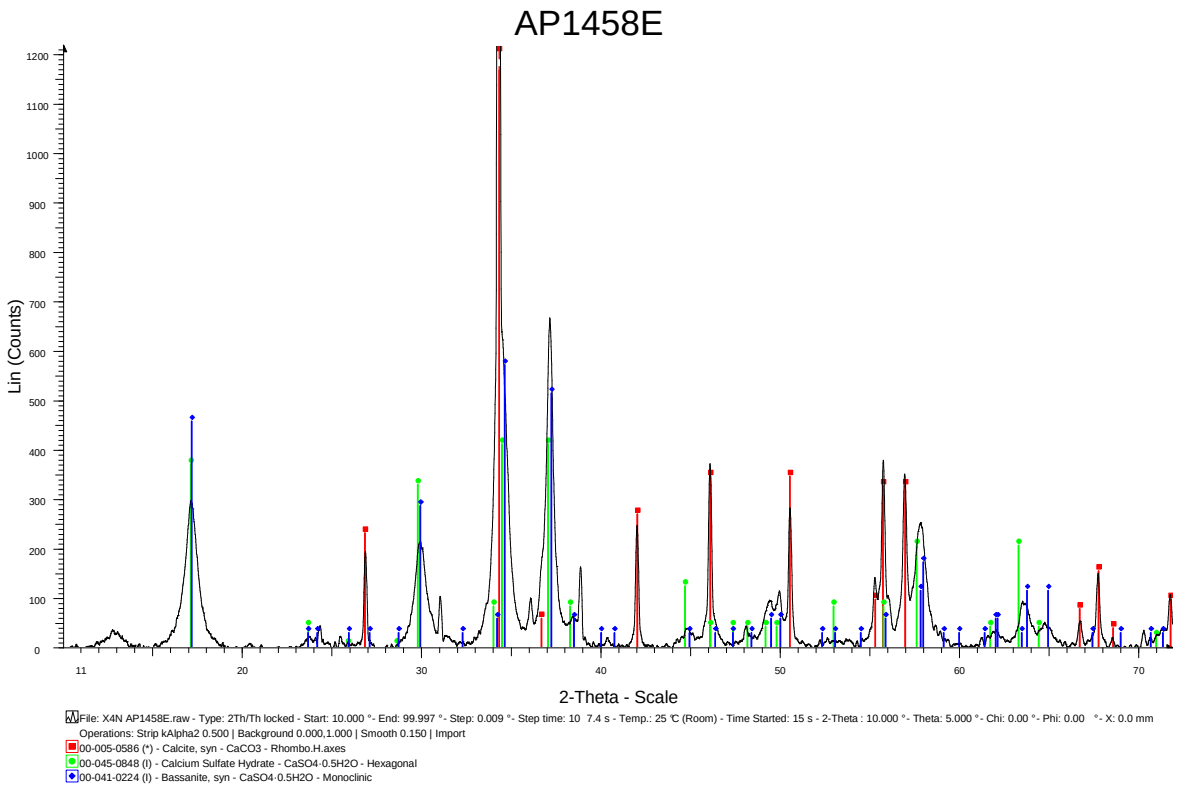

Figure 2-11 After dissoluion of white cement paste

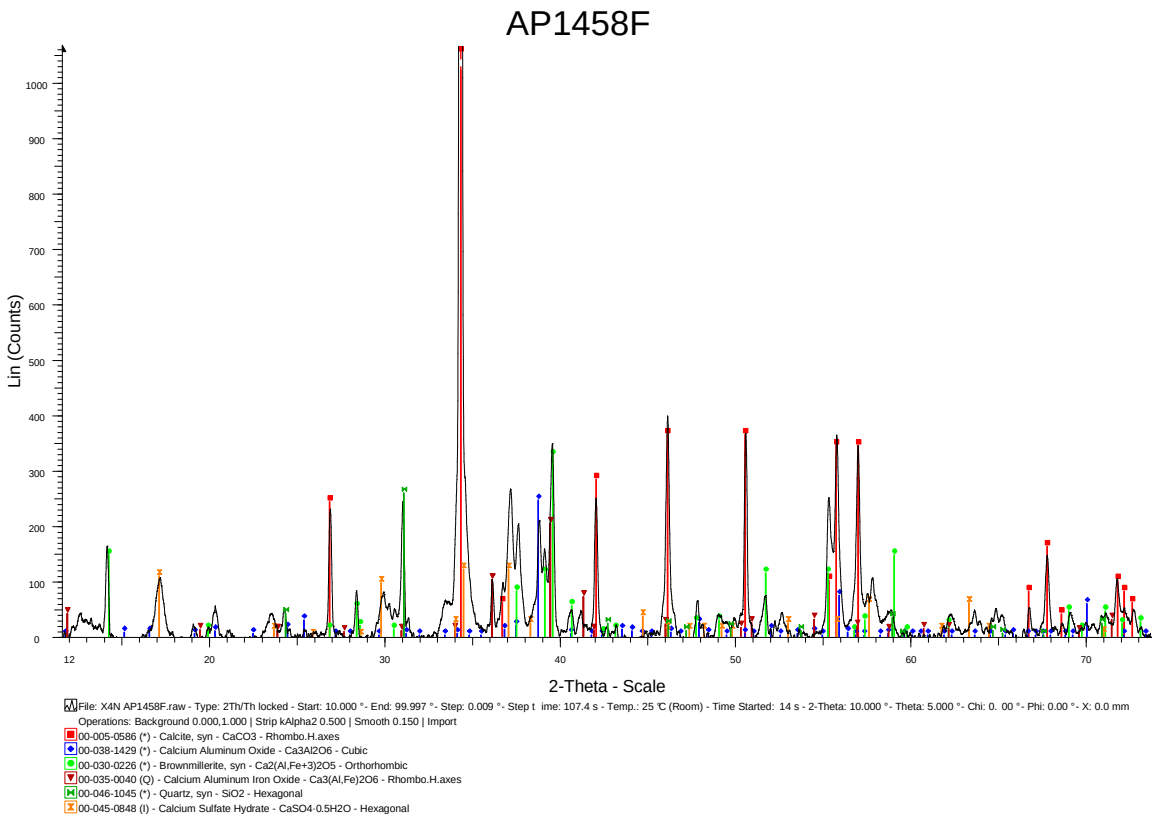

Figure 2-12 After dissoluion of grey cement paste

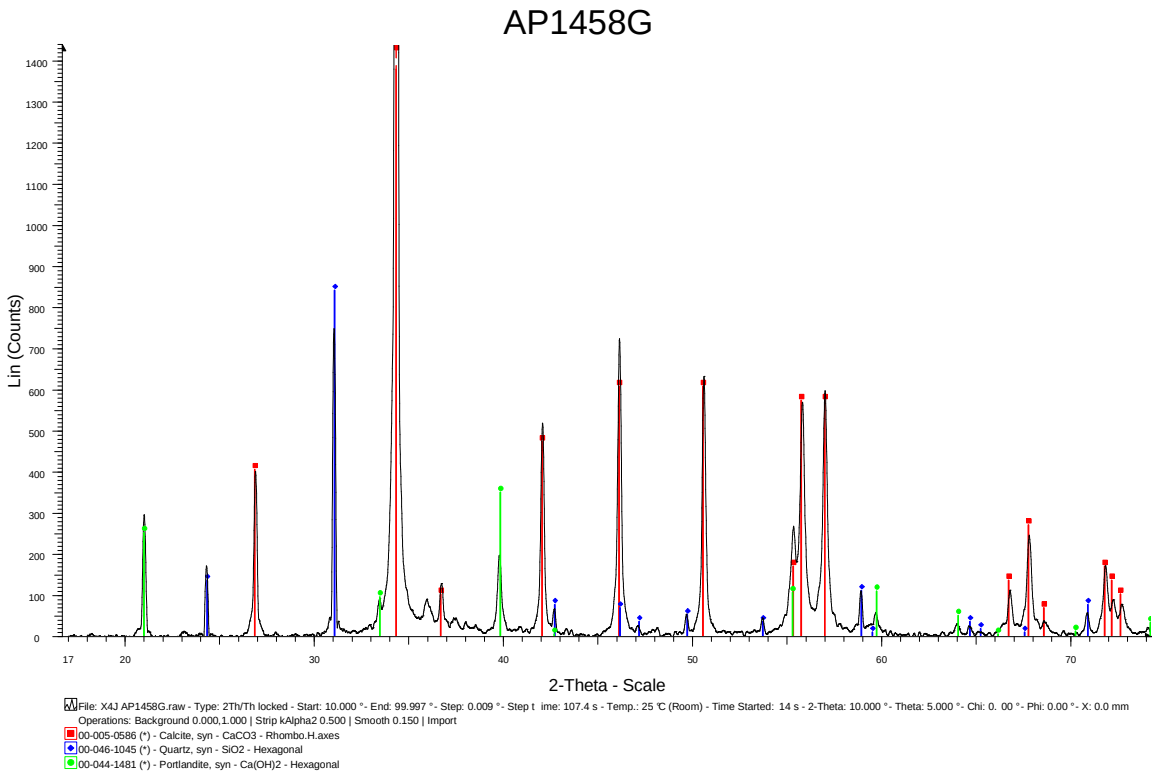

Figure 2-13 Before dissoluion of RCA-OC1-90 0.63/1.25mm

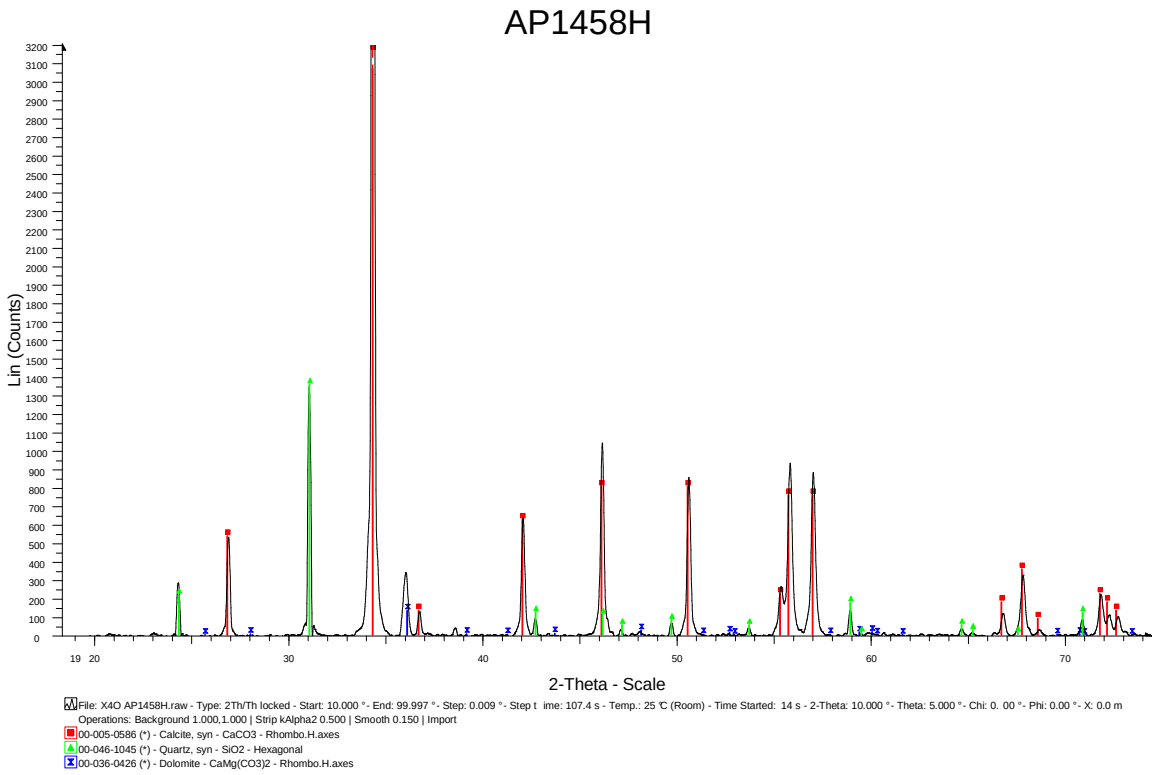

Figure 2-14 After dissoluion of RCA-OC1-90 0.63/1.25mm

From these results, salicylic acid is allowed to dissolve most of the phases contained in OPC cement paste but not of the main phases contained in natural aggregates and especially limestone (Table 2-4) [140-144]. Thus apart from calcium aluminate phases and their corresponding hydrates, all cement paste should be dissolved.

Table 2-4 Insoluble and soluble phases in salicylic acid and methanol

Insoluble phases	Soluble phases
C_3A, C_4AF,Gypsum	C_2S, C_3S
Quartz, Dolomite	CaO, $Ca(OH)_2$
Calcite (limestone)	C-S-H
C_3AH_6, Calcium monosulfoaluminate hydrate	Ettringite

Preliminary tests were carried out on natural aggregates alone and the two cement pastes already studied in XRD. Two kinds of natural aggregates were used: a crushed calcareous aggregate from Tournai (the same that was used for the production of concretes OC1, OC2 and OC3), and a siliceous sand complying with standard EN 196-1 [145]. Table 2-5 presents the results after dissolution. As can be seen, 95.6% of white cement paste and 62.99% of grey cement paste were dissolved while only 0.83% of siliceous aggregate and 3.21% of calcareous aggregates were dissolved. For white cement paste, soluble fraction in salicylic acid (SFSA) is almost identical to the cement paste content (CPC). This is the reason why white cement was chosen for the manufacture of original concretes. For the grey cement paste, as can be seen in Table 2-1, the cement has a larger content of C_3A, C_4AF and Calcite which do not dissolve in salicylic acid, so SFSA corresponds to only 62.99% of CPC. For grey cement paste, SFSA is always lower than CPC. So for industrial RCA generally containing a grey cement paste, SFSA does not give the exact value of CPC, but it will be demonstrated later that for a given RCA, SFSA is sufficient to correlate CPC with the other properties of RCA. This method was also chosen because it is easy to perform and a very small standard deviation is observed for all materials that confirms the robustness of the method.

Table 2-5 Results of preliminary tests with salicylic acid dissolution-1h (mass dissolved %)

	Test 1	Test 2	Test 3	Average value	Standard deviation value
White cement paste	95.46	96.35	94.89	95.57	0.74
Grey cement paste	62.56	63.08	63.33	62.99	0.39
Siliceous sand	0.76	0.86	0.88	0.83	0.06
Calcareous sand	3.42	3.03	3.18	3.21	0.20

2.3.4 Thermogravimetric analysis

Representative samples were pre-dried in the oven at a temperature of 105°C. A sample powder was then obtained by grinding the material to a maximum size of 0.2mm, and a thermogravimetric analysis with analysis of gas by mass spectrometry (MS) was then carried out using TGA NETZSCH STA449 F3 with QMS 403D (Figure 2-15). The heating was composed of three different phases:

- From ambient temperature to 105°C: heating rate of 2°C/min
- 30 mins at a constant temperature of 105°C
- From 105 to 1100°C, heating rate of 3°C/min.

Figure 2-15 TGA used machine

2.3.5 Mass loss between 105 and 600°C

A thermal method was used to determine the mass loss between 105 and 600°C ($ML_{105\text{-}600}$). $ML_{105\text{-}600}$ corresponds mainly to the loss of bound water of hydrated part of the cement paste; indeed, siliceous and calcareous aggregates do generally not decompose below 600°C. The experimental protocol used is as follows:

a) representative samples are grinded until passing 0.2mm sieve;

b) the grinded representative samples are pre-dried in the oven at 105°C, and constant mass (M_{105}) is achieved after 1 day;

c) dried samples are put in the oven at 600°C and constant mass (M_{600}) is achieved after 1 day;

d) then the $ML_{105\text{-}600}$ is calculated as follows:

$$ML_{105-600}(\%) = \frac{M_{105} - M_{600}}{M_{105}} \times 100 \qquad \text{Equation 2-2}$$

In order to validate this method, thermogravimetric Analysis (TGA) of cement paste, calcareous sand, siliceous mortar, and calcareous mortar (w/c ratio used was 0.5 for mortars and paste) were carried out (Figure 2-16). This figure shows that calcareous sand and mortar decarbonize over 600°C whereas most of the pure cement paste is dehydrated below 600°C. Indeed, several authors have shown that the dehydration of C-S-H is about 180-300°C and the dehydration of CH (Portlandite) is about 450-550°C [146-148]. Therefore, a heating at 600°C has been chosen for the measurement of $ML_{105\text{-}600}$ as it allows avoiding the decarbonation of aggregates. The mass loss at 600°C comes only from the dehydration of cement paste hydrates, and not from aggregates. It is therefore a good indicator of the part of cement paste corresponding to the hydrates whereas salicylic acid method also accounts for the unhydrated cement in the material.

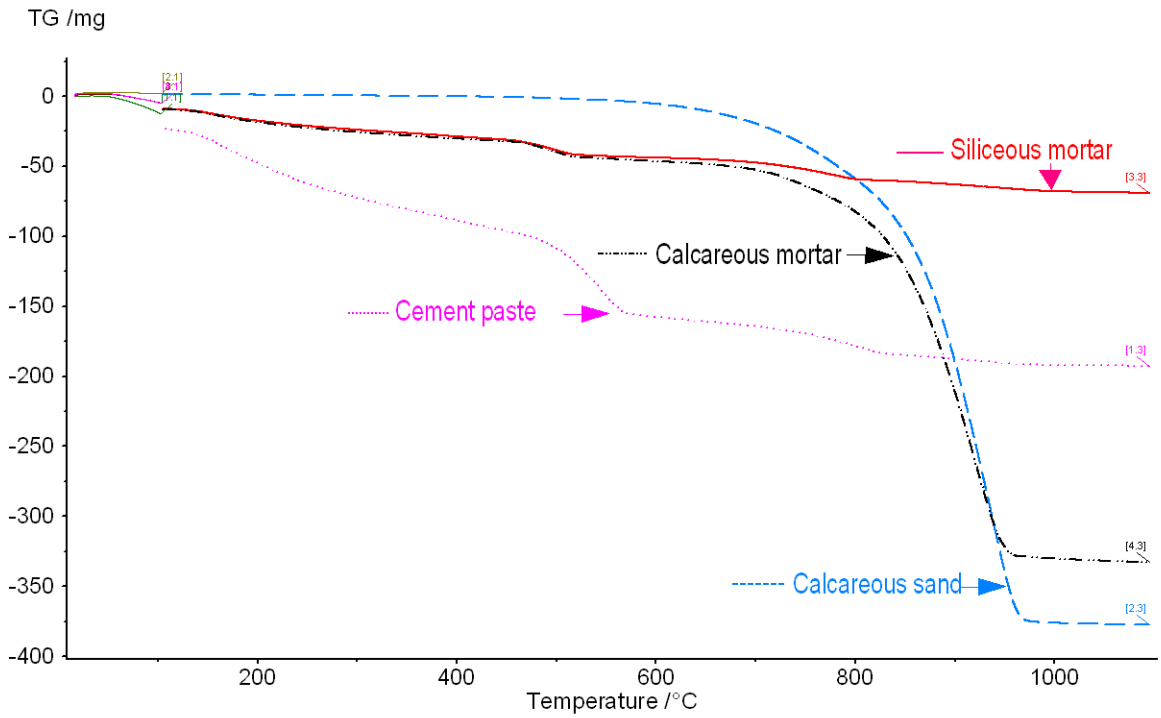

Figure 2-16 TGA results obtained on cement paste, calcareous sand, siliceous mortar and calcareous mortar

2.3.6 BET analysis

The specific surface area (SSA) of each granular class of each FRCA was measured by using BET (Brunauer-Emmett-Teller) analysis using N_2 adsorption (Micromeritics ASAP 2010 Figure 2-17). Representative samples were pre-dried in the oven at a temperature of 105°C and then cooled down in desiccators to room temperature. These samples were then used in the BET analysis. BJH (Barrett-Joyner-Halenda) analysis was also employed to determine pore area and specific pore volume on desorption isotherms [149].

Figure 2-17 BET analysis machine

2.4 Theoretical equations to calculate cement paste content, soluble fraction by salicylic acid and mass loss ($ML_{105-600}$)

Experimental methods for the measurement of SFSA and $ML_{105-600}$ have been shown in the previous section. In order to better understand the results, simple models allowing to calculate the cement paste content, to estimate the SFSA and the mass loss due to bound water are presented below.

Firstly, we assume that all the hydrates and unhydrated cement can dissolve in salicylic acid to calculate the CPC (in that case SFSA is equal to CPC). In the measurement of cement paste content by salicylic acid dissolution, as shown in Equation 2-1, dissolved phases (ΔM) can be considered as the mass of unhydrated cement and of hydrates. For a given percentage of reaction (α), mass of unhydrated cement (M_{uc}) and mass of hydrates (M_h) can be calculated from initial mass of cement (M_{ic}) respectively as shown in Equation 2-3 and Equation 2-4. As CPC or SFSA are considered for aged cement paste in the RCA, the kinetics of hydration of all cement phases is defined as being identical so the gain of mass due to hydration

corresponds to the stoichiometric water to cement ratio $(W/C)_{st}$ at a given percentage of reaction.

$$M_{uc} = (1-\alpha) \times M_{ic} \quad \text{Equation 2-3}$$

$$M_h = \alpha \times M_{ic} \times (1+(W/C)_{st}) \quad \text{Equation 2-4}$$

$(W/C)_{st}$ can be estimated from the mineralogical composition of the cement (see annex 1).

Then considering that aggregates are not dissolved, ΔM is depending on both (W/C)st as shown in Equation 2-5, the mass before dissolution (M_1) that also depends on ΔM and the mass of aggregate (M_a) as shown in Equation 2-6.

$$\Delta M = (1-\alpha) \times M_{ic} + \alpha \times M_{ic} \times (1+(W/C)_{st}) = (1+(W/C)_{st}\alpha) \times M_{ic} \quad \text{Equation 2-5}$$

$$M_1 = M_a + \Delta M = M_a + (1+(W/C)_{st}\alpha) \times M_{ic} \quad \text{Equation 2-6}$$

Cement paste content (CPC) can be calculated from Equation 2-7;

$$CPC(\%) = \frac{\Delta M}{M_1} \times 100 = \frac{(1+(W/C)_{st}\alpha) \times M_{ic}}{M_a + (1+(W/C)_{st}\alpha) \times M_{ic}} \times 100 \quad \text{Equation 2-7}$$

Hydrate paste content (HPC) can also be calculated from Equation 2-8;

$$HPC(\%) = \frac{M_h}{M_1} \times 100 = \frac{(1+(W/C)_{st})\alpha \times M_{ic}}{M_a + (1+(W/C)_{st}\alpha) \times M_{ic}} \times 100 \quad \text{Equation 2-8}$$

As shown previously dissolution in salicylic acid underestimates CPC as some phases are not dissolved. It is possible to estimate SFSA by making some corrections. First, the amount of insoluble phases contained in the cement has to be removed from M_{ic}. This can be done by adding a parameter A that represents the relative mass of soluble phases in the cement. Thus

A ranges from 0 to 1 and it can be calculated from the mineralogical composition of the cement or even better by an experiment of dissolution in salicylic acid on the cement as presented previously. However some of the insoluble phases such as C_3A (C_4AF) will hydrate whereas others such as calcite can be considered as inert in a first approximation. Thus another mass ratio C is defined; it corresponds to the relative mass of C_3S, C_2S, C_3A, C_4AF in the cement that will lead to the formation of hydrates that are soluble in salicylic acid such as C-S-H, portlandite and ettringite (see Annex 1). The mass gain thanks to hydration is also modified as some hydrates and especially AFm phases are not soluble. In a first approximation, it can be considered that hydration forms 3/4 of AFm and 1/4 of AFt phases, thus the stochiometric W/C has to be corrected by a factor B (being lower than 1) to account for the undissolved AFm phases (see annex 1). B can be estimated by calculation when the mineralogical composition of the cement is known and using the same chemical equations as those that were used to calculate the stochiometric W/C ratio (see annex 1). Thus the mass loss of the cement paste induced by dissolution in salicylic acid (ΔM_{SA}) can be written as Equation 2-9;

$$\Delta M_{SA} = (1-\alpha)\times A\times M_{ic} + \alpha\times M_{ic}\times C + \alpha\times M_{ic}\times\left(\left(B\times\left(W/C\right)_{st}\right)\right)$$
$$\Delta M_{SA} = \left(A+\alpha\left(C+B\left(W/C\right)_{st}-A\right)\right)\times M_{ic} \qquad \text{Equation 2-9}$$

Therefore the SFSA can be written as Equation 2-10. A, B and C are equal to 1 if all phases are soluble and thus similar equation as Equation 2-7 is found corresponding to a completely soluble cement paste.

$$SFSA(\%) = \frac{\Delta M_{SA}}{M_1}\times 100 = \frac{\left(A+\alpha\left(C+B\left(W/C\right)_{st}-A\right)\right)\times M_{ic}}{M_a+\left(1+\left(W/C\right)_{st}\alpha\right)\times M_{ic}}\times 100 \qquad \text{Equation 2-10}$$

$ML_{105\text{-}600}$ which corresponds to the bound water content of hydrated cement paste (M_{wh}) in FRCA can be calculated from Equation 2-11.

$$ML_{105-600}(\%) = \frac{M_{wh}}{M_1} \times 100 = \frac{(W/C)_{st}\,\alpha \times M_{ic}}{M_a + (1 + (W/C)_{st}\,\alpha) \times M_{ic}} \times 100 \qquad \text{Equation 2-11}$$

2.4.1 Application to the theoretical equations to calculate cement paste content and mass loss ($ML_{105\text{-}600}$) to OC1, OC2 and OC3

From the known compositions of original concrete (OC1, OC2 and OC3), the equivalent concrete composition (considering coarse aggregates and sand for M_a), mortar composition (considering sand for M_a), and paste composition are determined. Considering the stoichiometric water to cement ratio $(W/C)_{st}$ for the white portland cement is 0.44 (see annex 1), we can calculate the CPC and $ML_{105\text{-}600}$ based on these three kinds of equivalent compositions. Figure 2-18 show the calculated CPC and HPC based on equivalent compositions of concrete, mortar and paste for OC1. As it can be seen, both CPC and HPC increase as the hydration degree increases. The same trends are obtained for the other original concretes (OC2 and OC3). The CPC values based on concrete are lower than that with mortar and paste composition. Figure 2-19 and Figure 2-20 show the calculated value of CPC and HPC based on equivalent composition of mortar and concrete for OC1, OC2 and OC3 respectively. The CPC values increase with the increase of cement quantity. It can be noticed that the same CPC can be obtained with different hydration degrees and different cement quantities.

Figure 2-21 shows the calculated value $ML_{105\text{-}600}$ based on equivalent compositions of concrete, mortar and paste for OC1. Figure 2-22 shows the calculated value $ML_{105\text{-}600}$ based

on equivalent composition of mortar and concrete for OC1, OC2 and OC3. The $ML_{105\text{-}600}$ based on concrete is lower than the values obtained with mortar and paste composition. The value of $ML_{105\text{-}600}$ increases with the hydration degree.

Theoretical calculations of CPC and $ML_{105\text{-}600}$ show that the CPC and $ML_{105\text{-}600}$ increase with hydration degree. These calculations only concern equivalent compositions, the variations of CPC and $ML_{105\text{-}600}$ with particle size of RCA are not taken into account.

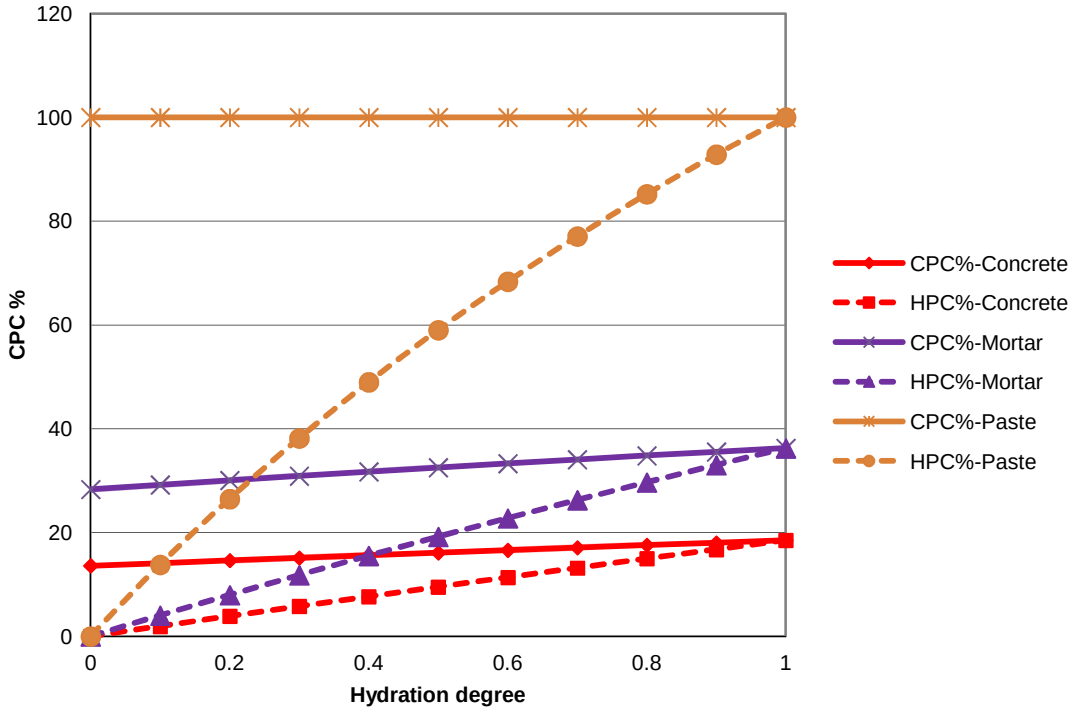

Figure 2-18 CPC as a function of hydration degree for OC1

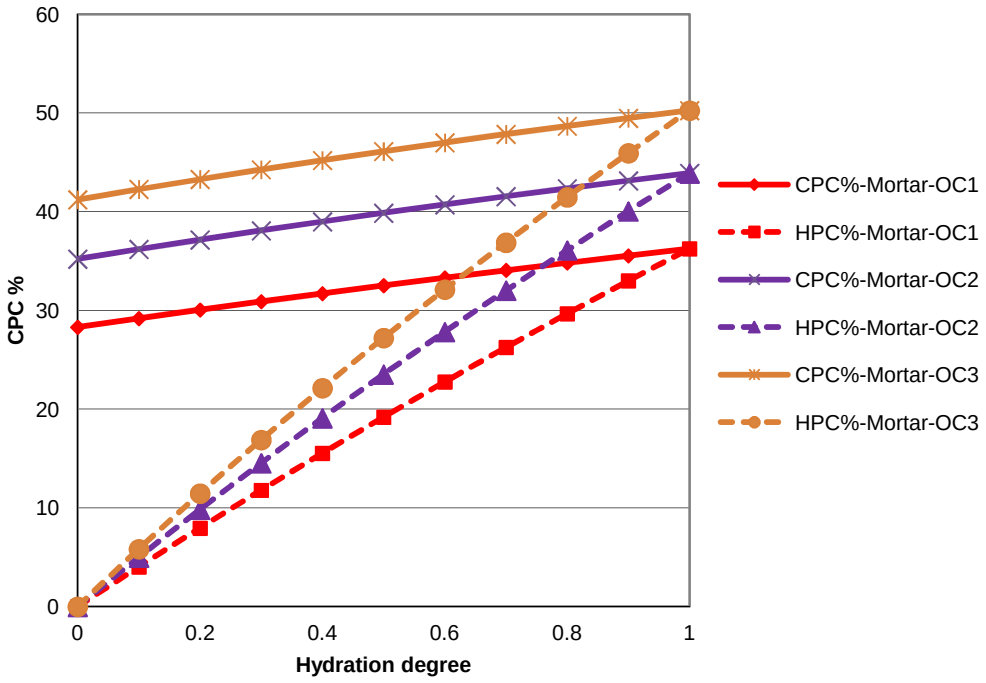

Figure 2-19 CPC based on mortar for OC1, OC2 and OC3 as a function of hydration degree

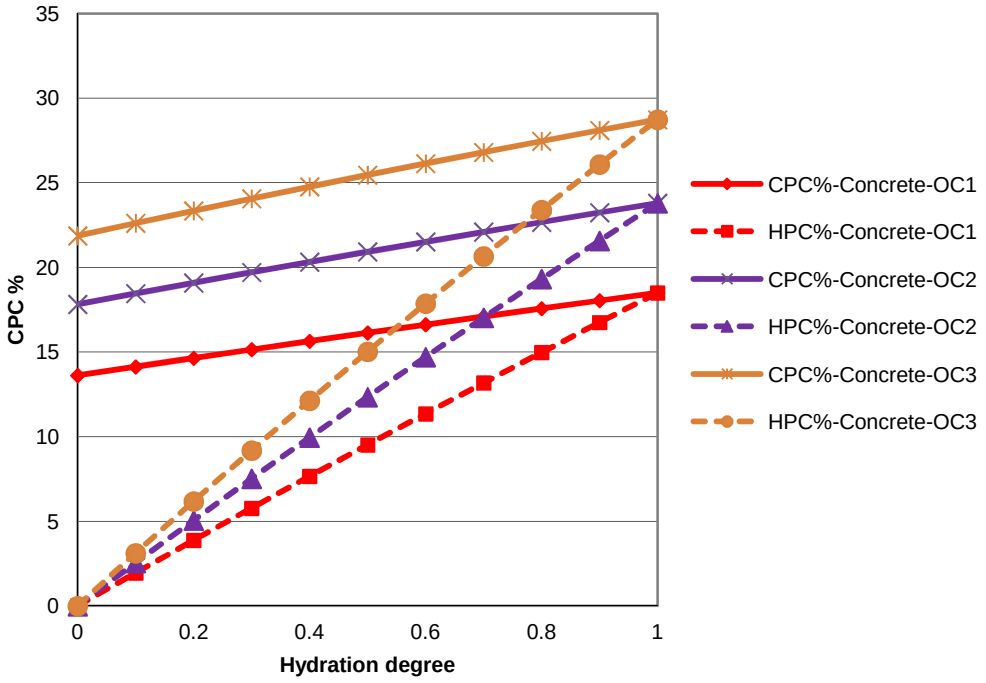

Figure 2-20 CPC based on concrete for OC1, OC2 and OC3 as a function of hydration degree

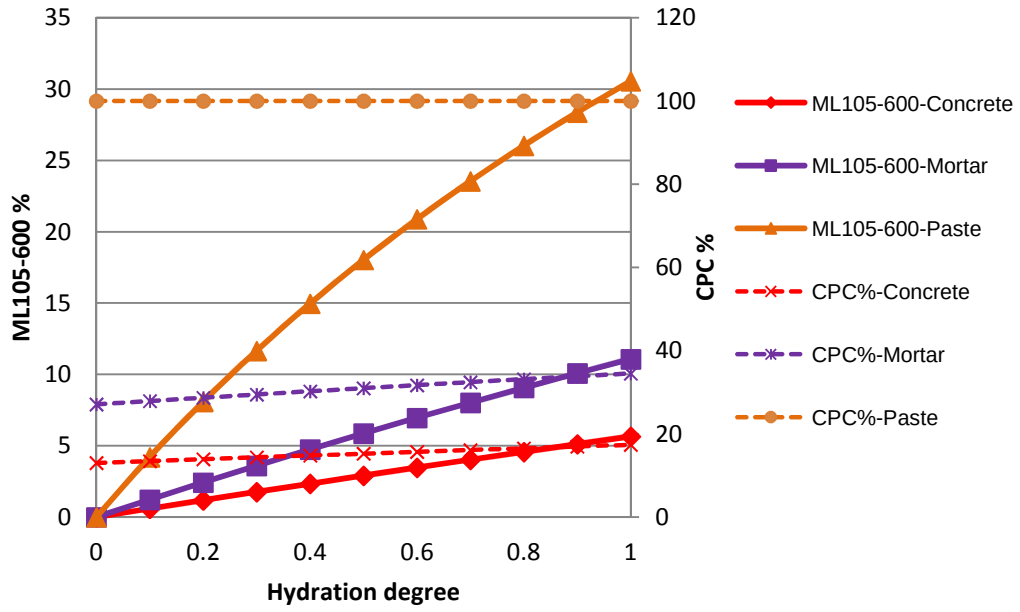

Figure 2-21 $ML_{105\text{-}600}$ and CPC as a function of hydration degree for OC1

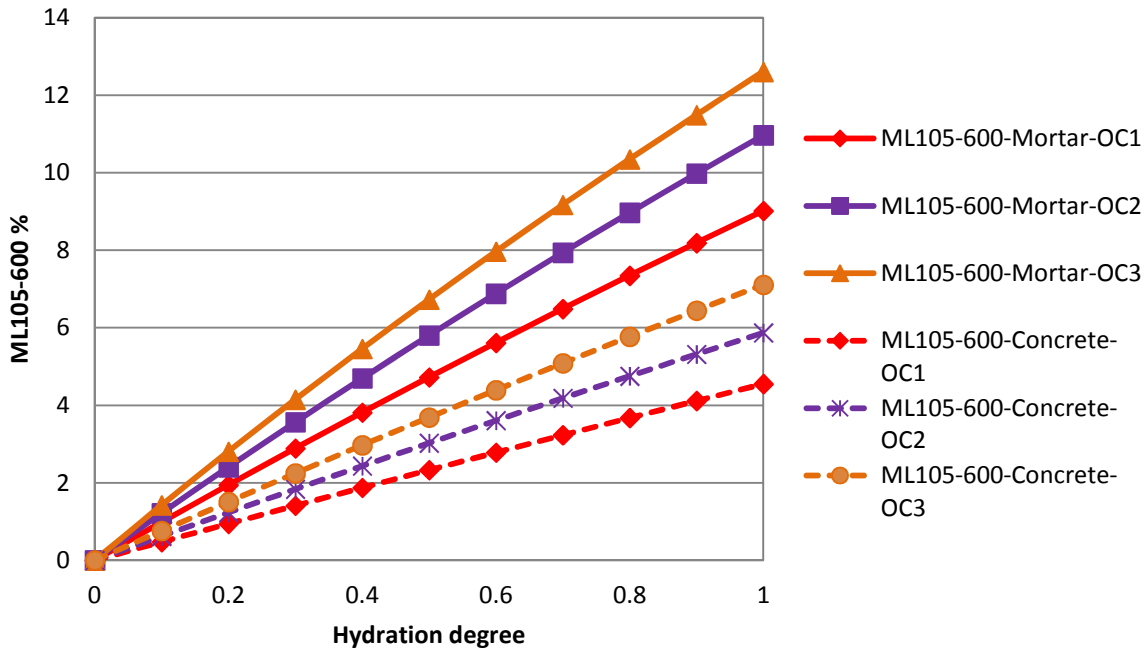

Figure 2-22 $ML_{105\text{-}600}$ based on mortar and concrete for OC1, OC2 and OC3 as a function of hydration degree

2.4.2 Application the theoretical equations to calculate soluble fraction by salicylic acid for the two cements used

The soluble fraction in salicylic acid (SFSA) can be estimated according to Equation 2-10. Coefficients A, B and C are shown in Annex 1. Figure 2-23 shows the comparison of calculated CPC and SFSA for the cement pastes manufactured with white and grey cements (W/C=0.5) which is used for the preliminary salicylic acid dissolution tests. As it can be seen, the values obtained of SFSA after considering only the soluble fraction are much lower than CPC for the grey cement, while they are similar for the white cement. The lower values obtained for grey cement might be due to the large amount of calcite and C_4AF. In the next chapter, we will show that the SFSA is sufficient to improve the measurement of properties of FRCA. If considering the hydration degree is 0.7 for both cement pastes used for the preliminary salicylic acid dissolution experiment, the calculated values of SFSA (96.4% for white cement paste, and 67.7% for grey cement paste) are slightly larger than observed in experimental results (95.6% for white cement paste, and 63.0% for grey cement paste). The difference is reasonable taking into account the simplification used for our calculation.

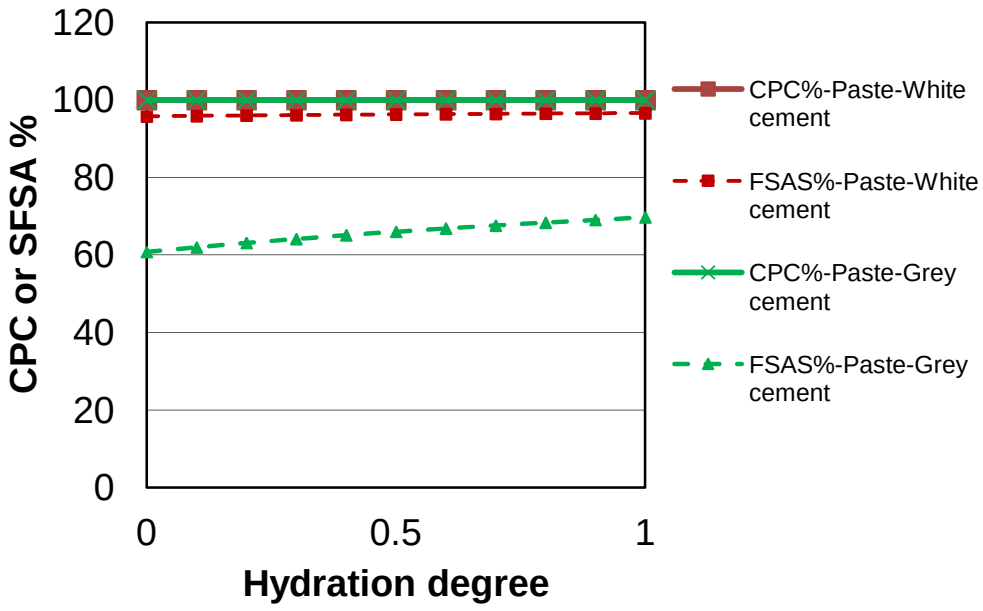

Figure 2-23 Comparison of calculated CPC and SFSA for the two cement pastes used in preliminary tests

Figure 2-24 and Figure 2-25 show the comparison of calculated CPC and SFSA for OC1 with the white and grey cements respectively. As it can be seen, the values obtained of SFSA after considering only the soluble fraction are much lower than CPC for the grey cement whatever considering concrete, mortar and paste compositions, while little differences are obtained for the white cement. The greater differences obtained for grey cement might be due to the large amount of calcite and C_4AF.

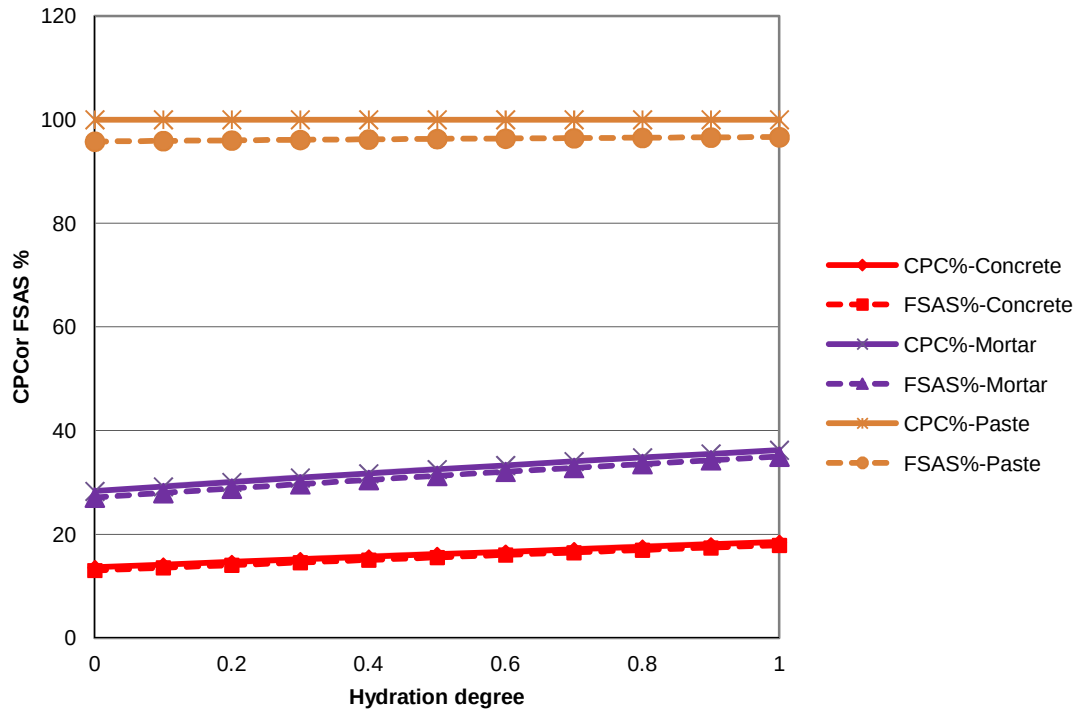

Figure 2-24 Calculated CPC and SFSA for OC1 as a function of hydration degree for white cement

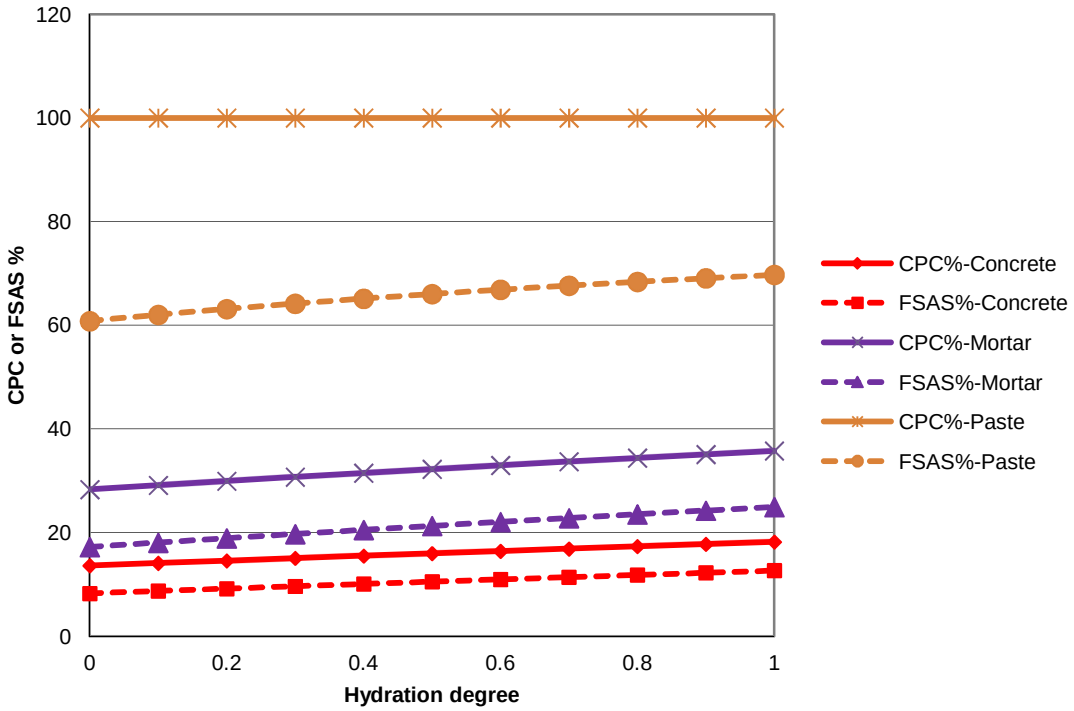

Figure 2-25 Calculated CPC and SFSA for OC1 as a function of hydration degree for grey cement

2.5 Experimental results

2.5.1 SFSA

Figure 2-26 and Table 2-6 present the variation of SFSA as a function of granular class for all the FRCA studied. The value of SFSA is the average of values obtained with three tests. The calculated value is obtained by the theoretical model based on the concrete and mortar compositions, considering that the hydration degrees at 28days and 90days are 0.7 and 0.9 respectively. As it can be seen, all experimental values are between the calculated values based on mortar and concrete compositions for all the studied fractions, which indicates that FRCA not only contain crushed mortar but also part of natural coarse aggregate of original concrete.

Table 2-6 SFSA of studied RCA

Fractions	RCA-OC1-28	RCA-OC1-90	RCA-OC2-28	RCA-OC2-90	RCA-OC3-28	RCA-OC3-90
0-0.63	26.54	27.28	32.66	39.01	37.31	38.36
0.63-1.25	24.98	25.72	29.51	32.63	35.68	35.86
1.25-2.5	23.25	23.60	27.06	27.79	31.53	33.22
2.5-5	19.35	20.76	23.16	25.35	28.29	29.34
Calculated value on concrete	16.49	17.42	21.31	22.44	25.84	27.14
Calculated value on mortar	32.85	34.32	40.06	41.65	46.14	47.77

The average standard deviation of SFSA for all the tests is 0.62. Figure 2-26 shows that the standard deviation is somewhat smaller than the size of symbols in the figure (example presented for RCA-OC1-28 and RCA-OC3-90). As can be seen in this figure, SFSA is higher as the average particle size decreases. A reasonable linear relation between SFSA and granular class is obtained. The correlation coefficients obtained (R^2) range from 0.82 to 1.00 (Table 2-7, the b value corresponds to the SFSA of the very fine fraction when the size of particle trends towards zero).

For all the FRCA, the values obtained for RCA-90 are slightly larger than those obtained for RCA-28. This can be attributed to the longer curing time in water (it is also confirmed by the theory calculation). The longer the curing in water, the higher hydration degree of cement paste, and then the higher the SFSA in the parent concrete. Indeed, the mass of hydrated cement paste is higher than the mass of initial anhydrous cement, because an additional quantity of water is added to the initial anhydrous cement during hydration.

For a given RCA, CPC is the cement paste content by mass of the considered granular fraction. If ρ_{NA} is the density of natural aggregates and ρ_{CP} is the density of cement paste, the cement paste content by volume of the considered granular fraction (noted X in the following), can be calculated with Equation 2-12:

$$CPC = \frac{1}{1+(\frac{1}{X}-1)\times\frac{\rho_{NA}}{\rho_{CP}}}$$ Equation 2-12

As can be seen with Equation 2-12, the cement paste content by mass (CPC) depends on volume of cement paste and densities of cement paste and natural aggregate. The larger values of SFSA obtained for RCA-OC2 comparatively to RCA-OC1 can be attributed to the higher volume of cement paste in the original composition (same W/C ratio). Similarly, the larger values obtained for RCA-OC3 comparatively to RCA-OC2 can be attributed to a lower W/C ratio in the original composition (same volume of cement paste), leading to a denser cement paste and therefore to a larger mass of cement paste for a similar paste volume (the theoretical calculation shows similar results). SFSA is almost identical to cement paste content (CPC) for the white cement. Therefore the cement paste content (or SFSA) of FRCA is influenced by the W/C ratio, the cement paste volume, and hydration degree of the original concrete.

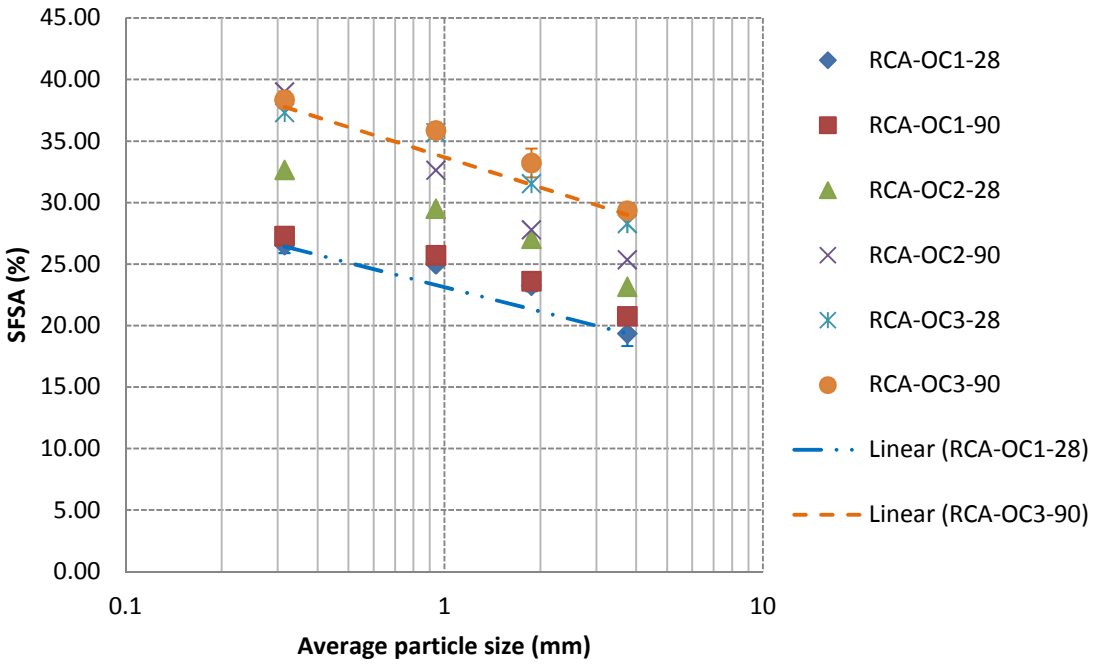

Figure 2-26 SFSA as a function of the average size of the four different granular classes considered (0/0.63, 0.63/1.25, 1.25/2.5, 2.5/5mm)

Table 2-7 Coefficients of the linear relationships between SFSA and particle sizes (y=ax+b)

Fractions	a	b	R^2
RCA-OC1-28	-2.06	27.08	1.00
RCA-OC1-90	-1.87	27.56	0.99
RCA-OC2-28	-2.63	32.62	0.96
RCA-OC2-90	-3.64	37.46	0.82
RCA-OC3-28	-2.67	37.79	0.96
RCA-OC3-90	-2.55	38.58	0.98

2.5.2 Content of paste using $ML_{105\text{-}600}$ based on thermal method

$ML_{105\text{-}600}$ corresponds essentially to the bound water of hydrated cement paste. Figure 2-27 and Table 2-8 show the $ML_{105\text{-}600}$ of FRCA based on thermal method as a function of granular class. The value of $ML_{105\text{-}600}$ is the average of values obtained with three tests. The calculated value is obtained by the theoretical model based on the concrete and mortar compositions, considering that the hydration degree of 28days and 90days are 0.7 and 0.9 respectively. As it can be seen, all experimental values are between the calculated values based on mortar and concrete compositions for all the studied fractions (except for the finer fraction 0-0.63mm of RCA-OC3-28), which indicates that there is part of natural coarse aggregate of original concrete crushed in the FRCA. The standard deviations of these tests are also shown in the figure (example presented for RCA-OC1-28 and RCA-OC3-90), the average standard deviation for all the tests is 0.32.

Table 2-8 $ML_{105\text{-}600}$ experiment results and calculated values of studied RCA

Fractions	RCA-OC1-28	RCA-OC1-90	RCA-OC2-28	RCA-OC2-90	RCA-OC3-28	RCA-OC3-90
0-0.63	6.83	8.13	7.17	10.63	7.83	11.59
0.63-1.25	6.44	7.66	6.83	9.21	7.48	10.53
1.25-2.5	6.16	7.23	6.26	8.40	6.77	9.46
2.5-5	5.96	7	6.03	8.05	6.26	8.67
Calculated value based on concrete	4.03	5.12	5.2	6.59	6.31	7.97
Calculated value based on mortar	8.02	10.08	9.78	12.24	11.27	14.03

As can be seen, $ML_{105-600}$ increases as the average particle size decreases for all FRCA. A reasonable linear relation between $ML_{105-600}$ and granular class is obtained, the correlation coefficients obtained (R^2) range from 0.76 to 0.95 (Table 2-9, the b value corresponds to the $ML_{105-600}$ of the very fine fraction when the size of particle trends towards zero). This confirms that SFSA varies quasi linearly with the four granular classes used. For all the FRCA, the larger values of $ML_{105-600}$ obtained for RCA-90 comparatively to RCA-28 can be attributed to the higher hydration degree (it is also confirmed by the theoretical calculation). The larger values obtained for RCA-OC2 comparatively to RCA-OC1 can be attributed to the higher volume of cement paste in the original composition. Similarly, the larger values obtained for RCA-OC3 comparatively to RCA-OC2 can be attributed to a lower W/C ratio in the original composition, leading to a denser cement paste and therefore to a larger mass of cement paste for a similar paste volume (the theoretical calculation shows similar results). Therefore the $ML_{105-600}$ is influenced by the W/C ratio, the cement paste volume, and hydration degree of the original concrete which is consistent with SFSA results.

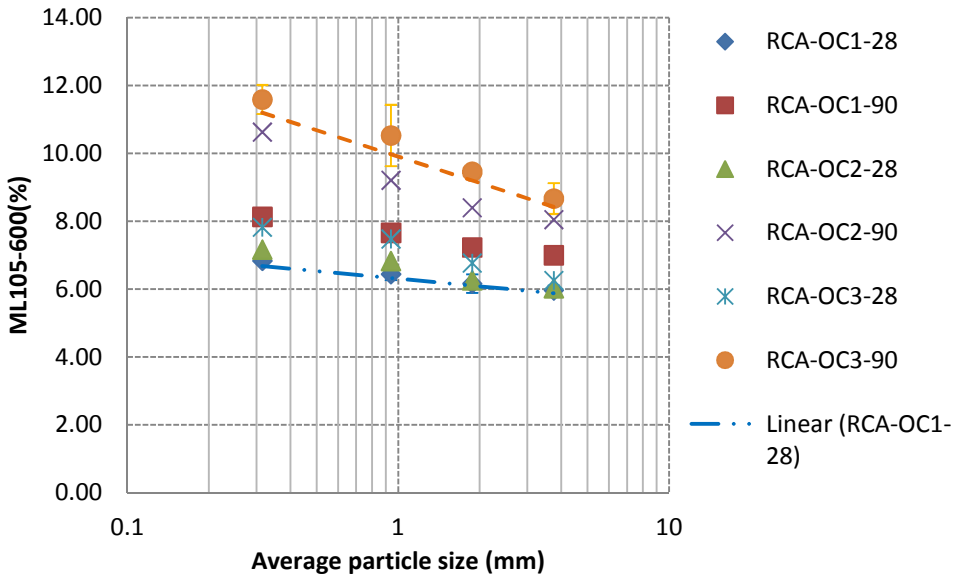

Figure 2-27 $ML_{105-600}$ as a function of the average size of the four different granular classes considered (0/0.63, 0.63/1.25, 1.25/2.5, 2.5/5mm)

Table 2-9 Coefficients of the linear relationships between $ML_{105-600}$ and particle sizes (y=ax+b)

Fractions	a	b	R^2
RCA-OC1-28	-0.23	6.75	0.85
RCA-OC1-90	-0.31	8.03	0.85
RCA-OC2-28	-0.33	7.13	0.88
RCA-OC2-90	-0.67	10.22	0.76
RCA-OC3-28	-0.46	7.87	0.95
RCA-OC3-90	-0.81	11.45	0.90

2.5.3 Estimation of the percentage of reaction of hydration of the cement paste contained in RCA

With Equation 2-7 and Equation 2-11, the value of $CPC/ML_{105-600}$ (Z) can be used to estimate the percentage of reaction as for white cement SFSA is almost identical to CPC:

$$Z = \frac{SFSA(\%)}{ML_{105-600}(\%)} = \frac{(1+(W/C)_{st}\alpha)\times M_{ic}}{(W/C)_{st}\alpha\times M_{ic}} = \frac{1+(W/C)_{st}\alpha}{(W/C)_{st}\alpha} = \frac{1+0.44\alpha}{0.44\alpha} \qquad \text{Equation 2-13}$$

Therefore the percentage of reaction (α) can be determined by the experimental results of SFSA and $ML_{105-600}$. As shown in Table 2-10, we chose the two finer fractions for this calculation because they have larger SFSA which decreases the errors. The mean hydration degree for the studied RCA is similar to 0.68 and 0.93 for the 28days and 90days concrete, which is close from the two values used in our calculations.

Table 2-10 α value determined by the results value of $SFSA/ML_{105-600}$

Fractions	RCA-OC1-28	RCA-OC1-90	RCA-OC2-28	RCA-OC2-90	RCA-OC3-28	RCA-OC3-90
0-0.63	0.788	0.965	0.639	0.851	0.604	0.984
0.63-1.25	0.789	0.964	0.684	0.894	0.603	0.945
Avergage	0.789	0.964	0.662	0.873	0.603	0.964

2.5.4 Density and porosity

Figure 2-28 presents the variation of density measured with the helium pycnometer as a function of granular class. The density of all the fractions of FRCA is lower than that of natural aggregates. This is due to the cement paste surrounding natural aggregates, which density is smaller than that of natural calcareous aggregates. Figure 2-28 also shows that the density of FRCA increases as the average particle size increases.

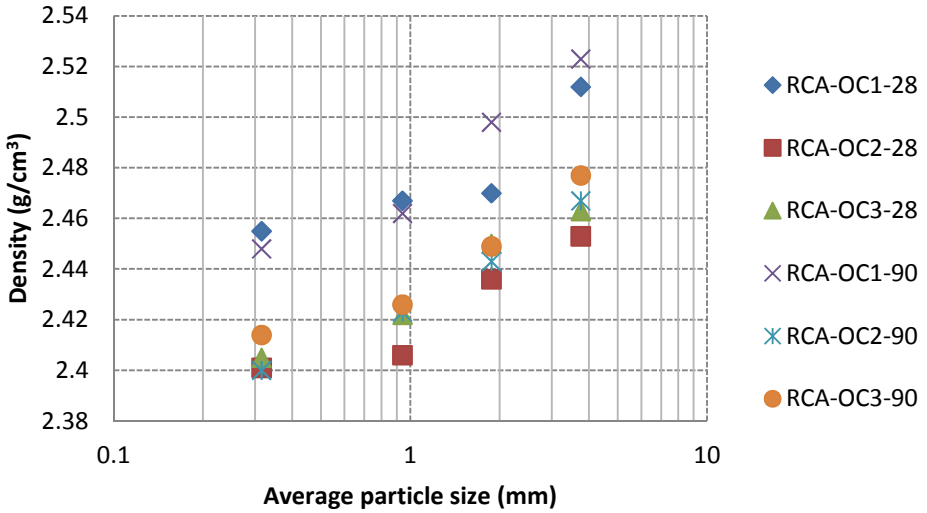

Figure 2-28 Density of FRCA as a function of the average size of the four different granular classes considered (0/0.63, 0.63/1.25, 1.25/2.5, 2.5/5mm)

Figure 2-29 shows the BJH porosity of all the granular classes of FRCA. The porosity of FRCA increases as the average particle size of FRCA decreases. The larger values obtained for RCA-OC2 comparatively to RCA-OC1 can be attributed to the higher volume of cement paste in the original composition of OC2 (same W/C ratio). Similarly, the larger values obtained for RCA-OC2 comparatively to RCA-OC3 can be attributed to a larger W/C ratio in the original composition of OC2 (same volume of cement paste), leading to a larger porosity of the cement paste. So, as expected, the porosity of FRCA is influenced by the W/C ratio and the cement paste volume of the original concrete. Generally, the porosity of RCA-90 is lower

than for RCA-28 which due to higher hydration degree of the cement paste (except for the fractions 0.63-1.25 and 2.5-5 for RCA-OC1 and for the fraction 2.5-5 for RCA-OC2).

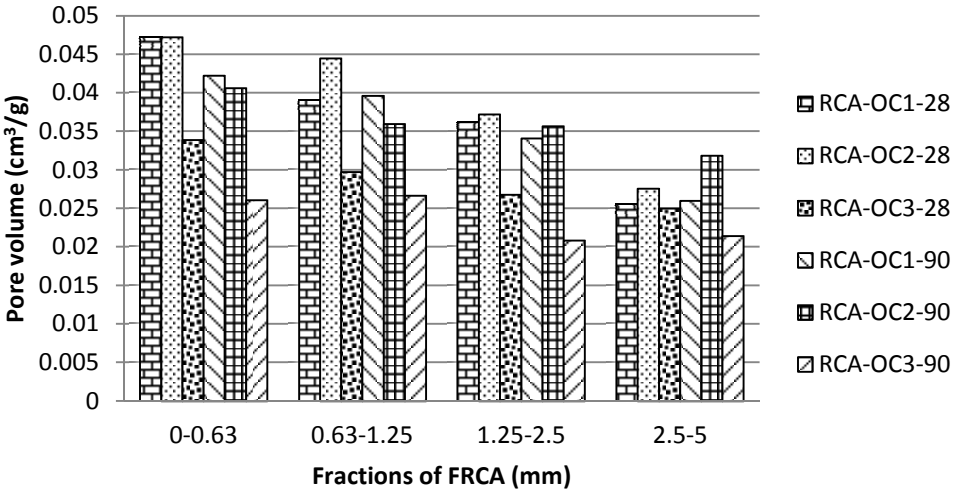

Figure 2-29 BJH porosity of FRCA as function of the average size of the four different granular classes considered (0/0.63, 0.63/1.25, 1.25/2.5, 2.5/5mm)

2.5.5 Water absorption

Figure 2-30 and Figure 2-31 show the variation of water absorption coefficient of RCA-28 and RCA-90 measured with the two methods EN1097-6 and IFSTTAR, noted as EN and IF in the figure and text. The value of water absorption is the average of three test values. The average standard deviation of all the tests is 0.53, for example the standard deviations of RCA-OC1-28-IF and RCA-OC1-90-IF are shown in Figure 2-30 and Figure 2-31 respectively. The results obtained for RCA-OC1 and RCA-OC3 are very similar, whatever the granular class. On the contrary, the water absorption coefficients obtained with all the granular classes of RCA-OC2 are significantly larger than those obtained with RCA-OC1 and RCA-OC3. The larger values obtained for RCA-OC2 comparatively to RCA-OC1 can be attributed to the higher volume of cement paste in OC2 compared to OC1. Similarly, the larger values obtained for RCA-OC2 comparatively to RCA-OC3 can be linked to a larger

W/C ratio of OC2 compared to OC3, leading to a greater porosity of the cement paste even if the volume of cement paste is similar.

The results obtained with the two experimental methods (EN1097-6 and IFSTTAR) are very close from one to another except for the smallest fraction (0/0.63mm). For all FRCA tested in our study, the water absorption coefficient increases when the average particle size decreases except for the fraction 0/0.63mm with the standard EN1097-6 showing a decrease of this coefficient. For the smallest fraction, the standard method does not allow to identify precisely the SSD state. Indeed, for very small angular particles (like those obtained from crushed concrete), some cohesion can occur between the grains even if all the water at the surface of particles has been removed. This prevents the collapse of the grains once the cone is removed [42]. The standard method therefore underestimates the water absorption coefficient for small particles. On the contrary, with IFSTTAR method, the water absorption coefficient increases a lot for the smaller fraction. Figure 2-32 presents an optical microscopy image of the fraction 0-0.63mm of RCA-OC1-28 at SSD state with IFSTTAR method. As it can be seen, agglomerates larger than 2mm (much larger than the maximum particle size of 0.63mm) are present. This result is due to the fact that very small particles tend to agglomerate during drying because of capillary forces. Absorbent paper allows drying the surface of these agglomerates, but the method used does not allow breaking them. IFSTTAR method therefore overestimates the water absorption coefficient of the finer fraction. The same trends are obtained for both RCA made with 28 or 90 days old concrete.

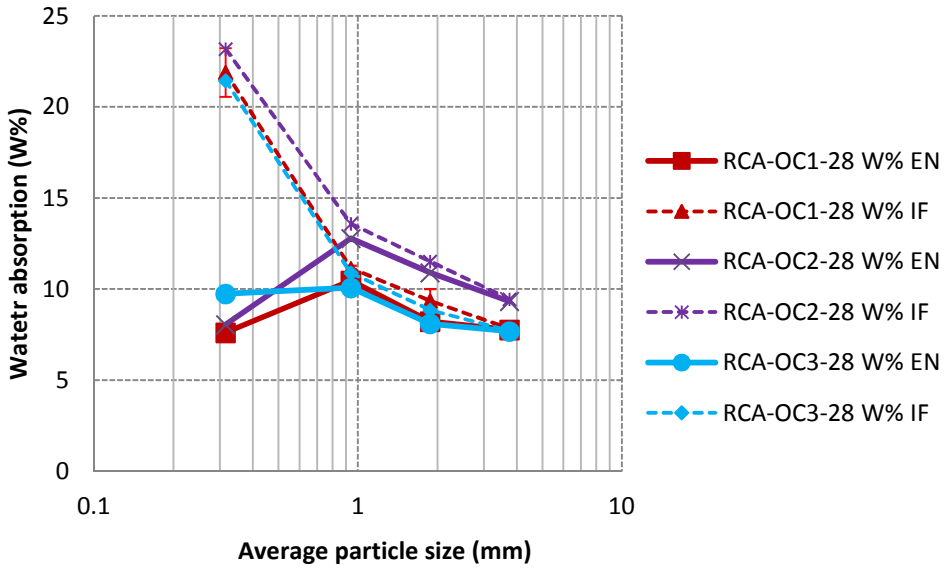

Figure 2-30 Water absorption of RCA-OC-28 measured by EN1097-6 and IFSTTAR methods as a function of the average size of the four different granular classes considered (0/0.63, 0.63/1.25, 1.25/2.5, 2.5/5mm)

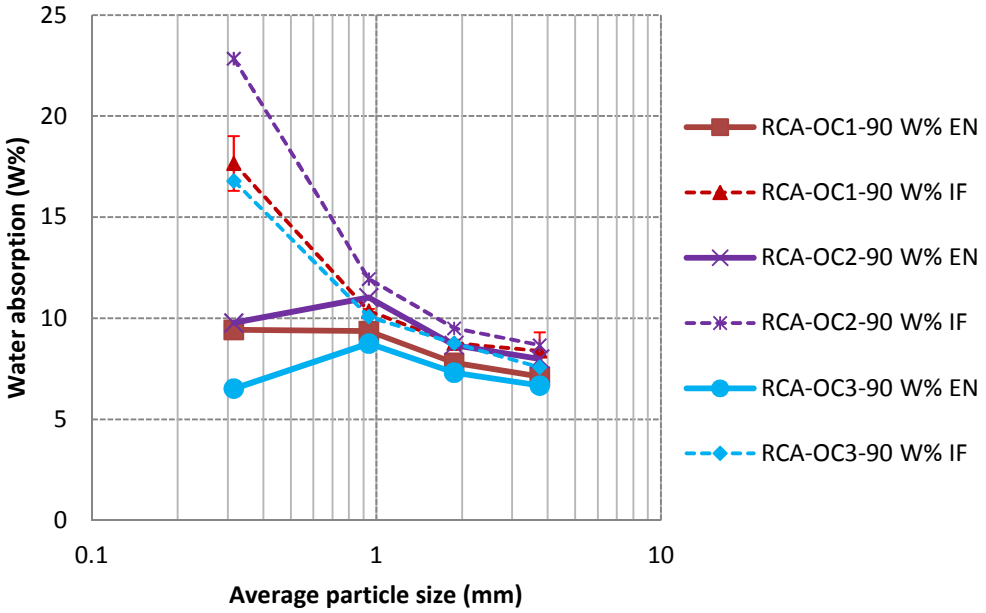

Figure 2-31 Water absorption of RCA-OC-90 measured by EN1097-6 and IFSTTAR methods as a function of the average size of the four different granular classes considered (0/0.63, 0.63/1.25, 1.25/2.5, 2.5/5mm)

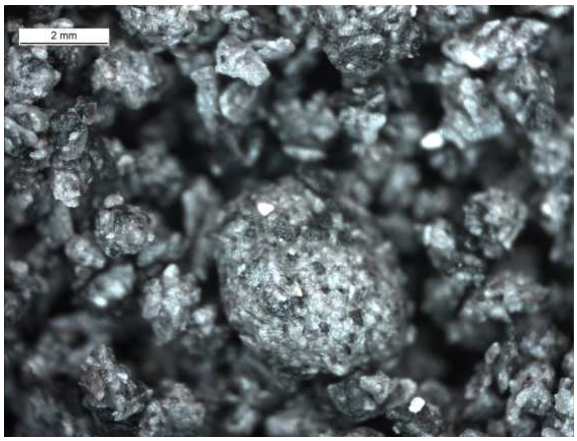

Figure 2-32 Optical microscopy of fraction 0/0.63mm of RCA-OC1-28 at SSD state by the IFSTTAR method

2.6 Relationships between SFSA and other properties of RCA

2.6.1 Relationship between SFSA and $ML_{105\text{-}600}$

Figure 2-33 shows the variation of $ML_{105\text{-}600}$ as a function of SFSA. For a given original concrete composition and a given hydration degree (the same for all concrete at the same time 28days or 90days), the $ML_{105\text{-}600}$ increases linearly with the SFSA (R^2 ranges from 0.87 to 1.00).

Table 2-11 presents the coefficients of the linear regressions obtained for all the FRCA between $ML_{105\text{-}600}$ and SFSA. The b value is not zero might due to the limited points and experimental errors of SFSA and $ML_{105\text{-}600}$. As can be seen, the slope of $ML_{105\text{-}600}$ to SFSA relations are close for RCA-OC1 and RCA-OC2, and that the slope for RCA-OC-90 is higher than RCA-OC-28. Indeed the mass dissolved in salicylic acid and the mass loss at 600°C both depend closely on the cement paste proportion in the material. However, salicylic acid leads to the dissolution of both hydrates and anhydrous phases (except C_4AF, C_3A is excepted to be consumed very quickly) whereas heating at 600°C only leads to the decomposition of all

hydrates but does not affect the anhydrous phases. Therefore, when comparing two cement pastes having different hydration degrees like in Figure 2-33, the mass loss at 600°C will be larger for the cement paste having the larger hydration degree. Indeed, for a given cement paste content (measured by the mass dissolved in salicylic acid), the paste with the larger hydration degree contains more hydrates than the one with the lower hydration degree.

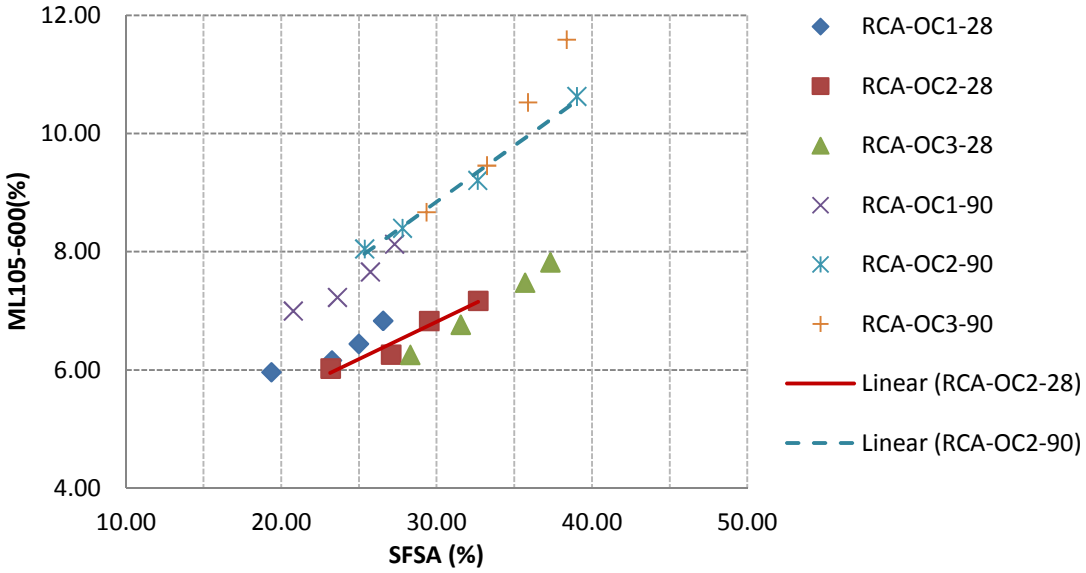

Figure 2-33 $ML_{105-600}$ versus SFSA

Table 2-11 Coefficients of the linear relationships between $ML_{105-600}$ and SFSA (y=ax+b)

	a	b	R^2
RCA-OC1-28	0.11	3.68	0.87
RCA-OC2-28	0.13	3.02	0.94
RCA-OC3-28	0.17	1.37	1.00
RCA-OC1-90	0.17	3.37	0.93
RCA-OC2-90	0.19	3.16	0.99
RCA-OC3-90	0.32	-1.04	0.97
RCA-OC-28	0.10	3.77	0.86
RCA-OC-90	0.24	1.74	0.95

2.6.2 Relationship between SFSA and density

Figure 2-34 shows the variation of specific density as a function of SFSA. When SFSA increases, specific density decreases linearly. The density of RCA directly depends on the densities of cement paste and of natural aggregates and on the proportion of cement paste. For a given RCA, if ρ_{NA} is the density of natural aggregates and ρ_{CP} is the density of cement paste, then the density of a given granular fraction of RCA (ρ_{RCA}) can be calculated with Equation 2-14:

$$\rho_{RCA} = \frac{\rho_{NA}}{1 + CPC \times \frac{\rho_{NA} - \rho_{CP}}{\rho_{CP}}} \qquad \text{Equation 2-14}$$

where CPC is the cement paste content by mass of the considered granular fraction. For concretes OC1, OC2, and OC3 which have been manufactured with the white cement, CPC in equation 2-20 can be replaced by SFSA (for this cement, SFSA is almost identical to CPC).

The density of each cement paste can then be obtained by fitting Equation 2-14 with our experimental results (Table 2-12). Table 2-12 shows that the densities of cement pastes in RCA-OC1-28 and RCA-OC2-28 (similarly for RCA-OC1-90 and RCA-OC2-90) are similar as expected. Indeed, cement paste of RCA-OC1 and RCA-OC2 have the same W/C ratio. Moreover, the larger values obtained for RCA-OC3 comparatively to RCA-OC1 and RCA-OC2 can be attributed to the lower W/C in the original composition. As the hydration degree of original concrete increases (from RCA-28 to RCA-90), the density of cement paste increases. Table 2-12 also shows that the correlation coefficients obtained between calculated and experimental value (R^2) range from 0.92 to 0.99.

Table 2-12 Densities of cement pastes calculated by fitting Equation 2-14 to experimental values of the densities of RCA.

	RCA-OC1-28	RCA-OC2-28	RCA-OC3-28	RCA-OC1-90	RCA-OC2-90	RCA-OC3-90
Density	2.00	1.96	2.07	2.04	2.04	2.10
R^2	0.95	0.92	0.97	0.98	0.96	0.99

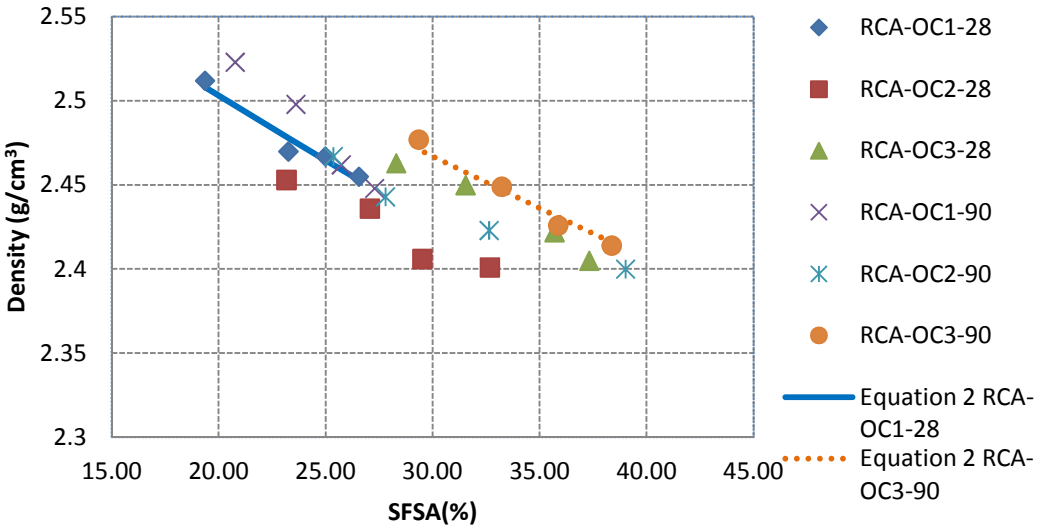

Figure 2-34 Correlation between SFSA and specific density

2.6.3 Relationship between SFSA and water absorption

Figure 2-35 presents the variation of water absorption (IFSTTAR method) with the SFSA: when SFSA increases, the water absorption increases too. As can be seen, the water absorption of all FRCA varies linearly with the SFSA for the three coarser average particle sizes of RCA. On the contrary, as discussed previously, the water absorption measured by standard or IFSTTAR method for the finer fraction seems to be either underestimated or overestimated respectively (example for RCA-OC3-90 shown on Figure 2-35). The water absorption of RCA directly depends on the water absorptions of cement paste and of natural aggregates and on the proportions of cement paste. For a given original concrete composition the water absorption coefficients of natural aggregates (WA_{NA}) and of the cement paste

(WA_{CP}) do not depend on the granular fraction considered. Therefore, the water absorption of a given granular fraction of RCA (WA_{RCA}) can be calculated with Equation 2-15.

$$WA_{RCA} = WA_{CP} \times CPC + WA_{NA} \times (1 - CPC) = CPC(WA_{CP} - WA_{NA}) + WA_{NA} \quad \text{Equation 2-15}$$

where CPC is the cement paste content of the considered granular fraction.

Equation 2-15 shows that the water absorption coefficient of RCA has to vary linearly with the cement paste content. Assuming that the composition of the cement paste does not depend on the size of particles, the ratio SFSA/CPC can be considered as constant. Therefore, the water absorption coefficient of the finer fraction (0/0.63mm) can be obtained by linear extrapolation of the relation between WA and SFSA determined with the three coarser fractions of RCA. Extrapolation carried out using both standard and IFSTTAR methods give similar values for the water absorption coefficient of the finer fraction (Table 2-14), the average difference between these two values obtained for the six FRCA is 1.06%. As expected, the value of water absorption coefficient of the finer fraction obtained is between the value obtained by the standard and IFSTTAR methods. In Figure 2-35, the water absorption coefficients of the smaller granular classes (0/0.63 mm) correspond to the extrapolated values from experimental results with IFSTTAR method. The values obtained by the standard and IFSTTAR methods are also reported for RCA-OC3-90 to demonstrate that these values are not appropriate.

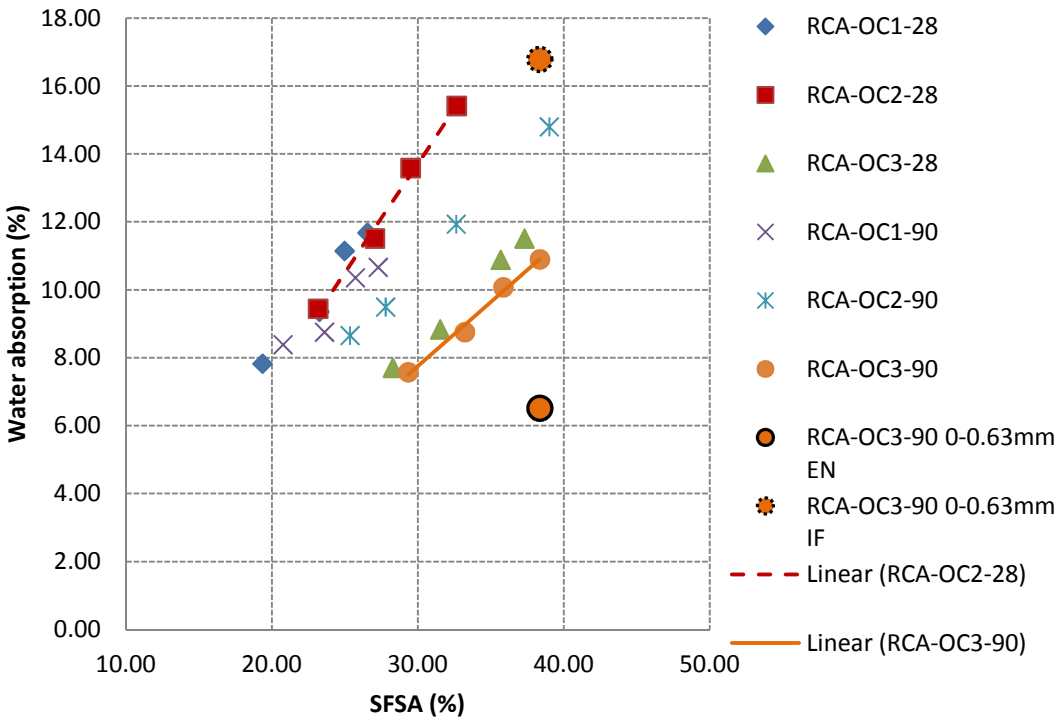

Figure 2-35 Correlation between water absorption (IFSTTAR method) and SFSA

Table 2-13 Coefficients of the linear relationships between water absorption (IFSTAAR method for three coarse fractions) and SFSA (y=ax+b)

	a	b	R^2
RCA-OC1-28	0.56	-3.09	0.93
RCA-OC2-28	0.64	-5.51	0.98
RCA-OC3-28	0.43	-4.64	0.99
RCA-OC1-90	0.38	0.24	0.83
RCA-OC2-90	0.46	-3.06	0.99
RCA-OC3-90	0.38	-3.58	0.98

Table 2-14 Extrapolated water absorption coefficient of Fraction 0-0.63mm from standard and IFSTTAR

	Tested value of IFSTTAR (%)	Tested value of EN 1097-6 (%)	Extrapolated value of IFSTTAR (%)	Extrapolated value of EN 1097-6 (%)	Difference of two extrapolated values (%)
RCA-OC1-28	21.9	7.61	11.68	10.50	1.19
RCA-OC2-28	23.18	8.05	15.42	15.87	-0.45
RCA-OC3-28	21.44	9.74	11.52	10.43	1.09
RCA-OC1-90	17.66	9.42	10.67	9.82	0.85
RCA-OC2-90	22.84	9.77	14.81	13.67	1.14
RCA-OC3-90	16.79	6.52	10.90	9.28	1.62

Therefore, we propose the following method to estimate the water absorption coefficient of the finer fraction (0-0.63mm) of FRCA. FRCA first have to be separated in different granular classes. In our study, the four classes 0/0.63, 0.63/1.25, 1.25/2.5, 2.5/5mm were retained because they allowed separating the FRCA into classes representing significant proportions of the aggregate. However, depending on the particle size distribution of the FRCA, different granular classes could be chosen. First the SFSA of each granular class have to be determined (alternatively, $ML_{105\text{-}600}$ or any quantity being proportional to the cement paste content could be used). Then, the water absorption coefficients of the three coarser fractions of FRCA have to be measured either with European standard EN 1097-6 or IFSTTAR method n°78 or other methods. Finally, the water absorption coefficient of the finer fraction (0/0.63 mm) can be obtained by a linear extrapolation between WA and SFSA of the three coarser classes. The accurate total water absorption of FRCA used (fraction 0/5mm) can be determined by knowing the proportion and water absorption coefficient of each fraction.

Additionally for a given RCA, the presence of insoluble phases of the cement paste will impact similarly all the four particle size classes. Thus the linear relationship between the SFSA and the average size of the four different granular classes will be kept. On the other hand, insoluble phases will impact the coefficients of the linear regression of the water absorption coefficient as a function of SFSA as this latter will decrease with an increase of the content of insoluble phases.

2.7 Properties of carbonated laboratory produced RCA

In order to study the influence of carbonation on the properties of RCA, laboratory produced RCA-OC1-90 were subjected to accelerated carbonation tests in laboratory (together with CP-0.4-90 and CP-0.6-90 with fraction 1.25/2.5mm). The objective was to have nearly complete

carbonation to maximize the effect of carbonation on the properties of RCA. First, RCA-OC1-90 were dried at 105°C and cooled down at room temperature. The sample was then put in a pure CO_2 carbonation cell at 20°C which is shown in Figure 2-36, supersaturated NaCl solution was used to obtain a constant relative humidity of 75%. After two weeks of carbonation, a solution of phenolphthalein was used as indicator to check the carbonation degree, as shown in Figure 2-37 (left sample is before carbonation, right sample is after carbonation). Figure 2-37 shows that, after carbonation, phenolphthalein does not turn pink, indicating that carbonation of the sample is almost complete at least at their surface. Before characterizing the properties of carbonated RCA, the samples were dried at 105°C. RCA-OC1-90 refers to RCA which is made by crushing original concrete OC1 at 90 days before carbonation. RCA-OC1-90-carbo refers to which is carbonated in the laboratory after carbonation. CP-0.6-90 refers to the cement paste which is made with w/c=0.6 and curing 90 days in water. CP-0.6-90-carbo refers to which is carbonated in the laboratory. The properties of RCA-OC1-90 and RCA-OC1-90-carbo (together with CP) were then tested in details.

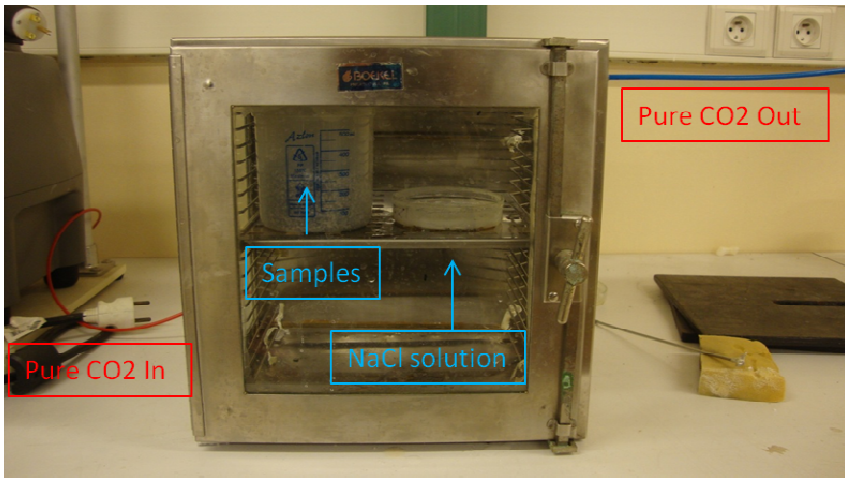

Figure 2-36 Carbonation cell used for RCA-OC1-90 and cement pastes

Figure 2-37 Carbonation tested by the solution of phenolphthalein (left: before carbonation; right: after carbonation)

2.7.1 TGA results with analysis of gas by mass spectrometry

Four different granular classes (0/0.63, 0.63/1.25, 1.25/2.5, 2.5/5mm) of RCA-OC1-90 have been tested with analysis of gas by MS. Figure 2-38 and Figure 2-39 present the TGA results with analysis of gas by MS for RCA-OC1-90 and RCA-OC1-90-carbo with fraction 0/0.63mm. In these figures, the peak at 150-175°C corresponds to a loss of water in C-S-H. The peak at 450°C corresponds to the loss of water in the portlandite (similar results are found in [146-148]) which almost disappears after the carbonation meaning that the portlandite has transferred to calcite. These results are confirmed with the cement paste samples. Figure 2-40 and Figure 2-41 present the TGA results with analysis of gas by MS for CP-0.6-90 and CP-0.6-90-carbo.

Figure 2-38 and Figure 2-40 first show that the loss of CO_2 in uncarbonated samples is negligible for tempartures lower than 600°C. This confirms that, in uncarbonated samples, the mass loss between 105 and 600°C comes essentially from the departure of water. However, for carbonated samples, Figure 2-39 and Figure 2-41 clearly show that part of the mass loss between 105 and 600°C comes from the departure of CO_2. Indeed, the loss of CO_2 in carbonated samples becomes significant at about 500°C.

Table 2-15 shows the values of mass loss between 105°C and 500°C ($ML_{105-500}$), between 500 and 600°C ($ML_{500-600}$), between 600 and 700°C ($ML_{600-700}$), and between 700 and 1095°C ($ML_{700-1095}$) based on TGA with gas, β and β´ are calculated by Equation 2-16 and Equation 2-17 respectively. As can be seen, after carbonation, $ML_{105-500}$ decreases which is due to the transfer of portlandite to calcite leading to a lesser loss of water (β´ smaller than 1). However, in the same time, $ML_{500-600}$ increases after carbonation due to a significant departure of CO_2 between 500 and 600°C. This suggests that the formation of amorphous carbonation products occurred during our accelerated carbonation tests [67-68]. As a consequence, after carbonation, $ML_{105-600}$ is no more related only to the departure of water, but also to the departure of part of the CO_2 coming from carbonation products. Table 2-15 also shows that, for RCA-OC1, carbonation leads to a systematic increase in the mass loss between 105 and 600°C (β larger than 1). On the contrary, carbonation leads to a decrease in mass loss between 105 and 600°C for the pure cement paste (β smaller than 1). For pure paste carbonation leads to greater quantities of calcite that decompose after 600°C. Thus we may suspect an important of calcareous aggregates on carbonation and thus on the different regimes of decarbonation.

Table 2-15 Mass loss based TGA with gas

	$ML_{105-500}$	$ML_{500-600}$	$ML_{600-700}$	$ML_{700-1095}$	$ML_{105-600}$	β	β´
RCA-OC1-90 0/0.63	3.08	0.35	1.59	29.33	3.43	1.41	0.62
RCA-OC1-90-carbo 0/0.63	1.91	2.91	3.54	29.39	4.82		
RCA-OC1-90 0.63/1.25	2.83	0.32	1.37	29.99	3.15	1.36	0.61
RCA-OC1-90-carbo 0.63/1.25	1.75	2.54	3.11	30.74	4.29		
RCA-OC1-90 1.25/2.5	2.54	0.3	1.22	30.85	2.84	1.31	0.59
RCA-OC1-90-carbo 1.25/2.5	1.5	2.23	2.8	31.63	3.73		
RCA-OC1-90 2.5/5	2.43	0.29	1.21	31.25	2.72	1.18	0.53
RCA-OC1-90-carbo 2.5/5	1.28	1.92	2.49	32.58	3.2		
CP-0.6-90 1.25/2.5	12.99	0.6	1.36	1.44	13.59	0.87	0.38
CP-0.6-90-carbo 1.25/2.5	4.94	6.87	6.45	16.19	11.81		

$$\beta = \frac{(ML_{105-600})carbo}{(ML_{105-600})}$$ Equation 2-16

where β is the ratio of $ML_{105\text{-}600}$-carbo to $ML_{105\text{-}600}$.

$$\beta' = \frac{(ML_{105-500})carbo}{(ML_{105-500})}$$ Equation 2-17

where β´ is the ratio of $ML_{105\text{-}500}$-carbo to $ML_{105\text{-}500}$.

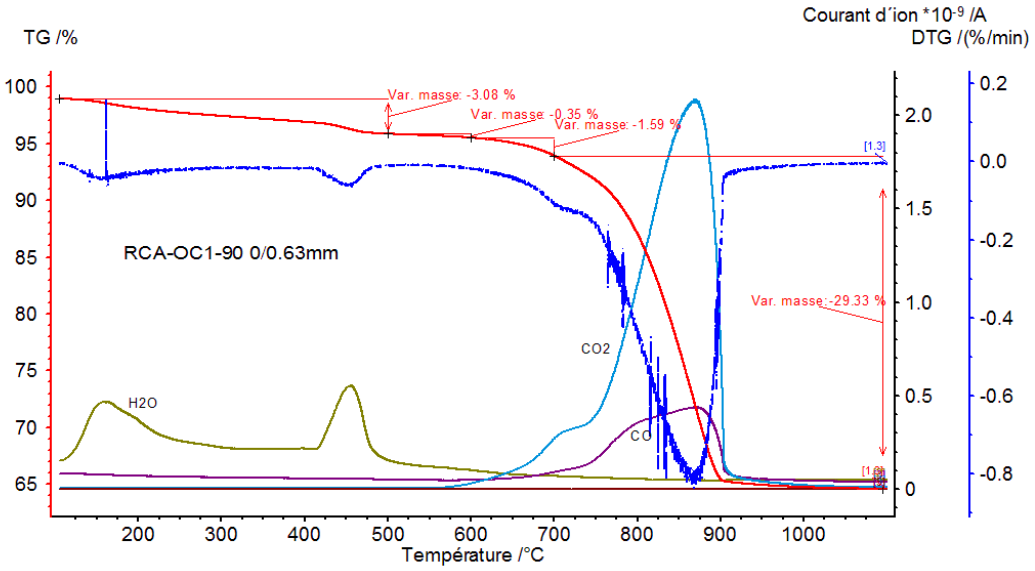

Figure 2-38 TGA with gas of RCA-OC1-90 0/0.63mm

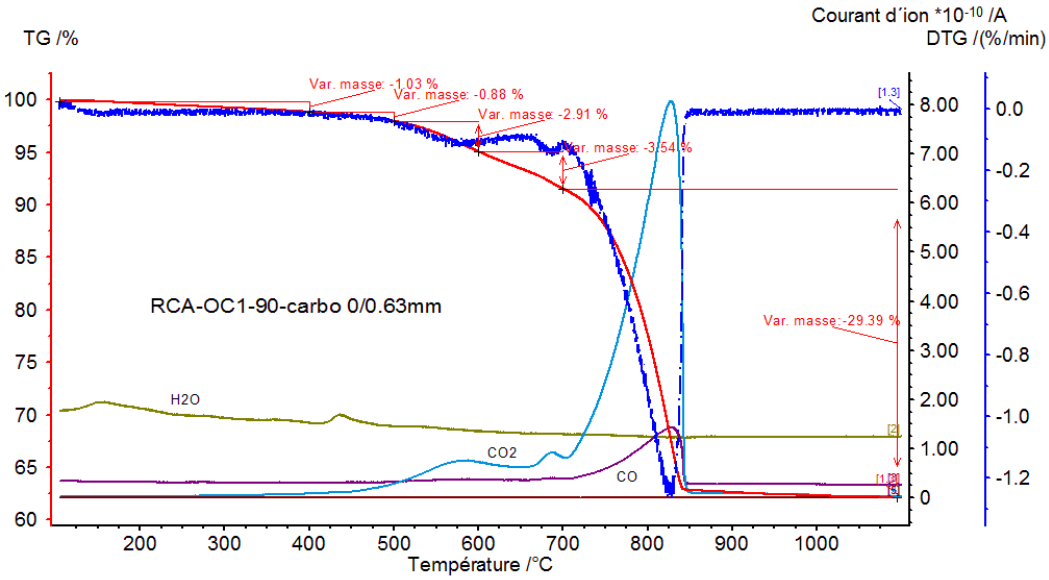

Figure 2-39 TGA with gas of RCA-OC1-90-carbo 0/0.63mm

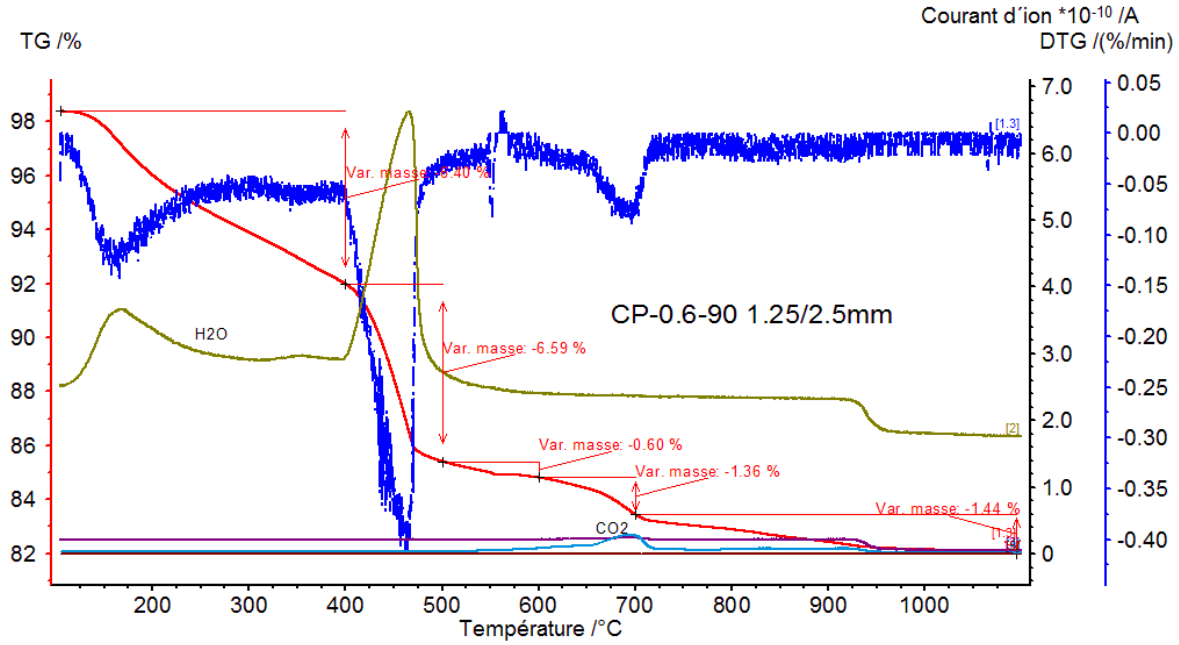

Figure 2-40 TGA with gas of CP-0.6-90 1.25/2.5mm

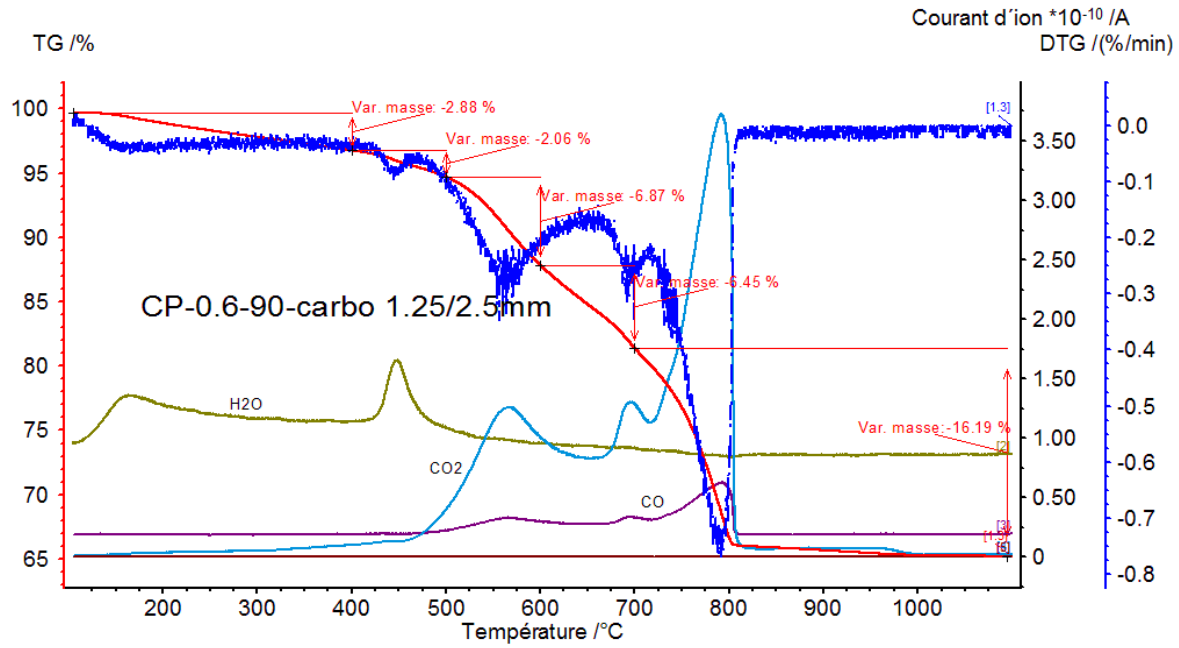

Figure 2-41 TGA with gas of CP-0.6-90-carbo 1.25/2.5mm

2.7.2 SFSA and $ML_{105\text{-}600}$

Figure 2-42 presents the variation of SFSA as a function of granular class for RCA-OC1-90 and RCA-OC1-90-carbo. As can be seen, SFSA increases as the average particle size decreases. After carbonation, part of the cement paste transfers to calcite which does not dissolve in the salicylic acid dissolution. Therefore the dissolved content decreases dramatically for all the four granular classes, moreover, the slope of SFSA to average particle size is larger than before carbonation (-0.60 for RCA-OC1-90-carbo, -1.87 for RCA-OC1-90).

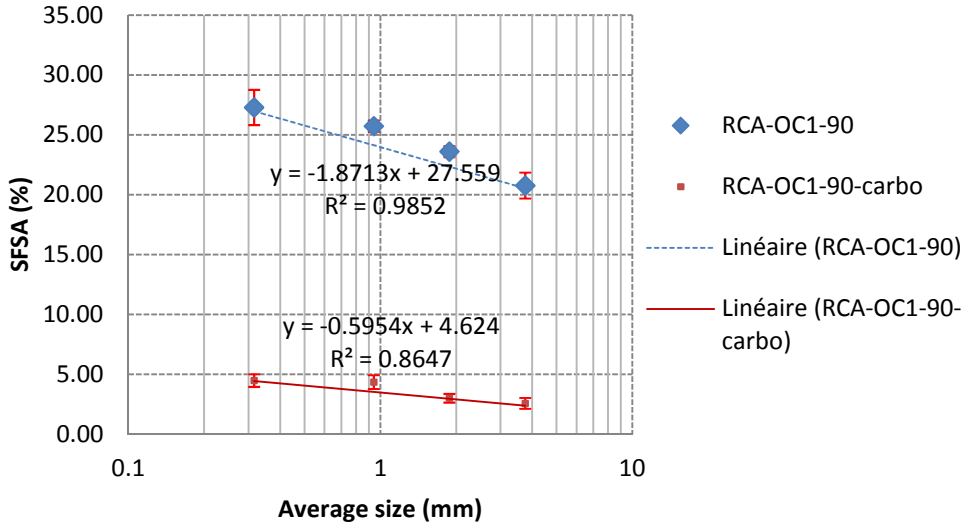

Figure 2-42 SFSA of RCA-OC1-90 as a function of average particle size of different granular classes considered (0/0.63, 0.63/1.25, 1.25/2.5, 2.5/5mm)

Figure 2-43 shows the variation of $ML_{105\text{-}600}$ of FRCA measured with the thermal method as a function of granular class for RCA-OC1-90 and RCA-OC1-90-carbo. As can be seen, $ML_{105\text{-}600}$ increases after the carbonation for all the granular classes. The β value (ratio of $ML_{105\text{-}600\text{-}carbo}$ to $ML_{105\text{-}600}$) based on thermal method is 1.37, 1.38, 1.33 and 1.30 for RCA fractions 0/0.63, 0.63/1.25, 1.25/2.5, 2.5/5mm respectively, which is consistent with the β value based on TGA method (Table 2-15). $ML_{105\text{-}600}$ obtained by thermal method is larger than the value

obtained by the TGA, which might due to the longer time in the oven (24h at 600°C for the thermal method, and about 3h from 105 to 600°C for TGA method). From the results of TGA (Figure 2-38 and Figure 2-39), $ML_{500\text{-}600}$ increases a lot for the carbonated cement paste or RCA. Therefore, in the case of carbonated materials, $ML_{105\text{-}600}$ does not correspond exclusively to the departure of bound water but also to that of CO_2, which comes from the transferred calcite in carbonated cement paste.

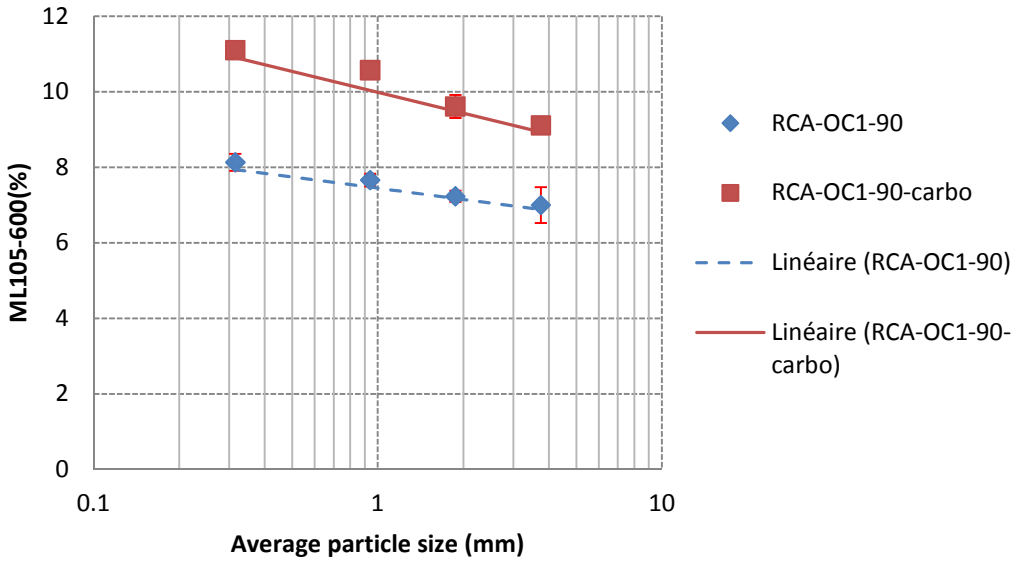

Figure 2-43 $ML_{105\text{-}600}$ of RCA-OC1-90 as a function of different granular classes considered (0/0.63, 0.63/1.25, 1.25/2.5, 2.5/5mm)

After carbonation, the dissolved content in salicylic acid of RCA-OC1-90-carbo decreases comparatively to RCA-OC1-90. Figure 2-44 shows the results of dissolved percentages by salicylic acid dissolution before and after carbonation for the two cement pastes. After carbonation, the soluble fraction decreases a lot both for CP-0.6-90 and CP-0.4-90. A lesser decrease is observed for cement paste with W/C=0.4 in comparison to that with W/C=0.6. Indeed, in the former case, the carbonation degree could be lower than in the later case because of a lower diffusivity of the cement paste. Therefore, carbonation changes the

mineralogical phases of cement pastes (such as forming calcite from portlandite), which could not dissolve in salicylic acid.

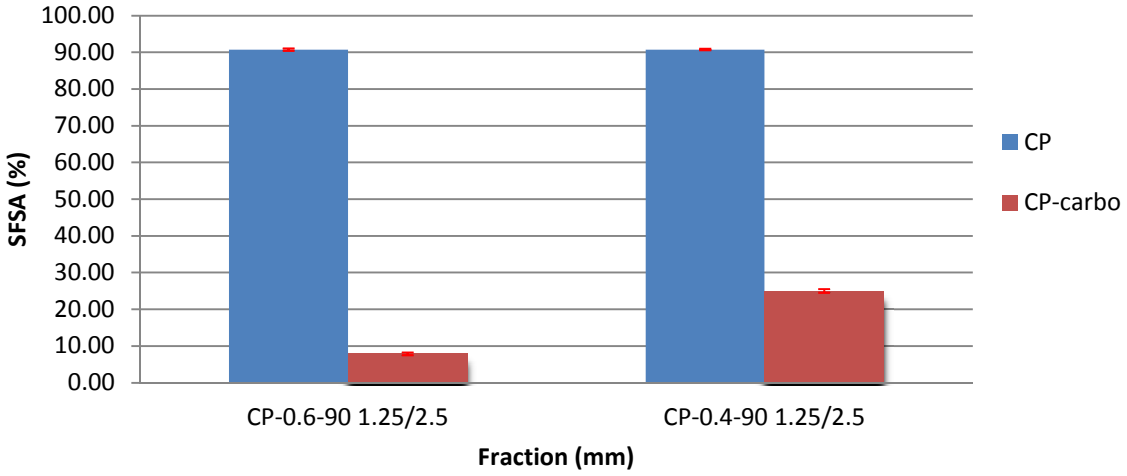

Figure 2-44 SFSA as a function of carbonation of pure cement pastes granular class (1.25/2.5mm)

2.7.3 Density

Figure 2-45 presents the variation of apparent density measured with the helium pycnometer as a function of granular class. The density of all the fractions of RCA-OC1-90-carbo is larger than that of RCA-OC1-90. This is due to transfer of portlandite to calcite, indeed calcite has larger density than portlandite. After carbonation, the slope of density to average particle size is lower than RCA-OC1-90 (0.01 for RCA-OC1-90-carbo, 0.02 for RCA-OC1-90), it can be explained by the fact that the finer fraction of RCA has higher SFSA, and the density of the latter increased by the carbonation.

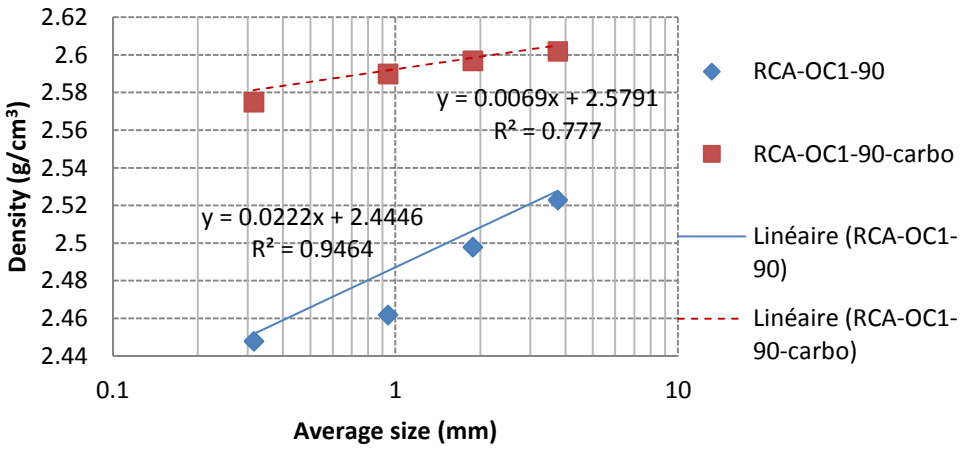

Figure 2-45 Density of RCA-OC1-90 as a function of average particle size of different granular classes considered (0/0.63, 0.63/1.25, 1.25/2.5, 2.5/5mm)

2.7.4 Porosity

Figure 2-46 shows the BET surface area of all the granular classes of RCA-OC1-90 before and after carbonation. The BET surface area increases as the average particle size of RCA decreases for both RCA-OC1-90 and RCA-OC1-90-carbo. Carbonation increases a lot specific surface area, which is due to the formation of small crystal calcite from portlandite [150].

In order to study the influence of carbonation on the porosity of cement paste and RCA, four samples (CP-0.6-90 1.25/2.5 and CP-0.6-90-carbo 1.25/2.5, RCA-OC1-90 2.5/5 and RCA-OC1-90-carbo 2.5/5) have been studied by using Mercury Intrusion Porosimetry (MIP) technique with machine MICROMERITICS AUTOPORE IV. Table 2-16 shows the MIP results of the cement paste and RCA before and after carbonation. The porosity decreases after the carbonation, which is also reported by Arandigoyen [73].

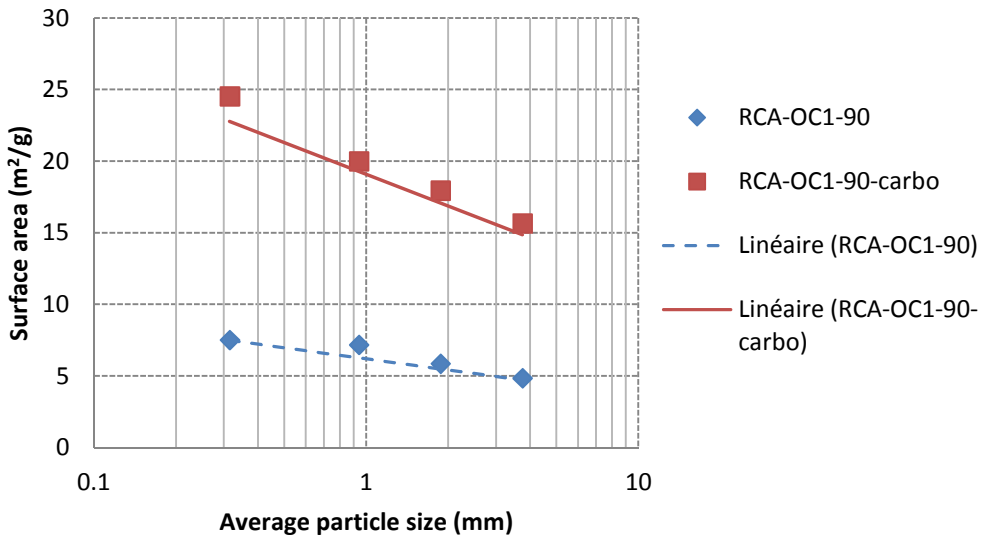

Figure 2-46 BET surface area of RCA-OC1-90 as a function of different granular classes considered (0/0.63, 0.63/1.25, 1.25/2.5, 2.5/5mm)

Table 2-16 MIP results of RCA and cement paste

		CP-0.6-90 1.25/2.5	CP-0.6-90-carbo 1.25/2.5	RCA-OC1-90 2.5/5	RCA-OC1-90-carbo 2.5/5
Total Intrusion Volume	mL/g	0.37	0.16	0.06	0.03
Total Pore Area	m²/g	31.87	14.84	5.31	3.25
Median Pore Diameter (Volume)	µm	0.08	0.15	0.06	0.14
Median Pore Diameter (Area)	µm	0.02	0.01	0.03	0.01
Average Pore Diameter (4V/A)	µm	0.05	0.04	0.05	0.04
Bulk Density at 0.10 psia	g/mL	1.17	1.63	2.25	2.45
Apparent (skeletal) Density	g/mL	2.05	2.19	2.62	2.66
Porosity	%	42.79	25.52	14.12	7.83

Figure 2-47 presents the pore size distribution of cement paste and RCA before and after carbonation measured by MIP. For the cement paste, pores comprised between 0.001-0.01 micron increase, pores between 0.01-0.1 micron decrease, pores between 0.1-1 micron increase after carbonation. The same changes can be found in RCA carbonation. Therefore, after the carbonation, pores between 0.01-0.1 micron could be filled by carbonation products, leaving smaller voids between them, comprised between 0.001-0.01 microns.

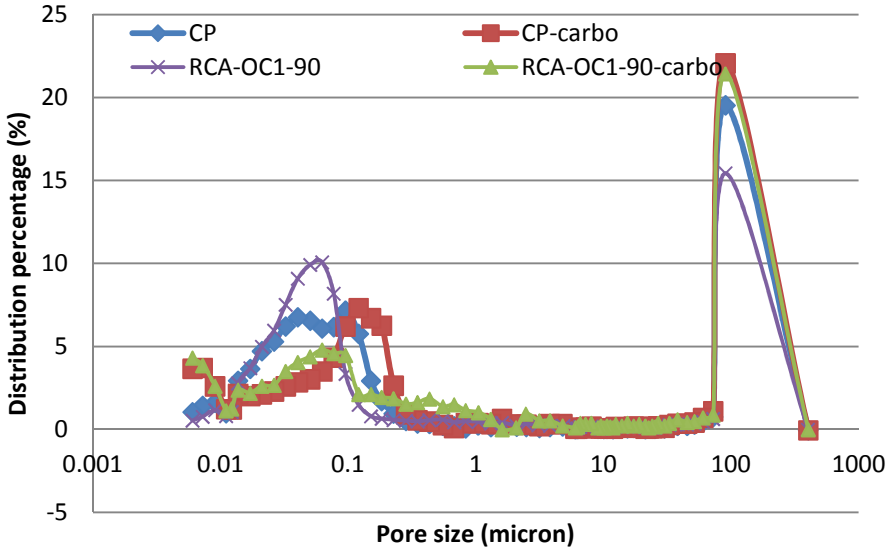

Figure 2-47 Pore distribution of cement paste and RCA-OC1-90 before and after carbonation measured by MIP

2.7.5 Water absorption

Table 2-17 and Figure 2-48 show the water absorption coefficients of the four granular fractions of RCA-OC1-90 and RCA-OC1-90-carbo measured with the two methods (EN1097-6 and IFSTTAR). The water absorption coefficients obtained with all the granular classes of RCA-OC1-90-carbo are significantly lower than those obtained with RCA-OC1-90. It can be attributed to the reduction of cement paste porosity due to carbonation. After the carbonantion, the water absorption of RCA decrease 26.3%, 28.5%, 33.1% for the fraction 2.5-5mm, 1.25-2.5mm, 0.63-1.25mm respectively, which is also reported by Grabiec [77].

Table 2-17 Water absorption of RCA-OC1-90 and RCA-OC1-90-carbo measured by the EN and IFSTTAR

size (mm)	RCA-OC1-90-EN	RCA-OC1-90-IF	RCA-OC1-90-carbo-EN	RCA-OC1-90-carbo-IF
0-0.63	9.42	17.66	-	13.1
0.63-1.25	9.37	10.36	6.27	7.14
1.25-2.5	7.79	8.76	5.57	6.05
2.5-5	7.12	8.39	5.25	5.64

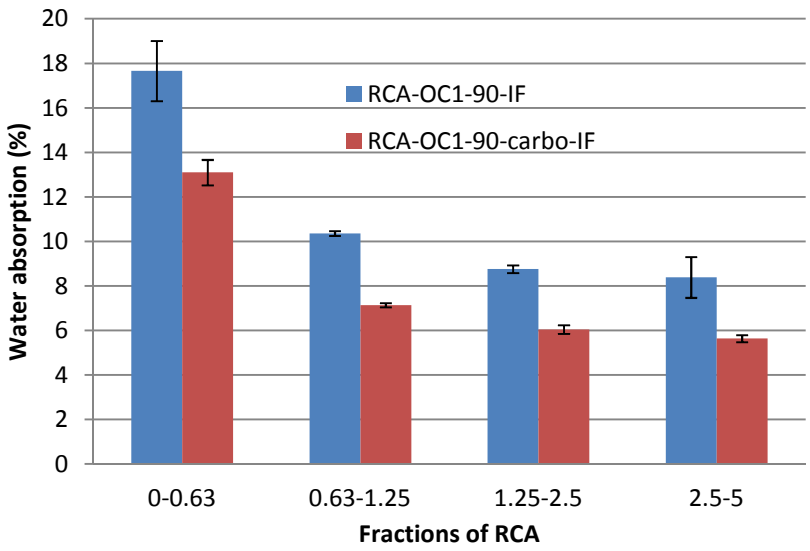

Figure 2-48 Water absorption of RCA-OC1-90 and RCA-OC1-90-carbo measured by IFSTTAR method as a function of different granular classes considered (0/0.63, 0.63/1.25, 1.25/2.5, 2.5/5mm)

2.8 Conclusions

Some of the major properties of FRCA produced in the laboratory from the crushing of concretes of known composition have been related to the cement paste content. A method based on the dissolution of the major part of the cement paste contained in FRCA by salicylic acid (SFSA) has been developed for the measurement of cement paste content (CPC). The properties of laboratory produced RCA have been tested.

With these results, questions 1 to 4 can be partly addressed.

Question 1: Can we define accurate experimental methods allowing to measure the water absorption coefficient and the adherent cement paste content of the different fractions of RCA?

⟹ A method based on the dissolution of the major part of the cement paste made with CEM I contained in FRCA by salicylic acid (SFSA) has been developed for the measurement of cement paste content. The method has been applied to concrete manufactured with a white OPC to obtain the most reliable results. From the theorical model, the SFSA is almost identical to the CPC for the white cement that did not contain C4AF and just a small amount

of C3A. For the grey cement, SFSA is always lower than CPC which is due to the presence of important amounts of insoluble phases such as Calcite and C_4AF. However for a given RCA, SFSA can be used to correlate the measured properties of RCA with CPC. Indeed the presence of insoluble phases of the cement paste will impact similarly all the particle size classes. Thus the linear relationship between SFSA and water absorption is kept for CPC with the same slope but an origin displaced to the right of the graph (toward higher CPC).

EN 1097-6 and IFSTTAR methods have been used to measure the water absorption of FRCA. For particle sizes larger than 0.63mm, EN 1097-6 and IFSTTAR methods give similar results, which suggest that these methods are relevant for the measurement of water absorption coefficient of FRCA (larger than 0.63mm). For these fractions, a quasi linear relation is found between the water absorption coefficient and the particle size, the former decreasing with the particle size. However, for the smaller particle size (<0.63mm), IFSTTAR method seems to overestimate the water absorption coefficient, and standard method (EN 1097-6) seems to underestimate it. The characterization of water absorption coefficient of very fine particles is known to be a difficult task, especially for FRCA. As the water absorption displays a linear relationship with SFSA of the three coarser granular classes, the absorption coefficient could be estimated with good accuracy for very fine RCA by extrapolating the relationship obtained between water absorption and SFSA with coarser granular class. The total water absorption of FRCA (fraction 0/5mm) can therefore be determined precisely which is very important in the mixture proportioning of recycled concrete.

Question 2: What is the link between properties of original concrete (W/C ratios, cement paste volume) and properties of RCA made with it?

⟹ The properties of RCA are influenced and connected with the properties of original concrete.

The SFSA of FRCA is influenced by the W/C ratio, the reaction degree and the cement paste volume of the original concrete. The larger values of SFSA obtained for RCA-OC2 comparatively to RCA-OC1 can be attributed to the higher volume of cement paste in the original composition (same W/C ratio). Similarly, the larger values obtained for RCA-OC3 comparatively to RCA-OC2 can be attributed to a lower W/C ratio in the original composition (same volume of cement paste), leading to a denser cement paste and therefore to a larger mass of cement paste for a similar paste volume.

The porosity and water absorption of FRCA are also influenced by the W/C ratio and the cement paste volume of the original concrete. The water absorption coefficients obtained with all the granular classes of RCA-OC2 are significantly larger than those obtained with RCA-OC1 and RCA-OC3.

Question 3: What is the link between size and properties of RCA (mortar or cement paste content, density, water absorption, porosity...)?

⟹ For the laboratory produced FRCA used in this study, the SFSA decreases linearly with the average particle size of four different granular classes (0/0.63, 0.63/1.25, 1.25/2.5, 2.5/5mm). This result has been confirmed by studying the variation of $ML_{105\text{-}600}$ of FRCA (mass loss at 600°C) as a function of average particle size. The properties of FRCA including specific density, water absorption, and porosity are strongly correlated to the SFSA, and therefore to the size of particles. The higher the SFSA, the higher the water absorption and porosity, and the lower the specific density at the exception of the absorption coefficient measured by EN 1097-6 standard for the smaller fraction (0/0.63mm).

Question 4: What is the influence of the conditions of conservation of the RCA (carbonation) on their properties?

⟹ After the carbonation of recycled aggregate, the dissolved fraction in salicylic acid (SFSA) decreases. The method can be also used for RCA that have been carbonated either before or during the fabrication or storage. In this case, the linear relationship between SFSA and water absorption is kept for CPC but with both different slope and origin; the slope is decreased while the origin displaced to the right of the graph.

$ML_{105\text{-}600}$ increases both for the thermal method and TGA method for RCA but not for pure cement paste. $ML_{105\text{-}500}$ based on TGA decreases, but $ML_{500\text{-}600}$ increases a lot, which are due to the transfer of portlandite to partly amorphous calcite, which decomposes from 500°C.

The density of RCA and the surface area increases, the porosity of RCA decrease, which leads to the decrease of water absorption.

Chapter 3 Characteristics of industrial RCA

3.1 Introduction

In the previous chapter, we have tested experimental methods with laboratory produced RCA, including measurement of SFSA and water absorption. Are these methods also suitable for industrial RCA where the initial composition of concrete is not known, especially the type of cement? What are the differences between laboratory produced RCA and industrial RCA? In order to answer these questions, three industrial RCA which have been sourced from different industrial platforms have been studied, particularly for SFSA and water absorption. The experimental methods used were the same as those used for laboratory produced RCA, which were presented in Chapter 2.

3.2 Experimental protocols

3.2.1 Industrial RCA

Three industrial RCA were collected from commercial plants. Two RCA were provided by the Colas Company, and are noted RCA-Colas1 and RCA-Colas2 in the following. RCA-Colas1 was produced in the site VALORMAT of Amiens. RCA-Colas2 was produced in the plant of Louvres. Figure 3-1 shows the site crushing machine for production of RCA-Colas1. RCA-PNR was the industrial FRCA produced for the French national project Recybéton. Figure 3-3 and Figure 3-4 show the granular distributions of the three industrial RCA. In this study, we are only considering the fraction 0/5mm of industrial RCA (Figure 3-2). Then they

were separated into four different granular classes (0/0.63, 0.63/1.25, 1.25/2.5, 2.5/5mm) in order to study the influence of granular size on the properties of industrial RCA. Each class was tested for SFSA, $ML_{105\text{-}600}$, density, porosity and water absorption.

Figure 3-1 Site crushing machine for production of RCA-Colas1

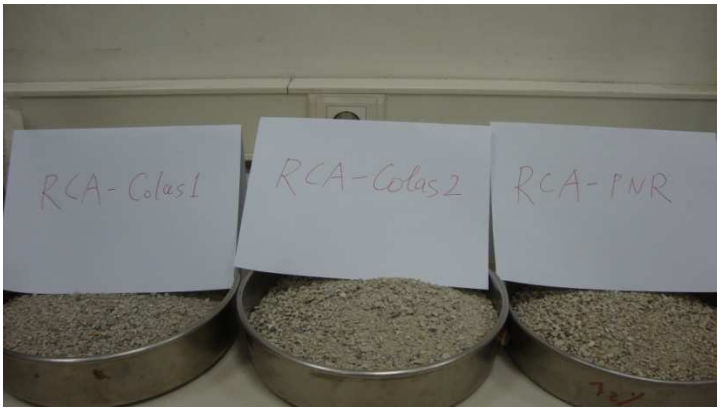

Figure 3-2 Three kinds of industrial RCA (Fraction 0/5mm)

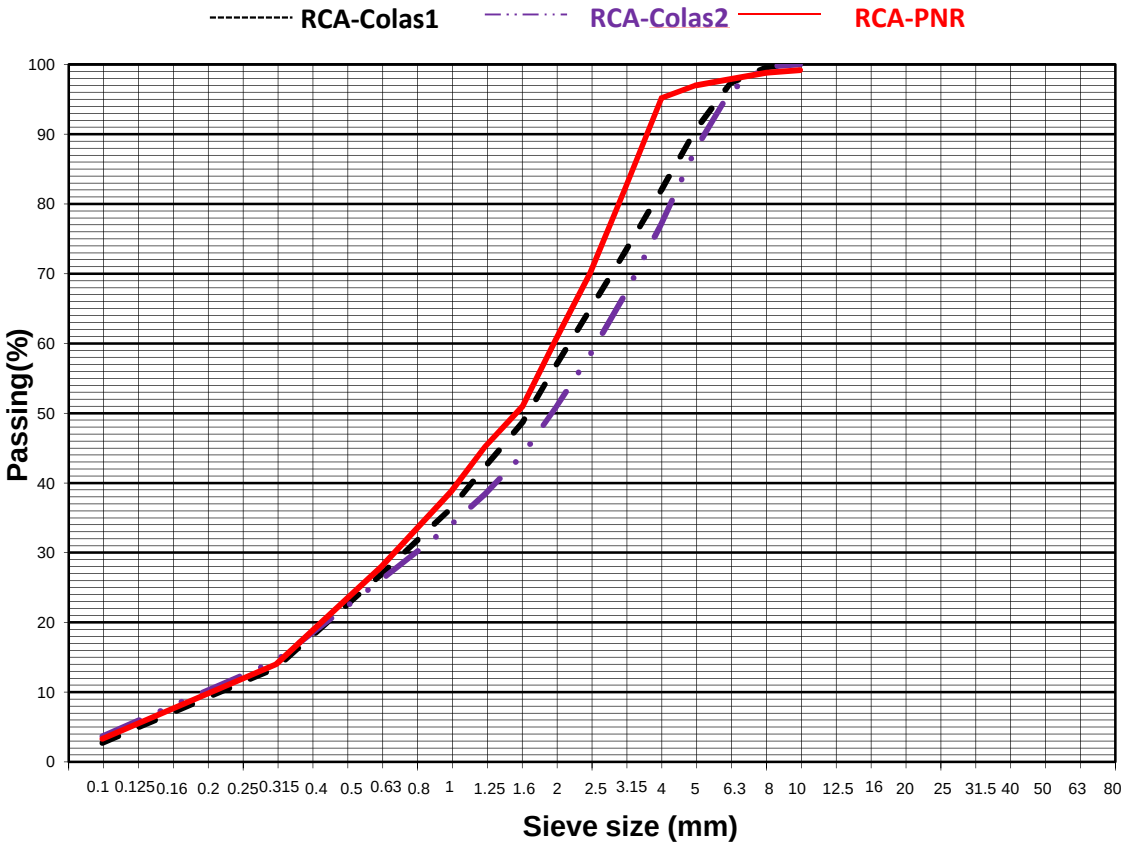

Figure 3-3 Cumulated particle size distributions of the three industrial RCA

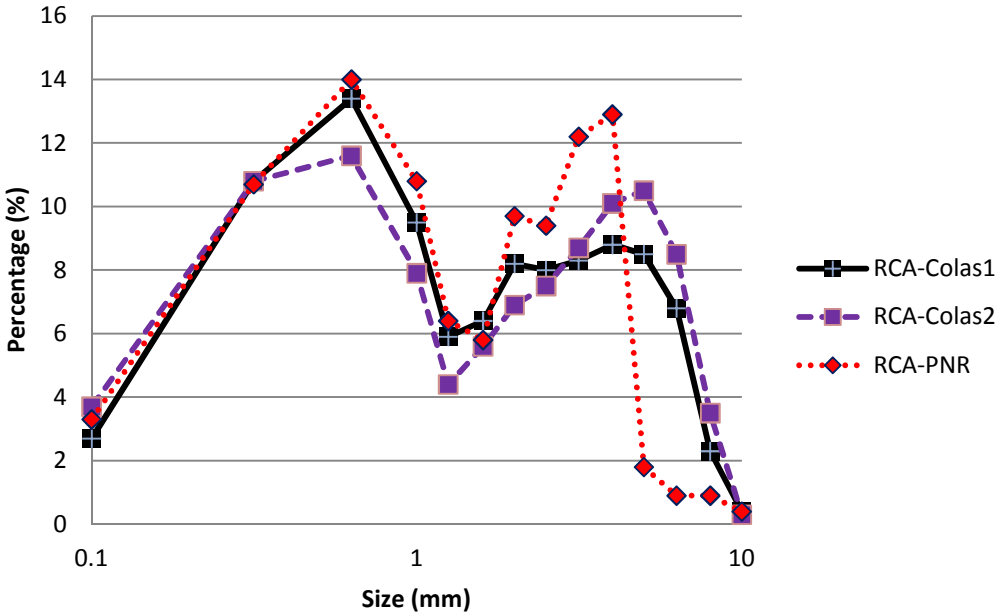

Figure 3-4 Partial particle size distributions of the three industrial RCA

3.2.2 Thermogravimetric analysis (TGA with analysis of gas by MS)

The four different granular classes (0/0.63, 0.63/1.25, 1.25/2.5, 2.5/5mm) of representative samples were tested with a thermogravimetric analysis with analysis of gas by MS. Figure 3-5 to Figure 3-7 present the TGA results for all the industrial RCA studied. As can be seen in these figures, for all the materials tested, a large peak of mass loss is obtained between 500 and 850°C due to the departure of CO_2 which suggest that all the industrial RCA studied contain calcareous aggregates. Moreover a significant decarbonation starts at 500°C showing that the industrial RCA are partly carbonated. The $ML_{105\text{-}600}$ includes therefore part of CO_2, as the three industrial RCA are partly carbonated.

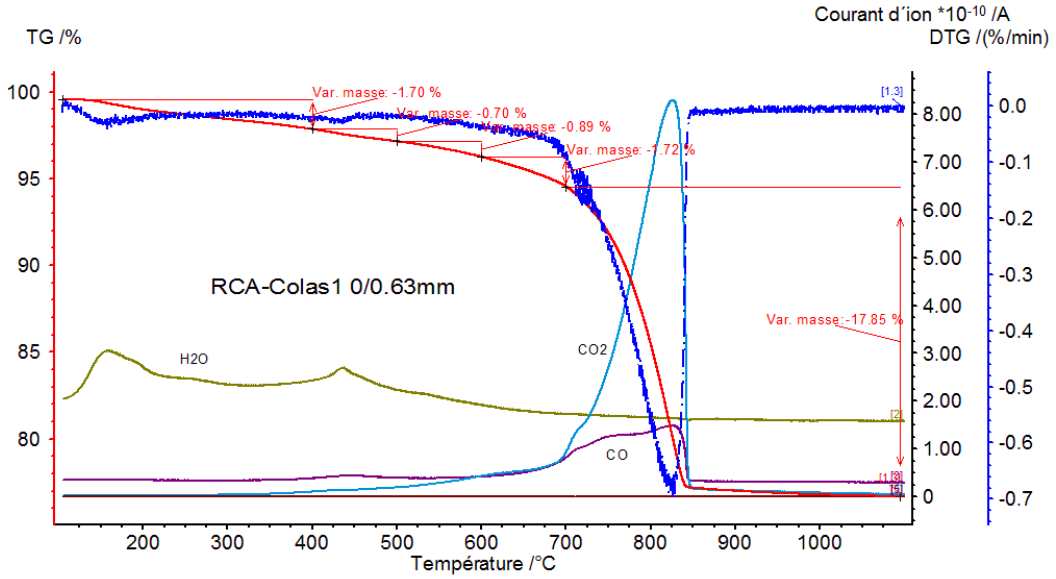

Figure 3-5 TGA with gas of RCA-Colas1 0/0.63mm

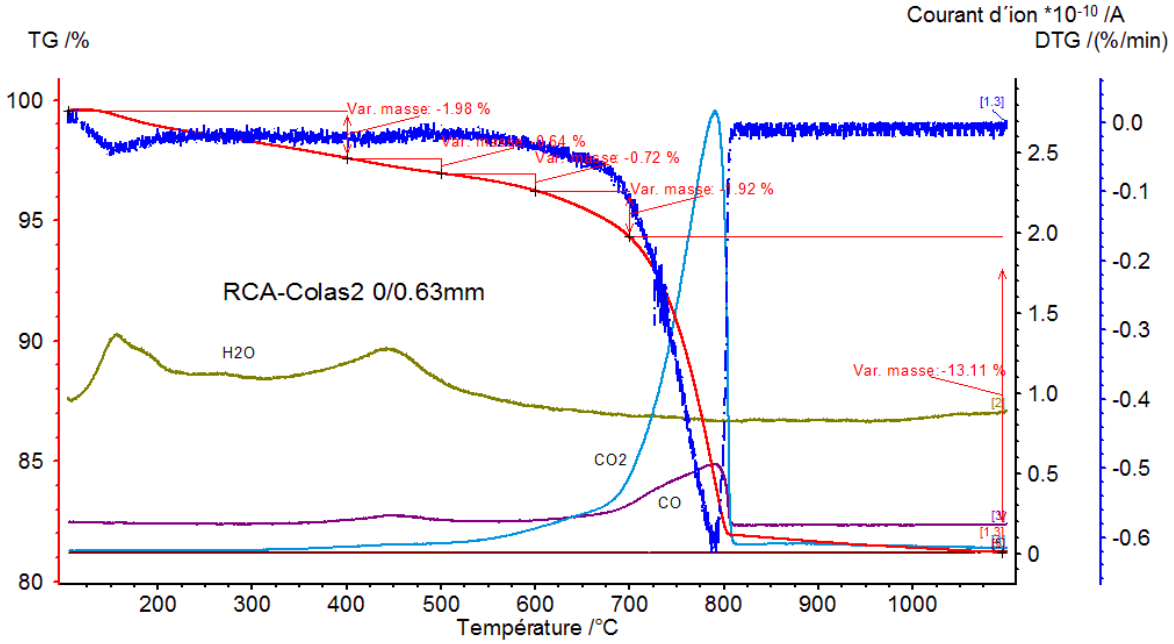

Figure 3-6 TGA with gas of RCA-Colas2 0/0.63mm

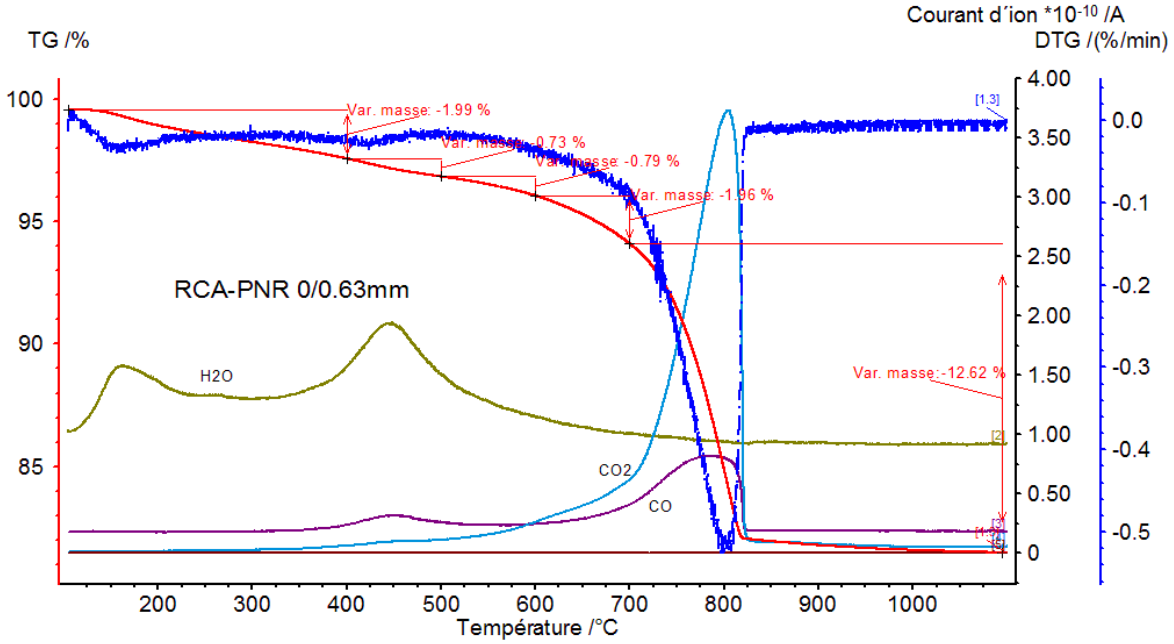

Figure 3-7 TGA with gas of RCA-PNR 0/0.63mm

From the TGA results, different mass losses can be calculated (Table 3-1): $ML_{700\text{-}1095}$ corresponds to the content of crystallized calcite in the sample. $ML_{400\text{-}500}$ corresponds partly to the water bounded by portlandite ($ML_{H2O\text{-}400\text{-}500}$) and some decarbonation of amorphous

calcite ($ML_{CO2-400-500}$). From the curves of gas by MS, the surface areas of H_2O (S_{H2O}) and CO_2 (S_{CO2}) could be estimated, then the mass ratio of H_2O can be calculated, thus $ML_{H2O-400-500}$ can be obtained from Equation 3-1.

$$ML_{H2O-400-500} = ML_{400-500} \times \frac{18 \times S_{H_2O}}{44 \times S_{CO_2} + 18 \times S_{H_2O}} \qquad \text{Equation 3-1}$$

Table 3-1 Mass loss based TGA with gas for industrial RCA

	$ML_{105-400}$	$ML_{400-500}$	$ML_{500-600}$	$ML_{600-700}$	$ML_{700-1095}$
RCA-Colas1 0/0.63	1.7	0.7	0.89	1.72	17.85
RCA-Colas1 0.63/1.25	1.43	0.56	0.97	1.8	20.71
RCA-Colas1 1.25/2.5	1	0.58	1.17	2.27	21.87
RCA-Colas1 2.5/5	0.91	0.54	1.07	2.08	22.43
RCA-Colas2 0/0.63	1.98	0.64	0.72	1.92	13.11
RCA-Colas2 0.63/1.25	1.68	0.55	0.57	1.5	17.19
RCA-Colas2 1.25/2.5	1.48	0.5	0.52	1.37	18.63
RCA-Colas2 2.5/5	1.34	0.47	0.73	1.62	19.28
RCA-PNR 0/0.63	1.99	0.73	0.79	1.96	12.62
RCA-PNR 0.63/1.25	1.48	0.55	0.69	1.6	12.92
RCA-PNR 1.25/2.5	1.36	0.5	0.65	1.51	14.54
RCA-PNR 2.5/5	1.32	0.5	0.64	1.5	15.33
RCA-OC1-90 0/0.63	2.04	1.04	0.35	1.59	29.33
RCA-OC1-90 0.63/1.25	1.81	1.02	0.32	1.37	29.99
RCA-OC1-90 1.25/2.5	1.53	1.01	0.3	1.22	30.85
RCA-OC1-90 2.5/5	1.44	0.98	0.29	1.21	31.25
RCA-OC1-90-carbo 0/0.63	1.03	0.88	2.91	3.54	29.39
RCA-OC1-90-carbo 0.63/1.25	0.94	0.8	2.54	3.11	30.74
RCA-OC1-90-carbo 1.25/2.5	0.81	0.69	2.23	2.8	31.63
RCA-OC1-90-carbo 2.5/5	0.68	0.6	1.92	2.49	32.58
RCA-OC2-90 0/0.63	2.49	1.82	0.46	2.14	25
RCA-OC3-90 0/0.63	2.66	1.79	0.4	1.3	25.03
RCA-OC3-90 0.63/1.25	2.51	1.66	0.38	1.3	25.73
RCA-OC3-90 1.25/2.5	2.19	1.47	0.36	1.35	27.14
RCA-OC3-90 2.5/5	2.18	1.51	0.36	1.27	27.2

Table 3-2 shows the calculated results of $ML_{H2O-400-500}$ and $ML_{CO2-400-500}$. As can be seen, the mass ratio of CO_2 in $ML_{400-500}$ changes as the carbonation degree changes. For uncarbonated laboratory produced RCA (RCA-OC1-90), $ML_{400-500}$ is totally from the bounded water by

portlandite. For carbonated laboratory produced RCA (RCA-OC1-90-carbo), $ML_{CO2-400-500}$ contains 92% in the $ML_{400-500}$. For industrial RCA, $ML_{CO2-400-500}$ contains 59%, 26%, 19% respectively for RCA-Colas1, RCA-Colas2 and RCA-PNR. On the other hand, the content of portlandite decreases from RCA-PNR to RCA-Colas2 and RCA-Colas1. This is in agreement with a stronger carbonation for RCA-Colas1 compared to RCA-Colas2 and RCA-PNR respectively. As a consequence, the portlandite content of industrial RCA is between the zone of uncarbonated RCA and carbonated RCA.

Table 3-2 $ML_{H2O-400-500}$ and $ML_{CO2-400-500}$ based on TGA with gas

	S_{H2O}	S_{CO2}	$ML_{400-500}$	$ML_{H2O-400-500}$	$ML_{CO2-400-500}$
RCA-Colas1 0/0.63	0.10	0.06	0.70	0.28	0.42
RCA-Colas2 0/0.63	0.42	0.06	0.64	0.47	0.17
RCA-PNR 0/0.63	1.25	0.12	0.73	0.59	0.14
RCA-OC1-90 0/0.63	0.50	0	1.04	1.04	0
RCA-OC1-90-carbo 0/0.63	0.03	0.12	0.88	0.07	0.81

All the industrial RCA have less portlandite than uncarbonated laboratory produced RCA, whatever the granular fraction considered. As shown in Figure 3-8, the calcite content decreases as the particle size decreases. This result is due to the larger SFSA in the smaller granular classes.

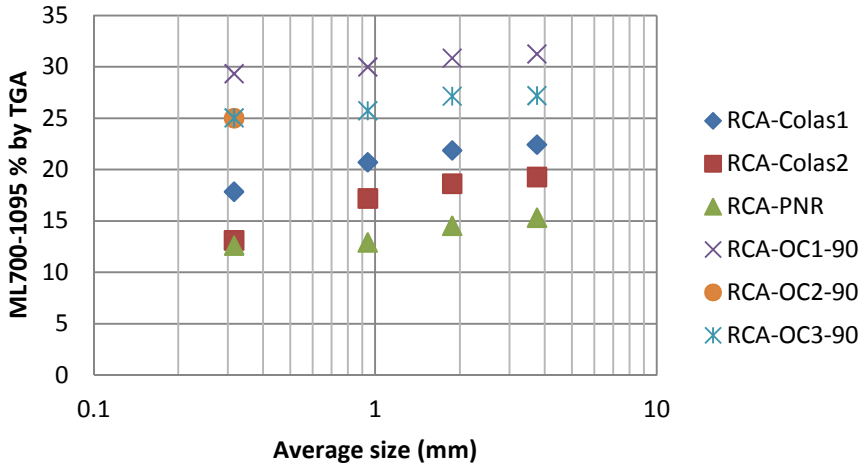

Figure 3-8 $ML_{700-1095}$ obtained by TGA as a function of the average size of the four different granular classes considered (0/0.63, 0.63/1.25, 1.25/2.5, 2.5/5mm)

3.2.3 Carbonation depth

Representative coarse RCA (about 20mm) of Colas1 and RCA-PNR were collected and pre-dried in the oven at a temperature of 105°C, and samples were cut in the middle with the diamond saw. The surfaces of RCA were then polished by using GBrot grinding and polishing machine. Then a solution of phenolphthalein was used to measure the carbonation depth. In the non-carbonated high alkaline part of the sample, a pink color is obtained. On the contrary, in the carbonated part of the sample, no coloration occurs due to the reduction of pH below 10 due to carbonation. For one sample, four images of the polished section were taken with an optical microscope. Carbonation depth was measured at about 6 different locations for each image in order to determine an average carbonation depth on 24 values. 14 samples were analyzed to estimate the variation of carbonation depth for RCA-Colas1 and RCA-PNR.

Figure 3-9 and Figure 3-10 show optical observations of carbonation depth of two samples for RCA-Colas1. Figure 3-11 and Figure 3-12 show optical observations of carbonation depth of two samples for RCA-PNR The average carbonation depth of RCA-Colas1 obtained from the 14 samples is about 1.5±0.9mm, while that of RCA-PNR is about 1.2±0.4mm (Table 3-3). As can be seen, there is a large variation of the carbonation depth for both RCA; some particle has a large carbonation depth whereas some particle just carbonates at the surface. This confirms that industrial RCA has been partly carbonated, RCA-Colas1 has been more carbonated than RCA-PNR in agreement with TGA results.

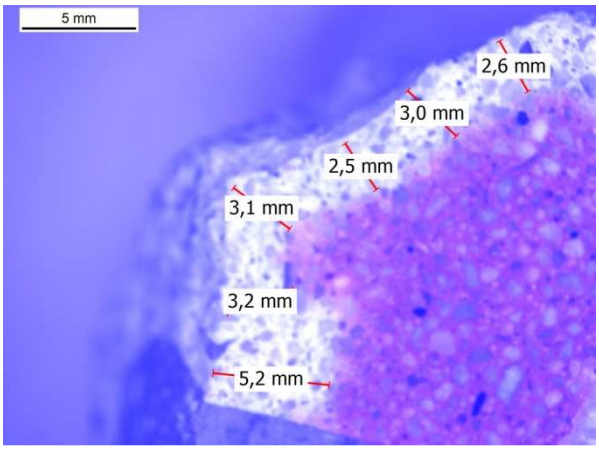

Figure 3-9 Optical observation of RCA-Colas1 (Sample 6)

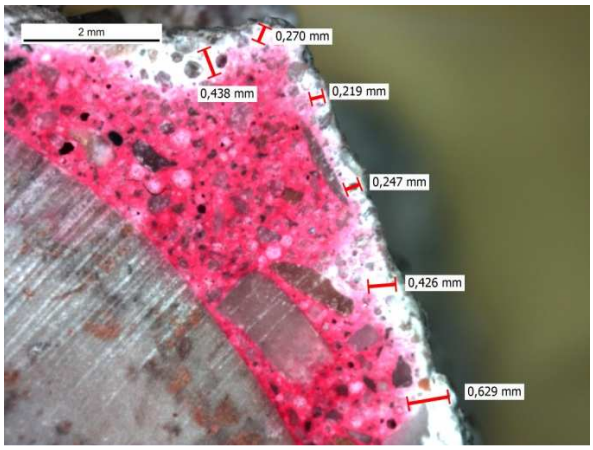

Figure 3-10 Optical observation of RCA-Colas1 (Sample 14)

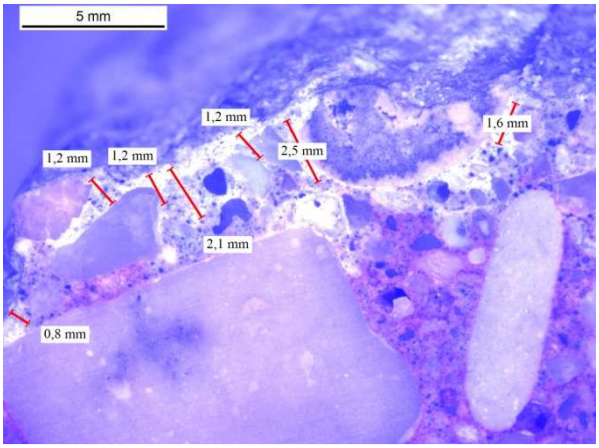

Figure 3-11 Optical observation of RCA-PNR (Sample 14)

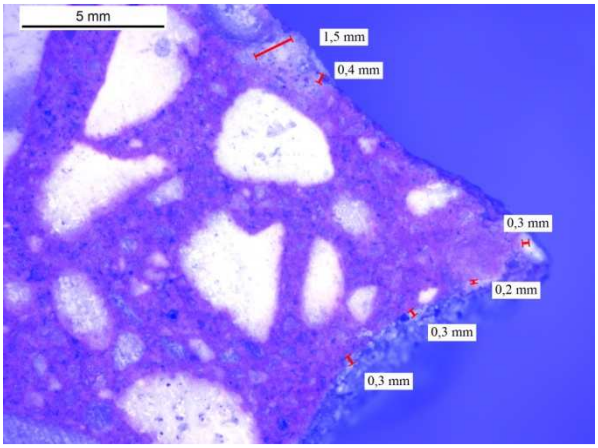

Figure 3-12 Optical observation of RCA-PNR (Sample 7)

Table 3-3 Mean carbonation depth obtained on 24 measurements at 14 different samples for two industrial RCA (mm)

	S1	S2	S3	S4	S5	S6	S7
RCA-Colas1	1.63	0.97	1.34	2.92	1.18	3.49	1.41
RCA-PNR	0.98	1.17	0.95	1.67	0.83	1.54	0.51
	S8	S9	S10	S11	S12	S13	S14
RCA-Colas1	0.70	1.75	2.39	0.68	0.92	0.63	0.50
RCA-PNR	1.17	1.61	1.24	1.15	1.26	0.86	1.86

3.3 Properties of industrial RCA

3.3.1 SFSA and $ML_{105\text{-}600}$

Figure 3-13 and Table 3-4 present the variation of SFSA as a function of granular class for all the FRCA studied. The value of SFSA is the average of three test values. The standard deviations are also shown in this figure (example for RCA-OC1-90 and RCA-Colas2). The average standard deviation for the three industrial RCA is 0.62. As can be seen in Figure 3-13, SFSA is higher as the average particle size decreases for all the industrial RCA. A reasonable linear relation between SFSA and granular class is obtained, similarly to what has been obtained with laboratory produced RCA. The correlation coefficients obtained (R^2) range from 0.77 to 0.92 (Table 3-5, b value corresponds to the SFSA when the particle size tends towards zero). The values obtained for industrial RCA are between the values of uncarbonated laboratory produced RCA and carbonated laboratory produced RCA (for example RCA-OC1-90 and RCA-OC1-90-carbo). As previously shown, the industrial RCA are partly carbonated, the carbonated phases cannot dissolve in salicylic acid, and therefore the lower value obtained for the three industrial RCA comparatively to uncarbonated laboratory produced RCA.

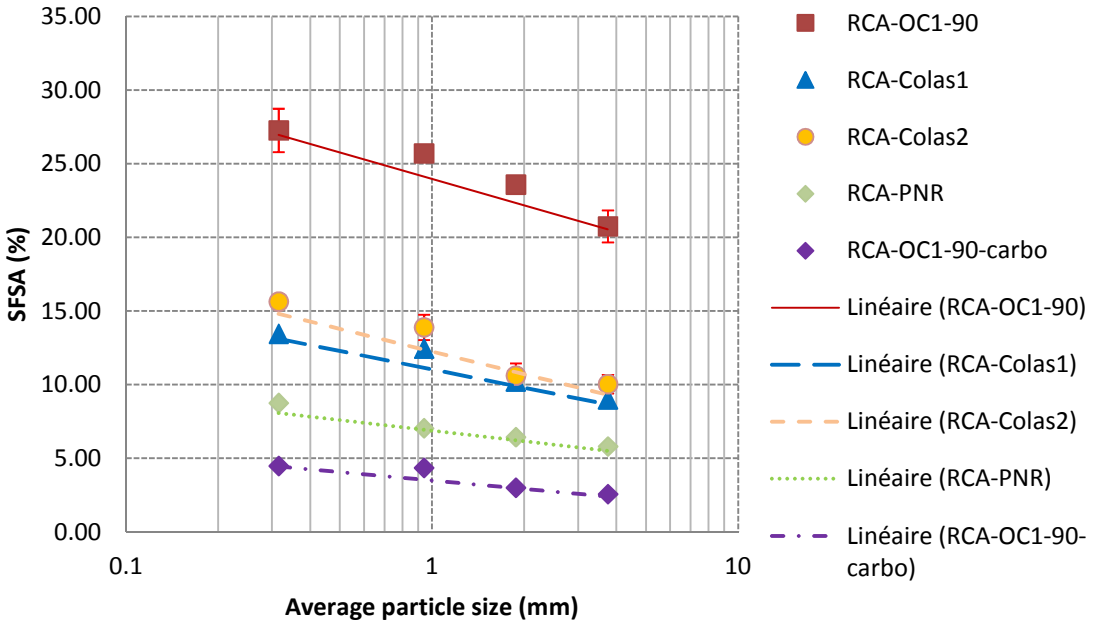

Figure 3-13 SFSA as a function of average size of the four different granular classes considered (0/0.63, 0.63/1.25, 1.25/2.5, 2.5/5mm)

Table 3-4 SFSA of industrial RCA

Fractions (mm)	RCA-OC1-90-carbo	RCA-Colas1	RCA-Colas2	RCA-PNR	RCA-OC1-90
0-0.63	4.48	13.46	15.65	8.76	27.28
0.63-1.25	4.35	12.45	13.90	7.04	25.72
1.25-2.5	3	10.22	10.62	6.44	23.60
2.5-5	2.57	9.00	10.04	5.81	20.76

Table 3-5 Coefficients of the linear relationships between SFSA and particle sizes for industrial RCA (y=ax+b)

Fractions	a	b	R^2
RCA-Colas1	-1.30	13.52	0.92
RCA-Colas2	-1.61	15.32	0.81
RCA-PNR	-0.74	8.29	0.77
RCA-OC1-90	-1.87	27.56	0.99
RCA-OC1-90-carbo	-0.60	4.62	0.86

Figure 3-14 shows the variation of $ML_{105\text{-}600}$ of FRCA based on the thermal method as a function of granular class. The standard deviation value is also shown in this figure (for

example for RCA-OC1-90 and RCA-Colas2), the average standard deviation of the three industrial RCA is 0.13. As can be seen, $ML_{105-600}$ increases as the average particle size decreases for all industrial FRCA, which is similar to the results obtained with laboratory produced FRCA. However, contrarily to laboratory produced RCA, the relation between $ML_{105-600}$ and granular class is not linear.

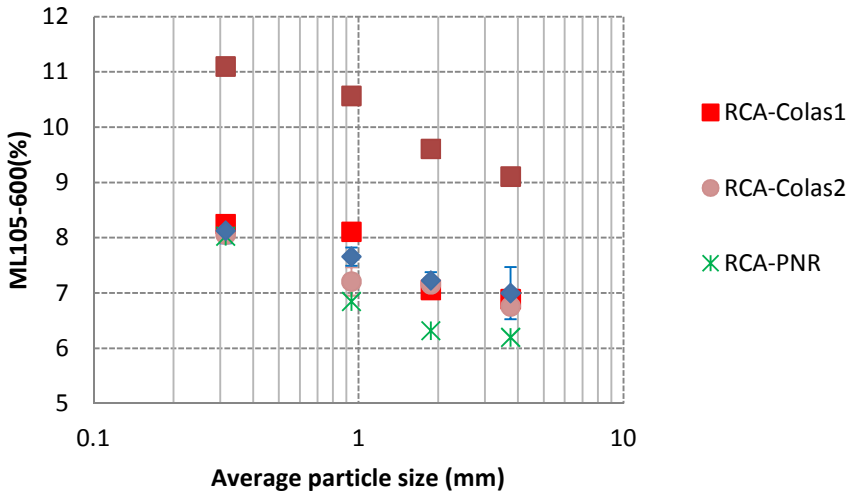

Figure 3-14 $ML_{105-600}$ as a function of the average size of the four different granular classes considered (0/0.63, 0.63/1.25, 1.25/2.5, 2.5/5mm)

3.3.2 Density and porosity

Figure 3-15 presents the variation of apparent density measured with the helium pycnometer as a function of granular class. It shows that the density of FRCA increases as the average particle size increases. The density of all the fractions of industrial FRCA is larger than that of laboratory produced RCA (for example RCA-OC1-90). As the industrial FRCA are partly carbonated, the carbonation degree is much larger than the laboratory produced RCA, the larger values of density are obtained for the industrial RCA could be due to the carbonation, however, the composition of RCA, the density of natural aggregate and density of cement paste in RCA could also change the density of industrial RCA, which are not known for industrial RCA.

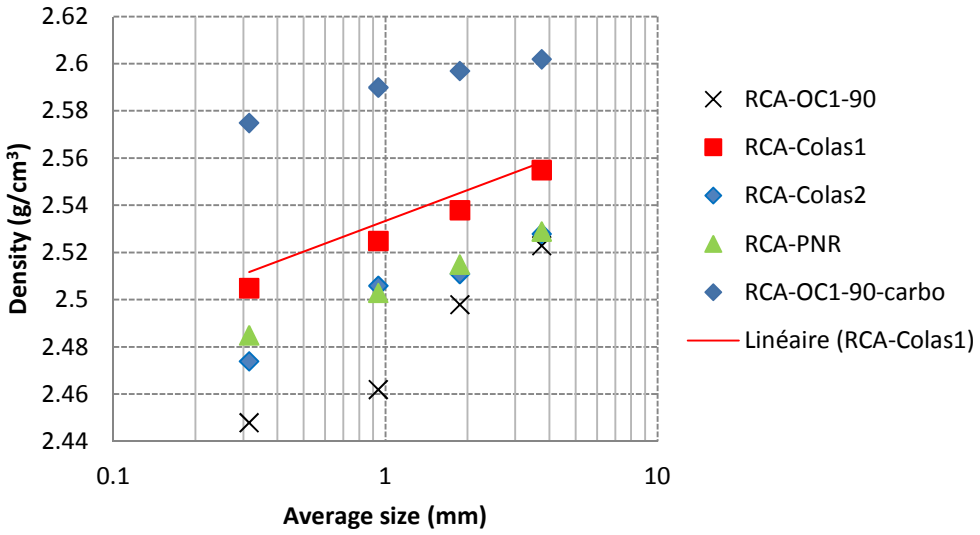

Figure 3-15 Density of FRCA as a function of the average size of the four different granular classes considered (0/0.63, 0.63/1.25, 1.25/2.5, 2.5/5mm)

Figure 3-16 shows the BET specific surface area of all the FRCA, and Figure 3-17 shows BJH porosity of all the granular classes of FRCA. The specific surface area of industrial RCA is lower than the laboratory produced RCA (for example RCA-OC1-90). As shown in chapter 2, the specific surface area increased after accelerated carbonation for laboratory produced RCA. However, in the case of industrial RCA, neither the composition nor the crushing method are known. Moreover, the kinetics of carbonation is very different from that used in our accelerated tests. It is therefore difficult to generalize the previous conclusions to naturally carbonated RCA. As can be seen, the specific surface area of FRCA increases as the average particle size of FRCA decreases. The porosity of industrial RCA is lower than that of laboratory produced RCA (for example RCA-OC1-90). As shown in Chapter 2, carbonation can decrease the porosity. The carbonation degree of industrial RCA is much larger than the laboratory produced RCA, therefore the lower value of porosity could be due to carbonation. The porosity of FRCA increases as the average particle size of FRCA decreases. The relationships between specific surface area or porosity and granular class might be different for three industrial RCA with different compositions. For RCA-Colas1, the relationships

between specific surface area or porosity and granular class are quasi linear. For the other two industrial RCA, the specific surface area and porosity of the finer fraction increases largely comparing with the coarser fractions. Therefore, the specific surface area and porosity can change much for the very fine fractions.

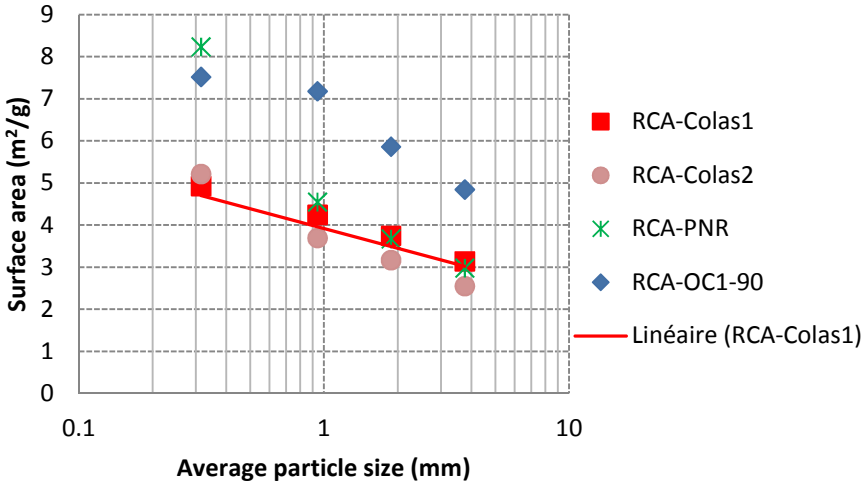

Figure 3-16 BET specific surface area of FRCA as function of the average size of the four different granular classes considered (0/0.63, 0.63/1.25, 1.25/2.5, 2.5/5mm)

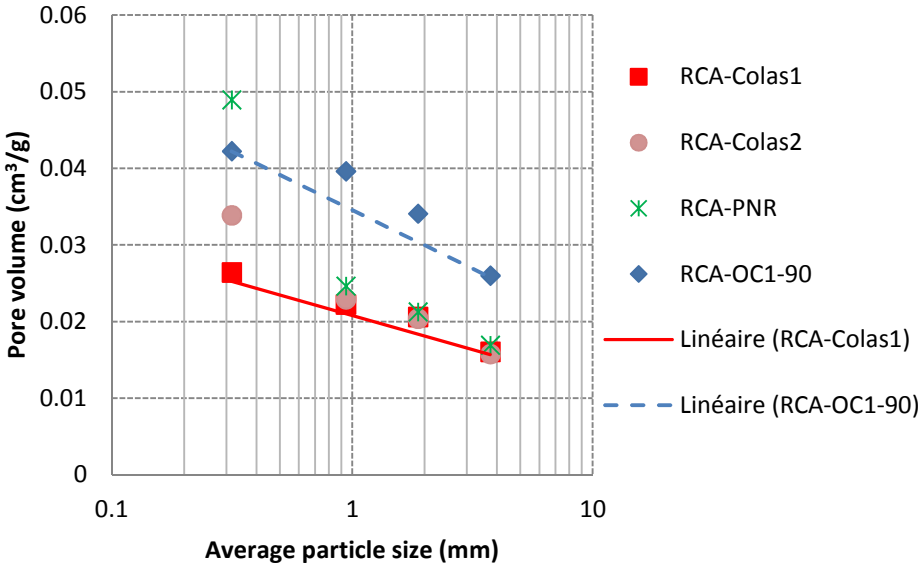

Figure 3-17 BJH porosity of FRCA as function of the average size of the four different granular classes considered (0/0.63, 0.63/1.25, 1.25/2.5, 2.5/5mm)

3.3.3 Water absorption

Figure 3-18 shows the variation of water absorption coefficient of industrial RCA measured with the two methods (EN1097-6 and IFSTTAR). The standard deviation of water absorption is shown for some fractions (for example RCA-PNR). The average standard deviation of all the industrial tests is 0.33. The results obtained with the two experimental methods (EN1097-6 and IFSTTAR) were very close from one to another except for the smaller fraction (0/0.63mm). For all the industrial FRCA tested in our study, the water absorption coefficient increased when the average particle size decreased except for the fraction 0/0.63mm with the standard EN1097-6. This result is similar to that obtained for laboratory RCA, the standard method underestimates the water absorption coefficient for small particles and the IFSTTAR method overestimates it. The results obtained for RCA-Colas2 are larger than the other two industrial RCA, while the RCA-Colas1 and RCA-PNR are similar, whatever the granular class.

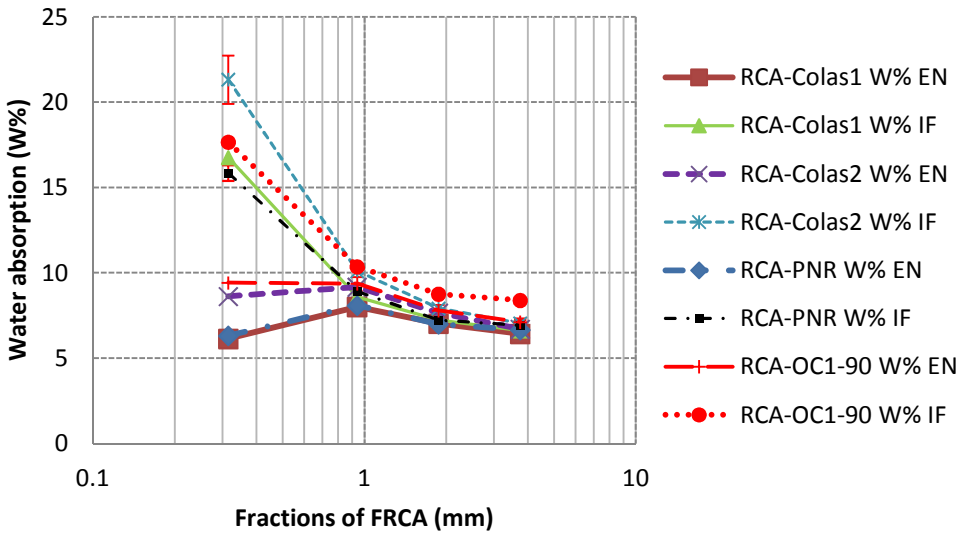

Figure 3-18 Water absorption of industrial RCA measured by EN1097-6 and IFSTTAR methods as a function of the average size of the four different granular classes considered (0/0.63, 0.63/1.25, 1.25/2.5, 2.5/5mm)

3.4 Relationship between SFSA and other properties of RCA

3.4.1 Relationship between SFSA and $ML_{105\text{-}600}$

Figure 3-19 shows the variation of $ML_{105\text{-}600}$ as a function of SFSA. For all studied RCA, the $ML_{105\text{-}600}$ increases linearly with the SFSA (R^2 ranges from 0.77 to 0.98). Table 3-6 shows the slope of $ML_{105\text{-}600}$ to SFSA. The b value is not zero which might be due to the limited number of points and experimental errors of SFSA and $ML_{105\text{-}600}$. The slopes of RCA-Colas1 and RCA-PNR are larger than those of laboratory produced RCA. The slope of $ML_{105\text{-}600}$ to SFSA increases after the carbonation for RCA-OC1-90 (from 0.17 to 0.92, the black circle shows the RCA-OC1-90 in Figure 3-19). The industrial RCA lie between RCA-OC1-90-carbo (high carbonation degree) and laboratory produced RCA (low carboantion degree). Consequently, the slope value depends on the weathering and other influences such as hydration degree and cement composition.

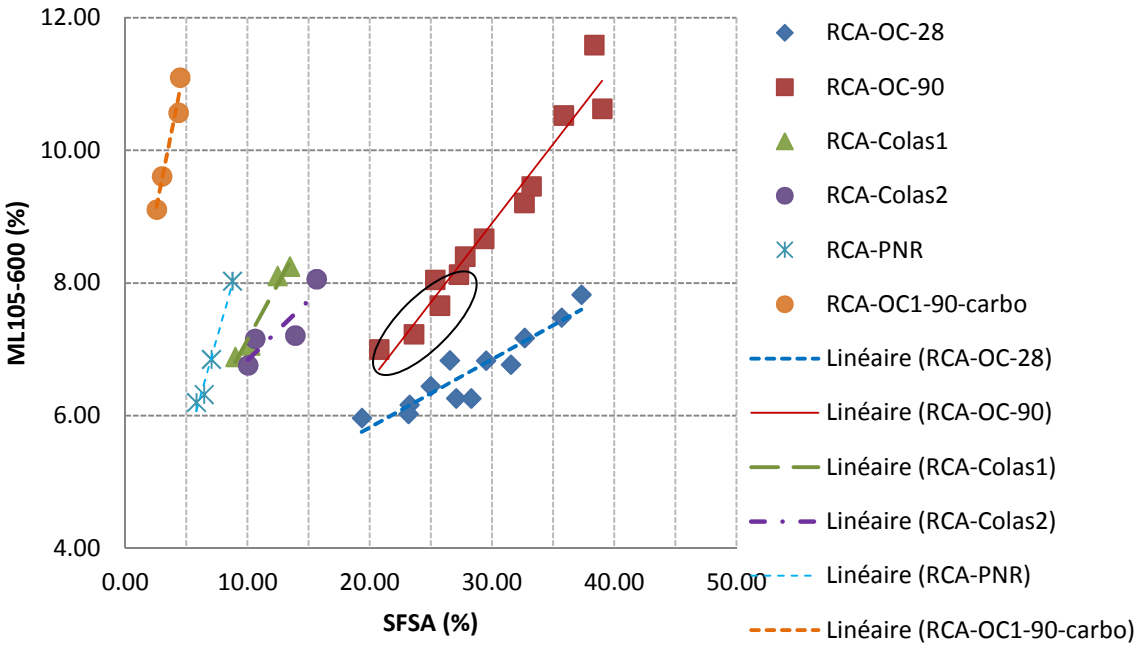

Figure 3-19 $ML_{105\text{-}600}$ versus SFSA

Table 3-6 Coefficients of the linear relationships between $ML_{105-600}$ and SFSA (y=ax+b)

	a	b	R^2
RCA-OC-28	0.10	3.77	0.86
RCA-OC-90	0.24	1.74	0.95
RCA-Colas1	0.34	3.76	0.96
RCA-Colas2	0.18	5.04	0.77
RCA-PNR	0.65	2.28	0.98
RCA-OC1-90	0.17	3.37	0.93
RCA-OC1-90-carbo	0.92	6.77	0.96

3.4.2 Relationship between SFSA and density

Figure 3-20 shows the variation of specific density as a function of SFSA. When SFSA increases, density decreases linearly. Indeed, density of RCA depends on the density of natural aggregate and density of cement paste and proportion of cement paste. Therefore, as the cement paste content increases, the SFSA also incerases and the density of RCA decreases for all the studied RCA. If we consider the intersection points of these relations with axis of coordinates (x=0), we can obtain the density of used natural aggregates. In the same way, when all the RCA is composed of cement paste (x=100%), we can obtain the density of used cement paste. As shown in Table 3-7, the density of cement paste of RCA-PNR is much smaller than that of other materials. This could be due to a larger W/C ratio in the original concrete. However, it has to be noted that, for the industrial RCA studied (as well as for carbonated RCA-OC1-90), the range of variation of SFSA is very limited (about 5%) which certainly leads to large uncertainties on the extrapolated values of NA and CP. The correlation coefficients between density and SFSA (R^2) range from 0.7 to 0.96. The slope of density to SFSA changes a little (from -0.012 to -0.011 after the carbonation, the black circle shows the RCA before carbonation in Figure 3-20).

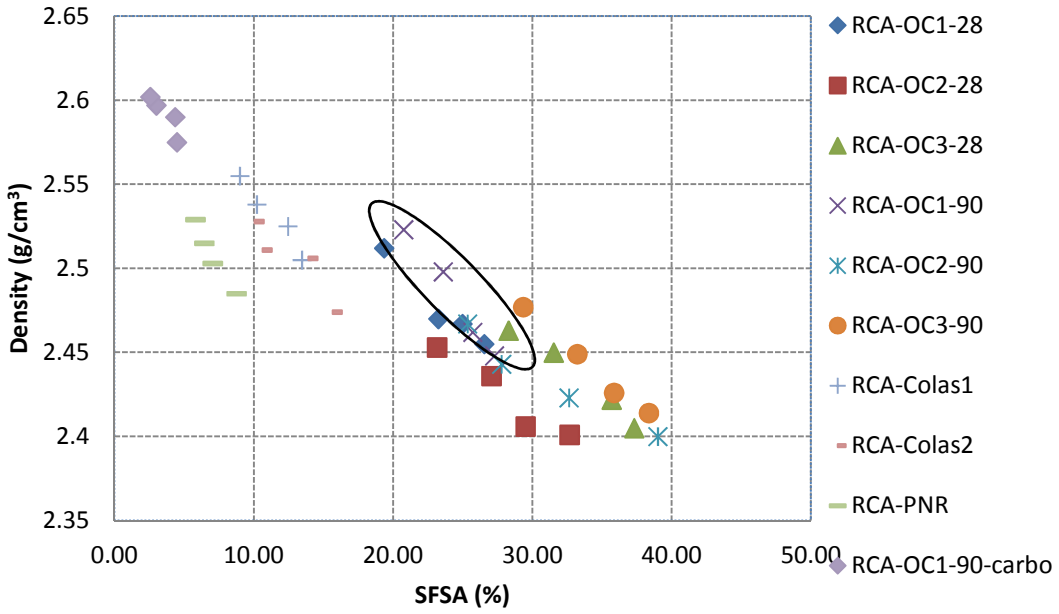

Figure 3-20 Correlation between density and SFSA

Table 3-7 Coefficients of the linear relationships between density and SFSA (y=ax+b)

	a	b	R^2	Density of NA (x=0)	Density of CP (x=100%)
RCA-Colas1	-0.010	2.64	0.95	2.64	1.64
RCA-Colas2	-0.008	2.60	0.82	2.60	1.84
RCA-PNR	-0.014	2.61	0.96	2.61	1.17
RCA-OC1-90	-0.011	2.63	0.78	2.63	1.55
RCA-OC1-90-carbo	-0.012	2.77	0.98	2.77	1.57

3.4.3 Relationship between SFSA and water absorption

Figure 3-21 presents the variation of water absorption (IFSTTAR method) with the SFSA: when SFSA increases, the water absorption increases too. As can be seen, the water absorption of all FRCA varies linearly with the SFSA for the three coarser average particle sizes of RCA. On the contrary, as discussed previously, the water absorption measured by standard or IFSTTAR method for the finer fraction seems to be either underestimated or

overestimated respectively. As discussed previously, the water absorption coefficient of the finer fraction (0/0.63mm) can be obtained by linear extrapolation of the relation between water absorption and SFSA determined with the three coarser fractions of RCA (Table 3-8). Extrapolation carried out using both standard and IFSTTAR methods give similar values for the water absorption coefficient of the finer fraction (Table 3-9), the average difference between these two values obtained for the industrial FRCA is 1.13%. As expected, the value of water absorption coefficient of finer fraction obtained is between the value obtained by the standard and IFSTTAR methods. The water absorption of RCA directly depends on the water absorptions of cement paste and of natural aggregates and on the proportions of cement paste. The water absorption of natural aggregates can be neglected comparing with the absorption of cement paste. The water absorption of cement paste depends on the property of cement paste. Therefore, the water absorption of RCA depends on the properties of cement pastes (W/C ratio, nature of cement, carbonation state) and proportions of cement paste. As shown in Figure 3-21, all the industrial RCA tested are comprised between the zone of laboratory produced RCA and carbonated RCA. Therefore, drawing the water absorption coefficient as a function of the SFSA can be a very convenient method to differentiate different sources of RCA for which the original concrete composition is generally unknown such as industrial RCA. Changes of the slope of this regression can also be used to estimate the effect of the weathering or some specific treatment after RCA being crushed.

Therefore, the proposed method to estimate the water absorption coefficient of the finer fraction (0/0.63mm) of FRCA is also suitable for industrial RCA.

The accurate total water absorption of FRCA used (fraction 0/5mm) can be determined by knowing the proportion and water absorption coefficient of each fraction. As shown in Table 3-10, the water absorption of all the studied FRCA (fraction 0/5mm) is calculated. The values of EN extrapolated are always larger than no extrapolated, which is due to the standard

method (EN 1097-6) which underestimates the water absorption of fraction 0/0.63mm. However, the values of IFSTTAR extrapolated are always larger than no extrapolated, which is due to the IFSTTAR method overestimating the water absorption of fraction 0/0.63mm. The average difference of water absorption between the extrapolated and non extrapolated values is about 0.6% for EN, and 1.7% for IFSTTAR respectively.

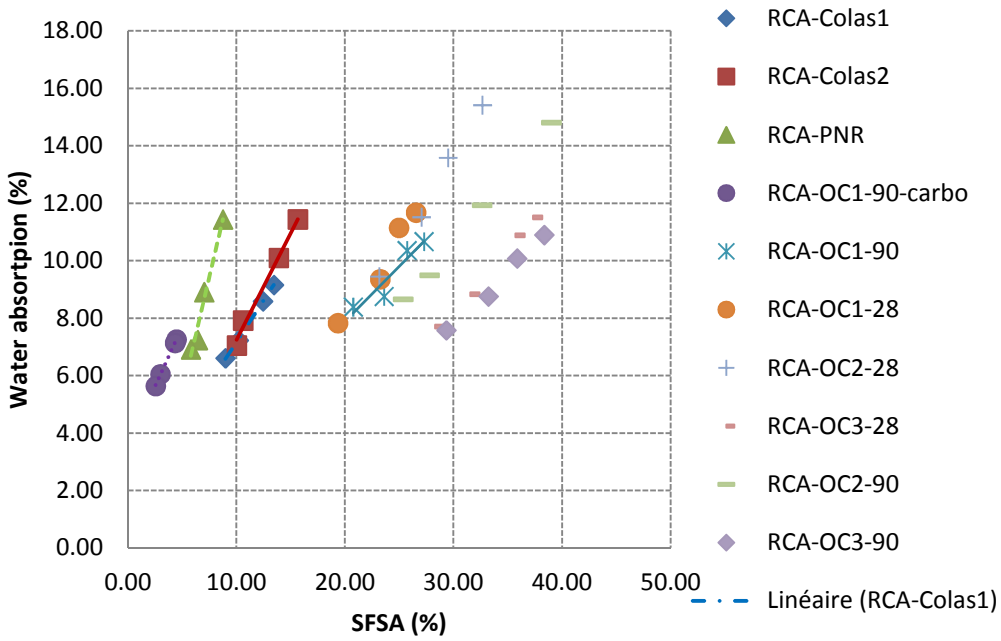

Figure 3-21 Correlation between water absorption (IFSTTAR method) and SFSA for all studied RCA including laboratory produced RCA, industrial RCA and carbonated RCA

Table 3-8 Coefficients of the linear relationships between water absorption (IFSTTAR method for three coarse fractions) and SFSA (y=ax+b) for industrial RCA and carbonated RCA

	a	b	R^2
RCA-Colas1	0.58	1.37	0.98
RCA-Colas2	0.75	-0.25	1.00
RCA-PNR	1.61	-2.65	0.86
RCA-OC1-90	0.83	3.52	1.00
RCA-OC1-90 carbo	0.38	0.24	0.83

Table 3-9 Extrapolated water absorption coefficient of Fraction 0-0.63mm from standard and IFSTTAR for industrial RCA and carbonated RCA

	Tested value of IFSTTAR (%)	Tested value of EN 1097-6 (%)	Extrapolated value of IFSTTAR (%)	Extrapolated value of EN 1097-6 (%)	Difference of two extrapolated values (%)
RCA-Colas1	16.76	6.14	9.16	8.48	0.68
RCA-Colas2	21.33	8.62	11.44	10.23	1.21
RCA-PNR	15.85	6.32	11.44	9.94	1.05
RCA-OC1-90	17.66	9.42	10.67	9.82	0.85
RCA-OC1-90 carbo	13.1	-	7.26	6.35	0.91

Table 3-10 Water absorption coefficient of Fraction 0-5mm calculated by the proposed method (%)

	EN 0/5 (extrapolated)	EN 0/5 (no extrapolated)	IFSTTAR 0/5 (extrapolated)	IFSTTAR 0/5 (no extrapolated)
RCA-OC1-28	8.83	8.24	9.47	11.54
RCA-OC2-28	11.27	9.94	11.51	12.83
RCA-OC3-28	8.57	8.45	9.05	10.77
RCA-OC1-90	8.09	8.02	9.17	10.44
RCA-OC2-90	9.53	8.88	10.36	11.70
RCA-OC3-90	7.53	7.07	8.75	9.73
RCA-Colas1	7.46	6.76	7.86	10.12
RCA-Colas2	8.31	7.83	8.98	11.93
RCA-PNR	7.95	6.90	8.66	9.93

3.5 Conclusions

Some of the major properties of three industrial FRCA have been studied. With these results, we can answer Question 1, 3.

Question 1: Can we define accurate experimental methods allowing to measure the water absorption coefficient and the adherent cement paste content of the different fractions of RCA?

⟹ The method based on the dissolution of the major part of the cement paste contained in FRCA by salicylic acid (SFSA) seem to be also applicable for the measurement of cement paste content of industrial RCA. The method is not applied to obtain the absolute adherent

cement paste content of industrial RCA, especially for carbonated RCA, as salicylic acid cannot dissolve the carbonated cement paste phases. However the insoluble phases of the cement paste will impact similarly all the particle size classes. Therefore, it can give the slope of SFSA with granluar class, and the relationship between SFSA and water absorption can be used to extrapolate the water absorption of the finer fraction. The method proposed for the water absorption is also adapted for industrial RCA.

Question 3: What is the link between size and properties of RCA (mortar or cement paste content, density, water absorption, porosity...)?

⟹ For the three industrial FRCA used in this study, the SFSA decreases with the average particle size of four different granular classes (0/0.63, 0.63/1.25, 1.25/2.5, 2.5/5mm). The properties of FRCA including specific density, water absorption, and porosity are strongly correlated to SFSA. The higher the SFSA, the higher the water absorption and porosity, and the lower the specific density at the exception of the absorption coefficient measured by EN 1097-6 standard for the smaller fraction (0/0.63mm).

From the relationship between water absorption and SFSA (also for the relationship between $ML_{105\text{-}600}$ and SFSA), drawing the water absorption coefficient as a function of the SFSA can be a very convenient method to differentiate different sources of RCA for which the original concrete composition is generally unknown such as industrial RCA. Changes of the slope of this regression can also be used to estimate the effect of the weathering or some specific treatment after RCA being crushed (carbonation).

Chapter 4 Recycled mortars with FRCA

4.1 Introduction

In the previous chapter, we have characterized the properties of FRCA such as SFSA and water absorption. Can we reuse these FRCA as sand in recycled mortars? This chapter presents the application of FRCA (RCA-Colas1) in recycled mortars. The properties of recycled mortars including fresh properties (slump), mechanical properties (compressive strength and splitting strength), and ITZ microstructure will be studied for different mortar compositions and for different states of saturation of the RCA (dried or saturated).

4.2 Materials

Different compositions of recycled mortars with different W/C ratios were designed and manufactured. Materials used in this study are as follows.

4.2.1 Cement

The cement used in recycled mortars was the white OPC (CEM I 52.5 “superblanc”) provided by Lafarge company whose mineralogical composition is shown in Table 2-1, and which was already used for the manufacture of laboratory produced RCA.

4.2.2 Natural sand and FRCA

The natural sand used in recycled mortars was sourced from Tournai and was the same as the one used for the manufacture of laboratory produced RCA. The water absorption of this sand was 1.05% according to the standard EN 1097-6.

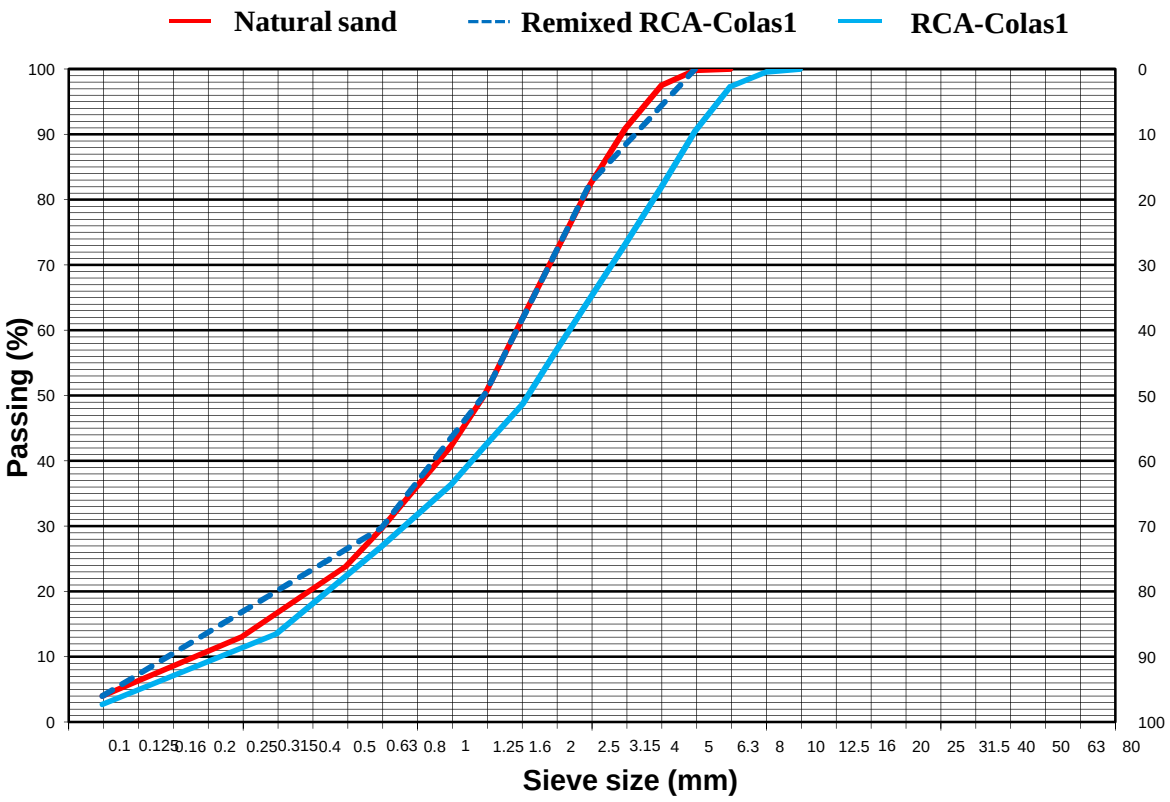

Figure 4-1 Particle size distributions of natural sand and RCA-Colas1 used in reycled mortars

The recycled sand used in the recycled mortars was RCA-Colas1. The size distributions of natural sand and FRCA are shown in Figure 4-1. The RCA-Colas1 was divided into four fractions (0/0.63, 0.63/1.25, 1.25/2.5, 2.5/5mm) and remixed to get a similar granular distribution than natural sand. The water absorption of remixed RCA-Colas1 was estimated from the method previously described in Chapter 2. The water absorption of fraction 0/0.63mm was extrapolated from the relationship between SFSA and water absorption of three coarser fraction values obtained by method EN 1097-6. With the particle size distribution of remixed RCA-Colas1, the water absorption coefficient of remixed FRCA was calculated as 7.54%. Two saturation states of FRCA (Dried RCA and Saturated RCA) were used in this study. For the saturated RCA, the sample was presaturated 24h before the fabrication of mortars.

4.3 Compositions of mortars

Several series of mortars were manufactured in the laboratory. Series I was used to study the influence of saturation state of RCA on the properties of recycled mortars. Series II was used to study the influence of proportions of recycled sand on the mechanical properties of recycled mortars. Series III was used to study the influence of granular fractions of recycled sand on the properties of recycled mortars. In all the series studied, natural calcareous sand was partially or totally replaced by the same volume of recycled sand (remixed RCA-Colas1).

Table 4-1 shows the compositions of mortars Series I manufactured with natural calcareous and recycled sands, noted respectively RM and CM. These mortars are noted RM-W/C-S or RM-W/C-D in the following, W/C referring to the efficient water to cement ratio, and S or D referring to the saturation state of aggregates (S refers to mortars manufactured with saturated sand, D refers to mortars manufactured with dry sand, and absorbed water is added in the mixer). Three W/C ratios of 0.5, 0.55, and 0.6 were studied.

Table 4-1 Compositions of mortars Series I

	Cement (g)	Recycled sand (g)	Efficient water (g)	Absorbed water (g)	W_{eff}/C at T0	Volume % of CP at T0
CM-0.5-S	450	1350*	225	14.18	0.5	41
CM-0.5-D	450	1350	225	14.18	0.53	42
RM-0.5-S	450	1291.1*	225	97.35	0.5	38
RM-0.5-D	450	1291.1	225	97.35	0.72	44
RM-0.55-S	450	1291.1*	247.5	97.35	0.55	40
RM-0.55-D	450	1291.1	247.5	97.35	0.77	45
RM-0.6-S	450	1291.1*	270	97.35	0.6	41
RM-0.6-D	450	1291.1	270	97.35	0.82	46

Remark :* Presaturated with efficient water 24 hours before mixing.

Table 4-2 shows the compositions of mortars Series II with W/C=0.5 manufactured with different proportion of recycled sand. These recycled mortars are noted RM-W/C-Proportion in the following, W/C referring to the efficient water to cement ratio, and Proportion referring to the volume replacement proportion of recycled sand. For example, RM-0.5-10 refers to the

recycled mortar manufactured with W/C of 0.5, and where 10% of natural sands are replaced by the same volume of recycled sand. Recycled mortars with W/C ratios of 0.6 were also studied just changing the efficient water quantity and the other quantities of materials used being the same as the recycled mortar with W/C ratios of 0.5. Both recycled sands and natural sands in Series II were presaturated 24 h before manufacture.

Table 4-2 Compositions of mortars Series II with W/C=0.5

	RM-0.5-0	RM-0.5-10	RM-0.5-20	RM-0.5-30	RM-0.5-50	RM-0.5-100
Recycled sand (g)	0.0	129.1	258.2	387.3	645.6	1291.1
Natural sand (g)	1350.0	1215.0	1080.0	944.9	675.0	0.0
Total Sand (g)	1350.0	1344.1	1338.2	1332.2	1320.6	1291.1
Cement (g)	450	450	450	450	450	450
Efficient water (g)	225	225	225	225	225	225
Absorbed water (g)	14.18	22.5	30.81	39.13	55.77	97.35

Table 4-3 Compositions of mortars Series III with W/C=0.5

	Control Mortar	RM-0.5-0/0.63	RM-0.5-0.63/1.25	RM-0.5-1.25/2.5	RM-0.5-2.5/5
Sand 0/0.63 (g)	399.60	*376.32*	399.60	399.60	399.60
Sand 0.63/1.25 (g)	278.10	278.10	*263.99*	278.10	278.10
Sand 1.25/2.5 (g)	433.35	433.35	433.35	*413.47*	433.35
Sand 2.5/5 (g)	238.95	238.95	238.95	238.95	*229.52*
Total sand (g)	1350.00	1326.72	1335.89	1330.12	1340.57
Cement (g)	450	450	450	450	450
Efficient water (g)	225	225	225	225	225
Absorbed water (g)	14.18	41.89	32.40	38.69	26.42

Remark : the value in red is the quantity of recycled sand while the others correspond to natural sand.

Table 4-3 show the compositions of mortars Series III with w/c=0.5 manufactured with replacing each fraction of natural sand with the corresponding fraction of recycled sand. These recycled mortars are noted RM-W/C-Fraction in the following, W/C referring to the efficient water to cement ratio, and Fraction referring to the replacement fraction of recycled sand. For example, RM-0.5-0/0.63 refers to the recycled mortar manufactured with W/C of 0.5, the fraction 0/0.63 mm of natural sand being replaced with the same volume of recycled

sand (the fractions from 0.63 up to 5mm correspond to natural sand). Mortars with W/C ratios of 0.6 were also studied just changing the efficient water quantity and the other quantities of materials used being the same as mortars with W/C ratios of 0.5. All the sands in Series III were presaturated 24 hours before manufacture.

4.4 Experimental methods

4.4.1 Mixing procedure for manufacture of mortars

For mortars manufactured with saturated RCA, the sand was presaturated with the efficient water 24h before the fabrication, and the absorbed water was added at the fabrication. The mixing procedure of mortar with saturated sand (M-S) is shown in Figure 4-2. For mortar manufactured with the dried RCA, the quantity of efficient water and absorbed water was added at the fabrication. The mixing procedure of mortar with dried sand (M-D) is also shown in this Figure 4-2.

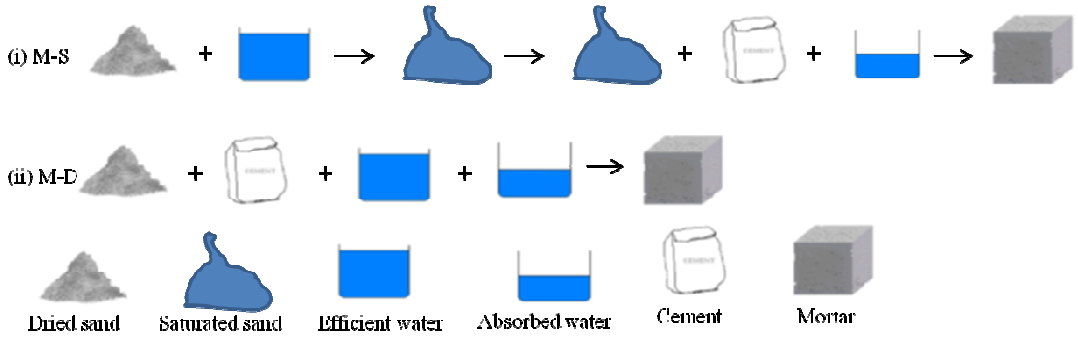

Figure 4-2 Mixing procedures of (i) M-S and (ii) M-D

The precise mixing procedure is as follows:

(1) Place the sand into the bowl, and then place the cement into the bowl, mix at low speed during 30s;

(2) Put the water in the mixer, and start to record the time (T0), mix at low speed during 30s, then switch the mixer to high speed and continue for 30s;

(3) Stop the mixer for 90s. During the first 30s, remove the mortar adhering to the wall and bottom of the bowl and place it in the middle of the bowl with a plastic scraper;

(4) Restart the mixer at high speed for 60s.

4.4.2 Slump test

After mixing, the slump of mortar was measured with the MBE cone (Mortier de Béton Equivalent) which is shown in Figure 4-3. The procedure of slump measurement is as follows:

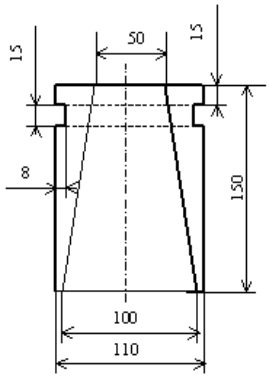

Figure 4-3 Cone MEB used for measuring slump of mortar (In the right figure the unit is mm)

(1) First, make sure that inner wall of mini cone is clean and slightly damp;

(2) Introduce the mortar into the mould in three layers of equal thickness. Compact each layer 15 times with the tamping rod, uniformly distribute the strokes over the cross-section of each layer. Level the top of the cone and remove spilled mortar from the base plate/surface carefully;

(3) Remove the mould by raising it carefully in a vertical direction as possible in 2-3 seconds.

Immediately after removal of the mould, measure and record the slump value by determining the difference between the height of the mould and that of the highest point of the slumped test specimen as shown in Figure 4-3.

(4) If the slump value is measured as a function of time, the specimen is put into the bowl of the mixer and is prevented from evaporation with plastics films during the waiting time. Before the new slump test, the specimen is remixed at high speed for 60s.

4.4.3 Mechanical properties

The preparation of specimens for mechanical strength tests is shown as follows:

(1) After the mixing of mortar, the specimens are placed into the mould (4x4x16cm) according to EN 196-1.

(2) Cover with plastics film and cure for 24h in the moist air room.

(3) Demold the specimens and cure in the water until the age of testing.

Flexural strength is determined with three-point bending test, with a loading at the rate of (50±10) N/s according to EN 196-1. Compressive strength is tested at the rate of (2400±200) N/s until fracture according to EN 196-1. These two mechanical tests are carried out with an INSTRON 5500R 4206-006 (loading capacity 1500 KN) which is shown in Figure 4-4.

Figure 4-4 INSTRON machine used for mechanical testing of mortars

4.4.4 ITZ characterization

After the compressive strength tests, small samples of mortar were collected in order to carry out microscopic observations. Samples were dried at 105°C until constant mass and were then impregnated in epoxy resin, under vacuum. Finally the specimens were polished and carbon coated. Scanning Electron Microscope (SEM) with Energy Dispersive X-ray Spectroscopy (EDS) analysis was carried out with a HITACHI S-4300SE/N which is shown in Figure 4-5.

Figure 4-5 SEM with EDS analysis used by the HITACHI S-4300 SE/N

4.5 Results and discussion

4.5.1 Influence of saturation state on the properties of recycled mortars

Figure 4-6 shows the changes of slump as a function of time for mortar Series I (Slump values are shown in Table 4-4). For the three different w/c ratios, the slump of RM-D is always higher than RM-S which is due to higher initial free water and higher initial paste volume. For example, in the mortar RM-0.5-D at the beginning, the efficient W/C is 0.72, while it is 0.5 for RM-0.5-S. Moreover, the volume proportion of paste in RM-0.5-D is 44% (additional

water doesn't go immediately into the recycled sand), it is only 38% for RM-0.5-S. Therefore, the slump of RM-0.5-D is much higher than RM-0.5-S.

The rate of slump loss of RM-D is quicker than that of RM-S, which could be due to the absorption of free water in recycled sand but also to the higher initial slump value (for example the slope of RM-0.5-S is almost zero due to the very small initial slump value, the slope of slump loss for RM-0.5-S is 0.37 with an initial slump value of 44mm, as shown in Table 4-5). However, whatever the w/c ratio used, the slump value of mortars manufactured with dried aggregates is always larger than that of mortars manufactured with saturated aggregates. This result suggests that the absorption of water by dried aggregates in the mortar is lower and/or slowly than the absorption determined with standard procedures. It could be due first to the kinetics of absorption (the time of immersion of aggregates into mixing water before placing is much smaller than the 24h immersion used in the standards). But it could also be due to a lesser water absorption capacity of aggregates when they are immersed into the cement paste. Indeed, the large specific surface area of cement grains leads to an increase in apparent viscosity of mixing water, preventing is from draining into aggregates. Moreover, some surface porosity of RCA could be filled with small cement particles, reducing the absorption capacity of RCA.

Table 4-4 Slump values (in mm) of mortars Series I as a function of time

Time (T0+mins)	5	15	30	45	60	75	90	105	120
CM-0.5-S	13	10	7	6	6				
CM-0.5-D	33	33	28	18	12	9	6		
RM-0.5-S	6	5	5	4					
RM-0.5-D	44	43	41	37	24	15	11	7	
RM-0.55-S	22	21	19	17	16	13	10	7	4
RM-0.55-D	50	49	45	40	33	28	20	13	9
RM-0.6-S	55	48	41	34	27	23	22	15	13
RM-0.6-D	89	82	76	66	61	50	40	37	22

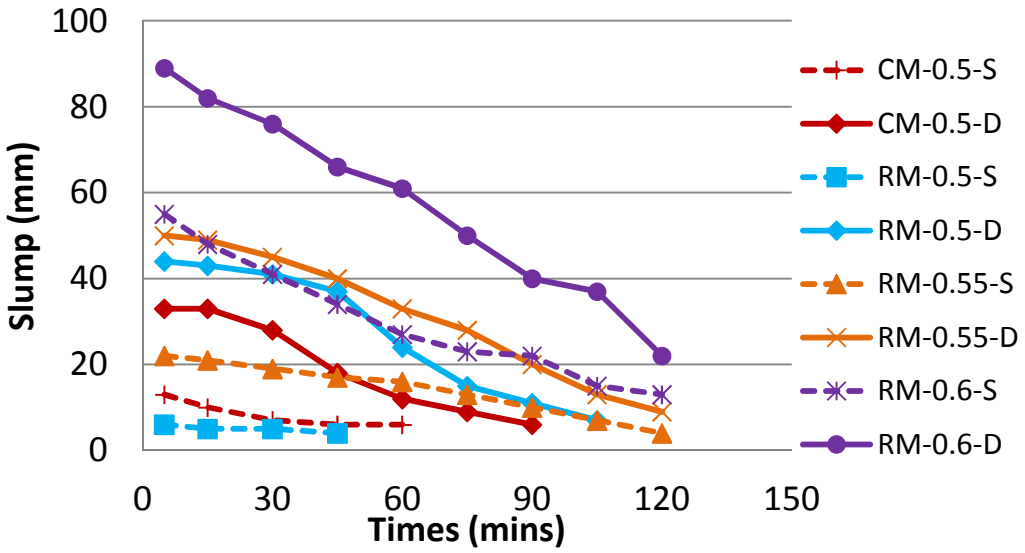

Figure 4-6 Changes of slump as a function of time for mortar Series I

Table 4-5 Coefficients of the linear relationships between slump and time (y=ax+b)

	a	b	R^2
CM-0.5-S	-0.13	12.34	0.88
CM-0.5-D	-0.35	36.02	0.97
RM-0.5-S	-0.01	6.00	1.00
RM-0.5-D	-0.37	39.02	0.99
RM-0.55-S	-0.15	23.71	0.98
RM-0.55-D	-0.38	54.94	0.99
RM-0.6-S	-0.36	52.54	0.96
RM-0.6-D	-0.56	91.90	0.99

Table 4-6 shows the mechanical properties of mortars of Series I. As can be seen, with the same volume of aggregates, the flexural strength of recycled mortar is lower than that of calcareous mortar (the flexural strength of RM-0.5-S decreases 26.8% comparing with CM-0.5-S, while the flexural strength of RM-0.5-D decreases 27.7% comparing with CM-0.5-D). The compressive strength of recycled mortars is lower than for the calcareous mortar (the compressive strength of RM-0.5-S decreases 32.3% comparing with CM-0.5-S, while the compressive strength of RM-0.5-D decreases 30.8% comparing with CM-0.5-D). These lower properties are caused by the poorer properties of recycled sand in comparison to calcareous

sand used (the presence of adherent cement paste leads to higher porosity and water absorption comparing with the calcareous sand).

As can be seen, flexural strengths of mortars with the saturated and dried aggregates are almost the same both for the recycled mortar and calcareous mortar. The compressive strength of mortars (either with natural or recycled sand) with dried aggregates is always larger than with saturated aggregates (increase by 7.9% for calcareous sand, increase by 10.2%, 5.4%, and 4.3% with w/c ratio 0.5, 0.55, and 0.6 respectively for recycled aggregates).With dried aggregates, porous aggregates absorb water which could also drive some cement grains at the surface of aggregates, improving their ITZ [151], which leads to better compressive strengths than with saturated aggregates.

Table 4-6 Properties of mortars Series I

	CM-0.50-S	CM-0.50-D	RM-0.50-S	RM-0.50-D	RM-0.55-S	RM-0.55-D	RM-0.60-S	RM-0.6-D
Fresh density (g/cm^3)	2.40	2.36	2.15	2.14	2.16	2.13	2.16	2.12
28 days saturated density (g/cm^3)	2.40	2.38	2.15	2.15	2.18	2.15	2.17	2.13
Flexural strength (MPa)	11.97	12.15	8.76	8.78	8.10	8.15	7.72	7.80
Compressive strength(MPa)	66.75	72.00	45.22	49.84	43.01	45.34	41.96	43.76

4.5.2 Influence of recycled sand on the mechanical properties of recycled mortar

Two series of recycled mortars with two different w/c ratios are used to study the influence of recycled sand on the properties of recycled mortars. Series II is used to study the influence of proportions of recycled sand on the mechanical properties of recycled mortars. Series III is used to study the influence of granular fractions of recycled sand on the properties of recycled mortars.

Table 4-7 shows the properties of mortars Series II. As can be seen, for both water to cement ratios, the fresh density decreases as the percentage of sand replacement increases, which is due to the lower density of recycled sand. The compressive strength of recycled mortars decreases as the replacement of recycled sand increases. The compressive strength of mortar can be predicted with different methods. One of the more efficient methods has been proposed by De Larrard and Sedran [152-153]. However, we use here in a first approximation the simple equation of Bolomey (Equation 4-1)[154].

$$R_c = G\sigma\left(\frac{C}{E} - 0.5\right) \qquad \text{Equation 4-1}$$

In Equation 4-1, C/E represents cement to efficient water ratio, G is a granular coefficient depending only on the aggregates, and σ is the 28 days compressive strength of normal cement mortar (65 MPa with the white cement used).

Knowing R_c, σ, and C/E, the G value can be calculated. For a given mixture between natural and recycled sand, if the efficient water is correctly known, the G value of two corresponding mortars having different W/C should be the same. Table 4-7 shows that the G values of mortars having the same sand composition with W/C of 0.5 and 0.6 are very close from one to another (the G values are very close for RCA content lower than or equal to 30%, a larger difference is obtained for 50 and 100% RCA). This suggests that the efficient water in these mortars is correctly predicted (so that the water absorption coefficients are correctly determined).

Moreover, we assume that the granular coefficient G_{mix} of a mixture of recycled sand (of granular coefficient G_{RCA}) with natural sand (of granular coefficient G_{NA}) can be calculated as following:

$$G_{mix} = XG_{RCA} + (1 - X)G_{NA} \quad \text{Equation 4-2}$$

where X represents the fraction of recycled sand in the mixture.

For all the mixtures of sands used in mortar Series II, a calculated G coefficient (based on Equation 4-2) can therefore be compared with an average measured G coefficient (calculated with G values obtained with the two different W/C). The comparison between calculated and average measured G values is presented in Figure 4-7. The slope of the regression between calculated and measured G values is 1.01 (Figure 4-7), which suggests that the granular coefficient of the sand mixture can be approximated with Equation 4-2, and that the efficient water is correctly predicted in the mortar compositions. The value of water absorption of recycled sand used seems therefore to be correct.

Table 4-7 Properties of recycled mortars Series II

W/C=0.5	RM-0.5-0	RM-0.5-10	RM-0.5-20	RM-0.5-30	RM-0.5-50	RM-0.5-100
Slump (mm)	27	17	19	29	8	5
Fresh density(g/cm^3)	2.37	2.37	2.34	2.30	2.26	2.15
Flexural strength (MPa)	12.14	13.06	12.05	10.86	10.53	8.54
Compressive strength (MPa)	67.77	66.63	64.58	57.23	53.84	42.09
G	0.70	0.68	0.66	0.59	0.55	0.43
W/C=0.6	RM-0.6-0	RM-0.6-10	RM-0.6-20	RM-0.6-30	RM-0.6-50	RM-0.6-100
Slump (mm)	105	93	80	76	70	55
Fresh density(g/cm^3)	2.31	2.27	2.27	2.26	2.20	2.15
Flexural strength (MPa)	10.63	10.55	10.21	10.00	9.16	8.00
Compressive strength (MPa)	55.98	51.17	49.32	47.37	46.92	39.14
G	0.74	0.67	0.65	0.62	0.62	0.52
Average mesured G value	0.72	0.68	0.66	0.61	0.59	0.47
Calculated G value	0.72	0.69	0.67	0.64	0.60	0.47

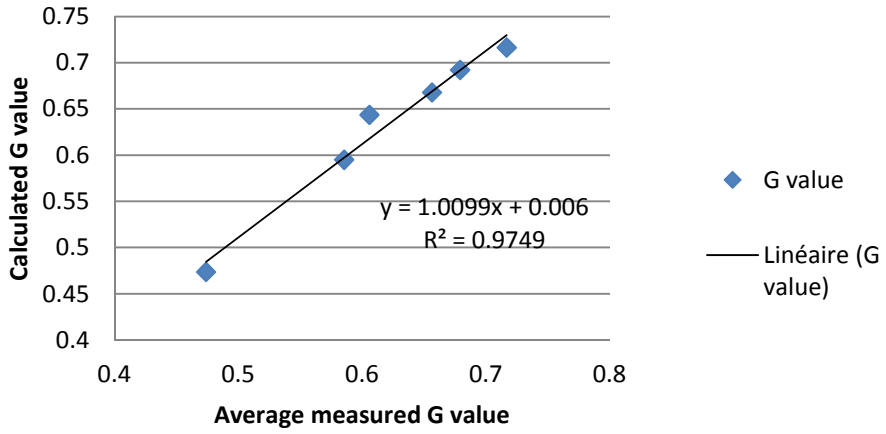

Figure 4-7 Relationship between calculated G value and average measured G value

Figure 4-8 shows the compressive strength of mortar series II with w/c=0.5 and 0.6. We can first observe that the strength of recycled mortars varies linearly with the replacement ratio of calcareous sand by recycled sand, for both water to cement ratios. The slope of compressive strength of w/c=0.5 is larger than w/c=0.6. The compressive strength of recycled mortar (w/c=0.5) decreases 1.7%, 4.7%, 15.6%, 20.6%, 37.9% as the replacement ratio is 0, 10, 20, 30, 50, 100% comparing with the reference mortar respectively.

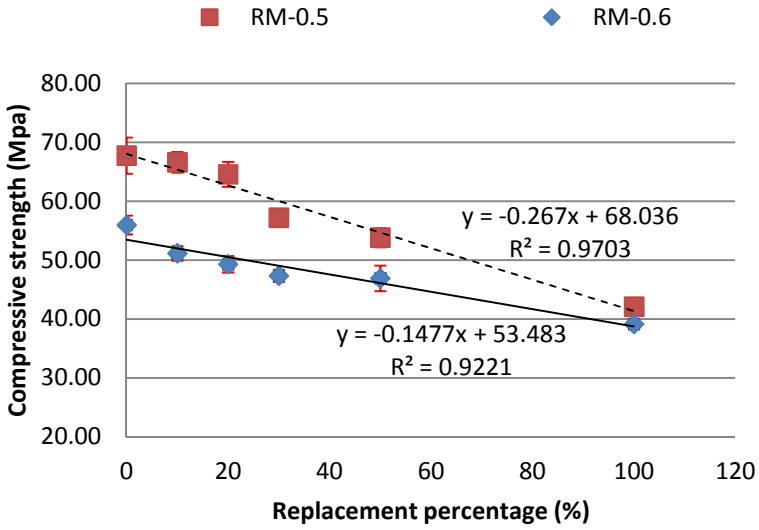

Figure 4-8 Compressive strength of recycled mortar vs replacement percentage

Table 4-8 shows the properties of mortars Series III. As can be seen, for both water to cement ratios, the fresh density decreases when each fraction of natural sand is replaced with recycled sand, which is due to the lower density of recycled sand. Figure 4-9 shows the compressive strength of recycled mortars with each fraction replacement. For both w/c ratios, the compressive strength of mortars containing recycled sand is lower than the control mortar (for example, the compressive strengths of RM-0.6-0/0.63, RM-0.6-0.63/1.25, RM-0.6-1.25/2.5, RM-0.6-2.5/5, decrease 17.58%, 6.85%, 5.37%, 3.08% respectively comparing with the control mortar for w/c=0.6.)

Table 4-8 Properties of recycled mortars III

W/C=0.5	Control Mortar	RM-0.5-0/0.63	RM-0.5-0.63/1.25	RM-0.5-1.25/2.5	RM-0.5-2.5/5
Slump (mm)	20	9	13	12	21
Fresh density (g/cm3)	2.36	2.28	2.28	2.27	2.37
Flexural strength (MPa)	11.01	10.19	9.66	9.83	11.22
Compressive strength (MPa)	63.71	45.55	52.54	52.22	58.32
W/C=0.6	Control Mortar	RM-0.6-0/0.63	RM-0.6-0.63/1.25	RM-0.6-1.25/2.5	RM-0.6-2.5/5
Slump (mm)	103	93	83	82	90
Fresh density (g/cm3)	2.30	2.21	2.29	2.25	2.25
Flexural strength (MPa)	9.95	9.24	9.67	9.77	10.38
Compressive strength (MPa)	53.74	44.29	50.06	50.85	52.08

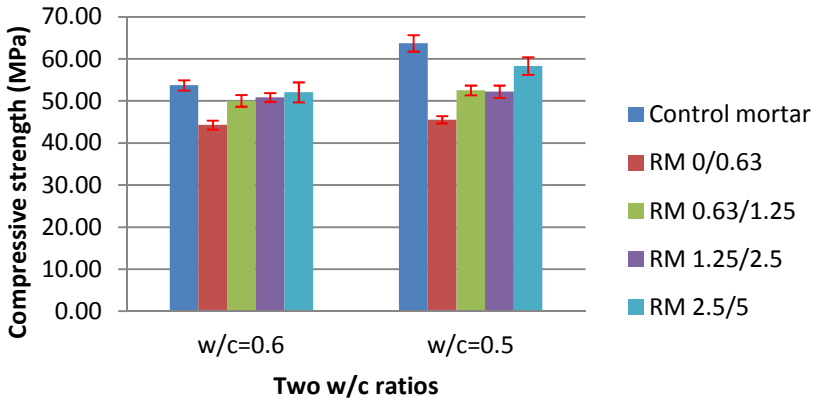

Figure 4-9 Compressive strength of recycled mortar Series III with each fraction replacement

In mortars of Series III, two parameters are varying simultaneously: the granular class of recycled sand and the replacement fraction. Indeed, the four granular fractions studied do not represent the same volume of aggregates. In order to study only the effect of granular class of FRCA on the properties of mortars, the results of Series III have been compared to those obtained with series II. Figure 4-10 shows the relationship between the relative strength of recycled mortars and replacement proportion of recycled sand obtained from mortars of Series II. The relative compressive strengths of Series III are compared with Series II on Figure 4-10 and in Table 4-9. The volume fraction of recycled sand in mortars Series III is calculated. The relative strength is the compressive strength of recycled mortar reported to that of the control mortar. According to the linear relationship between the relative strength of Series II and replacement percentage, a calculated relative strength is obtained. The difference between the relative strength of Series III and calculated relative strength from series II gives the influence index of each fraction of recycled sand. As can be seen in Table 4-9, the difference between series II and Series III for the smaller fraction (0/0.63) is larger than for the coarser one (a similar result is obtained for mortars having a W/C of 0.6). This means that the finer fraction of RCA (fraction 0/0.63) has a worse influence than the larger fractions. It is partly due to the higher cement paste content, higher water absorption and lower mechanical property of the finer fraction of recycled aggregates. Therefore, the finer fractions of recycled aggregates have the worse influence on the properties of recycled mortars.

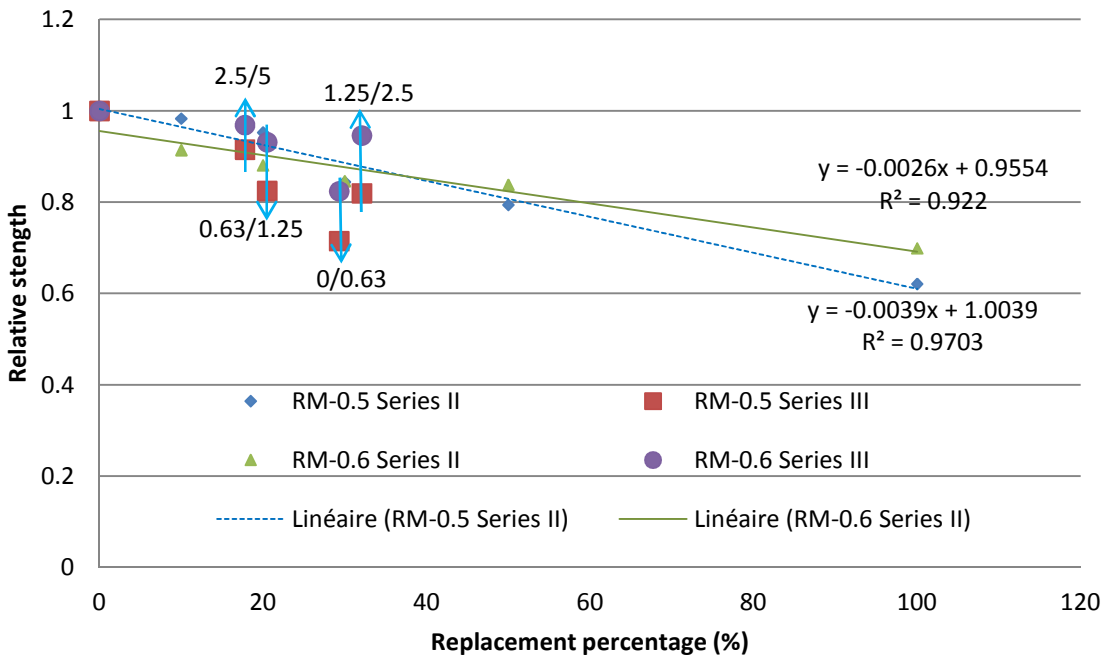

Figure 4-10 Relationship between relative compressive strength of mortars and replacement percentage

Table 4-9 Comparasion compressiver strength of Series III with Series II

W/C=0.5	RM-0.5-0/0.63	RM-0.5-0.63/1.25	RM-0.5-1.25/2.5	RM-0.5-2.5/5
Recycled sand by volume (%)	29.31	20.50	32.08	17.79
Relative strength of Series III	0.72	0.82	0.82	0.91
Calculated relative strength	0.89	0.92	0.88	0.93
Difference value	-0.17	-0.10	-0.06	-0.02
W/C=0.6	RM-0.6-0/0.63	RM-0.6-0.63/1.25	RM-0.6-1.25/2.5	RM-0.6-2.5/5
Recycled sand by volume (%)	29.31	20.50	32.08	17.79
Relative strength of Series III	0.82	0.93	0.95	0.97
Calculated relative strength	0.88	0.90	0.87	0.91
Difference value	-0.06	0.03	0.07	0.06

4.5.3 Microstructure of ITZ

In order to study the microstructure of ITZ of recycled mortars with saturated RCA and dried RCA, SEM with EDX were carried out after the compressive strength tests.

Preliminary observations showed that the observation of ITZ in recycled mortars containing recycled concrete aggregates was difficult. Therefore a simpler system of ITZ was first studied. Model RCA was first manufactured by crushing a sample of old white cement paste (particles from CP-0.6-90 with fraction 2.5/5mm). These model aggregates were incorporated in a new cement paste with cement HTS (cement Lafarge Durabat X-Trem CEM I 52.5). The old white cement paste aggregate has no ferrite phase, while the new cement paste with cement HTS contains ferrite which should allow to identify the ITZ for SEM observations. Two saturation states for the old white cement paste aggregate were studied (24h saturated old cement paste and dried old cement paste). The dried or saturated particle of old white cement paste aggregate was placed in the centre of small cylinder mould (2cm×2cm×1cm). The curing conditions were the same as for recycled mortars. After 28days curing in water, the samples were dried at 105°C and polished for ITZ observations. Here CPS refers to cement paste with saturated old white cement paste aggregate, and CPD refers to the cement paste with dried old white cement paste aggregate in the simple system of ITZ.

Figure 4-11 and Figure 4-12 show the SEM results (backscattered electrons on flat polished section) obtained on simple model system of ITZ made with saturated or dried model RCA named respectively CPS and CPD. Figure 4-13 shows the results of the mapping by EDS of iron and silicon. From the elemental distribution of iron, the cement paste corresponding to the model RCA aggregate is identified by the area where no Fe element is detected contrarily to the new paste. Indeed during hydration, iron ions tend to precipitate close to the initial position on or nearby C_4AF grains as they do not diffuse far way from anhydrous phases due to the very low solubility of iron containing hydrates. Thus iron mapping enables us to determine the localization of ITZ (red curve on Figure 4-13) but it cannot be used to estimate its thickness. On the other hand, silicate ions also do not diffuse far away from cement grains leading generally to ITZ poorer in silicon while it is richer in calcium as portlandite is

abundant in ITZ. The area with a lower silicon concentration and close to the ITZ localization by iron content therefore corresponds to the ITZ which is initially filled with water. This area is well defined for the model aggregate that was saturated leading to ITZ thickness between 20-80 µm (two yellow curves on Figure 4-13). On the other hand, ITZ corresponding to the dried model aggregate appears to be finer with a thickness ranging from 5-10 µm (two yellow curves on Figure 4-13). The ITZ is therefore influenced by the saturation states of the cement paste contained in FRCA. The following explanation can therefore be proposed for the ITZ microstructure of mortars depending on the saturation state of FRCA (Figure 4-14). With saturated FRCA, water goes from the surface of the cement paste of FRCA to the new paste, increasing locally the W/C ratio at the surface of aggregate and thus leading to a large ITZ. On the contrary, for the dried FRCA, water moves from the bulk into the dried aggregate even if this process is not instantaneous as demonstrated by the slump loss. The cement grains are dragged together with water, reducing locally the (W_{eff}/C) at the surface of aggregate and leading new hydrates to precipitate at the surface or near the inside of cement paste of FRCA. This leads to an improved ITZ in mortars manufactured with dried RCA in comparison to those manufactured with saturated ones. Compressive strengths obtained for mortars manufactured with dried aggregates are all larger than those obtained for saturated aggregates. This result shows that the improvement of mechanical properties of the ITZ in mortars containing dried aggregates is able to compensate the decrease in mechanical properties of the bulk paste of these mortars due to the larger initial (W_{eff}/C). These results are obtained in a simple system; they also need to be verified with a statistical approach for several ITZ and for other materials. Nevertheless the micro-cracks observed in both samples and probably induced by the preparation of samples (heating at 105 °C and then polishing) confirms that ITZ in the sample made with saturated model RCA has some weak mechanical properties as the micro-crack passes through it (Figure 4-13). On the other hand, the micro-cracks of the

sample made with the dried model RCA passes either in the cement paste or in the ITZ leading to consider close mechanical properties (Figure 4-13).

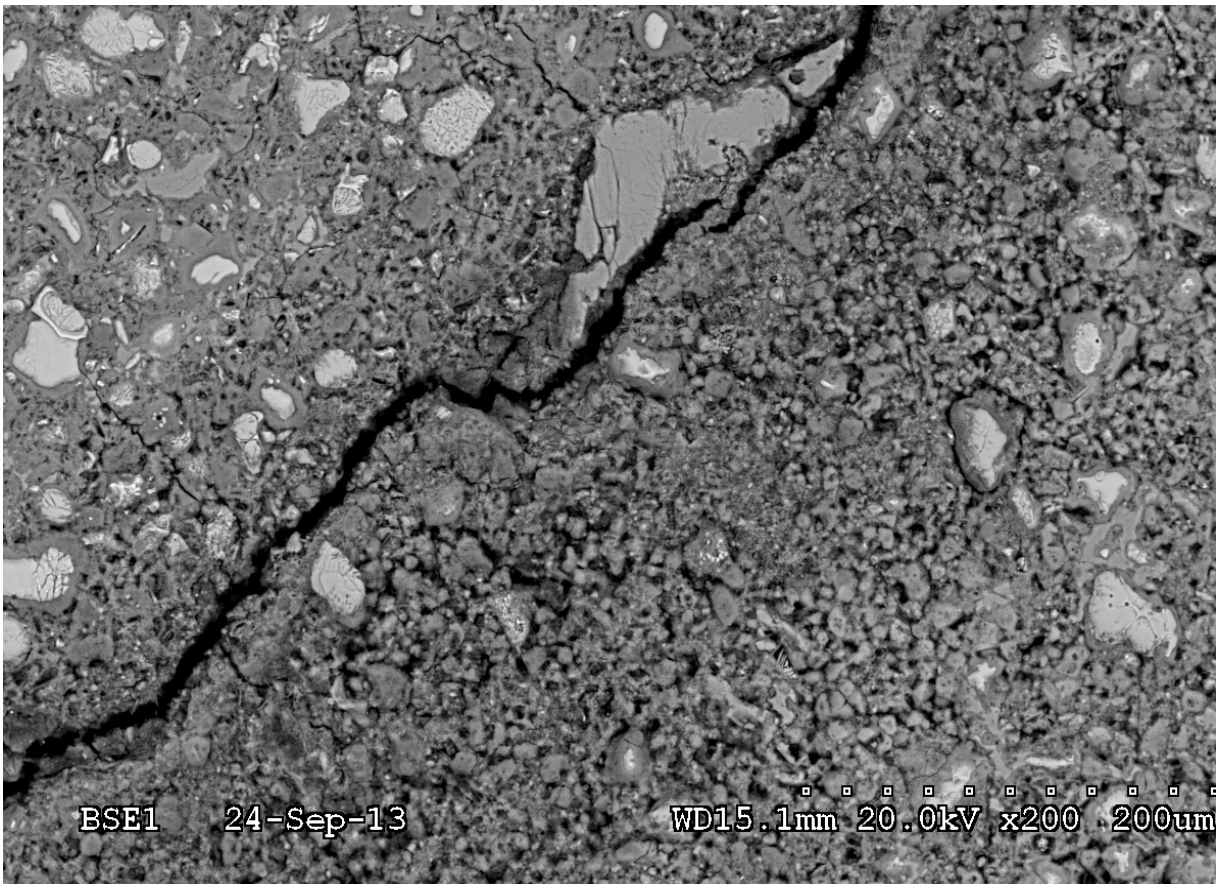

Figure 4-11 SEM results of ITZ of CPS

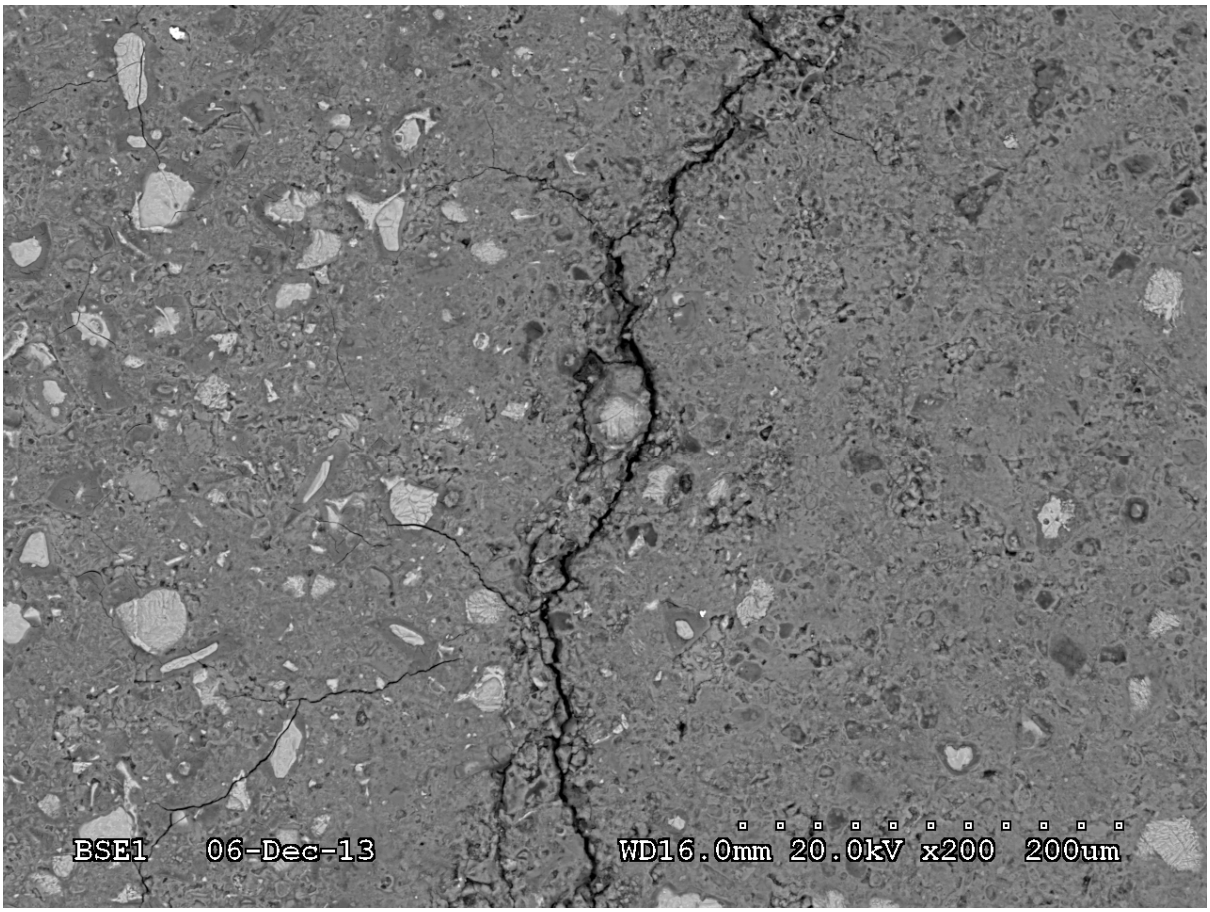

Figure 4-12 SEM results of ITZ of CPD

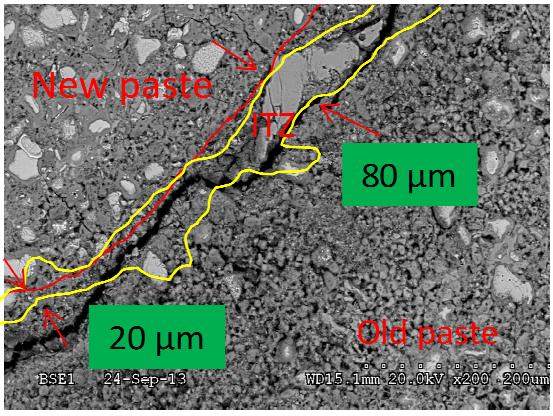

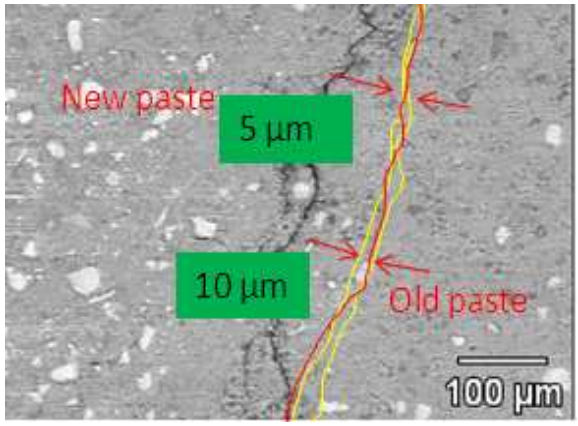

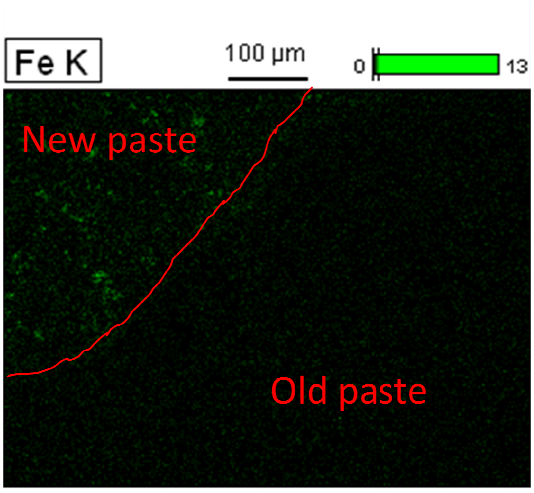

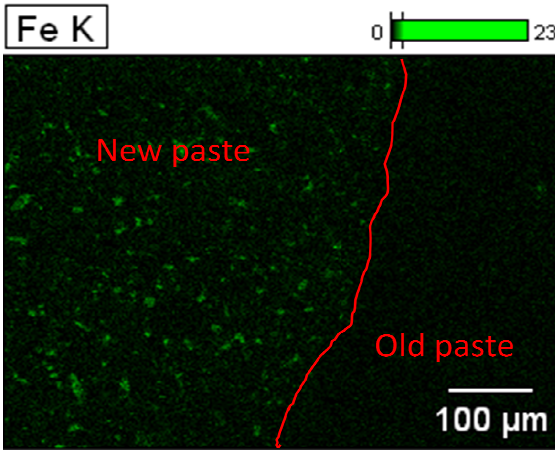

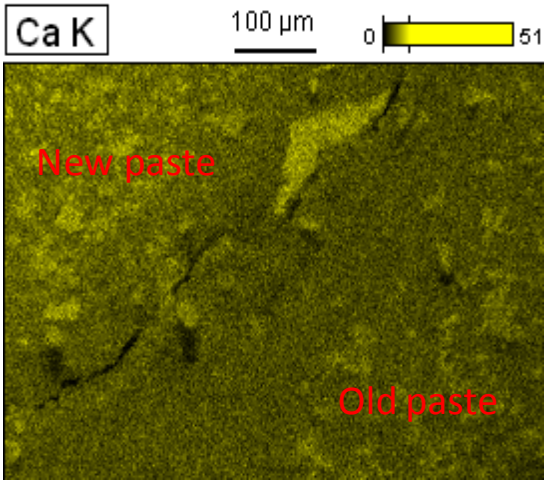

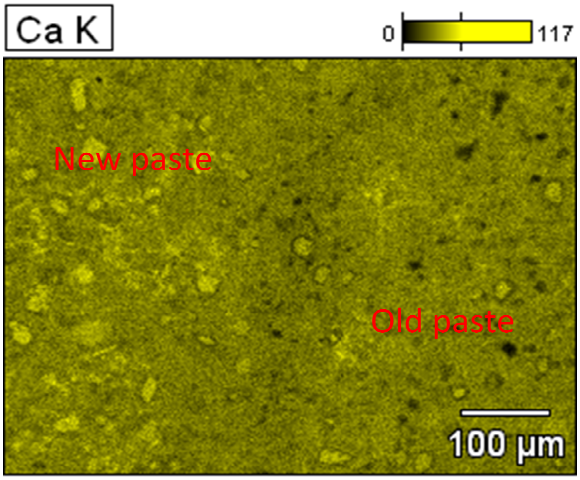

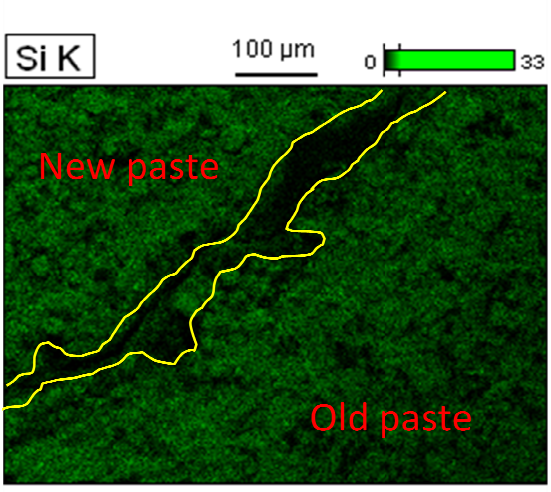

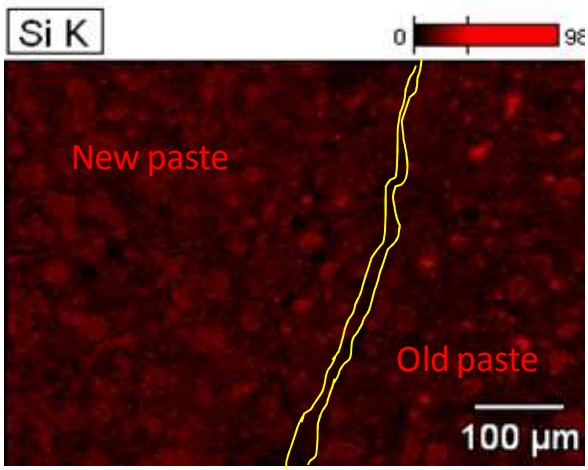

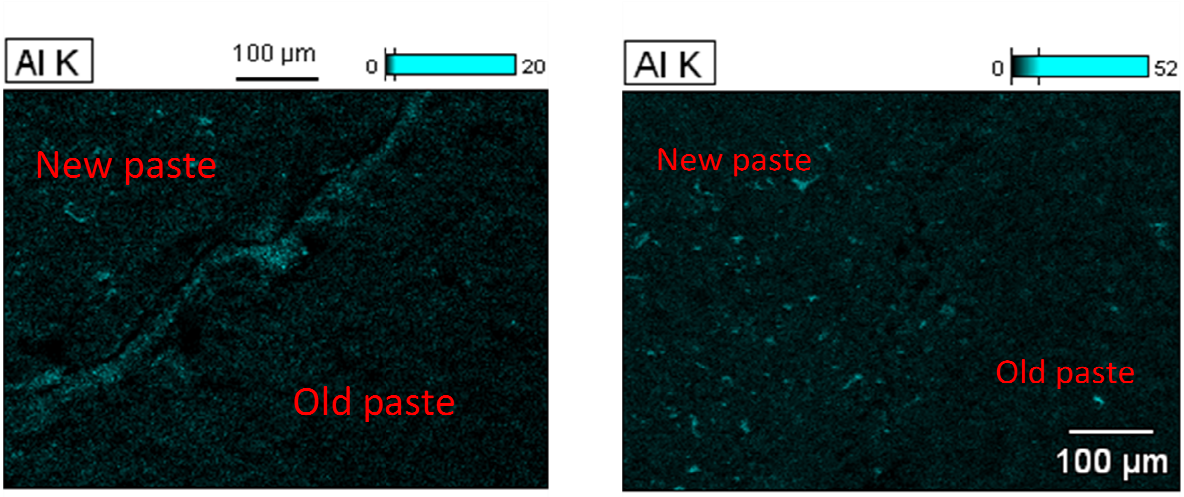

Figure 4-13 Elemental analysis with EDS results of ITZ of CPS (left) and CPD (right)

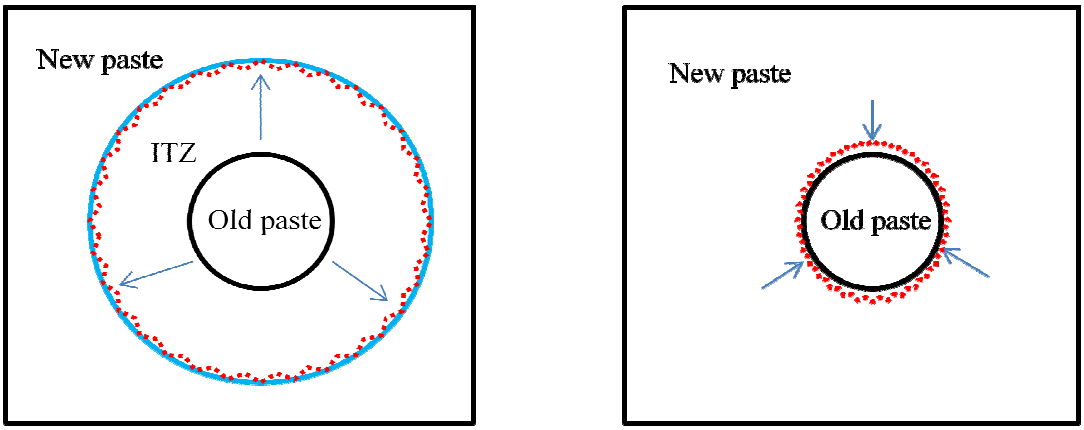

Figure 4-14 Models of ITZ for CPS (left) and CPD (right) , here red point refers to the hydrates, blue circle refers to the front between new paste and ITZ, black circle refers to the front between old paste and ITZ, arrow refers to moving direction of water

Similar SEM observations have then been carried out on mortars containing dry or saturated RCA-Colas1. For mortar with saturated RCA, different zones can be distinguished on the elemental maps, depending on the intensity of the recorded signal (Figure 4-15). Limits separating these zones are reported on the figures: the red curve is determined from the grey levels of the BSE image, the yellow curve is determined from the silicium concentration obtained by EDS mapping.

As shown in Figure 4-15, the thickness of ITZ can be estimated about 10 µm for saturated RCA. However, in the mortar with dried RCA, the ITZ between dried RCA and new paste cannot be found clearly, it is thinner than that with saturated RCA, which means that the property of ITZ is improved in the mortar with dried RCA. As proposed by model for dried paste, it is due to the absorption of water during the fabrication, water moves from the bulk into the dried RCA, the cement grains also move with the water, leading to better properties of ITZ. Therefore the better properties of ITZ for recycled mortar with dried RCA, confirms that the compressive strength of recycled mortars with dried RCA is larger than that with saturated RCA. These results are obtained by the two ITZ, and should be checked in the quantities of ITZ and in the other materials.

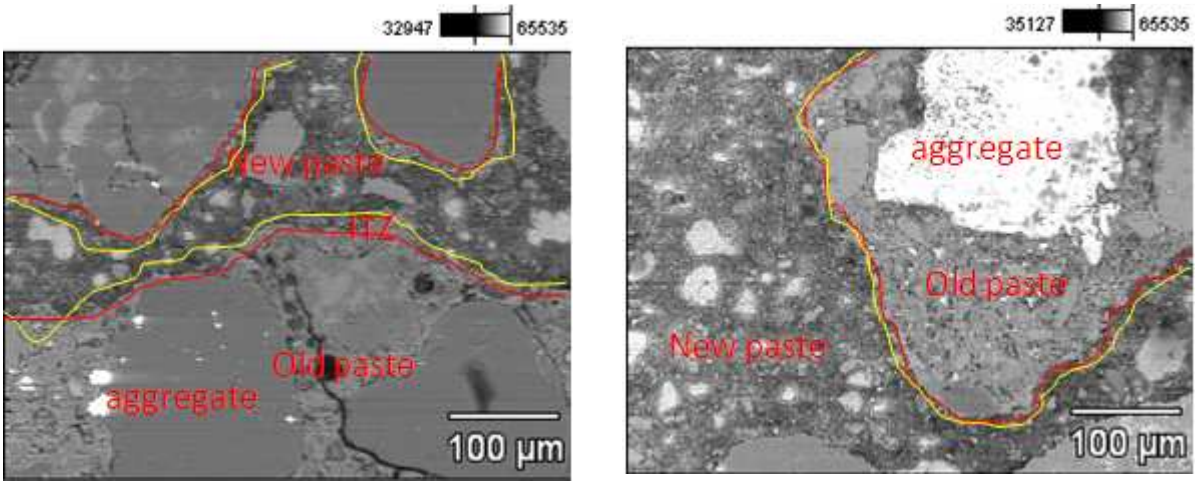

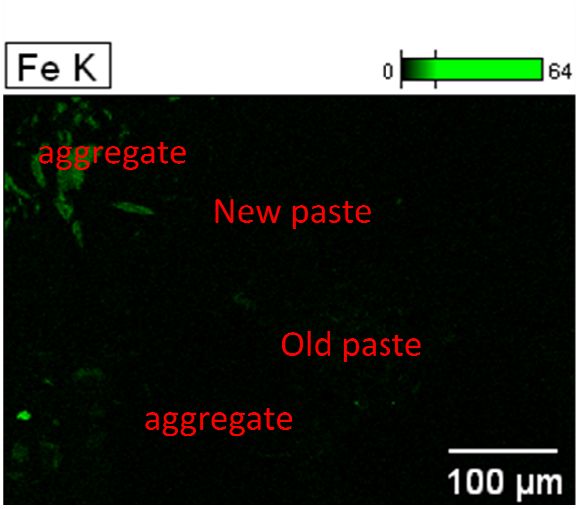

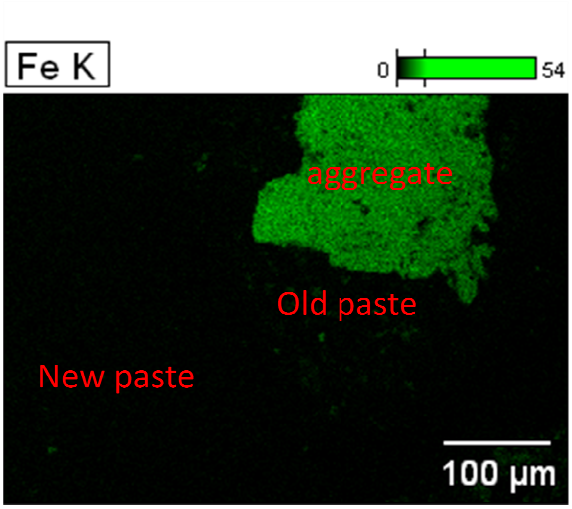

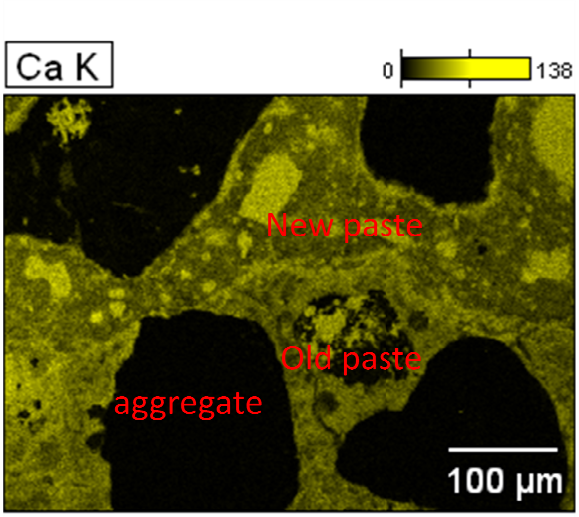

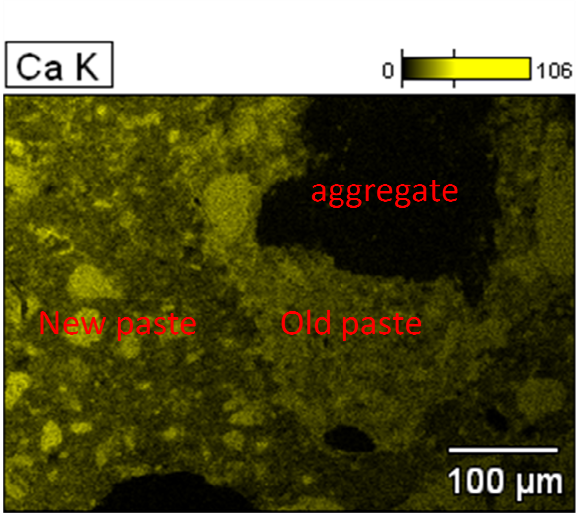

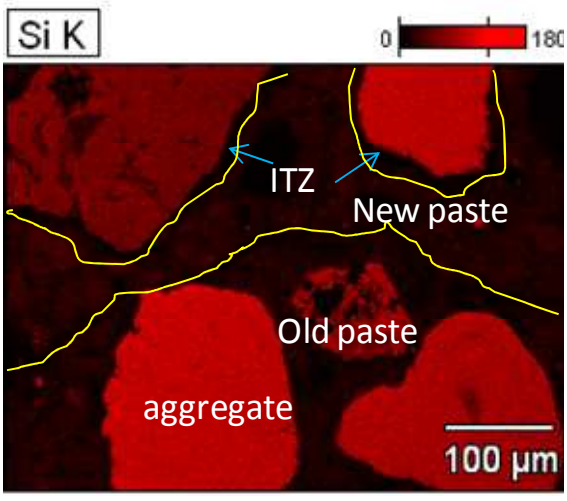

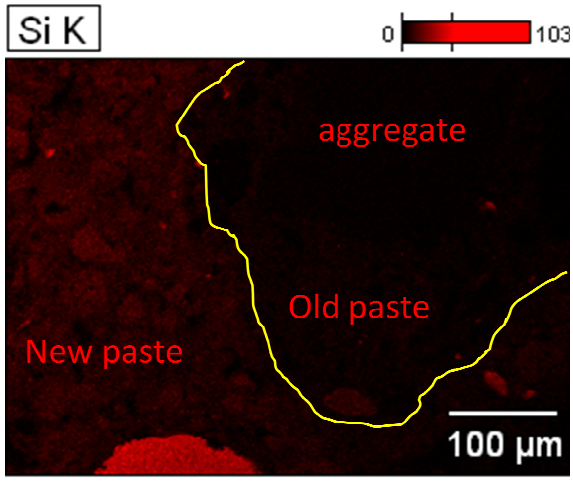

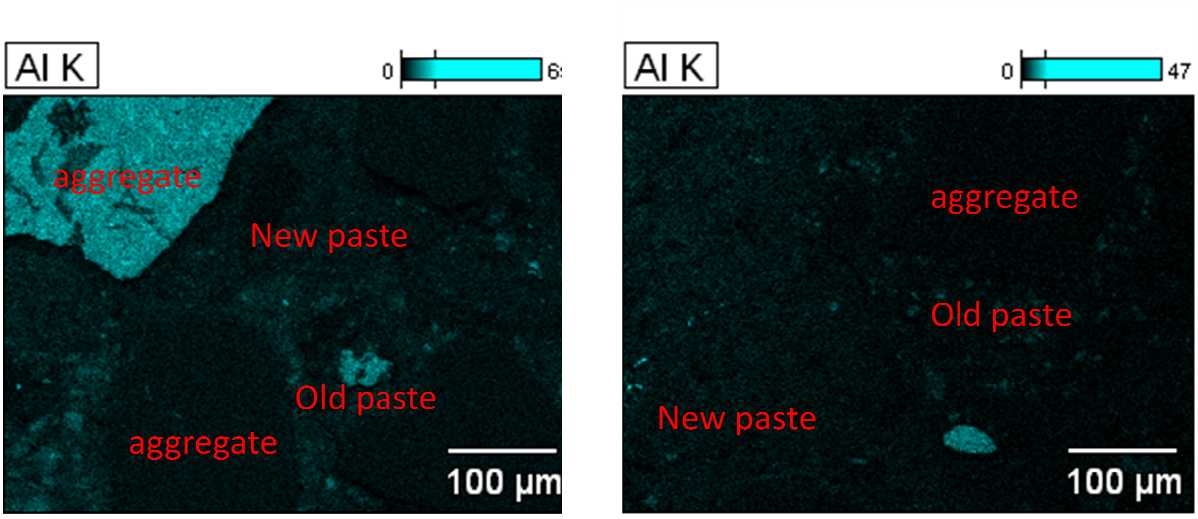

Figure 4-15 Elemental analysis with EDS results of ITZ of recycled mortars with saturated RCA (left) and dried RCA (right)

4.6 Conclusions

The properties of recycled mortars including the fresh properties, mechanical properties, and ITZ microstructure have been studied. Three series of different compositions of recycled mortars have been tested. With the results, we can answer Questions 5 and 6.

Question 5: What is the influence of FRCA (replacement percentage and replacement fraction) on the properties of recycled mortars?

⟹With replacing the natural sand with FRCA, the fresh density decreases which is due to the lower density of recycled sand. The compressive strength of recycled mortar decreases as the replacement ratio increases. The relationship between the compressive strength and replacement ratio is quasi linear.

The compressive strength of recycled mortar with each fractions replacement is lower than the control mortar for both w/c ratios (w/c=0.5, 0.6).

Moreover, the finer fraction of RCA (fraction 0/0.63) has a worse influence than the larger fractions, which is partly due to the higher cement paste content, higher water absorption and lower mechanical properties of finer fraction of recycled aggregates.

Question 6: What is the influence of the moisture state of FRCA on the properties of recycled mortars?

⟹ The slump of recycled mortar with dried FRCA is higher than that with saturated FRCA, which is due to higher initial free water and higher paste volume. The rate of slump loss of RM-D is quicker than RM-S, which could be partly due to the higher initial slump value, and also due to the decrease of free water by the absorption of recycled sand. However, whatever the w/c ratio used, the slump value of mortars manufactured with dried aggregates is always larger than that of mortars manufactured with saturated aggregates. This result suggests that the absorption of water by dried aggregates in the mortar is lower than the absorption determined with standard procedures. It could be due first to the kinetics of absorption. But it could also be due to a lesser water absorption capacity of aggregates when they are immersed into the cement paste. Indeed, small cement particles could be drained at the surface of RCA, filling some surface porosity. Moreover, the large specific surface area of cement grains could lead to an increase in apparent viscosity of mixing water, preventing is from draining into aggregates.

The recycled mortars with dried aggregates have better compressive strengths than the ones with saturated aggregates for the three different w/c ratios studied.

SEM observations of recycled mortars with saturated FRCA demonstrated that the ITZ between old cement paste and new cement paste is larger than that with dried FRCA. It means the properties of ITZ are improved by the water absorption of FRCA. The studies of properties of ITZ for saturated and dried FRCA, confirm that the higher compressive strength with dried FRCA are due to the stronger properties of ITZ, which shows that the improvement of mechanical properties of the ITZ in mortars containing dried aggregates is able to compensate the decrease in mechanical properties of the bulk paste of these mortars due to the larger initial (W_{eff}/C).

Conclusions and perspectives

Since many old buildings and other structures have overcome their limits of use and need to be demolished, a lot of C&DW are generated, and it is really important to make good use of these wastes to maximize economic and environmental benefits. This study deals with the reuse of FRCA to make new mortar and concrete. The properties of RCA especially the FRCA and the properties of recycled mortar made with FRCA have been studied.

Several questions have been asked after the literature review. The results presented in this manuscript allow to draw the following answers.

Question 1: Can we define accurate experimental methods allowing to measure the water absorption coefficient and the adherent cement paste content of the different fractions of RCA?

⟹ For an estimation of the adherent cement paste content (CPC), a method based on the dissolution of the major part of the cement paste contained in FRCA by salicylic acid (SFSA) was developed. The method was applied successfully to RCA manufactured in the laboratory with a white OPC and three industrial RCA made with grey OPC. Despite that SFSA underestimates CPC even more markedly that the content of insoluble phases increases, the insoluble phases of the cement paste will impact similarly all the particle size classes, and the method can be used to determine the variation of SFSA as a function of particle size of RCA. In all the cases, a quasi linear relation has been found between SFSA and the granular class of the RCA.

Based on the preceding results, a method allowing the measurement of water absorption coefficient of RCA has been proposed. We have used EN 1097-6 and IFSTTAR methods to

measure the water absorption of FRCA as a function of their particle sizes (both for laboratory produced RCA and three industrial RCA). For particle sizes larger than 0.63mm, EN 1097-6 and IFSTTAR methods give similar results. However, for the smaller particle size (<0.63mm), IFSTTAR method seems to overestimate the water absorption coefficient, and standard method (EN 1097-6) seems to underestimate it. The water absorption coefficient of the finer fraction (0-0.63mm) can be estimated by extrapolating the relationship obtained between water absorption and SFSA with coarser granular classes. The total water absorption of FRCA (fraction 0/5mm) can therefore be determined precisely from the granular distribution. This method has been used for estimating the water absorption of RCA-Colas1 and the results of compressive strengths obtained on recycled mortars containing this RCA has shown that the efficient water is correctly predicted, based on Bolomey equation.

Question 2: What is the link between properties of original concrete (W/C ratios, cement paste volume) and properties of RCA made with it?

⟹ The cement paste content of FRCA is influenced by the W/C ratio and the cement paste volume of the original concrete. The cement paste content by mass (CPC) depends on volume of cement paste and densities of cement paste and natural aggregate. The larger values of cement paste content obtained for RCA-OC2 comparatively to RCA-OC1 can be attributed to the higher volume of cement paste in the original composition (same W/C ratio). Similarly, the larger values obtained for RCA-OC3 comparatively to RCA-OC2 can be attributed to a lower W/C ratio in the original composition (same volume of cement paste), leading to a denser cement paste and therefore to a larger mass of cement paste for a similar paste volume. The porosity and water absorption of FRCA are also influenced by the W/C ratio and the cement paste volume of the original concrete. The water absorption coefficients obtained with

all the granular classes of RCA-OC2 (larger pate volume and larger W/C ratio) are significantly larger than those obtained with RCA-OC1 and RCA-OC3.

Question 3: What is the link between size and properties of RCA (mortar or cement paste content, density, water absorption, porosity...)?

⟹ For the laboratory produced and industrial FRCA used in this study, the SFSA decreases quasi-linearly with the average particle size. The properties of FRCA including specific density, water absorption, and porosity are strongly correlated to the SFSA. The higher SFSA, the higher the water absorption and porosity, and the lower the specific density at the exception of the absorption coefficient measured by EN 1097-6 standard for the smaller fraction (0/0.63mm).

From the relationship between water absorption and SFSA (also for the relationship between $ML_{105\text{-}600}$ and SFSA), drawing the water absorption coefficient as a function of the SFSA can be a very convenient method to differentiate different sources of RCA for which the original concrete composition is generally unknown such as industrial RCA. Changes of the slope of this regression can also be used to estimate the effect of the weathering or some specific treatment after RCA being crushed (carbonation).

Question 4: What is the influence of the conditions of conservation of the RCA (carbonation) on their properties?

⟹ After the carbonation of recycled aggregate, the dissolved percentage in salicylic acid decreases; $ML_{105\text{-}600}$ increases both for the thermal method and TGA method for RCA but not for pure cement paste. $ML_{105\text{-}500}$ based on TGA decreases, but $ML_{500\text{-}600}$ increases a lot, which are due to the transfer of portlandite to partly amorphous calcite, which decomposes from 500°C.

The density of RCA and the surface area increase, the porosity of RCA decrease, which leads to the decrease of water absorption.

Question 5: What is the influence of FRCA (replacement percentage and replacement fraction) on the properties of recycled mortars?

⟹Replacing the natural sand with FRCA, the fresh density decreases which is due to the lower density of recycled sand. The compressive strength of recycled mortars decreases as the replacement percentage increases. The relationship between the compressive strength and replacement ratio is quasi linear, therefore the choice of replacement ratio can be determined according to the objective compressive strength.

The compressive strength of recycled mortar with different fractions replacement is lower than the control mortar for both w/c ratios (w/c=0.5, 0.6).

Moreover, the finer fraction of RCA (fraction 0/0.63) has a worse influence than the larger fractions, which is partly due to the higher cement paste content and higher water absorption and lower mechanical property for finer fraction of recycled aggregates.

Question 6: What is the influence of the moisture state of FRCA on the properties of recycled mortars?

⟹ The slump of recycled mortar with dried FRCA is higher than that with saturated FRCA, which is due to higher initial free water and higher paste volume. The slump loss depends on the quantity of free water and paste volume. The rate of slump loss of RM-D is quicker than RM-S. However, whatever the w/c ratio used, the slump value of mortars manufactured with dried aggregates is always larger than that of mortars manufactured with saturated aggregates.

The recycled mortar with dried aggregates has better mechanical properties than the one with saturated aggregates for the three different w/c ratios. The compressive strength of recycled mortar with dried aggregates is larger than with the saturated aggregate. This is confirmed by the SEM studies of the microstructure of mortars, the recycled mortar with dried FRCA has stronger properties of ITZ. In the SEM of recycled mortar with saturated FRCA, the ITZ between old cement paste and new cement paste can clearly be seen, while with dried FRCA, the ITZ zone between old cement paste and new cement paste is thinner than that with saturated FRCA, indicating that the properties of ITZ are improved by the water absorption of FRCA.

Perspectives

There is still a lot of work that should be done such as follows.

(1) In this study, the cement paste content has been estimated by a simple method corresponding to its dissolution in the salicylic acid. It would be interesting to study the robustness of this method for others RCA and also by other laboratories. Soluble fraction in salicylic acid (SFSA) decreases almost linearly when the average particle size of FRCA increases with the four fractions. It would also be interesting to study many more granular fractions especially the finer fractions (less than 0.63mm) to verify the extend of the linearity of the relationship between SFSA and particle size.

(2) In this study, the water absorption of recycled aggregates has been studied. However, the kinetics of water absorption of recycled aggregates is not included. The water absorption of recycled aggregates in the mortar or concrete is not the same as in the experimental conditions used for testing the water absorption (EN 1097-6). It would be interesting to study the kinetics of water absorption of recycled aggregates in the mortar or concrete and the influence on the properties of recycled mortar or concrete.

(3) The influence factors such as weathering (carbonation) on the properties of FRCA have been partly studied and have shown that carbonation could improve the quality of RCA by reducing their porosity and water absorption. Methods to improve the properties of FRCA in order to make good use of the recycled concrete such as accelerated carbonation could therefore be studied, however, the difference between real carbonation and accelerate laboratory carbonation should also be interesting to study.

(4) The properties of ITZ have been studied partially. But there is still a lot of work to be done in this direction. First the observation and analysis methods should be improved in order to better identify the ITZ in saturated or dry RCA. Then, the saturation states on the properties of on the properties of ITZ, and the properties of ITZ measured by nano-indentation are also interesting to study.

(5) In this study, the applications of FRCA are just focused on the recycled mortar with recycled aggregates, so the use of FRCA in the recycled concrete should be confirmed. For example, the influence of the properties of FRCA on the properties of recycled concrete such as fresh properties and mechanical properties is also interesting to study.

References

[1] DAO D-T. (multi-) recyclage du béton hydraulique [Thèse]: Ecole Central de Nantes; 2012.
[2] Larrañaga ME. Experimental study on microstructure and structural behaviour of recycled aggregate concrete [Thesis]: Universitat Politècnica de Catalunya; 2004.
[3] Christian Fischer MW. EU as recycling society, Present recycling levels of municipal waste and construction and demolition waste in the EU. 2009.
[4] Arab HB. Study aggregates from construction and demolition waste in Europe. 2006.
[5] GRONDIN A. Valorisatin des granulats recyclés de béton: Etude des caractéristiques physiques et mécaniques des bétons de granulats recyclés de béton [Thèse]: INSA de Strasbourg; 2011.
[6] Xiao J, Xie H, Zhang C. Investigation on building waste and reclaim in Wenchuan earthquake disaster area. Resources, Conservation and Recycling. 2012;61(0):109-17.
[7] Shi J, Xu Y. Estimation and forecasting of concrete debris amount in China. Resources, Conservation and Recycling. 2006;49(2):147-58.
[8] Xiao J, Li W, Fan Y, Huang X. An overview of study on recycled aggregate concrete in China (1996–2011). Construction and Building Materials. 2012;31(0):364-83.
[9] Xuping L. Recycling and reuse of waste concrete in China: Part I. Material behaviour of recycled aggregate concrete. Resources, Conservation and Recycling. 2008;53(1–2):36-44.
[10] Yu AT, Poon C, Wong A, Yip R, Jaillon L. Impact of Construction Waste Disposal Charging Scheme on work practices at construction sites in Hong Kong. Waste Management. 2012.
[11] Fong WFK, Yeung JSK, Poon C. HONG KONG EXPERIENCE OF USING RECYCLED AGGREGATES FROM CONSTRUCTION AND DEMOLITION MATERIALS IN READY MIX CONCRETE. Civil Engineering Department, Hong Kong SAR Government, Hong Kong; Yue Xiu Concrete Co Ltd, Hong Kong; Department of Civil and Structural Engineering, Hong Kong Polytechnic University, Hong Kong. 2002.
[12] Poon C-S, Chan D. The use of recycled aggregate in concrete in Hong Kong. Resources, Conservation and Recycling. 2007;50(3):293-305.
[13] Hansen TC. Recycled aggregates and recycled aggregate concrete second state-of-the-art report developments 1945–1985. Materials and Structures. 1986;19(3):201-46.
[14] Xing W. Quality improvement of granular secondary raw building materials by separation and cleansing techniques. 2004.
[15] Commission E. Construction and demolition waste management practices, and their economic impacts. Final Report to DGXI European Commission by Symonds, ARGUS, COWI Consulting Engineers and Planners and PRC Boucentrum. 1999.
[16] Oikonomou ND. Recycled concrete aggregates. Cement and Concrete Composites. 2005;27(2):315-8.
[17] Sani D, Moriconi G, Fava G, Corinaldesi V. Leaching and mechanical behaviour of concrete manufactured with recycled aggregates. Waste Management. 2005;25(2):177-82.
[18] Xiao J, Xie H, Zhang C. Investigation on building waste and reclaim in Wenchuan earthquake disaster area. Resources, Conservation and Recycling. 2012;61:109-17.
[19] Bianchini G, Marrocchino E, Tassinari R, Vaccaro C. Recycling of construction and demolition waste materials: a chemical–mineralogical appraisal. Waste Management. 2005;25(2):149-59.

[20] Batayneh M, Marie I, Asi I. Use of selected waste materials in concrete mixes. Waste Management. 2007;27(12):1870-6.
[21] Etxeberria M, Vázquez E, Marí A, Barra M. Influence of amount of recycled coarse aggregates and production process on properties of recycled aggregate concrete. Cement and Concrete Research. 2007;37(5):735-42.
[22] Ulsen C, Kahn H, Hawlitschek G, Masini EA, Angulo SC. Separability studies of construction and demolition waste recycled sand. Waste Management. 2012.
[23] Ogawa H, Nawa T. Improving the Quality of Recycled Fine Aggregate by Selective Removal of Brittle Defects. Journal of Advanced Concrete Technology. 2012;10(12):395-410.
[24] Tam VW, Tam C. Crushed aggregate production from centralized combined and individual waste sources in Hong Kong. Construction and Building Materials. 2007;21(4):879-86.
[25] Nik.D O. Recycled concrete aggregates. Cement and Concrete Composites. 2005;27(2):315-8.
[26] Jiménez J, Ayuso J, Galvín A, López M, Agrela F. Use of mixed recycled aggregates with a low embodied energy from non-selected CDW in unpaved rural roads. Construction and Building Materials. 2012;34:34-43.
[27] Roesler JR, Lange D. Batching Effects on Properties of Recycled Concrete Aggregates for Airfield Rigid Pavements Andres Salas Postdoctoral Researcher. Urbana.51:61801.
[28] Hansen TC. RECYCLED CONCRETE AGGREGATE AND FLY-ASH PRODUCE CONCRETE WITHOUT PORTLAND-CEMENT. Cement and Concrete Research. 1990;20(3):355-6.
[29] Park T. Application of construction and building debris as base and subbase materials in rigid pavement. Journal of Transportation Engineering-Asce. 2003;129(5):558-63.
[30] Huang Y, Bird RN, Heidrich O. A review of the use of recycled solid waste materials in asphalt pavements. Resources, Conservation and Recycling. 2007;52(1):58-73.
[31] Barbudo A, Agrela F, Ayuso J, Jiménez J, Poon C. Statistical analysis of recycled aggregates derived from different sources for sub-base applications. Construction and Building Materials. 2012;28(1):129-38.
[32] Poon CS, Yu ATW, Ng LH. On-site sorting of construction and demolition waste in Hong Kong. Resources, Conservation and Recycling. 2001;32(2):157-72.
[33] Rao A, Jha KN, Misra S. Use of aggregates from recycled construction and demolition waste in concrete. Resources, Conservation and Recycling. 2007;50(1):71-81.
[34] de Juan MS, Gutiérrez PA. Study on the influence of attached mortar content on the properties of recycled concrete aggregate. Construction and Building Materials. 2009;23(2):872-7.
[35] Nagataki S, Gokce A, Saeki T, Hisada M. Assessment of recycling process induced damage sensitivity of recycled concrete aggregates. Cement and Concrete Research. 2004;34(6):965-71.
[36] Abbas A, Fathifazl G, Fournier B, Isgor OB, Zavadil R, Razaqpur AG, et al. Quantification of the residual mortar content in recycled concrete aggregates by image analysis. Materials Characterization. 2009;60(7):716-28.
[37] Hansen TC, Narud H. Strength of recycled concrete made from crushed concrete coarse aggregate. Concrete International. 1983;5(1):79-83.
[38] Topcu IB, Sengel S. Properties of concretes produced with waste concrete aggregate. Cement and Concrete Research. 2004;34(8):1307-12.
[39] Yagishita F, Sano M, Yamada M. Behaviour of reinforced concrete beams containing recycled coarse aggregate. Demolition and reuse of concrete. 1994.

[40] EN B. 1097-6: 2000. Tests for mechanical and physical properties of aggregates-Part 6: determination of particle density and water absorption.
[41] ASTM-C127. Standard test method for density, relative density (specific gravity), and absorption of coarse aggregate. 2008.
[42] ASTM-C128. Standard test method for density, relative denstiy (specific gravity), and absorption of fine aggregate. 2004.
[43] Tam VW, Gao X, Tam C, Chan C. New approach in measuring water absorption of recycled aggregates. Construction and Building Materials. 2008;22(3):364-9.
[44] Djerbi Tegguer A. Determining the water absorption of recycled aggregates utilizing hydrostatic weighing approach. Construction and Building Materials. 2012;27(1):112-6.
[45] Mechling J-M, Lecomte A, Merriaux K. Measurement of the absorption of water of the mineral admixtures in concrete by evaporometry. Materials and Structures. 2003;36(255):32-9.
[46] Poon CS, Shui ZH, Lam L. Effect of microstructure of ITZ on compressive strength of concrete prepared with recycled aggregates. Construction and Building Materials. 2004;18(6):461-8.
[47] José M.V G-S. Porosity of recycled concrete with substitution of recycled concrete aggregate: An experimental study. Cement and Concrete Research. 2002;32(8):1301-11.
[48] Martín-Morales M, Zamorano M, Ruiz-Moyano A, Valverde-Espinosa I. Characterization of recycled aggregates construction and demolition waste for concrete production following the Spanish Structural Concrete Code EHE-08. Construction and Building Materials. 2011;25(2):742-8.
[49] Tam VWY, Gao XF, Tam CM. Carbonation around near aggregate regions of old hardened concrete cement paste. Cement and Concrete Research. 2005;35(6):1180-6.
[50] Nixon P. Recycled concrete as an aggregate for concrete—a review. Materials and Structures. 1978;11(5):371-8.
[51] Khalaf FM, DeVenny AS. Recycling of demolished masonry rubble as coarse aggregate in concrete: Review. Journal of materials in civil engineering. 2004;16(4):331-40.
[52] Lamond JF, Campbell Sr RL, Giraldi A, Jenkins NJ, Campbell TR, Halczak W, et al. Removal and reuse of hardened concrete. ACI Mater J. 2002;99(3):300-25.
[53] Debieb F, Courard L, Kenai S, Degeimbre R. Mechanical and durability properties of concrete using contaminated recycled aggregates. Cement and Concrete Composites. 2010;32(6):421-6.
[54] Institution BS. Methods for determination of aggregate crushing value. BS 812-110. 1990.
[55] Padmini AK, Ramamurthy K, Mathews MS. Influence of parent concrete on the properties of recycled aggregate concrete. Construction and Building Materials. 2009;23(2):829-36.
[56] Tam VWY, Wang K, Tam CM. Assessing relationships among properties of demolished concrete, recycled aggregate and recycled aggregate concrete using regression analysis. Journal of hazardous materials. 2008;152(2):703-14.
[57] Limbachiya MC, Marrocchino E, Koulouris A. Chemical–mineralogical characterisation of coarse recycled concrete aggregate. Waste Management. 2007;27(2):201-8.
[58] Tomas J, Schreier M, Gröger T, Ehlers S. Impact crushing of concrete for liberation and recycling. Powder Technology. 1999;105(1):39-51.
[59] Schubert W, Khanal M, Tomas J. Impact crushing of particle–particle compounds—experiment and simulation. International Journal of Mineral Processing. 2005;75(1):41-52.
[60] Molin C, Larsson K, Arvidsson H. Quality of reused crushed concrete strength, contamination and crushing technique. RILEM Publications; 2004. p. 150.

[61] Xiao J, Li J, Zhu B, Fan Z. Experimental study on strength and ductility of carbonated concrete elements. Construction and Building Materials. 2002;16(3):187-92.
[62] Fernandez Bertos M, Simons S, Hills C, Carey P. A review of accelerated carbonation technology in the treatment of cement-based materials and sequestration of CO< sub> 2</sub>. Journal of Hazardous Materials. 2004;112(3):193-205.
[63] Yamasaki A, Iizuka A, Kakizawa M, Katsuyama Y, Nakagawa M, Fujii M, et al. Development of a carbon sequestration process by the carbonation reaction of waste streams containing calcium or magnesium. Fifth Annual Conference on Carbon Capture & Sequestration, May2006. p. 8-11.
[64] Chang C-F, Chen J-W. The experimental investigation of concrete carbonation depth. Cement and Concrete Research. 2006;36(9):1760-7.
[65] Song H-W, Kwon S-J. Permeability characteristics of carbonated concrete considering capillary pore structure. Cement and Concrete Research. 2007;37(6):909-15.
[66] Roy SK, Poh KB, Northwood Do. Durability of concrete—accelerated carbonation and weathering studies. Building and Environment. 1999;34(5):597-606.
[67] Thiery M, Villain G, Dangla P, Platret G. Investigation of the carbonation front shape on cementitious materials: effects of the chemical kinetics. Cement and Concrete Research. 2007;37(7):1047-58.
[68] Villain G, Thiery M, Platret G. Measurement methods of carbonation profiles in concrete: thermogravimetry, chemical analysis and gammadensimetry. Cement and Concrete Research. 2007;37(8):1182-92.
[69] Martinez-Ramirez S, Sanchez-Cortes S, Garcia-Ramos J, Domingo C, Fortes C, Blanco-Varela M. Micro-Raman spectroscopy applied to depth profiles of carbonates formed in lime mortar. Cement and Concrete Research. 2003;33(12):2063-8.
[70] López-Arce P, Gómez-Villalba LS, Martínez-Ramírez S, Álvarez de Buergo M, Fort R. Influence of relative humidity on the carbonation of calcium hydroxide nanoparticles and the formation of calcium carbonate polymorphs. Powder Technology. 2011;205(1):263-9.
[71] Ngala V, Page C. Effects of carbonation on pore structure and diffusional properties of hydrated cement pastes. Cement and Concrete Research. 1997;27(7):995-1007.
[72] Johannesson B, Utgenannt P. Microstructural changes caused by carbonation of cement mortar. Cement and Concrete Research. 2001;31(6):925-31.
[73] Arandigoyen M, Bicer-Simsir B, Alvarez JI, Lange DA. Variation of microstructure with carbonation in lime and blended pastes. Applied surface science. 2006;252(20):7562-71.
[74] Lawrence RM, Mays TJ, Rigby SP, Walker P, D'Ayala D. Effects of carbonation on the pore structure of non-hydraulic lime mortars. Cement and Concrete Research. 2007;37(7):1059-69.
[75] Hendriks CF, Xing W. Quality Improvement of Granular Wastes by Separation Techniques. PRO 40: International RILEM Conference on the Use of Recycled Materials in Buildings and Structures (Volume 1): RILEM Publications; 2004. p. 142.
[76] Tsujino M, Noguchi T, Tamura M, Kanematsu M, Maruyama I, Nagai H. Study on the application of low-quality recycled coarse aggregate to concrete structure by surface modification treatment. University of Tokyo. 2006.
[77] Grabiec AM, Klama J, Zawal D, Krupa D. Modification of recycled concrete aggregate by calcium carbonate biodeposition. Construction and Building Materials. 2012;34:145-50.
[78] Tam VWY, Tam CM, Le KN. Removal of cement mortar remains from recycled aggregate using pre-soaking approaches. Resources, Conservation and Recycling. 2007;50(1):82-101.
[79] Ahn J-W, Kim H-S, Han G-C. Recovery of Aggregates from Waste Concrete by Heating and Grinding. Geosystem Engineering. 2001;4(4):117-22.

[80] Nakagawa M, Iizuka A, Fujii M, Kumagai K, Yamasaki A, Hikino K, et al. Development of a New Recycling Process of Fine Aggregate from Waste Concrete Particles Using High-Pressure Carbon Dioxide Solution. The 2005 Annual Meeting2005.
[81] prEN 933-11:Tests for chemical properties of aggregates. Part 11: classification test for the constituents of coarse recycled aggregate. 2005.
[82] BS 8500-2: Concrete-Complementary British Standard to BS EN 206-1. Part 2. Specification for constituent materials and concrete. 2002.
[83] Recommendation R. Specification for concrete with recycled aggregates. Materials and Structures. 1994;27(173):557.
[84] JIS A. 5021: Recycled aggregate for concrete-class H. Japanese Standards Association. 2005.
[85] JIS A. 5022: Recycled concrete using recycled class M. Japanese Standards Association. 2007.
[86] JIS A. 5023: Recycled concrete using recycled aggregate class L. Japanese Standards Association. 2006.
[87] JIS. Recycled concrete using recycled aggregate. JIS Technical Report, TRA 0006. 2000.
[88] Society SCS. Technical code on the application of recycled concrete (DG/TJ08-2018-2007). Shanghai. 2007.
[89] Sagoe-Crentsil KK, Brown T, Taylor AH. Performance of concrete made with commercially produced coarse recycled concrete aggregate. Cement and Concrete Research. 2001;31(5):707-12.
[90] J.M K. Properties of concrete incorporating fine recycled aggregate. Cement and Concrete Research. 2005;35(4):763-9.
[91] Tam VWY, Gao XF, Tam CM. Microstructural analysis of recycled aggregate concrete produced from two-stage mixing approach. Cement and Concrete Research. 2005;35(6):1195-203.
[92] Tam VWY, Gao XF, Tam CM, Ng KM. Physio-chemical reactions in recycle aggregate concrete. Journal of hazardous materials. 2009;163(2–3):823-8.
[93] Tam VWY, Tam CM, Wang Y. Optimization on proportion for recycled aggregate in concrete using two-stage mixing approach. Construction and Building Materials. 2007;21(10):1928-39.
[94] Tam VWY, Tam CM. Diversifying two-stage mixing approach (TSMA) for recycled aggregate concrete: TSMA(s) and TSMA(sc). Construction and Building Materials. 2008;22(10):2068-77.
[95] Kou S-C, Poon C-S. Properties of concrete prepared with crushed fine stone, furnace bottom ash and fine recycled aggregate as fine aggregates. Construction and Building Materials. 2009;23(8):2877-86.
[96] Poon CS, Shui ZH, Lam L, Fok H, Kou SC. Influence of moisture states of natural and recycled aggregates on the slump and compressive strength of concrete. Cement and Concrete Research. 2004;34(1):31-6.
[97] Poon C, Kou S, Lam L. Influence of recycled aggregate on slump and bleeding of fresh concrete. Materials and Structures. 2007;40(9):981-8.
[98] Evangelista L, de Brito J. Mechanical behaviour of concrete made with fine recycled concrete aggregates. Cement and Concrete Composites. 2007;29(5):397-401.
[99] Poon CS, Kou SC, Lam L. Use of recycled aggregates in molded concrete bricks and blocks. Construction and Building Materials. 2002;16(5):281-9.
[100] Xiao J, Li J, Zhang C. Mechanical properties of recycled aggregate concrete under uniaxial loading. Cement and Concrete Research. 2005;35(6):1187-94.
[101] Xiao JZ, Li JB, Zhang C. On relationships between the mechanical properties of recycled aggregate concrete: An overview. Materials and Structures. 2006;39(6):655-64.

[102] Pereira P, Evangelista L, De Brito J. The effect of superplasticisers on the workability and compressive strength of concrete made with fine recycled concrete aggregates. Construction and Building Materials. 2012;28(1):722-9.
[103] Hansen TC, Boegh E. Elasticity and Drying Shrinkage Concrete of Recycled-Aggregate. ACI; 1985.
[104] Valeria C. Mechanical and elastic behaviour of concretes made of recycled-concrete coarse aggregates. Construction and Building Materials. 2010;24(9):1616-20.
[105] Amnon K. Properties of concrete made with recycled aggregate from partially hydrated old concrete. Cement and Concrete Research. 2003;33(5):703-11.
[106] Topcu IB, Şengel S. Properties of concretes produced with waste concrete aggregate. Cement and Concrete Research. 2004;34(8):1307-12.
[107] Tabsh SW, Abdelfatah AS. Influence of recycled concrete aggregates on strength properties of concrete. Construction and Building Materials. 2009;23(2):1163-7.
[108] Mas B, Cladera A, Olmo Td, Pitarch F. Influence of the amount of mixed recycled aggregates on the properties of concrete for non-structural use. Construction and Building Materials. 2012;27(1):612-22.
[109] Casuccio M, Torrijos M, Giaccio G, Zerbino R. Failure mechanism of recycled aggregate concrete. Construction and Building Materials. 2008;22(7):1500-6.
[110] Lee C-H, Du J-C, Shen D-H. Evaluation of pre-coated recycled concrete aggregate for hot mix asphalt. Construction and Building Materials. 2012;28(1):66-71.
[111] Choi YW, Moon DJ, Kim YJ, Lachemi M. Characteristics of mortar and concrete containing fine aggregate manufactured from recycled waste polyethylene terephthalate bottles. Construction and Building Materials. 2009;23(8):2829-35.
[112] Miranda LFR, Selmo SMS. CDW recycled aggregate renderings: Part I - Analysis of the effect of materials finer than 75 mu m on mortar properties. Construction and Building Materials. 2006;20(9):615-24.
[113] Dapena E, Alaejos P, Lobet A, Pérez D. Effect of recycled sand content on characteristics of mortars and concretes. Journal of Materials in Civil Engineering. 2011;23:414.
[114] Braga M, de Brito J, Veiga R. Incorporation of fine concrete aggregates in mortars. Construction and Building Materials. 2012;36:960-8.
[115] I.Vegas IA, A.Juarrero, M.Frias. Design and performance of masonry mortars made with recycled concrete aggregates. Materiales de Construccion. 2009;59(295):5-18.
[116] Lee S-T. Influence of recycled fine aggregates on the resistance of mortars to magnesium sulfate attack. Waste Management. 2009;29(8):2385-91.
[117] Corinaldesi V, Giuggiolini M, Moriconi G. Use of rubble from building demolition in mortars. Waste Management. 2002;22(8):893-9.
[118] Corinaldesi V, Moriconi G. Behaviour of cementitious mortars containing different kinds of recycled aggregate. Construction and Building Materials. 2009;23(1):289-94.
[119] Corinaldesi V. Mechanical behavior of masonry assemblages manufactured with recycled-aggregate mortars. Cement & Concrete Composites. 2009;31(7):505-10.
[120] Diamond S, Huang J. The ITZ in concrete–a different view based on image analysis and SEM observations. Cement and concrete composites. 2001;23(2):179-88.
[121] Diamond S. Considerations in image analysis as applied to investigations of the ITZ in concrete. Cement and concrete composites. 2001;23(2):171-8.
[122] Gokce A, Nagataki S, Saeki T, Hisada M. Freezing and thawing resistance of air-entrained concrete incorporating recycled coarse aggregate: The role of air content in demolished concrete. Cement and Concrete Research. 2004;34(5):799-806.
[123] Li G, Xie H, Xiong G. Transition zone studies of new-to-old concrete with different binders. Cement and concrete composites. 2001;23(4):381-7.

[124] Ollivier J, Maso J, Bourdette B. Interfacial transition zone in concrete. Advanced Cement Based Materials. 1995;2(1):30-8.
[125] Kong D, Lei T, Zheng J, Ma C, Jiang J, Jiang J. Effect and mechanism of surface-coating pozzalanics materials around aggregate on properties and ITZ microstructure of recycled aggregate concrete. Construction and Building Materials. 2010;24(5):701-8.
[126] Wang XH, Jacobsen S, He JY, Zhang ZL, Lee SF, Lein HL. Application of nanoindentation testing to study of the interfacial transition zone in steel fiber reinforced mortar. Cement and Concrete Research. 2009;39(8):701-15.
[127] Garboczi EJ, Bentz DP. Analytical formulas for interfacial transition zone properties. Advanced Cement Based Materials. 1997;6(3):99-108.
[128] Delagrave A, Bigas J, Ollivier J, Marchand J, Pigeon M. Influence of the interfacial zone on the chloride diffusivity of mortars. Advanced Cement Based Materials. 1997;5(3):86-92.
[129] Bentur A, Alexander M. A review of the work of the RILEM TC 159-ETC: Engineering of the interfacial transition zone in cementitious composites. Materials and Structures. 2000;33(2):82-7.
[130] Hashin Z, Monteiro P. An inverse method to determine the elastic properties of the interphase between the aggregate and the cement paste. Cement and Concrete Research. 2002;32(8):1291-300.
[131] Stutzman P. Scanning electron microscopy imaging of hydraulic cement microstructure. Cement and concrete composites. 2004;26(8):957-66.
[132] Scrivener KL. Backscattered electron imaging of cementitious microstructures: understanding and quantification. Cement and concrete composites. 2004;26(8):935-45.
[133] Bentz DP. Influence of internal curing using lightweight aggregates on interfacial transition zone percolation and chloride ingress in mortars. Cement and concrete composites. 2009;31(5):285-9.
[134] Xiao J, Li W, Sun Z, Lange DA, Shah SP. Properties of interfacial transition zones in recycled aggregate concrete tested by nanoindentation. Cement and concrete composites. 2013;37:276-92.
[135] Li W, Xiao J, Sun Z, Kawashima S, Shah SP. Interfacial transition zones in recycled aggregate concrete with different mixing approaches. Construction and Building Materials. 2012;35:1045-55.
[136] Xiao J, Li W, Corr DJ, Shah SP. Effects of interfacial transition zones on the stress–strain behavior of modeled recycled aggregate concrete. Cement and Concrete Research. 2013;52:82-99.
[137] Lee GC, Choi HB. Study on interfacial transition zone properties of recycled aggregate by micro-hardness test. Construction and Building Materials. 2013;40(0):455-60.
[138] EN N. 933-1. Tests for geometrical properties of aggregates. Determination of particle size distribution Sieving method. 1997.
[139] IFSTTAR. Test N° 78:2011. Tests on granulats in concrte: measurment of total water absorption of crushed sand.
[140] Gutteridge WA. On the dissolution of the interstitial phases in Portland cement. Cement and Concrete Research. 1979;9(3):319-24.
[141] Ohsawa S, Asaga K, Goto S, Daimon M. Quantitative determination of fly ash in the hydrated fly ash - CaSO4·2H2O□Ca(OH)2 system. Cement and Concrete Research. 1985;15(2):357-66.
[142] Luke K, Glasser FP. Selective dissolution of hydrated blast furnace slag cements. Cement and Concrete Research. 1987;17(2):273-82.

[143] Le Saout G, Lécolier E, Rivereau A, Zanni H. Chemical structure of cement aged at normal and elevated temperatures and pressures: Part I. Class G oilwell cement. Cement and Concrete Research. 2006;36(1):71-8.
[144] Lothenbach B, Le Saout G, Ben Haha M, Figi R, Wieland E. Hydration of a low-alkali CEM III/B–SiO2 cement (LAC). Cement and Concrete Research. 2012;42(2):410-23.
[145] EN T. 196-1 Methods of testing cement–Part 1: Determination of strength. European Committee for Standardization. 2005:26.
[146] DeJong MJ, Ulm F-J. The nanogranular behavior of CSH at elevated temperatures (up to 700 C). Cement and Concrete Research. 2007;37(1):1-12.
[147] Kojima Y, Numazawa M, Umegaki T. Fluorescent properties of a blue-to green-emitting Ce3+, Tb3+ codoped amorphous calcium silicate phosphors. Journal of Luminescence. 2012;132(11):2992-6.
[148] Alarcon-Ruiz L, Platret G, Massieu E, Ehrlacher A. The use of thermal analysis in assessing the effect of temperature on a cement paste. Cement and Concrete Research. 2005;35(3):609-13.
[149] Brunauer S, Emmett PH, Teller E. Adsorption of gases in multimolecular layers. Journal of the American Chemical Society. 1938;60(2):309-19.
[150] Morandeau A. Carbonatation atmosphérique des systèmes cimentaires à faible teneur en portlandite [Thèse]: Université Paris-Est; 2013.
[151] Nguyen TD. Étude de la zone d'interphase'granulats calcaires poreux-pâte de ciment': Influence des propriétés physico-mécaniques des granulats; Conséquence sur les propriétés mécaniques du mortier [Thèse]: Ecole Nationale Supérieure des Mines de Saint-Etienne; 2013.
[152] De Larrard F. Structures granulaires et formulation des bétons: Laboratoire Central des Ponts et Chaussées; 2000.
[153] SEDRAN T. RHEOLOGIE ET RHEOMETRIE DES BETONS. APPLICATION AUX BETONS AUTOINVELANTS [Thèse]: Ecole Nationale des Ponts et Chaussees; 1999.
[154] Bolomey J. Granulation et prévision de la résistance probable des bétons. Travaux. 1935;19(30):228-32.

Annex

Annex 1 : stoichimetric W/C and coefficients A, B and C to estimate SFSA

The stoichimetric W/C can be calculated according to the Rietveld results of clinker phases (Table 2-1). Equation A- 1 to Equation A- 6 show the general reactions of main clinker phases. Equation A- 1 and Equation A- 2 show that 5.5 and 4.5 moles of water are bounded due to the formation of portlandite and C-S-H from C_3S and C_2S respectively, according to these equations, the $(W/C)_{st,C3S}$ and $(W/C)_{st,C2S}$ can be calculated as 0.434 and 0.471 respectively. Similarly, $(W/C)_{st,C3A}$ for ettringite can be calculated as 1.733 according to Equation A- 3, (W/C)st,C3A for monosulfosluminate can be calculated as 0.667 according to Equation A- 4 (here we made a simplification, the content of gypsum is not included). Moreover, considering that 25% of ettringite and 75% of monosulfoaluminate are formed during hydration of C_3A and C_4AF, the $(W/C)_{st,C3A}$ and $(W/C)_{st,C4AF}$ can be estimated as shown in Table A- 1.

Table 2-1 Mineralogical composition of cements determined by XRD-Rietveld

	C_3S	C_2S	C_3A	C_4AF	Anhydrite	Calcite	Periclase	Gypsum
CEM I 52.5 Superblanc (%)	73.90	21.87	1.46	-	0.52	1.53	0.72	-
Grey cement CEM II 52.5 (%)	52.74	8.07	8.92	8.95	0.74	18.06	0.46	2.06

$$C_3S + 5.5H \rightarrow C_{1.7}SH_{4.2} + 1.3CH \qquad \text{Equation A- 1}$$

$$C_2S + 4.5H \rightarrow C_{1.7}SH_{4.2} + 0.3CH \qquad \text{Equation A- 2}$$

$$C_3A + 3C\bar{S}H_2 + 26H \rightarrow C_6A\bar{S}_3H_{32}\,(ettringite) \qquad \text{Equation A- 3}$$

$$C_3A + C\bar{S}H_2 + 10H \rightarrow C_4A\bar{S}H_{12}(AFm)$$ Equation A- 4

$$C_4AF + 3C\bar{S}H_2 + 30H \rightarrow CH + FH_3 + C_6A\bar{S}_3H_{32}(ettringite)$$ Equation A- 5

$$C_4AF + C\bar{S}H_2 + 14H \rightarrow CH + FH_3 + C_4A\bar{S}H_{12}(AFm)$$ Equation A- 6

Table A- 1 Calculation of $(W/C)_{st}$ for clinkers phases, Ett and MS means ettringite and monosulfoaluminate respectively

	C_3S	C_2S	C_3A		C_4AF	
$(W/C)_{st}$	0.434	0.471	Ett:1.733 MS:0.667	0.933	Ett:1.111 MS:0.519	0.667

Therefore the $(W/C)_{st}$ obtained from the composition of Rietveld are 0.44 and 0.41 respectively for white cement and grey cement used (Table A- 2).

Coefficients A, B and C are used to estimated SFSA by making some corrections.

Parameter A represents the relative mass of soluble phases in salicylic acid (C_3S, C_2S) in the cement. The A values of white cement and grey cement can be calculated as 0.9577 and 0.6081 from the mineralogical composition of cements.

Parameter C corresponds to the relative mass of C_3S, C_2S, C_3A, C_4AF leading to the formation of hydrates that are soluble in salicylic acid such as C-S-H, portlandite and ettringite. It can be calculated by the Equation A- 7. 0.25 refers to the first approximation that hydration forms 1/4 AFt phases for C_3A and C_4AF. The C values of white cement and grey cement can be calculated as 0.9614 and 0.6528 from the mineralogical composition of cements.

$$C = C_3S + C_2S + 0.25 \times (C_3A + C_4AF)$$ Equation A- 7

where the clinker phase corresponds to the quantity result of Rietveld analysis.

Parameter B represents the ratio between soluble fractions and total fractions which is shown as Equation A- 8. 0.25 and 0.75 refer to the first approximation that hydration forms 1/4 of AFt and 3/4 of AFm phases for C_3A and C_4AF. Therefore the B values can be estimated by calculation as 0.9773 and 0.8061 for the white cement and grey cement when the mineralogical composition of the cement is known and using the same chemical equations as those that were used to calculate the stochiometric W/C ratio. The values of coefficients A, B and C are shown in Table A- 2.

$$B = \frac{0.434C_3S + 0.471C_2S + 1.733C_3A \times 0.25 + 1.111C_4AF \times 0.25}{0.434C_3S + 0.471C_2S + (1.733 \times 0.25 + 0.667 \times 0.75)C_3A + (1.111 \times 0.25 + 0.519 \times 0.75)C_4AF} \quad \text{Equation A- 8}$$

where the clinker phase corresponds to the quantity result of Rietveld analysis.

Table A- 2 (W/C)st and coefficients A, B and C for the white and grey cements

	$(W/C)_{st}$	A	B	C
White cement CEM I 52.5 Superblanc (%)	0.44	0.9577	0.9773	0.9614
Grey cement CEM II 52.5 (%)	0.41	0.6081	0.8061	0.6528